Tampere University

TEEMU TIAINEN

Discrete Steel Frame and Truss Sizing Optimization under Code-based Constraints

Tampere University Dissertations 464

Tampere University Dissertations 464

TEEMU TIAINEN

Discrete Steel Frame and Truss Sizing Optimization under Code-based Constraints

ACADEMIC DISSERTATION
To be presented, with the permission of
the Faculty of Built Environment
of Tampere University,
for public discussion in the Lecture room RG202
of the Rakennustalo, Korkeakoulunkatu 5, Tampere,
on 17 September, at 12 o'clock.

ACADEMIC DISSERTATION
Tampere University, Faculty of Built Environment
Finland

Responsible supervisor and Custos	Assistant Professor Kristo Mela Tampere University Finland	
Pre-examiners	Professor Amir Oded Technion - Israel Institute of Technology, Israel	Professor Mathias Stolpe Technical University of Denmark Denmark
Opponents	Principal Scientist Ludovic Fulop VTT Finland	Professor Mathias Stolpe Technical University of Denmark Denmark

The originality of this thesis has been checked using the Turnitin OriginalityCheck service.

Copyright ©2021 author

Cover design: Roihu Inc.

ISBN 978-952-03-2082-9 (print)
ISBN 978-952-03-2083-6 (pdf)
ISSN 2489-9860 (print)
ISSN 2490-0028 (pdf)
http://urn.fi/URN:ISBN:978-952-03-2083-6

PunaMusta Oy – Yliopistopaino
Joensuu 2021

Abstract

The topic of this thesis is discrete sizing optimization of steel frames and trusses used as load bearing structures in buildings. Instead of only stress or displacement limits, steel structures should comply with design codes and meet their requirements. Thus the resulting design optimization problem is complemented with constraints that can be derived from steel design standards and include fire design as well. The code-based constraints together with discrete design variables originating from availability of steel profiles in certain sizes and types result in design problem to which the variety of available solution approaches is limited. In this thesis, the goal is to assess and further develop such approaches to find best performing procedure in terms of computational cost and quality of the obtained solution.

Three types of optimization approaches are considered. Firstly the popular meta-heuristics, secondly the mixed-integer linear programming (MILP) approach and thirdly the two-phase approach. Meta-heuristics are known to be flexible and easy to implement. However, the optimality of the obtained solution cannot be proven and convergence can be considered slow. Mixed-integer scheme is based on strict mathematical formulation and gives guaranteed global optimum of the problem. However, the computational effort needed for the solution becomes high. Moreover, the strict requirement of problem mathematical properties can be restricting when code-based resistance and stability constraints are applied. Approximations may be needed to ensure compliance with the requirements. The third approach uses continuous relaxation in the first phase after which a subset of the original discrete set around the continuous solution is searched with a suitable method. With the two-phase approach promising results are obtained in comparison with both meta-heuristics and MILP approach.

However, based on multiple example calculations the best approach cannot be selected with respect to all criteria. It seems that choice of approach and method should be done according to properties of the optimization problem being considered.

Preface

This thesis for doctor of science in engineering was written based on research on steel structures and structural optimization in 2015–19 in Tampere University and its predecessor Tampere University of Technology.

The author would like to thank the following persons and entities for contributing the progress of the research work and this thesis: *assistant professor Kristo Mela* as co-author in the publications and for guidance in optimization, *professor emeritus Markku Heinisuo* as co-author and guidance in structural engineering in steel structures, *MSc Timo Jokinen*, *PhD Roxane van Mellaert*, *associate professor Mattias Schevenels*, *professor Geert Lombaert* as co-authors, all other colleagues in steel and optimization research communities and conferences for presenting and sharing their work thus giving new ideas, and co-workers in Tampere University Faculty of Built Environment.

The valuable comments to enhance the thesis given by the pre-examiners *professor Mathias Stolpe* and *professor Oded Amir* are highly appreciated by the author.

The support of friends and family is also important for a doctoral candidate. It is most valuable to have possibilities to relax from research work every now and then and widen one's perspective to other areas of life. In this respect, the author would like to thank especially his wife *Liina* and two sons, *Urho* and *Kuisma*.

The thesis was partly funded by Finnish Cultural Foundation, Pirkanmaa Regional Fund. Their financial support is gratefully acknowledged by the author.

Tampere
2021

Teemu Tiainen

List of original publications

The thesis is based on the following original publications that are referred to in the text as Publication I-VI.

I Jokinen T., Mela K., Tiainen T. & Heinisuo M. (2016), 'Optimization of tubular trusses using intumescent coating in fire', *Journal of Structural Mechanics* **49**(4), pp. 160–170.

II Tiainen T., Mela K., Heinisuo M. & Jokinen T. (2017), 'The effect of steel grade in weight and cost of Warren-type welded tubular trusses', *Proceedings of the Institution of Civil Engineers - Structures and Buildings* **170**(11), pp. 854-872.

III Van Mellaert, R., Mela, K., Tiainen, T., Heinisuo, M., Lombaert, G. & Schevenels, M. (2018), 'Mixed variable approach for global discrete sizing optimization of frame structures', *Structural and Multidisciplinary Optimization* **57**(2), pp. 579–593.

IV Tiainen, T., Mela, K. & Heinisuo, M. (2018), Buckling length in mixed-integer linear frame optimization, *in* A. Schumacher, T. Vietor, S. Fiebig, K. Bletzinger & K. Maute, eds, 'Advances in Structural and Multidisciplinary Optimization Proceedings of the 12th World Congress of Structural and Multidisciplinary Optimization (WCSMO12)', Springer–Verlag, pp. 1923–1936.

V Tiainen T. & Heinisuo M. (2018), 'Buckling length of a frame member', *Journal of Structural Mechanics* **51**(2), pp. 49–61.

VI Tiainen T., Mela K. (2021), 'Two-phase approach in discrete sizing optimization of steel frames'. Manuscript submitted for review.

The Publications I-III and V are published in peer-reviewed journals. The Publication IV is published in conference proceedings. The Publication VI is a manuscript submitted for review.

Author's contribution in the publications

I The author implemented the example design problem and calculations with Jokinen. The author finished the manuscript.

II The author implemented the example design problem and calculations with Jokinen. The author prepared the manuscript with Heinisuo.

III Mela and van Mellaert prepared the manuscript and derived most of the equations in the proposed method. The author implemented the proposed method and completed the example calculations. During implementation, the author enhanced the method's details. Beyond the example problems, the author applied the method to numerous other test problems to find out the limits and behaviour of the method.

IV The author prepared the manuscript, implemented the proposed method and performed the example calculations.

V The author prepared the manuscript, implemented the proposed method and performed the example calculations.

VI The author prepared the manuscript, implemented the proposed method and performed the example calculations.

Contents

1 Introduction

In design of steel frames, finding dimensions of members is a standard task for structural engineers. The member dimensions have to be large enough to ensure the structure can withstand the expected loads occurring during the expected service time of the structure. On the other hand, unnecessarily large dimensions would mean unwanted extra investment cost for the owner of the structure. Alternatively to manual sizing, the dimensioning task can be formulated as an *optimization problem* and the solution to the problem can be searched with the help of computers. With the help of optimization, (at least partly) automated design procedure can be obtained.

The special feature of steel frame or truss design optimization is that the member sections should be chosen from a set of commercially available alternatives (Figure 1.1). This implies that the respective optimization problem has discrete design variables instead of continuous. The second special feature is that steel structures are typically slender and thus stability phenomena play an important role in the design. Thirdly, steel structures as part of buildings should comply with design codes which may contain limitations that are not necessarily easy to express with mathematical functions. These three features make the design optimization of steel structures mathematically challenging.

In the following, variety of optimization, structural analysis and cost calculation literature is reviewed. On structural optimization alone, thousands of articles had been published already in the 1990s (Cohn 1994). The review cannot thus be exhaustive and it is limited to scope of the thesis. Optimization and structural analysis literature is considered mainly focusing on the availability with the steel design codes and standards. The cost calculation literature review focuses on steel structures.

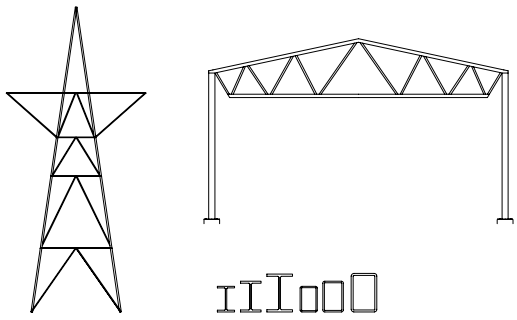

Figure 1.1: Typical steel structures are constructed of commercially available set of profile sizes and types.

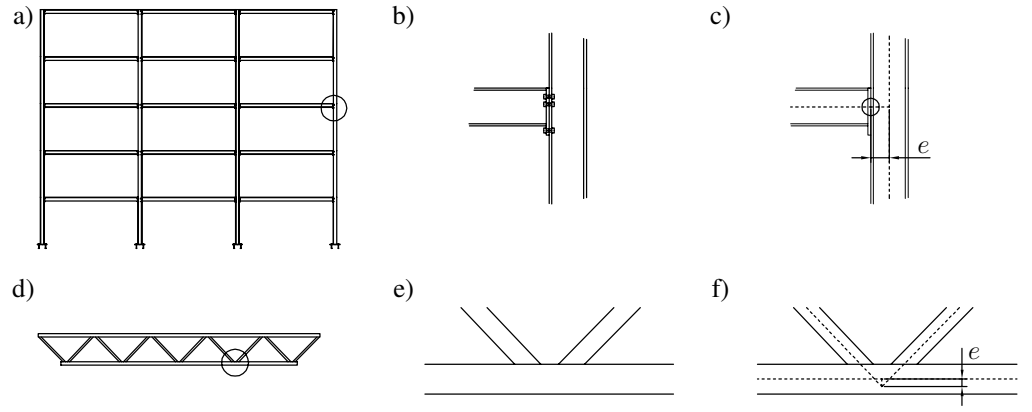

Figure 1.2: Frame and truss. Example joints and finite element modeling. a) frame constructed of hot-rolled I sections b) end plate joint in frame c) finite element model and eccentricity e at the joint d) tubular truss e) tubular truss joint f) tubular truss joint eccentricity e. Example joint locations in structures marked with circle in subfigures a) and d).

1.1 Steel design standards and optimization

Steel structures found in buildings are designed following standards and codes. In the standards, guidance to ensure the resistance and stability of load bearing structures is given. In a typical steel frame design procedure, the designer constructs a finite element model of the structure where loads (due to self-weight, snow, wind etc.) given in design codes are applied. With the internal forces obtained from the finite element analysis and the member dimension values chosen by the designer, the respective resistances are calculated according to the steel design code or standard.

In European Union, the Eurocode standards are used. The most relevant Eurocode standards for steel frame design are EN 1993-1-1, EN 1993-1-8, EN 1993-1-12 and EN 1993-1-2. They include member (EN 1993-1-1 2006) and joint (EN 1993-1-8 2006) resistance evaluation procedure as well as conditions on joint geometry on several different structure and joint types. Two typical steel joint types are shown in Figure 1.2. Moreover, EN 1993-1-8 (2006) gives guidance for the structural model used in analysis. For example in tubular trusses bending moments occurring in the chords and conditionally the eccentricities (Figure 1.2 d-f) of the joints are taken into account. This means that instead of truss or bar elements beam or frame elements should be used to model the chord members.

In finite element modeling of trusses and frames, traditionally only ideally hinged or rigid joints are considered. However, many typical joint designs are *semi-rigid* and their stiffness properties should conditionally be included in the design model (EN 1993-1-8 2006).

The standard EN 1993-1-12 (2007) gives rules how to apply EN 1993-1-1 and EN 1993-1-8 with steels with yield strength higher than 460 MPa up to 700 MPa. EN 1993-1-2 (2006) gives guidance to structural fire design and the resistance assessment at elevated temperatures.

From optimization perspective, the design codes include several challenging features. Depending on the optimization formulation, even the application of code formulas and procedures can

be challenging. Some of the design rules include conditional function definitions, for example flexural buckling of a member in both EN 1993-1-1 and the AISC specification (ANSI/AISC 360 16 2016). This may imply discontinuity of the functions but at least discontinuity of the derivative of such function which may limit the usable optimization methods or require mathematical treatment or approximation techniques.

In the resistance evaluation of a frame structure, stability is a fundamental issue. According to EN 1993-1-1, stability can be taken into account by a geometrically non-linear analysis procedure with initial imperfections or by the separated column approach where *buckling length* is determined for each compressed member.

In an optimization procedure, the latter option seems more tempting due to considerably lower computational effort needed for a single analysis. Thus, a methodology for obtaining the correct buckling length or critical axial force is essential for optimization. For trusses, constant values for buckling length factors are given in EN 1993-1-1. However, it was found by Boel (2010) and Snijder, Boel, Hoenderkamp & Spoorenberg (2011) that the code values for tubular trusses may be inaccurate and based on rigorous finite element analyses a simple method was given to evaluate correct lengths. Moreover, the joint rotational stiffness for both in-plane and out-of-plane can be determined by using the tabulated data given by Boel (2010).

In frames, the critical force of a single member is usually affected by the stiffening system of the whole frame, stiffness of the neighbouring members and/or stiffness of the joints. To evaluate the critical force numerous simplified methods have been presented. The method widely used is given by Dumonteil (1992). Semi-rigid joints in member stability have been considered by Mageirou & Gantes (2006). Enhanced method also taking into account the axial load in adjoining columns has been proposed by Webber, Orr, Shepherd & Crothers (2015). In optimization, the usability of a buckling assessment method is dependent of the problem formulation. In practically all the buckling length assessment methods some information on the stiffness of the neighbouring members is needed which may cause difficulties.

1.2 Optimization approaches

1.2.1 Classification of formulations

Typically structural optimization of truss or frame structures is classified in three categories: sizing, geometry and topology optimization (Kirsch 1993). The features of these categories are illustrated in Figure 1.3. In each category there are specific problem formulations and solution procedures. In all categories, it is important to recognize the mathematical properties of the problem formulation since the efficiency and applicability of solution techniques depend on them.

Clearly, problem considering sizing of a steel frame made of cross-sections of a commercially available selection has discrete design variables instead of continuous (Arora, Huang & Hsieh 1994). Arguably this feature is responsible for most of the challenges in steel frame optimization. The discrete sizing optimization of a truss with stress and displacement constraints has been proven to be NP-hard (Yates, Templeman & Boffey 1982). This implies that the computational effort to solve the discrete truss problem increases exponentially as the problem size increases. The author is not aware of a mathematical proof of the NP-hardness of frame problems, however similar behaviour is to be expected for frame optimization problems.

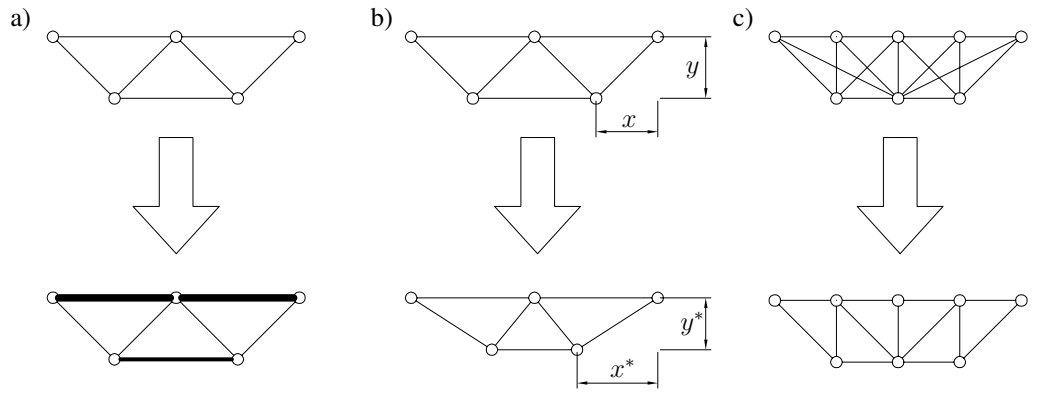

Figure 1.3: Structural optimization problem types a) sizing, b) geometry, c) topology with a truss example. In sizing problem, only member sections are chosen by optimization. In geometry optimization, also node coordinates may be added as design variables. In topology optimization, the structure topology is governed by the design variables.

1.2.2 Optimality criteria methods

Approaches that write a condition for optimality based on either engineering judgement or rigorous mathematics are called *optimality criteria methods*. These type of methods became popular in the 1970s (Kirsch 1993). The most well-known is probably the *fully stressed design* (FSD) approach where the maximum allowable stress present in all members is considered the criterion for optimality. While this holds for sizing optimization of isostatic structures with one loading condition and it has been shown in beginning of 1900s (Michell 1904) it has also been shown to result in suboptimal designs in hyperstatic structures (Razani 1965).

However, these methods have turned out to be very effective and they have been extended to cover discrete design variables and displacement constraints (Patnaik, Gendy, Berke & Hopkins 1998). In a contribution by Schevenels, McGinn, Rolvink & Coenders (2014), displacement constraints, code-based resistance constraints and manufacturability constraints are included in this type of approach. Still, it is acknowledged that optimality criteria methods cannot verify the optimality of the obtained solution.

1.2.3 Mathematical programming

In majority of contributions in the field of structural optimization, general mathematical programming methods are applied to structural optimization problems. The optimization problem is formulated in a standard form and a suitable method is applied to it to find a optimum candidate design.

A structural design problem can be formulated in multiple ways resulting in the same optimal design. Kociecki & Adeli (2005) have reviewed the formulations ending up in three categories: 1. nested approach 2. simultaneous analysis and design (SAND) approach and 3. two-phase approach. In the first category, only actual design variables are used and the structural analysis is nested in the formulation. This implies that typically the derivatives of constraint functions can be

only obtained numerically. In the SAND approach, state variables (displacement and/or forces) are introduced in the optimization problem. This means that the number of variables grows but the mathematical structure of the problem can be utilized in the solution procedure because the constraint functions can be explicitly written in terms of the design variables. This feature is not generally available in nested approach except for some particular structures such as isostatic trusses. The third approach is that state variables and design variables are handled at separate phases or sub-problems. It is shown by Kociecki & Adeli (2005) that choosing the formulation affects the computational effort needed in the solution procedure. However, no general remarks about the most efficient approach can be drawn from the examples presented by Kociecki & Adeli (2005).

In nested approach, the responses of the structure (forces, displacements etc.) needed for constraint evaluation are solved separately, for example with finite element approach. In structural optimization, the relevant responses are member forces $\mathbf{q}$ and nodal displacements $\mathbf{u}$. This "black box" structural analysis means that $\mathbf{q}$ and $\mathbf{u}$ are in general implicit functions of design variables $\mathbf{x}$. In an optimization problem constrained by resistance and displacement, the nested problem could be written as

$$\begin{aligned} &\min_{\mathbf{x}} f(\mathbf{x}) \\ &\quad \mathbf{g}_r(\mathbf{q}(\mathbf{x}), \mathbf{x}) \leq 0 && \text{resistance} \\ &\quad \mathbf{g}_d(\mathbf{u}(\mathbf{x})) \leq 0 && \text{displacement} \end{aligned} \tag{1.1}$$

In SAND formulation, the equations of structural analysis, such as compatibility and equilibrium, are taken into optimization problem as equality constraints and the responses are included as state variables in the formulation. Thus the resistance and displacement constraints have explicit mathematical structure. In this thesis, the state equations, equilibrium and compatibility, are written separately. The previous nested problem reformulated as SAND, could be written as:

$$\begin{aligned} &\min_{\mathbf{x},\mathbf{q},\mathbf{u}} f(\mathbf{x}) \\ &\quad \mathbf{g}_e(\mathbf{q}) = 0 && \text{equilibrium} \\ &\quad \mathbf{g}_c(\mathbf{x}, \mathbf{q}, \mathbf{u}) = 0 && \text{compatibility} \\ &\quad \mathbf{g}_r(\mathbf{q}, \mathbf{x}) \leq 0 && \text{resistance} \\ &\quad \mathbf{g}_d(\mathbf{u}) \leq 0 && \text{displacement} \end{aligned} \tag{1.2}$$

The equilibrium constraints are in fact in many cases linear without modifications and thus the derivatives become constant. Moreover, in an isostatic structure without limits for the displacement, the compatibility constraints are not needed and they can be removed from the optimization problem formulation.

With stress and displacement constraints and cross-sectional areas as design variables, the optimization problem becomes non-linear and possibly non-convex (Svanberg 1984). However, multiple gradient based methods and approaches have been applied to the continuous design problem.

These include for example sequential linear programming (SLP) approach (Haftka & Gürdal 1992), methods of feasible directions (Zoutendijk 1960), sequential quadratic programming (SQP)

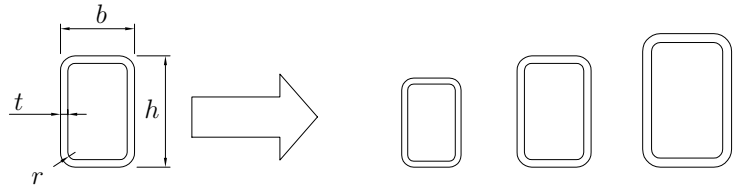

Figure 1.4: For optimization of a structure with rectangular hollow section profiles, the three dimensions (h, b and t) would be a natural choice for design variables for each member. In discrete problem, only certain sizes are available and a single index defining the chosen alternative can be used.

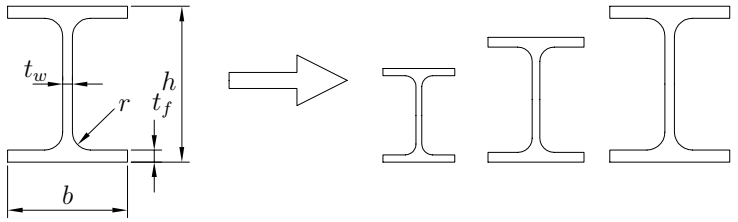

Figure 1.5: I profile dimensions and discrete sizes.

methods (Han 1976, Schittkowski 1983). SLP approaches were popular still in the 1990s owing to the fact that reliable LP packages were available (Haftka & Gürdal 1992, p. 231) despite the fact that SQPs have been found to have superior rate of convergence (Han 1976, Schittkowski 1983). SQP methods have been studied widely with some steps summarized by Sargent (1997). Today many contemporary software for spreadsheet and numerical computation have included implementations of different SQP and interior point methods to suit the needs of the user.

Many classical approaches use continuous design variables to determine the size of a section. However, as stated before, steel frame design is a discrete design problem, and the continuous solution candidate does not necessarily tell which discrete design choices to make. Therefore, rounding or other techniques must be used to make the discrete selection. Rounding, however, may result in suboptimal design as shown by textbook examples for integer programming, for example (Wolsey 1998, p. 4).

Other possibilities of treating the transfer from continuous to discrete design are considered by Arora & Huang (1996). Depending on the formulation, different schemes are possible. Hager & Balling (1988) presented a two-phase procedure where in the first phase continuous problem having larger dimension than the original sizing problem, i.e. possibly two or more continuous sizing variables are used for each member. Hager & Balling (1988) used cross-sectional properties as design variables whereas later contributors, such as Arora & Huang (1996), used profile dimensions (see Figure 1.4 an example for rectangular hollow sections and Figure 1.5 for I profiles). In the second phase, either the well-known *branch-and-bound* method (Land & Doig 1960) or meta-heuristics (see Section 1.2.4) can be used with the reduced discrete search space in the neighbourhood of the continuous solution.

By adopting the SAND approach, truss topology (and sizing) optimization problem with discrete sizing variables can be formulated as *mixed integer linear program* (MILP) (Ghattas &

Grossmann 1991). Probably the most important feature with MILP is that the problem can be solved to its global optimum by branch-and-bound method or its variants such as the *branch-and-cut* method (Padberg & Rinaldi 1987, Padberg & Rinaldi 1991) based on which several efficient commercial computer software are available (Gurobi Optimization 2018, IBM 2018). Moreover, the efficiency of MILP solution by branch-and-cut can be further enhanced with different heuristics.

Also, some other possibilities of using MILP including dynamic considerations are shown by Stolpe (2007). Mela (2014) included the EN 1993-1-1 member design constraints in tubular steel truss MILP formulation. Moreover, Mellaert, Lombaert & Schevenels (2016) included the EN 1993-1-8 joint design rules into constraints for a statically determinate truss. Especially sizing optimization of a tubular truss is very efficient with the MILP approach (Mela & Heinisuo 2017). However, with the truss model and MILP approach, the EN 1993-1-1 requirement for structural model being able to model the bending of chords cannot be taken into account accurately. The bending is taken into account with pre-approximated bending moment values and joint eccentricities (Figure 1.2 e-f) are disregarded. Therefore, the design obtained with these approaches may need manual post-processing after optimization to ensure that the design is fully compliant with EN 1993 rules.

The frame topology optimization problem with beam elements can be formulated as MILP similarly to the approach presented for truss elements. This means that two more independent force and two more displacement state variables are introduced for each member. This approach has been used for finding topologies in special structures, such as structures exhibiting negative thermal expansion (Hirota & Kanno 2015) and negative Poisson's coefficient (Kureta & Kanno 2014).

1.2.4 Meta-heuristic approaches

In the last two decades, meta-heuristic optimization techniques have become popular among the scientific community. For example, genetic algorithms (GA (Holland 1975)), particle swarm optimization (PSO, (Kennedy & Eberhart 1995)), harmony search (HS (Degertekin 2008)), tabu search (TS (Bennage & Dhingra 1995)), simulated annealing (SA (Balling 1991)), antcolony optimization (ACO (Camp, Bichon & Stovall 2005)), mine blast algorithm (MBA (Sadollah, Bahreininejad, Eskandar & Hamdi 2012)), symbiotic organisms search (SOS (Li, Huang & Liu 2009)), Big Bang–Big Crunch algorithm (BBBCA (Kaveh & Talahatari 2009)) have been shown to be usable in various design problems. The list above is not exhaustive and, moreover, improved versions of many of the mentioned methods have been presented in the literature.

The meta-heuristic optimization methods are typically relatively easy to implement and understand and they typically pose no restraints for the problem formulation in terms of mathematical properties of constraint and objective functions. Moreover, most of the methods can handle discrete design variables. Thus code-based constraints in discrete steel frame design can be used easily as has been done by several authors (Saka & Kameshki 1998, Jalkanen 2007, Kaveh & Talahatari 2009).

As there are plenty of meta-heuristic methods with various versions it is of interest to know which one to choose. When new methods are published their performance is evaluated against existing techniques and results found in literature usually with a finding that the new or improved method is better than the old ones.

However, some comparative studies have been presented with inconsistent results. For example, Jalkanen (2007) compared the performance of TS, GA, PSO, SA in tubular truss optimization problems in his thesis with a conclusion that none of the methods was the best in all of the example problems but overall performance imply greater efficiency for PSO and TS over SA and GA. Degertekin (2007) compared simulated annealing and genetic algorithms with finding that genetic algorithms converge faster but SA found better designs. Hasançebi, Çarbas, Dogăn, Erdal & Saka (2010) compared GA, SA, evolution strategies, PSO, TS, ACO and HS. In their test problems the difference in objective function value of best found design was quite large but different methods seemed to success in different problems. Alberdi & Khandelwal (2015) optimized frames with connection topology variables in addition to sizing variables using GA, HS, TS and ACO which in a comparison seemed to perform similarly well. Thus based on the references mentioned in this paragraph no general information about performance of the mentioned methods seems to be available.

In contrary to mathematical programming techniques, in the meta-heuristic methods there is no verification of optimality of the obtained design. Moreover, the convergence of such methods is typically slow. The number of function evaluations needed for even decent results is very high thus implying low efficiency and long computational time. Many of the methods require careful tuning of algorithmic parameters. In problems with clear mathematical structure in which other types of methods can be applied, considerably more efficient procedure can be obtained as shown by Stolpe (2011). Still, it could be said that mathematical programming and meta-heuristics should not be seen as competitors but to complement each other (Stolpe 2016).

In addition to meta-heuristic methods with relatively broad area of application presented above, many other heuristics have been used and developed since 1950s. For example greedy and local search algorithms for combinatorial discrete problems presented in Wolsey (1998) are said to date at least to 1950s or 60s. These types of heuristics are specific to problem formulation and many rely extensively on the notion of a solution neighborhood. However, this neighborhood is typically tailored to the structure of the problem being solved. For MILP type of problem, the relaxation induced neighbourhood search (RINS) has been proposed (Danna, Rothberg & Pape 2005). In the variable neighbourhood search (VNS) method (Mladenovic & Hansen 1997), the basic idea is to perform local search and to systematically vary the neighborhood in which the local search is performed. In last two decades, multiple improvements to this basis have been developed and proposed (Hansen, Mladenovic & Perez 2009).

The meta-heuristic approaches typically include a stochastic component in the algorithm whereas mathematical programming methods are deterministic. This means that multiple runs need typically to be performed to obtain ”good enough” results with acceptable probability with most meta-heuristic methods. In research, the behaviour of such methods should be evaluated with statistical measures rather than only the best found objective function value (Le Riche & Haftka 2012).

1.2.5 Cost as objective function in optimization

From optimization perspective, structural weight is a convenient choice for objective function. Several researchers, however, have analyzed the cost distribution of steel structures (Nethercot 1998, Carter, Murray & Thornton 2000, Evers & Maatje 2000, Salokangas 2009, Jalkanen 2007). Although there is some variation in the figures given by the references due to different types of

structures and differences in assumed manufacturing technologies, a general conclusion is that not only material cost but also manufacturing cost plays an important role in the economy of steel structures.

If only sizing optimization is performed, weight and cost optimization seem to correlate quite well (Jalkanen 2007). However, for example when the performance of different steel grades is compared it is clear that higher steel strength will result in lower weight but in overall economy the benefit is not clear without the knowledge of material cost difference. Moreover, if different topologies are compared, material cost alone becomes irrelevant, since large share of costs in steel structures is related to manufacturing actions (welding, cutting, drilling et cetera) needed in joints. Furthermore, some steel structures need to be designed to maintain their load bearing capacity during fire. This may require additional protection of the steel structures. If protection is done by intumescent coating a considerable additional cost is introduced and the cost is related to member dimensions (Iso-Mustajärvi & Inha 1999). Thus, if manufacturing cost of a steel frame including possible fire protection can be reliably calculated, it would serve as meaningful objective function for optimization.

Various cost functions with varying degree of detail have been proposed in the literature (Watson, Dallas, Van der Kreek & Main 1996, Jármai & Farkas 1999, Sarma & Adeli 2000, Jármai & Farkas 2001, Farkas, Simões & Jármai 2005, Pavlovčič, Krajnc & Beg 2004, Haapio 2012). With cost as objective function rather than the structural weight, the convenient mathematical properties may be lost depending on the structure and the used cost function. It turns out, however, that with careful formulation seemingly complicated cost functions can be included in formulations. For example, the highly detailed and mathematically complicated cost expressions proposed by Haapio can be included effectively to cost optimization of steel trusses with a relatively restricting MILP formulation (Mela 2013).

1.3 Outline of the study

In traditional formulations in structural optimization, the constraints are based on stress measures or displacements. Since the resistance of steel structures is typically connected to stability phenomena as well and standards governing structural design pose their restrictions to the design, the simplified model based only stresses or other structural responses may fail to produce usable designs.

The code-based constraints have been considered by numerous contributors in the literature. However, in majority of those contributions meta-heuristics have been used even though these methods are known for slow convergence and that the optimality of the obtained solution cannot be verified.

Moreover, design optimization is in most structural engineering applications multi-objective and multidisciplinary. Still, majority of structural optimization literature do not consider other objective functions than the structural weight. From practitioner's point of view this may limit the usability of an optimization approach since the typical client would be more interested in the cost of the structure rather than the weight.

Therefore, the objective of the thesis is to find the best possible methodology for steel frame optimization under code-based constraints. This is done by improving, complementing and possibly

combining the existing frame optimization schemes found in literature. The focus is on following aspects: i) the reliability of the solution procedure, ii) the computational effort needed to find an optimum candidate to the problem, iii) the possibility to use code-based constraints and objective functions alternative to structural weight. In the examples found in the literature by the author, only one or two of the mentioned aspects can be simultaneously fulfilled.

1.3.1 Research question

The outline of the thesis can be written as the following research question:

How should discrete sizing optimization problem of a frame structure be

1. formulated
2. attempted to be solved

taking into account

1. computational efficiency
2. quality of the solution candidate
3. flexibility to multiple types of objective functions
4. flexibility to use code-based constraints?

1.3.2 The scope of the thesis

This thesis is limited to cover sizing optimization of a steel frame structure under static deterministic loadings. A frame structure is understood within the thesis as a structure consisting of members in which both bending moments and axial forces can occur. However, the methods considered in the thesis are generally applicable to wider range of skeletal structures, such as pin-jointed trusses with axial force as the only internal force appearing in the members. Thus, also truss examples are covered to some extent. The example calculations are limited to planar structures. In structural analysis, linear models with respect to both material and geometrical behaviour is used. The proposed methods and approaches are tested on example problems covering steel members and design codes.

1.3.3 Main contribution of the thesis

The main contribution can be summarized as follows:

- Cost-efficiency of high strength steel assessed in tubular trusses
- Fire design procedure of tubular trusses assessed

- MILP approach tested for frame sizing optimization with practical selection of profiles
- Code-based member and cross-section design procedures formulated as MILP
- Novel techniques for buckling length assessment
- Two-phase techniques tested for structural sizing optimization comparing them to MILP and meta-heuristics

2 Discrete optimization and code-based constraints

As found in Chapter 1, the design optimization problems of skeletal steel structures are discrete and mathematically challenging. Therefore, the selection of available approaches to efficiently formulate and to find optimum candidates in such problems is limited. In this chapter, the typical constraints in steel frames are presented when applying the Eurocode 3 standards. Moreover, approaches of continuous relaxation are discussed.

2.1 Eurocode 3 and optimization

For steel frames, the Eurocode 3 standards include basically three types of resistance evaluation

1. Cross-section resistance evaluation
2. Member resistance evaluation (compressed members)
3. Joint resistance evaluation

In addition, depending on the problem formulation, other types of constraints may need to be included to the problem to ensure applicability of the resistance evaluation formulas.

Moreover, in structural design also serviceability limit states need to be verified. In a static problem, they include typically displacement limits for both horizontal sway and vertical deflections. These kind of constraints are widely applied and studied in the structural optimization literature and do not cause additional difficulties when Eurocode or other standards are applied. In some steel structures, the serviceability limit states connected to vertical deflections can be handled with pre-camber in the manufacturing process and thus the displacement constraints can be left out.

2.1.1 Cross-sectional properties and relaxation

The basis of resistance and serviceability verification is that the cross-sectional properties of the members are known. When a discrete problem is considered, tabulated values of all the relevant cross-sectional properties given by the material suppliers can be used. However, if in the optimization the discrete design variables need to be relaxed as continuous, different techniques may need to be used.

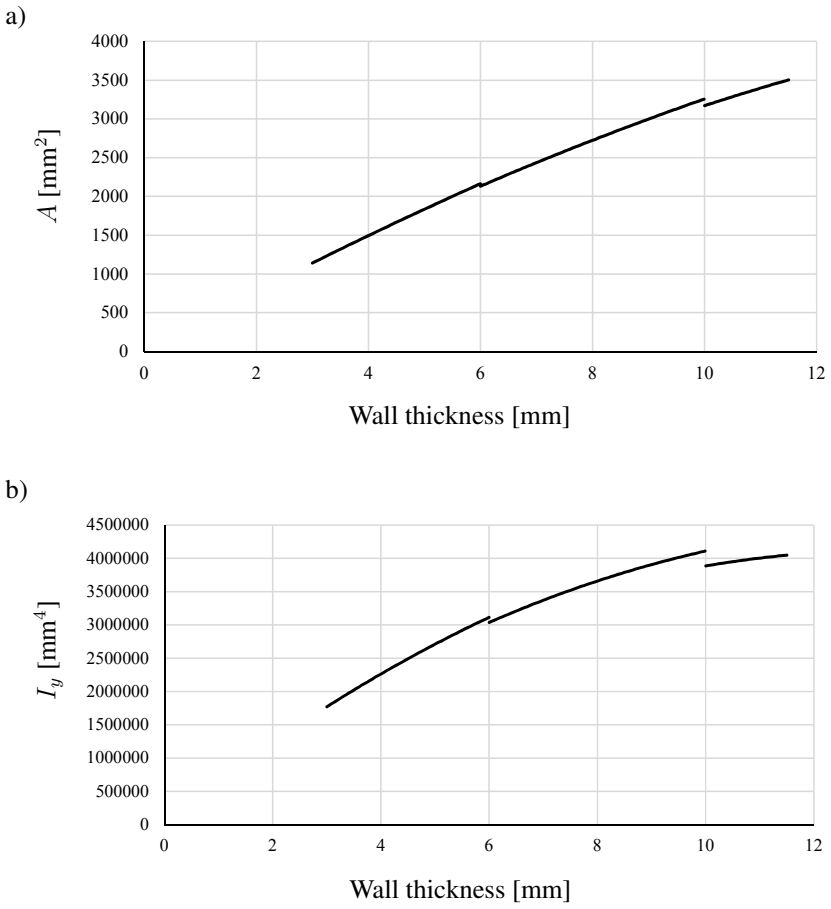

Figure 2.1: a) The cross-sectional area A and b) second moment I_y for a cold-formed square hollow section with external dimensions 100x100 as function of wall thickness.

For a cold-formed rectangular hollow section, the standard (EN 10219-2 2006) Annex B gives formulas to calculate the cross-sectional properties of a section with arbitrary dimensions b, h and t (see Figure 1.4). The corner rounding inner radius r is defined piecewise as (EN 10219-2 2006):

$$r\left(t\right) = \begin{cases} t & \text{if } t \leq 6 \text{ mm} \\ 1.5t & \text{if } 6 \text{ mm } < t \leq 10 \text{ mm} \\ 2t & \text{if } t > 10 \text{ mm} \end{cases} \tag{2.1}$$

This causes the cross-sectional properties to be non-differentiable or even non-continuous functions of the wall thickness t which is illustrated for cross-sectional area A and second moment I_y in Figure 2.1.

For I or H sections (see Figure 1.5), the cross-sectional properties are given in tables that can be obtained from the material suppliers. For continuous relaxation, multiple techniques can be used.

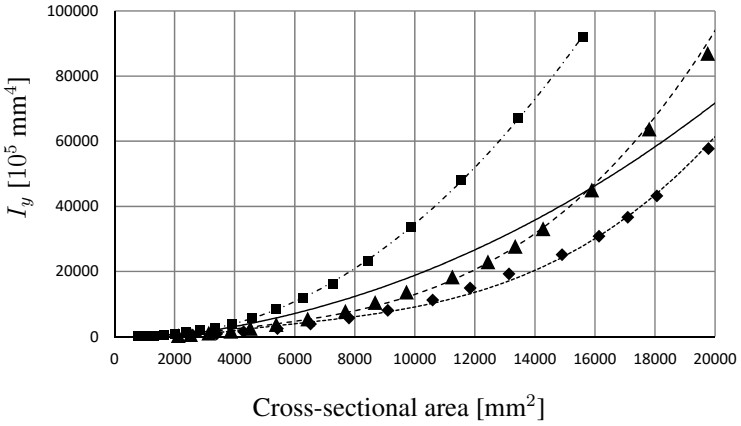

Figure 2.2: Three series of European hot-rolled I sections: IPE (square), HEA (triangle) and HEB (diamond). Strong axis second moment I_y plotted as function of cross-sectional area A. The dependency between I_y and A can be approximated with a polynomial fit: IPE (dash dot line), HEA (long dash), HEB (short dash), all profile types (solid line). In the plot, third degree polynomial is used.

Classical approach is to make curve fitting with respect to cross-sectional area. This approach according to Haftka & Gürdal (1992, p. 18) was first proposed by Moses & Onoda (1969). However, if different types of profiles are used – for example the European HEA and IPE series – the curve fitting scheme does not work particularly well since instead of one curve, several curves, one for each profile type, should be used (Figure 2.2).

Another option is to use the dimensions depicted in Figure 1.5 and calculate the cross-sectional properties directly from them. For example, the cross-sectional area of an I section can be calculated as

$$A = 2bt_f + (h - 2t_f)\, t_w + (4 - 2\pi)\, r^2 \tag{2.2}$$

When only certain series is used, relatively simple rules can be found for relations between dimensions. When relations are used in the relaxed problem the dimension of the problem reduces as only two variables need to be used for each member instead of four shown in Figure 2.3–2.5. With European IPE series it seems that linear approximations for relation of the dimensions fit well with the values in the catalogue.

2.1.2 Cross-section resistance

The EN 1993-1-1 uses cross-section classification to verify whether plastic or elastic cross-section resistance evaluation should be used. The classification is based on dimensions and strength of the cross-section material. In classes 1 and 2, plastic bending resistance can be reached before local buckling phenomena occur. In class 3, the stress due to bending may exceed yield limit in some part of the cross-section but full plastic capacity cannot develop. In class 4, the stress does not exceed the yield limit before some part of the cross-section locally buckles.

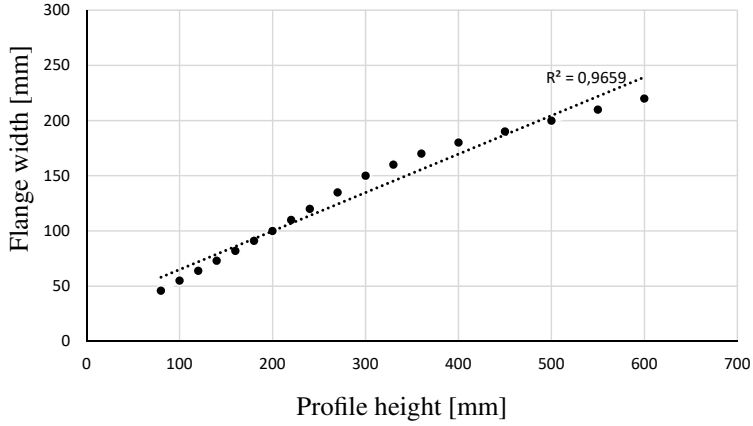

Figure 2.3: IPE series profile dimensions and linear fit with R^2 value shown in plot.

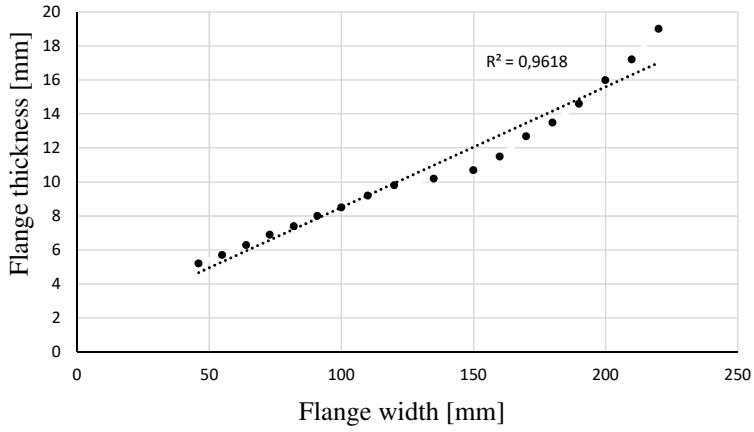

Figure 2.4: IPE series profile dimensions and linear fit with R^2 value shown in plot.

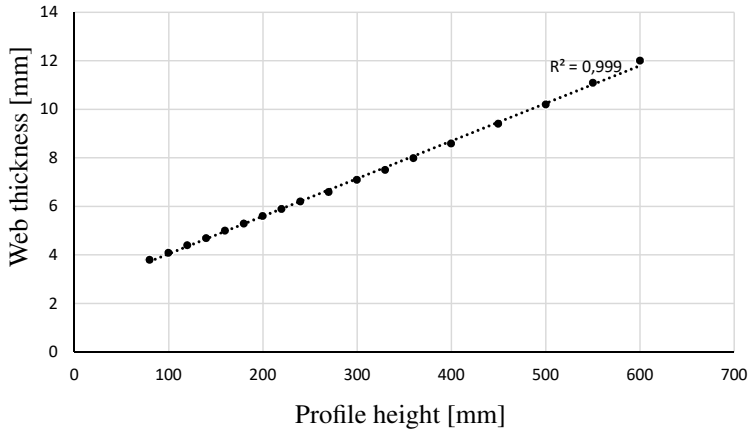

Figure 2.5: IPE series profile dimensions and linear fit with R^2 value shown in plot.

The cross-section resistance evaluation of EN 1993-1-1 in plastic cross-section classes 1 and 2 results in a set of linear constraints with respect to the internal forces N_{Ed} and M_{Ed}

$$\frac{N_{Ed}}{N_{Rd}} + k\frac{M_{Ed}}{M_{Rd}} \leq 1 \tag{2.3}$$

$$\frac{M_{Ed}}{M_{Rd}} \leq 1 \tag{2.4}$$

$$\frac{N_{Ed}}{N_{Rd}} \leq 1 \tag{2.5}$$

where N_{Ed} and M_{Ed} are the axial force and bending moment, respectively, present in the cross-section and N_{Rd} and M_{Rd} are the respective plastic resistances, and k is the interaction factor and a function of cross-section dimensions. The interaction factor k is a conditionally defined function of cross-sectional area and section dimensions. For an I section with cross-sectional area A, width b and flange thickness t_f, the k is calculated as

$$k = 1 - 0.5\left[\min\left(\frac{A - 2bt_f}{A}; 0.5\right)\right] \tag{2.6}$$

In cross-section class 3, elastic theory is used and the actions can be linearly combined by

$$\frac{N_{Ed}}{N_{Rd}} + \frac{M_{Ed}}{M_{Rd}} \leq 1 \tag{2.7}$$

where the resistances N_{Rd} and M_{Rd} are the elastic resistances.

The cross-section resistance evaluation based on cross-section classification thus implies discontinuity in resistance constraint functions for the relaxed problem (Figure 2.6).

Three notions can be made:

1. In both cases, problem formulation as MILP does not require linearization

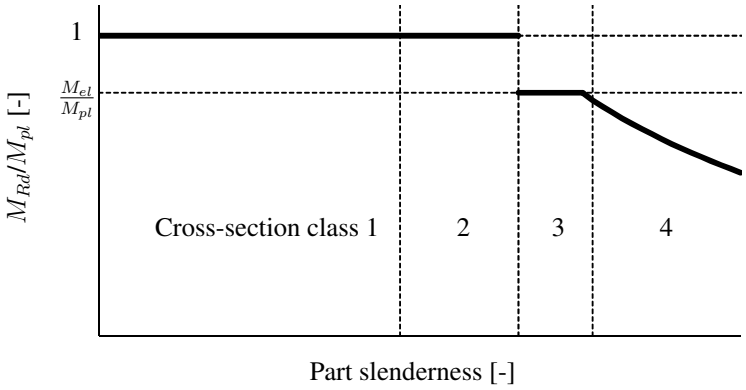

Figure 2.6: Discontinuity in bending moment resistance due to cross-section classification.

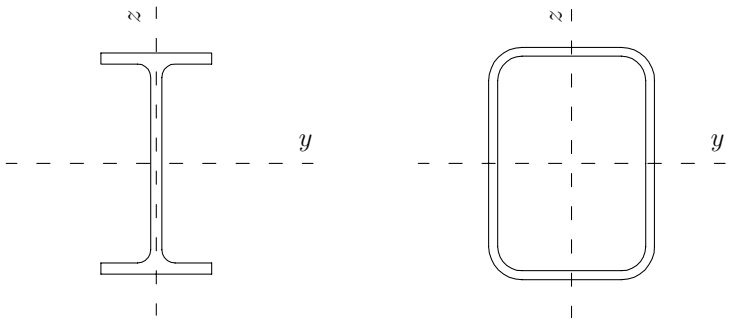

Figure 2.7: Axis definition.

2. In both cases, when a continuous relaxation in nested formulation is used, the resulting constraint is non-linear and most likely non-convex

3. In continuous relaxation, when cross-section class is changed from 2 to 3 there is a discontinuity in the constraint function (Figure 2.6)

2.1.3 Member resistance evaluation

In planar case with member not susceptible to torsion, the EN 1993-1-1 member resistance evaluation formulas 6.61 and 6.62 for compressed members reduce to

$$\frac{N_{Ed}}{\chi_y N_{Rd}} + k_{yy}\frac{M_{Ed}}{\chi_{LT} M_{Rd}} \leq 1 \tag{2.8}$$

$$\frac{N_{Ed}}{\chi_z N_{Rd}} \leq 1 \tag{2.9}$$

where χ_y and χ_z are reduction factors taking into account the flexural buckling around y and z axis (axis definition Figure 2.7), respectively, and k_{yy} is the interaction factor.

The χ_y is a function of member bending stiffness EI_y but also a function of bending stiffness of other members in the structure through buckling length. Moreover, k_{yy} is a non-continuous function of cross-section class, piecewise defined function of dimensionless slenderness $\bar{\lambda}$ and continuous function of design axial force N_{Ed} which in a hyperstatic structure is function of member stiffness and their distribution in the structure. The dimensionless slenderness $\bar{\lambda}$ is a function of elastic buckling load N_{cr}, cross-sectional area and yield strength

$$\bar{\lambda} = \sqrt{\frac{N_{cr}}{f_y A}} \tag{2.10}$$

The critical load N_{cr}, on the other hand, is a function of buckling length L_{cr}, flexural stiffness and material's Young's modulus

$$N_{cr} = \pi^2 \frac{EI}{L_{cr}^2} \tag{2.11}$$

In the mixed-integer formulation, the resistance evaluation in Eq. (2.8) can be shown nonlinear with respect to force variables. It is also possibly non-convex (Tiainen, Mela & Heinisuo 2018).

When continuous relaxations in nested formulations are considered, the internal forces are not state variables in the optimization leaving only the cross-section dimensions as design variables. Practically regardless of continuous relaxation technique the constraints are then non-linear:

$$\min f(\mathbf{x}) \tag{2.12}$$

$$\frac{N_{Ed,i}(\mathbf{x})}{\chi_{y,i}(\mathbf{x}) N_{Rd,i}(\mathbf{x})} + k_{yy,i}(\mathbf{x}) \frac{M_{Ed,i}(\mathbf{x})}{M_{Rd,i}(\mathbf{x})} \leq 1 \tag{2.13}$$

$$\frac{N_{Ed,i}(\mathbf{x})}{\chi_{z,i}(\mathbf{x}) N_{Rd}(\mathbf{x})} \leq 1 \tag{2.14}$$

2.1.4 Joint resistance evaluation

The joint resistance evaluation formulas are heavily dependent on which type of structure is being analyzed. For hollow section welded trusses (Figure 1.2 d-f), the joint design is relatively straightforward task. The resistance evaluation is done by checking relevant failure modes.

For example, probably the most important failure mode for K-joints (Figure 1.2 e), the chord face failure, is calculated by (Ongelin & Valkonen 2016, EN 1993-1-8 2006)

$$N_{i,Rd} = \frac{8.9 k_n f_{y0} t_0^2}{\sin \theta_i} \frac{b_1 + h_1 + b_2 + h_2}{4 b_0} \sqrt{\frac{b_0}{2 t_0}}, \; i = 1, 2 \tag{2.15}$$

where k_n is a factor taking into account the compressive stress in the chord face, f_{y0} is the yield strength of the chord material, t_0 is the chord wall thickness, θ_i is the angle between chord and brace member, b_i and h_i are the dimensions of the members with subscript 0 referring to chord and 1 and 2 referring to braces.

The resulting constraint in optimization can be written as

$$\frac{N_{i,Ed}}{N_{i,Rd}} \leq 1 \tag{2.16}$$

Thus, it can be seen that constraint is non-linear with respect to relaxed problem design variables b_i, h_i and t_i, $i = 0, 1, 2$. Moreover, the joint resistance is function of dimensions of all connecting members.

In frames with I and H profiles, multiple types of bolted connections are used depending on whether pinned, rigid or semi-rigid behaviour is wanted. Typically, additional steel parts such as welded fin plates, end plates, stiffeners and bolts are needed. To effectively include these types of joints in the optimization the dimensions of the additional parts may need to be taken into the optimization problem as design variables thus adding the dimension of the problem. Multiple failure modes need typically to be evaluated. In the design optimization examples found in this thesis, bolted connections are not considered.

3 Optimization methods and formulations

In this Chapter, the optimization methods used in the Publications I-IV and VI are presented briefly. Moreover, application of a specific method may need reformulation of the optimization problem. This will also be discussed in this Chapter.

In the publications I-IV and VI, multiple type of optimization algorithms are needed. In order to directly attemp to solve a discrete design problem of nested type, the set of available procedures becomes limited. The metaheuristics have been widely used in this type of problems. In this thesis, two methods, namely PSO and GA were utilized.

When an optimization approach involving a continuous relaxation, that may be nonlinear, is applied, a well-established algorithm for constrained continuous optimization is needed. In this subproblem, the SQP method was chosen mainly for three reasons: 1) the SQP methods are shown to have good converge characteristics 2) the SQP methods tolerate unfeasible starting point 3) multiple SQP method implementations are available in numerical calculation computer programs.

When a structural design problem is reformulated as MILP it would be possible to apply metaheuristics to the optimization problem as well. However, as the number of constraints and variables will become large this type of approach becomes practically unusable. The method called *branch-and-cut* is very efficient in this problem type and can handle the large amount of constraints and variables involved the reformulation.

3.1 Metaheuristics

The metaheuristics used in this thesis include PSO and GA. Both rely on a set of solutions that move or evolve in the design space. In terms of problem formulation, the methods allow different approaches. In this thesis, when applying metaheuristics the optimization problem is formulated as nested problem with the variable values implying an index which refers to a row in a Table to obtain the cross-sectional properties of the members.

With metaheuristics, multiple possibilities to implement the algorithm with different variations around the basic idea can be made. In the following subsections, the notation and equations to describe the algorithm are mostly based on the highly cited comparison article by Elbeltagi, Hegazy & Grierson (2005).

3.1.1 Particle swarm algorithm

The particle swarm optimization (PSO) algorithm mimics the behaviour of a bird flock or a swarm of bees searching for food. While trying to find a good place in the design space (with low objec-

tive function value and feasible constraint function values) the members of the swarm communicate with each other. Moreover, the members of the swarm, or *particles*, have memory of their locations.

For the algorithm N typically random designs are generated in the S-dimensional design space. Three values, namely current position of the ith member (X_i), the best position it has reached during previous rounds (P_i), and flying velocity (V_i). These are written as

$$X_i = (x_{i1}, x_{i2}, \ldots, x_{iS}) \tag{3.1}$$
$$P_i = (p_{i1}, p_{i2}, \ldots, p_{iS}) \tag{3.2}$$
$$V_i = (v_{i1}, v_{i2}, \ldots, v_{iS}) \tag{3.3}$$

In each round, the position (P_g) of the best particle is calculated as the best objective function value of all particles.

The new velocity for round $j+1$ of ith particle is calculated by

$$V_i^{j+1} = \omega V_i^j + c_1 \cdot rand_1 \cdot \left(P_i^j - X_i^j\right) + c_2 \cdot rand_2 \cdot \left(P_g^j - X_i^j\right) \tag{3.4}$$

where c_1 and c_2 are positive constants, $rand_1$ and $rand_2$ are random values in the range $[0, 1]$ and ω is an inertia parameter. Typical choices for the first two algorithmic parameters are $c_1 = c_2 = 2$. The operator ω balances the global search and the local search and it has been proposed to decrease linearly as the algorithm progresses from value of 1.4 to 0.5.

The updated position is obtained by using the updated velocity by

$$X_i^{j+1} = X^j + V_i^{j+1} \tag{3.5}$$

The velocity of the particle can be limited to set values as

$$-V_{max} \leq V_i \leq V_{max} \tag{3.6}$$

The typical algorithm implementation can be expressed by following steps (steps based on appendix D (Elbeltagi et al. 2005))

Step 1 Generate random population of N solutions (particles) and evaluate objective and constraint function values. Initialize weight factor ω.

Step 2 For each particle;
Set p_{Best} as the best position of particle i;
If fitness(i) is better than p_{Best};

p_{Best}(i)=fitness (i);
End;
Set g_{Best} as the best fitness of all particles;

Step 3 For each particle;
Calculate particle velocity according to (3.4);
Update particle position according to (3.5);
End;

Step 4 Update the value of the weight factor, ω;

Step 5 Check termination criteria. If true, go to Step 6, else go to step 2.

Step 6 Algorithm completed

Stopping criterion can be based on improvement of the best found design or when the number of iterations reaches the maximum value given by the user.

The method does not include mechanism to check the convergence against any mathematical optimality criteria. Thus, the quality of the obtained solution cannot be assessed.

Together with randomness involved within the algorithm it can be difficult to choose the parameter values c_1, c_2 and ω in best possible way. However, the method is relatively easy to implement and ready implementations are available in numerical calculation software.

3.1.2 Genetic algorithm

The genetic algorithm mimics the evolutionary principle among a population of individuals. Randomly generated set of designs is evaluated for objective and constraint function values. Based on their *fitness*, some of the individuals are chosen to produce offspring. The design variable values are coded as strings of genomes and the genomes of the offspring are combined from the genomes of the parents following algorithm rules for crossover. Alternatively, the process may also include *mutation* in which some part or parts of the string are altered randomly.

The algorithm can be implemented by completing following steps (steps based on appendix D (Elbeltagi et al. 2005))

Step 1 Generate random population of P solutions (chromosomes) and calculate their fitness (i)

Step 2 Select an operation (crossover and/or mutation);

If crossover;
Select two parents at random i_a and i_b;
Generate on offspring i_c=crossover(i_a and i_b);
Else If mutation;
Select one chromosome i at random;
Generate an offspring i_c=mutate(i);
End if;

Step 3 Calculate the fitness of the offspring i_c;

If i_c is better than the worst chromosome then replace the worst chromosome by i_c;

Step 4 Check termination criteria. If true, go to Step 2, else go to step 5.

Step 5 Algorithm completed

Within the genetic algorithm there are multiple tunable parameters and choices that must be made within the implementation of the method such as

- Number of individuals in the population
- Number of cross-over points
- Method of choosing the parent chromosomes
- Rule for mutation
- Binary coding vs. other type of coding
- Termination criteria

As it is the case with the PSO method, with randomness involved within the genetic algorithm it is very difficult to choose the parameter values in best possible way. However, the method is relatively easy to implement and ready implementations are available in numerical calculation software.

Moreover, similarly to the PSO method, there is no information available on the quality of the optimum candidate obtained with the genetic algorithm.

3.2 Branch-and-cut

Branch-and-cut method is used to solve convex mixed-integer programs. With the formulation described by Ghattas & Grossmann (1991) discrete binary variables are used for choosing the profile alternative. Nodal forces and displacements are continuous state variables. This type of formulation can be linear. As linear problem is always convex the mixed-integer linear program (MILP) can be solved to its global optimum.

The mixed-integer linear formulation can be written as

$$\min_{\mathbf{x},\mathbf{y}} \ \mathbf{a}^T\mathbf{x} + \mathbf{b}^T\mathbf{y} \tag{3.7}$$

$$\mathbf{A}\mathbf{x} = \mathbf{c} \tag{3.8}$$

$$\mathbf{C}\mathbf{y} = \mathbf{d} \tag{3.9}$$

where in case of structural optimization formulations typically, $\mathbf{a} = \mathbf{0}$, $\mathbf{b}$, $\mathbf{c}$ and $\mathbf{d}$ are constant vectors, $\mathbf{A}$ and $\mathbf{C}$, are constant matrices, $\mathbf{x}$ is the vector of continuous variables (forces and displacements), and $\mathbf{y}$ is the vector of binary variables.

A problem formulated as MILP can be solved using branch-and-bound approach. When the LP relaxation is complemented with additional cuts, the algorithm is called branch-and-cut. The branch-and-cut algorithm can be summarized by following steps (based on flowchart in (Wolsey 1998, page 158))

Step 1 Add the initial MILP to L, the list of active problems

Step 2 Set y = null and $f^* = \infty$

Step 3 Continue step if L is not empty

1. Select and remove (de-queue) a problem from L
2. Solve the LP relaxation of the problem.
3. If the solution is infeasible, go back to Step 3. Otherwise denote the solution by y with objective value f.
4. If $f \geq f^*$, go back to Step 3.
5. If y is integer, set $f^* \leftarrow f,\ y^* \leftarrow y$ and go back to Step 3.
6. If desired, search for cutting planes that are violated by y. If any are found, add them to the LP relaxation and return to Step 3.2.
7. Branch to partition the problem into new problems with restricted feasible regions. Add these problem to L and go back to Step 3

Step 4 Algorithm completed.

In addition to different type of cuts, the problem solving philosophy differs to that of branch-and-bound such that any other aids to solve the subproblem are welcome and utilized by the commercial solvers. These include heuristics (Wolsey 1998, section 2.6 and chapter 12), for example feasibility pump (Fischetti, Glover & Lodi 2005) and relaxation induced neigbourhood search (RINS) (Danna et al. 2005). Typically the utilization of such methods and branching strategy can be set by the user.

In this type of problem formulation, the matrices and vectors have typically a very large dimension. Thus programmable procedures are needed to 1) generate the matrices and vectors and 2) obtain for example the actual profile choices proposed by the procedure from the result data.

3.3 Sequential quadratic programming

Sequential quadratic programming (SQP) methods have been developed since 1970s (Belegundu & Chandrupatla 1999, p. 183) and have various versions of which an overview can be obtained from (Nocedal & Wright 2006*a*, chapter 18). They rely on quadratic approximation of the Lagrangian of the design problem. The problem can be formulated in well-known nested procedure (see Eq. 1.1). The SQP method is used for problems with continuous design variables, thus in the context of structural steel design optimization with typically discrete variables it can be used only for solving relaxed continuous subproblem.

The problem Lagrangian is written (notation following (Belegundu & Chandrupatla 1999))

$$L = f + \sum_{i=1}^{m} \mu_i g_i + \sum_{j=1}^{l} \lambda_j h_j \tag{3.10}$$

and the quadratic direction finding subproblem can be written as

$$\min_{\mathbf{d}} \ \frac{1}{2}\mathbf{d}^T\mathbf{B}\mathbf{d} + \nabla f^T\mathbf{d} \tag{3.11}$$

$$\nabla g_i^T\mathbf{d} + g_i^k \leq 0 \qquad i \in I_1 \tag{3.12}$$

$$\nabla h_i^T\mathbf{d} + h_i^k \leq 0 \qquad i \in I_2 \tag{3.13}$$

$$\mathbf{x}^L \leq \mathbf{x}_k + \mathbf{d} \leq \mathbf{x}^U \tag{3.14}$$

where $\mathbf{d}$ is the direction vector, $\mathbf{B}$ is the (approximation of) Hessian matrix of problem Lagrangian (Eq. (3.10)), g_i^k is inequality constraint function i evaluated at $\mathbf{x}_k$, h_i^k is equality constraint function i evaluated at $\mathbf{x}_k$, ∇f, ∇g and ∇h are gradient vectors evaluated at $\mathbf{x}_k$, $\mathbf{x}^L$ and $\mathbf{x}^U$ are vectors of lower and upper bounds, respectively, for problem design variables and I_1 and I_2"active sets" including problem active constraints.

When the direction is found, *line search* is performed to find the correct step length.

The stopping criterion can be based on optimality

$$\|\mathbf{d}\| \leq \epsilon_{KKT} \tag{3.15}$$

where ϵ_{KKT} is tolerance for direction vector length, or improvement of the solution candidate in terms of objective function value f

$$\|f_k - f_{k-n}\| \leq \epsilon_f \tag{3.16}$$

where n is number of consecutive iterations to which the objective function value is compared and ϵ_f is the desired tolerance. Belegundu & Chandrupatla (1999, p. 186) recommends value $n = 3$.

The algorithm can be summarized by following steps (steps based on (Belegundu & Chandrupatla 1999, p. 183–187))

Step 1 Set $k = 1$

Step 2 Solve the QP subproblem described on Eq. (3.11) to determine $\mathbf{d}_k$.

Step 3 Compute the step length α_k and set $\mathbf{x}_{k+1} = \mathbf{x}_k + \alpha_k \mathbf{d}_k$.

Step 4 Compute B_{k+1}.

Step 5 If stopping criterion is satisfied, continue, otherwise, go to step 2.

Step 6 Algorithm completed.

It should be noted, however, that some SQP algorithms use identity matrix instead of (approximation of) Hessian. Thus in those SQP versions, the step 4 is not needed.

The SQP methods converge to local minimum of a constrained optimization problem. The requirement for proven convergence is the C1 continuity of the objective and constraint functions. If the problem is convex and C1 continuity holds the optimum candidate given by the method is the global optimum of the problem. However, as discussed within the Chapter the given conditions are rarely fulfilled for structural design problems.

In this thesis, the SQP method was chosen after set of test runs on practical problems with high non-linearity and discontinuities present in the constraint functions. The interior point methods, another well-established type of methods (Nocedal & Wright 2006*b*, Chapter 19), suitable for constrained continuous optimization, seemed to fail in the test runs more frequently than SQP type of method.

4 Discussion

4.1 Contribution of the publications

The Publications I and II consider a tubular truss where geometry is modeled including eccentricity of the joints and all the relevant requirements of EN 1993-1-1 and EN 1993-1-8 are included as constraints. The main scope of Publication I was to assess two design approaches when fire protection design is included in the problem. In optimization this means slightly longer for a single function evalution due to critical temperature assessment. Since metaheuristic PSO method was applied, no theoretical obstacles to include the fire design were present.

In Publication II, the main scope was to find out whether or not it is economical to use higher strength steel than the widely used S355 (with yield strength $f_y = 355$ MPa).

In both Publications I and II, the cost of the structure is needed for comparison instead of weight.

The Publication I demonstrates by a calculation example that fire design and protection increase the cost of a tubular truss considerably and that the design of the truss itself remarkably affects the cost of the fire protection. The widely used approach to design the structure in room temperature after which fire protection is considered results in more expensive structures than a more holistic approach where fire design is included in the optimization problem.

In Publication II, it is demonstrated that in many cases using high strength steel reduces the total cost of the structure. Hybrid solutions with high strength steel in chords and lower strength steel in braces seem very promising in particular.

When fire protection needs to be applied the benefit of high strength steel is not clear without further calculations as the protection adds the total cost considerably. As the profiles are likely to become lighter and smaller, the outer surface area to be covered with the intumescent paint is likely to diminish but in the same time smaller wall thickness leads to thicker and thus more expensive intumescent coating. The scenario with both high strength steel and fire protection thus is an interesting topic for further research.

Regarding optimization in Publications I and II, several major findings can be made: 1) all the relevant Eurocode design formulas can be included in a truss design optimization problem 2) cost of such a structure can be optimized even with fire design constraints and protective coating 3) the approach allows direct optimization with given total height (from lower surface of bottom chord to the top surface of top chord) of the truss 4) eccentricities in the joints can be taken into account. Typically in structural optimization literature the height is based on mid-lines of the truss members and eccentricities are omitted. It can also be said that to obtain the results, a relatively large amount of computational effort was needed. Thus, the PSO method seems inefficient in the discrete truss design problem with code-based constraints.

In Publication III, a completely different optimization approach is adopted. The mixed-integer formulation previously used in the literature with truss structures and special frame structures is applied to a frame design problem with stress and displacement constraints. In the paper, general framework for applying MILP in building frame sizing is given. Moreover, the performance is compared to genetic algorithm, a popular method for similar frame optimization problems. Rather than a code-based resistance evaluation straightforward stress and displacement constraints are applied.

Three findings can be addressed. It seems that with a practical catalogue of profiles, the size of optimized frame is limited to modest size of structures due to high computational effort needed and, in comparison with the MILP, the genetic algorithm seems to be more efficient option. However, it should be noted that optimal design itself is found in a relatively short time and most of the computational effort is spent on proving the optimality of the design. Secondly, numerical problems are possible with the MILP implementation. Thirdly, the method is not easy to implement since existing finite element codes cannot be used at least directly.

During implementation and test runs it turned out that MILP problems are prone to numerical problems. It happened for example that two commercial programs (Gurobi Optimization 2018, IBM 2018) gave slightly different results claiming them to be the global optimum of the same problem. Also, another problem for which a solution could be found was claimed infeasible when more profile options were added. The numerical problems may originate from several sources. Firstly, big-M technique used in compatibility constraint requires user-defined large value and incorrect value may have been used. Secondly, the scaling of the variables and constraints is difficult due to multiple dimensions found in structural analysis and design equations. For example, rotational displacement, translational displacement, axial force and bending moment have their own dimension and the choice of unit system for example is strongly related to scaling.

In Publication IV, it is demonstrated that the EN 1993-1-1 member design rules can be linearized to fit the MILP scheme implying that guaranteed global optimum of the design problem can be obtained. However, the buckling length assessment methods presented in the literature cannot be included in the MILP scheme. The buckling length problem is tackled by a sequential approach in which the change in buckling length is handled by performing sequentially optimization and buckling analysis. In the numerical examples, it is demonstrated that this approach results in finding the global optimum for example structures of small size. However, as found out in Publication III, the practical problem size is limited with the MILP approach. When applying the proposed sequential approach the MILP has to be solved multiple times during one optimization making the computational effort needed even greater. Moreover, sequential technique requires a programmable procedure for buckling assessment. In the article, however, the lowest positive eigenmode was used as a conservative approximation.

Publication V considers the buckling length problem arisen in Publication IV. In Publication V, two rather simple but efficient and robust methods for assessing the buckling length factors are presented. Both approaches rely on the well-known finite element discretization. The first approach uses geometric stiffness matrix only in elements belonging to the member being assessed. The second approach is based on strain energy measure. Both of the methods are general in the sense that they can be used for many kinds of skeletal structures including tapered beams and/or semi-rigid connections.

However, both methods lack generality in other ways. The one based on local geometric stiffness matrix has limited application range such that only braced frames (or frames with horizontal sup-

ports) can be handled. The strain energy based approach includes an important tunable parameter that governs which eigenmode is chosen. Value for this parameter resulting in correct buckling mode in all possible design scenarios has - however - not been found.

Although the programmable procedures proposed in Publication V were created with applicability in optimization in mind, they can be applied for any design problem and procedure with or without optimization. Implementation requires some knowledge of finite element programming and possibility to add own procedures in collecting the geometrical stiffness matrix.

In Publications I-IV, the direct application of metaheuristics or MILP reformulation were found to be inefficient. Therefore in Publication VI, alternatively, a two-phase technique using continuous relaxation of discrete design variables in the first phase and limited discrete design space in the second phase is utilized.

Theoretically, when utilizing deterministic gradient-based optimization methods in the first phase the relaxation should be differentiable and continuous for guaranteed convergence. However, these properties are not necessarily available (see Chapter 2) when code-based constraints are used. Based on the example calculations, it seems however, that this methodology can be used for solving such problems.

Even fairly simple continuous sizing problems with only stress constraints may be non-convex (Svanberg 1984). This feature was seen in the examples in a way that the continuous search converged into several different designs within the set of runs performed with random initial designs.

In the two-phase procedure, multiple possibilities to relax the discrete design variables continuous are available (see also Chapter 2). The type is preferably chosen to meet the problem features as is done in the examples found in the Publication VI. In many cases, the relaxation of discrete design variables can be performed without adding the dimension of the problem.

The performance of the two-phase approach is evaluated in several examples. The first one is the 3x3 example used also in the Publication III. It is found that the two-phase approach outperforms both MILP and direct application of GA in terms of computational efficiency. In this example, the relaxation is based on one variable, namely the height of the profile. Other cross-sectional properties are expressed as continuous and differentiable functions of the profile height.

In the second example, a benchmark problem studied widely by researchers on metaheuristic methods, a 52-member truss, is optimized with stress constraints. In the relaxation, the cross-sectional areas can be used directly. The problem can be solved to its global optimum by the MILP approach. However, this is computationally a very demanding task. With the two-phase approach, a design with slightly lower objective function value than designs produced by alternative methods in the literature is found.

In the third example problem, a tubular truss similar to those found in Publications I and II is optimized with relevant EN 1993-1-1 and EN 1993-1-8 based constraints. It is found that results are obtained with less computational effort and with less deviation. Thus, lower number of shorter computer runs are needed for similar results.

In the fourth example, a 24-story 3-bay frame is considered. The constraints are based on the AISC design code. With the two-phase approach, a better design is found than with state-of-the-art metaheuristics. However, the metaheuristics converge in the examples with low amount of function evaluations. On the other hand, in the tests performed by the author the GA found worse

Table 4.1: Features of different approaches in frame sizing problems.

Feature	MILP	metaheuristic	two-phase
Cost as objective	possibly	yes	yes
Member design rules	approximate	exact	exact
Buckling assessment	approximate	exact	exact
Joint design rules	in some cases	yes	yes
Semi-rigid joints	possibly	yes	yes
Calculation time	long	long	moderate
Implementation	difficult	easy	moderate
Verification of optimality	yes	no	no

design with higher computational effort than the two-phase approach. Thus it would be of interest to try the performance of the newest metaheuristics in the second phase.

4.2 Summary of the main results

In the original Publications I-VI three types of frame optimization techniques are used:

1. Direct application of metaheuristic approaches
2. Mixed-integer linear programming (MILP) approach
3. Two-phase approach

Based on the publications and the work done within the topics, features of different approaches are described in qualitative fashion (Table 4.1). All of the aspects, such as semi-rigid joints, are not covered in the Publications I-VI included in the thesis but this feature has been tested by the author. The aspect of cost as objective has been considered in contributions related to tubular trusses (Publications I and II) but not in the others.

In the original publications, the ease of implementation is not considered directly. All of the methods have multiple tunable parameters. They were run with default values with commercial computer programs and with parameter values selected based on literature when university-made codes were used. The effect of varying the tunable parameters were thus not covered by the thesis. However, it should be acknowledged that performance of some methods may be sensitive to parameter choices.

It seems thus, that none of the approaches presented is better than others with respect to all criteria mentioned in Table 4.1. This implies that optimization approach should be chosen according to features needed in the specific application at hand. Possibly parallel or sequential use of the approaches would be beneficial. Based on performance in numerical examples in the publications I-IV and VI, however, the two-phase approach can be considered best performing of the considered optimization approaches.

The MILP approach has been found to be effective in roof truss optimization (Mela 2013). However, in truss sizing optimization problem in Publication VI the MILP approach seems to be very

time consuming. That is also the case in Publication III and IV in which moderately sized frames are optimized. This may be due to fact that in the roof truss topologies considered by Mela constraints were added to prevent bracing members to cross each other to ensure manufacturability of the truss. While it has not been rigorously proven that those constraints result in a statically determinate design it has been noted that all the resulting topologies were statically determinate. Thus, the compatibility constraints can be considered inessential. In the truss in Publication VI and frames in Publications III and IV, the structures are statically indeterminate to a high degree meaning that compatibility constraints are needed. If MILP truss sizing optimization is complemented with a displacement constraint when using software described by Mela, Alinikula, Tiainen, Heinisuo & Sorsa (2015) the solution slows down considerably. These findings may imply that the computational difficulty is located in the compatibility constraints.

4.3 Future work on the topic

As implied by Table 4.1, several paths are open for future research in the area of discrete code-based based steel frame optimization. The semi-rigid nature of joints could be incorporated to MILP, but it would be meaningful only if the cost of the joints could be incorporated to the scheme as well. This maybe possible through a database of different joints for which resistance, stiffness and cost would be evaluated. The approximate cost could then be obtained through suitable response surface in resistance-stiffness space. Similar work has been carried out by Díaz, Victoria, Querin & Martí (2012).

In the thesis, only planar structures were considered. Theoretically, there are no obstacles on moving to 3D structures. However, 3D structures involve complicated 3D stability issues, more complicated resistance assessment and more degrees of freedom in the analysis model. The first two points may mean challenges in implementation of the optimization and the last one means increased computational effort.

When moving to 3D problem, the buckling length assessment becomes more complicated. The methods proposed in Publication V need to be generalized to recognize in-plane and out-of-plane eigenmodes from 3D analysis. Moreover, the methods in Publication V could be generalized to include lateral torsion buckling modes. This, however, would require the use of finite element that includes warping as degree of freedom. Suitable element has been proposed by Barsoum & Gallagher (1970).

Also, the effect of fire protection and improved steel strength on structure cost could be studied on other structures than tubular trusses as well. Requirement for this is clearly a well suited formulation and cost assessment and a robust optimization procedure.

The two-phase approach was originally proposed around thirty years ago. However, for some reason it has not been used widely during that time but different metaheuristics have been developed. It seems, however, that the two-phase approach might be usable in structural optimization and, even though the performance is demonstrated in Publication VI in some numerical examples, the full potential of the approach is not yet exploited.

5 Conclusions

Motivation for this study is to find an optimization approach for discrete sizing optimization under code-based constraints. The approaches found in the literature seem to have issues with regard to computational efficiency and/or the quality of solution. In some optimization approaches, the code-based constraints may be unusable due to their mathematical structure.

Within this thesis, three kinds of approaches have been adopted: direct applying of metaheuristics, direct applying of mixed-integer reformulations, and applying a two-phase approach in which the problem is relaxed continuous in the first phase and either mixed-integer or metaheuristics are used in the second phase with limited discrete design space. All of the approaches seem to have some advantages and drawbacks when compared to each other.

The results obtained in the thesis imply that the most promising branch for further development is the two-phase approach. Even though the optimality cannot usually be proven, the computational efficiency in comparison to directly applying metaheuristics seems high. Theoretically the relaxed problems should have certain mathematical properties but based on test in example problems it did not matter even if they did not possess those properties. Thus when comparing to MILP reformulations, the two-phase approach does not seem to have as strict limitations for mathematical properties of the objective and constraint functions.

Moreover, even though the member resistance evaluation of EN 1993-1-1 could be linearized to fit MILP scheme, it seems that computational efficiency of this approach is low compared to other approaches. Still, the MILP approach possesses the good feature of being able to give guaranteed optimum of the problem. Thus, it could be used for scientific purposes for finding the global optimum of benchmark problems and to help to verify the performance of other approaches.

Within the thesis, some knowledge is obtained from the structural design itself. Based on the work done with cost optimization, it can be said that truss design approach should be such that it includes the fire design assessment in some degree even if the actual fire protection design would be completed by an expert in the field of fire protection. Moreover, when considering roof structures with no requirement for fire protection with intumescent paint, for example due to automatic fire extinction system, the high strength steels or hybrid solutions can be a tempting option.

Bibliography

Alberdi, R. & Khandelwal, K. (2015), 'Comparison of robustness of metaheuristic algorithms for steel frame optimization', *Engineering Structures* **100**, 276–292.

ANSI/AISC 360 16 (2016), *Specification for Structural Steel Buildings*, American Institute of Steel Construction.

Arora, J. S. & Huang, M.-W. (1996), 'Discrete structural optimization with commercially available sections', *J. Struct. Mech. Earthquake Eng., JSCE* **1996**(549), 1–18.

Arora, J. S., Huang, M. W. & Hsieh, C. C. (1994), 'Methods for optimization of nonlinear problems with discrete variables: A review', *Structural Optimization* **8**, 69–85.

Balling, R. (1991), 'Optimal steel frame design by simulated annealing', *Journal of Structural Engineering* **117**, 1780–1795.

Barsoum, R. W. & Gallagher, R. H. (1970), 'Finite element analysis of torsional and torsional-flexural stability problems', *International Journal for Numerical Methods in Engineering* **2**, 335–352.

Belegundu, A. D. & Chandrupatla, T. R. (1999), *Optimization Concepts and Applications in Engineering*, Prentice Hall.

Bennage, W. & Dhingra, A. (1995), 'Optimization of truss topology using tabu search', *International Journal for Numerical Methods in Engineering* **38**, 4035–4052.

Boel, H. (2010), Buckling length factors of hollow section members in lattice girders, Master's thesis, Eindhoven University of Technology.

Camp, C. V., Bichon, B. J. & Stovall, S. P. (2005), 'Design of steel frames using ant colony optimization.', *Journal of Structural Engineering* **131**, 369–379.

Carter, C. J., Murray, T. M. & Thornton, W. A. (2000), 'Cost-effective steel building design', *Progress in structural engineering and materials* **2**, 16–25.

Cohn, M. Z. (1994), 'Theory and practice of structural optimization', *Structural Optimization* **7**, 20–31.

Danna, E., Rothberg, E. & Pape, C. L. (2005), 'Exploring relaxation induced neighborhoods to improve mip solutions', *Mathematical Programming* **102**, 71–90.

Degertekin, S. O. (2007), 'A comparison of simulated annealing and genetic algorithm for optimum design of nonlinear steel space frames', *Structural and Multidisclipinary Optimization* **34**, 347–359.

Degertekin, S. O. (2008), 'Optimum design of steel frames using harmony search algorithm', *Structural and Multidisclipinary Optimization* **36**, 393–401.

Díaz, C., Victoria, M., Querin, O. & Martí, P. (2012), 'Optimum design of semi–rigid connections using metamodels', *Journal of Constructional Steel Research* **78**, 97–107.

Dumonteil, P. (1992), 'Simple equations for effective length factors', *Engineering Journal AISC* **29**(3), 111–115.

Elbeltagi, E., Hegazy, T. & Grierson, D. (2005), 'Comparison among five evolutionary-based optimization algorithms', *Advanced Engineering Informatics* **19**(1), 43–53.
URL: *http://www.sciencedirect.com/science/article/pii/S1474034605000091*

EN 10219-2 (2006), *Cold formed welded structural hollow sections of non-alloy and fine grain steels. Part 2: Tolerances, dimensions and sectional properties*, CEN.

EN 1993-1-1 (2006), *EN-1993-1-1. Eurocode 3: Design of steel structures. Part 1-1: General rules and rules for buildings.*, CEN.

EN 1993-1-12 (2007), *EN-1993-1-12. Eurocode 3: Design of steel structures. Part 1-12: Additional rules for the extension of EN 1993 up to steel grades S 700* ., CEN.

EN 1993-1-2 (2006), *EN-1993-1-2. Eurocode 3: Design of steel structures. Part 1-2: General rules – structural fire design.*, CEN.

EN 1993-1-8 (2006), *EN-1993-1-8. Eurocode 3: Design of steel structures. Part 1-8: Design of joints.*, CEN.

Evers, H. G. A. & Maatje, I. F. (2000), Cost based engineering and production of steel constructions, *in* 'Connections in steel structures IV', Roanoke, Virginia, USA, pp. 14–22.

Farkas, J., Simões, L. M. C. & Jármai, K. (2005), 'Minimum cost design of a welded stiffened square plate loaded by biaxial compression', *Structural and Multidisciplinary Optimization* **29**, 298–303.

Fischetti, M., Glover, F. & Lodi, A. (2005), 'The feasibility pump', *Mathematical Programming* **104**, 91–104.

Ghattas, O. & Grossmann, I. E. (1991), MINLP and MILP strategies for discrete sizing structural optimization problems, *in* O. Ural & T. L. Wang, eds, 'Proceedings of the 10th conference on electronic computation', ASCE, pp. 197–204.

Gurobi Optimization, L. (2018), 'Gurobi optimizer reference manual'.
URL: *http://www.gurobi.com*

Haapio, J. (2012), Feature-Based Costing Method for Skeletal Steel Structures based on the Process Approach, Phd thesis, Tampere University of Technology.

Haftka, R. T. & Gürdal, Z. (1992), *Elements of structural optimization*, Kluwer academic publishers.

Hager, K. & Balling, R. (1988), 'New approach for discrete structural optimization', *Journal of Structural Engineering* **114**(5), 1120–1134.

Han, S. (1976), 'Superlinearly convergent variable metric algorithms for general nonlinear programming problems', *Mathematical Programming* **11**, 263–282.

Hansen, P., Mladenovic, N. & Perez, J. A. M. (2009), 'Variable neighbourhood search: methods and applications', *Annals of Operations Research* **175**, 367–407.

Hasançebi, O., Çarbas, S., Dogăn, E., Erdal, F. & Saka, M. (2010), 'Comparison of non-deterministic search techniques in the optimum design of real size steel frames', *Computers and Structures* **88**, 1033–1048.

Hirota, M. & Kanno, Y. (2015), 'Optimal design of periodic frame structures with negative thermal expansion via mixed integer programming', *Optimization and Engineering* **16**, 767–809.

Holland, J. (1975), *Adaptation in Natural and Artificial Systems*, University of Michigan Press.

IBM (2018), *Cplex cp optimizer*.

Iso-Mustajärvi, P. & Inha, T. (1999), *Fire protection of load bearing structures (Kantavien rakenteiden palosuojaus)*, Rakennustieto. In Finnish.

Jalkanen, J. (2007), Tubular Truss Optimization Using Heuristic Algorithms, Phd thesis, Tampere University of Technology.

Jármai, K. & Farkas, J. (1999), 'Cost calculation and optimisation of welded steel structures', *Journal of Constructional Steel Research* **50**, 115–135.

Jármai, K. & Farkas, J. (2001), 'Optimum cost design of welded box beams with longitudinal stiffeners using advanced backtrack method', *Structural and Multidisciplinary Optimization* **21**, 52–59.

Kaveh, A. & Talahatari, S. (2009), 'A particle swarm ant colony optimization for truss structures with discrete variables', *Journal of Constructional Steel Research* **65**, 1558–1568.

Kennedy, J. & Eberhart, R. (1995), Particle swarm optimization, *in* 'IEEE International Conference on Neural Networks, Vol. 4', pp. 1942–1948.

Kirsch, U. (1993), *Structural optimization*, Springer-Verlag.

Kociecki, M. & Adeli, H. (2005), 'Review of formulations for structural and mechanical system optimization', *Structural and Multidisclipinary Optimization* **30**, 251–272.

Kureta, R. & Kanno, Y. (2014), 'A mixed integer programming approach to designing periodic frame structures with negative poisson's ratio', *Optimization and Engineering* **15**, 773–800.

Land, A. H. & Doig, A. (1960), 'An automated method of solving discrete programming problems', *Econometrica* **28**, 497–520.

Le Riche, R. & Haftka, R. (2012), 'On global optimization articles in smo', *Structural and multidisclipinary optimization* **46**(5), 627–629.

Li, L., Huang, Z. & Liu, F. (2009), 'A heuristic particle swarm optimization method for truss structures with discrete variables', *Computers and Structures* **87**, 435–443.

Mageirou, G. E. & Gantes, C. J. (2006), 'Buckling strength of multi-story sway, non-sway and partially-sway frames with semi-rigid connections', *Journal of Constructional Steel Research* **62**(9), 893 – 905.
URL: *http://www.sciencedirect.com/science/article/pii/S0143974X05002087*

Mela, K. (2013), Mixed Variable Formulations for Truss Topology Optimization, Phd thesis, Tampere University of Technology.

Mela, K. (2014), 'Resolving issues with member buckling in truss topology optimization using a mixed variable approach', *Structural and Multidisclipinary Optimization* **50**, 1037–1049.

Mela, K., Alinikula, M., Tiainen, T., Heinisuo, M. & Sorsa, I. (2015), Suunnittelutyökalu putkiristikoiden mitoitukseen ja optimointiin (Design tool for dimensioning and optimization of tubular trusses), *in* R. Kouhia, J. Mäkinen, S. Pajunen & T. Saksala, eds, 'Proceedings of the XII Finnish mechanics days', Finland, pp. 136–141. In Finnish.

Mela, K. & Heinisuo, M. (2017), Mixed variable approach for topology optimization of roof trusses, *in* 'WCSMO-12', Braunschweig, Germany.

Mellaert, R. V., Lombaert, G. & Schevenels, M. (2016), 'Global size optimization of statically determinate trusses considering displacement, member, and joint constraints', *Journal of Structural Engineering* **142**, 04015120.

Michell, A. (1904), 'The limits of economy of material in frame-structures.', *The London, Edinburgh, and Dublin Philosophical magazine and journal of science* **8**, 589–597.

Mladenovic, N. & Hansen, P. (1997), 'Variable neighborhood search', *Computers & Operations Research* **24**, 1097–1100.

Moses, F. & Onoda, S. (1969), 'Minimum weight design of structures with application to elastic grillages', *International Journal of numerical methods in engineering* **1**, 311–331.

Nethercot, D. A. (1998), 'Towards a standardization of the design and detailing of connections', *Journal of constructional Steel Research* **46**, 3–4.

Nocedal, J. & Wright, S. J. (2006*a*), *Numerical optimization*, Springer. second edition.

Nocedal, J. & Wright, S. J. (2006*b*), *Numerical Optimization*, Springer.

Ongelin, P. & Valkonen, I. (2016), *Structural Hollow Sections*, SSAB.

Padberg, M. & Rinaldi, G. (1987), 'Optimization of a 532-city symmetric traveling salesman problem by branch and cut', *Operations research letters* **6**(1), 1–7.

Padberg, M. & Rinaldi, G. (1991), 'A branch and cut algorithm for the resolution of large-scale symmetric traveling salesman problems', *SIAM Review* **33**(1), 60–100.

Patnaik, S. N., Gendy, A. S., Berke, L. & Hopkins, D. A. (1998), 'Modified fully utilized design (mfud) method for stress and displacement constraints', *International Journal for Numerical Methods in Engineering* **41**, 1171–1194.

Pavlovčič, L., Krajnc, A. & Beg, D. (2004), 'Cost function analysis in the structural optimization of steel frames', *Structural and Multidisciplinary Optimization* **28**, 286–295.

Razani, R. (1965), 'Behavior of fully-stressed design of structures and its relationship to minimum-weight design.', *AIAA J* **3**, 2262–2268.

Sadollah, A., Bahreininejad, A., Eskandar, H. & Hamdi, M. (2012), 'Mine blast algorithm for optimization of truss structures with discrete variables', *Computers and Structures* **102–103**, 49–63.

Saka, M. & Kameshki, E. (1998), 'Optimum design of unbraced rigid frames', *Computers and Structures* **69**, 433–442.

Salokangas, J. (2009), *Costs in steel construction (Teräsrakentamisen kustannukset)*, Teräsrakenneyhdistys. In Finnish.

Sargent, R. (1997), The development of the sqp algorithm for nonlinear programming, *in* L. T. Biegler, T. F. Coleman, A. R. Conn & F. N. Santosa, eds, 'Large-Scale Optimization with Applications. Part II: Optimal Design and Control', Springer–Verlag, pp. 1–19.

Sarma, K. C. & Adeli, H. (2000), 'Cost optimization of steel structures', *Engineering Optimization* **32**, 777–802.

Schevenels, M., McGinn, S., Rolvink, A. & Coenders, J. (2014), 'An optimality criteria based method for discrete design optimization taking into account buildability constraints', *Structural and multidisclipinary optimization* **50**, 755–774.

Schittkowski, K. (1983), 'On the convergence of a sequential quadratic programming method with an augmented lagrangian line search function', *Mathematische Operationsforschung und statistik* **14**, 197–216.

Snijder, H., Boel, H., Hoenderkamp, J. & Spoorenberg, R. (2011), Buckling length factors for welded lattice girders with hollow section braces and chords, *in* 'Eurosteel 2011', Budapest, Hungary.

Stolpe, M. (2007), 'On the reformulation of topology optimization as linear or convex quadratic mixed 0-1 programs', *Optimization and Engineering* **8**, 163–192.

Stolpe, M. (2011), 'To bee or not to bee—comments on "discrete optimum design of truss structures using artificial bee colony algorithm"', *Structural and Multidisciplinary Optimization* **44**(5), 707–711.
URL: *http://dx.doi.org/10.1007/s00158-011-0639-6*

Stolpe, M. (2016), 'Truss optimization with discrete design variables: a critical review', *Structural and multi-disclipinary optimization* **53**, 349–374.

Svanberg, K. (1984), On local and global minima in structural optimization, *in* E. Atrek, R. H. Gallagher, K. M. Ragsdell & O. C. Zienkiewicz, eds, 'New Directions in Optimum Structural Design', John Wiley & Sons Ltd, pp. 327–341.

Tiainen, T., Mela, K. & Heinisuo, M. (2018), Buckling length in mixed-integer linear frame optimization, *in* A. Schumacher, T. Vietor, S. Fiebig, K. Bletzinger & K. Maute, eds, 'Advances in Structural and Multidisciplinary Optimization Proceedings of the 12th World Congress of Structural and Multidisciplinary Optimization (WCSMO12)', Springer–Verlag, pp. 1923–1936.

Watson, K. B., Dallas, S., Van der Kreek, N. & Main, T. (1996), 'Costing of steelwork from feasibility through to completion', *Journal of Australian Steel Construction* **30**, 2–9.

Webber, A., Orr, J., Shepherd, P. & Crothers, K. (2015), 'The effective length of columns in multi-storey frames', *Engineering Structures* **102**, 132–143.

Wolsey, L. A. (1998), *Integer Programming*, John Wiley & Sons.

Yates, D., Templeman, A. & Boffey, T. (1982), 'The complexity of procedures for determining minimum weight trusses with discrete member sizes', *International Journal of Solids and Structures* **18**, 487–495.

Zoutendijk, G. (1960), *Methods of feasible directions*, Elsevier.

6 Original publications

Original publications reprinted on kind permission of the respective rightholders. They are reprinted as published. The errors found by the author are listed in Section 6.1.

Publication I

Title: Optimization of tubular trusses using intumescent in fire
Authors: Timo Jokinen, Kristo Mela, Teemu Tiainen and Markku Heinisuo
Journal: Rakenteiden Mekaniikka (Journal of Structural Mechanics)
Volume: 49
Issue: 4
Pages: 160–175

Print permission based on CC BY-SA 4.0 license.

Original available at `http://rmseura.tkk.fi/rmlehti/2016/nro4/RakMek_49_4_2016_1.pdf`

Rakenteiden Mekaniikka (Journal of Structural Mechanics)
Vol. 49, No 4, 2016, pp. 160 – 175
rmseura.tkk.fi/rmlehti/
©The authors 2016.
Open access under CC BY-SA 4.0 license.

VERTAISARVIOITU
KOLLEGIALT GRANSKAD
PEER-REVIEWED
www.tsv.fi/tunnus

Optimization of tubular trusses using intumescent coating in fire

Timo Jokinen, Kristo Mela, Teemu Tiainen[1] and Markku Heinisuo

Summary. In steel structures, the cost of fire protection can be significant. They are typically designed to resist loads at room temperature after which the fire protection is considered. This widely used approach may result in expensive and unpractical solutions. On the other hand, automatic design systems utilizing optimization allow taking fire design aspects into account simultaneously. In this research, these two approaches are compared in a tubular roof truss case where intumescent coating is used as fire protection. The results show clearly the benefits of combined structural and fire engineering design. Design with Finnish national and ETA approvals of intumescent coating are compared for 30 and 60 minutes resistance to standard fire. It is shown, that ETA-approved rules indicate increased costs to tubular structures for 60 minutes fire. For 30 minutes the difference between the two approval systems were less significant.

Key words: tubular steel truss, optimization, fire, intumescent coating

Received 9 September 2016. Accepted 4 December 2016. Published online 30 December 2016

Introduction

Tubular welded trusses are widely used in buildings due to their aesthetically pleasing appearance, good load bearing capacity and cost effectiveness. An essential property of a truss is its fire resistance, because all buildings have to fulfill local fire regulations. The fire scenario is defined for each given project, and typically either ISO-834 fire or natural fire is employed. The resistance of the structure in fire can be accomplished without any additional protection, or by using either passive or active fire protection. These approaches can also be combined such that appropriate structural performance in fire is achieved by increasing the member sizes as well as applying fire protection. As different methods for attaining a suitable fire resistance are available, the designer is faced with the task of finding the most economical approach for the structure at hand.

The purpose of the present study is to assess the economy of welded single span tubular roof trusses under ISO-834 fire when intumescent paint is employed as fire protection (Fig. 1). Two design approaches are compared. The first approach emulates a "conventional" engineering practice, where the truss is first designed in room temperature and the required paint thickness in fire conditions is determined in a second design phase. In the second approach, member sizing and determination of paint thickness are performed

[1]Corresponding author. teemu.tiainen@tut.fi

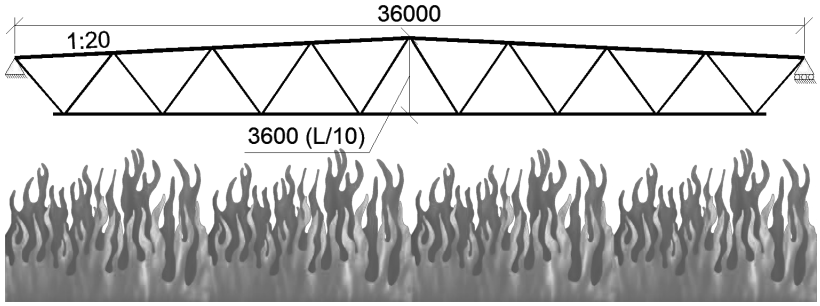

Figure 1. Considered case.

simultaneously such that the total cost of the truss is minimized. This more advanced approach relies on iterative optimization methods as finding the minimum cost design requires a compromise between minimizing the member sizes and minimizing the amount of paint.

The design of trusses is governed by the Eurocode EN 1993. For fire design, EN 1993-1-2 [5] is employed. The standard enables the use of various approaches for showing sufficient structural safety in fire conditions. In this study, the method of the critical temperature is adopted. The idea is to determine the (critical) temperature at which the structure collapses under the loads of fire situation. The paint producers provide tables that give the required intumescent coating thickness for given critical temperature at and cross-section section factor at specific time.

The method for the intumescent design in Finland is moving from nationally approved certified product declarations from the Finnish Constructional Steelwork Association (FCSA) to European Technical Approval (ETA) specifications. This affects the testing method and ultimately the required fire paint thickness. In this study, the ETA approved intumescent FIRETEX FX2002 is used [14]. This is compared with the older FIRETEX FX2000 which is approved by FCSA [2] in R30-R60 (valid until June 1st 2016). Requirements R30 and R60 mean that structure is supposed to withstand loads for 30 and 60 minutes, respectively, after the beginning of fire. As the range of validity and the thickness of the intumescent coating is different for the two approvals, it is interesting to examine the influence of the newer ETA system on the total cost of the truss, compared with the older FCSA approval. This comparison is included in the present study.

For minimizing the cost of the truss, the costs of the different fabrication phases need to be evaluated. Several methods for estimating the fabrication costs of steel structures have been presented in the literature [20, 11, 17, 15, 13, 7]. In this study, a feature-based costing method [8] adopted. The cost of material, blasting, sawing, welding, painting and intumescent painting are included in the cost function. The unit costs and fabrication times are estimated based on discussions with local workshops.

In order to minimize the costs, the truss design task must be formulated as a mathematical programming problem with clearly defined design variables, objective and constraints functions. The cost minimization problem of tubular trusses in fire conditions according to the Eurocode leads to a nonlinear discrete optimization problem where some of the functions are known only implicitly with respect to the design variables. For such problems, the variety of applicable solution methods is rather limited. In this study, a meta-heuristic population-based Particle Swarm Optimization (PSO) method is employed. This method has been found reliable for discrete truss optimization in previous

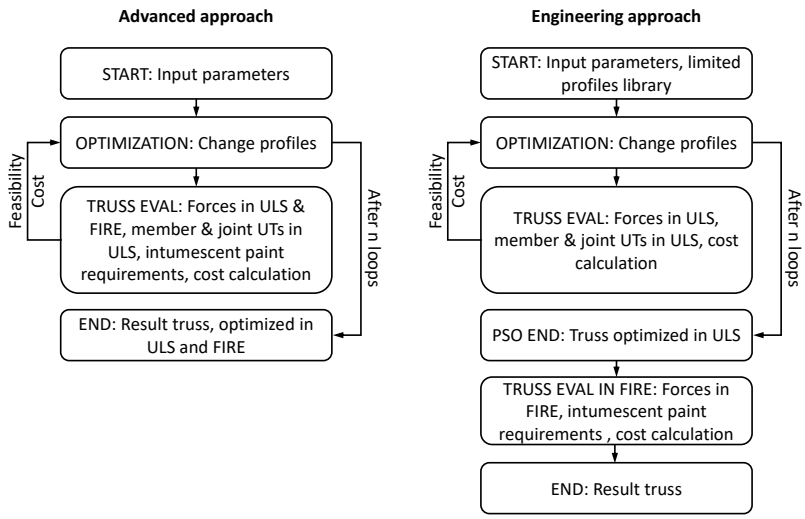

Figure 2. Advanced approach and engineering approach for truss design in fire conditions.

research [10].

The paper is organized as follows. Firstly, the two approaches for truss design in fire conditions considered in this study are described. Then, the cost optimization problem is presented, including details of structural modelling and design according to the Eurocode. The results of optimization are treated in detail, and finally, the implications of the study are discussed.

Tubular truss design in fire conditions

Designing trusses for fire safety using intumescent coating involves determining the member profiles and the thickness of the coating. The required amount of the fire paint depends on the dimensions of the cross-section. For tubular profiles, the key factor is the wall thickness, i.e. for thicker profiles, less paint is required. Consequently, the minimum cost design is a compromise between reducing the member sizes and the amount of intumescent paint. In general, this is not a simple task to be solved relying only on experience and engineering skills.

In this study, two approaches for truss design in fire conditions are considered. The first approach emulates a conventional engineering process, whereas in the second the cost minimization task is treated more comprehensively. In both approaches, the design is governed by the Eurocodes EN 1993-1-1 [4], EN 1993-1-8 [6] for members and joints in ambient conditions, and EN 1993-1-2 [5] for fire design. In this study, the recommended values of all parameters are used, i.e. no national annexes are employed.

The two approaches are schematically illustrated in Fig. 2.

Engineering approach

A typical design procedure is to first design the truss in ambient conditions (room temperature), and then to determine the required fire paint thickness for the obtained member profiles.

The design of the truss in ambient conditions is carried out by applying an optimization procedure. This emulates a seasoned engineer, who conventionally tries to find the most economical solution based on experience and judgment.

Advanced approach

It is clear the the engineering approach might lead to relatively thick intumescent coating, because the member profiles are made a small as possible in ambient conditions. In order to obtain more economical solution, sizing of the member profiles should be coupled with the determination of the coating thickness. The method of critical temperature is employed along with manufacturer's tables for finding the required intumescent paint thickness.

The minimum cost design is determined using a similar optimization procedure as for the engineering approach. The main difference is that now the cost of the intumescent paint is included in the cost function, whereas for the engineering approach, the cost of the paint is calculated only after the optimization has been terminated.

Cost minimization

Both approaches to truss design in fire conditions rely on optimization. Consequently, the truss design task must be formulated as an optimization problem, which includes the definition of design variables, objective function and constraints. This is described in the following along with details on structural modelling and fire design according to the Eurocode.

Structural modelling and design

For evaluating the performance of the truss in elevated temperature, structural analysis in fire conditions must be performed. The truss considered in this study is globally statically determinate truss of Fig. 1. Due to the structural analysis model used in this study the truss is internally statically indeterminate, but is has been shown that when the global support conditions are statically determinate, linear analysis predicts rather well the ultimate situation of the truss in fire [1]. This is especially true when dealing with the stress resultants of the truss.

The resistance of members and joints is verified in the Ultimate Limit State (ULS) in fire. The deflections are handled with pre-cambering, and they are not included in the analysis. The height of truss is $L/10$ ($L = 36\,\mathrm{m}$ is the span) at mid-span and it is measured from the bottom of the bottom chord to the top of the top chord. The slope of the top chord is 1:20. The truss consists of K-joints, with the gap of 50 mm at each joint. The joints are located evenly at the chords.

The design load in ambient conditions is a uniform load 23.5 kN/m at the top chord and in fire conditions the load is approximated as $0.4 \cdot 23.5\,\mathrm{kN/m}$.

The gaps and profile dimensions induce eccentricities at the joints, which cause secondary bending moments in the members. This is taken into account by introducing rigid eccentricity elements at the joints (Fig. 3). An eccentricity element is created between the mid-line of the chord and the intersection of the mid-lines of the connecting braces such that the element is perpendicular to the chord. The location of the nodes of the eccentricity element is calculated from the member profile dimensions, gap size and angles of the braces. Such structural model based on the accurate geometry is an important feature for

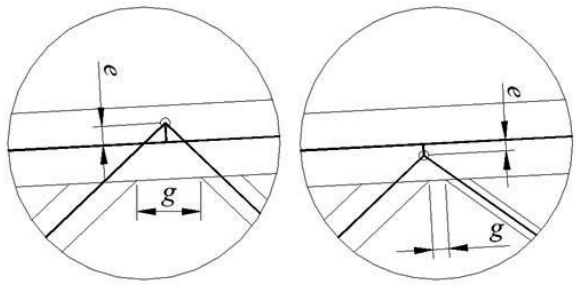

Figure 3. Local structural models of K-joints following EN 1993-1-8.

structural analysis and optimization according to the Eurocode, when the joint design is included in the procedure, because the details of the joints have an impact on the global structural model and therefore on the internal forces of the members.

The chords are modelled as continuous beams and diagonals are hinged at both ends. Euler-Bernoulli beam elements are used for the members and for the local models of the joints [10]. The buckling length of each member is 0.9 times the system length, which is defined as in [3], see also [9].

Fire design of members is performed using the method of critical temperatures of EN 1993-1-2 and calculating the minimum required intumescent thickness for each member. For compressed members the critical temperature is dependent on the elastic modulus temperature reduction in addition to yield strength reduction. This means that the critical temperature method is not directly applicable for compressed members, unless some iteration is performed. Three iterations for each compressed member proved to be sufficient to get the critical temperatures within 1°C accuracy.

The critical temperature $\theta_{\mathrm{a,cr}}$ (°C) is calculated as

$$\theta_{\mathrm{a,cr}} = 39.19 \cdot \ln\left(\frac{1}{0.9674\mu_0^{3.833}} - 1\right) + 482, \quad \mu_0 \geq 0.013 \tag{1}$$

where μ_0 is the degree of utilization of the member in fire. When the μ_0 of the member is known the critical temperature of the member can be calculated using Eq. (1). For square tubes the section factor value $A/V \approx 1/t$ can be used (see EN 1993-1-2). In this expression t is the wall thickness of the tube in meters. When the critical temperature $\theta_{\mathrm{a,cr}}$ and the section factor A/V are known the required intumescent cover thickness is retrieved from the tables of the coating fabricators.

The method for the intumescent design in Finland is moving from nationally approved certified product declarations from the Finnish Constructional Steelwork Association (FCSA) to European Technical Approval (ETA) specifications. This affects the testing method and ultimately the required fire paint thickness. In this study, the ETA approved intumescent FIRETEX FX2002 is used [14]. This is compared with the older FIRETEX FX2000 which is approved by FCSA [2] in R30-R60 (valid until June 1st 2016). Different calculation methods are employed for ETA and for FCSA. The ETA gives tables for paint thicknesses when critical temperatures are known and FCSA gives formulas for temperatures when the paint thickness is known. For a straightforward comparison, the intumescent coating thickness tables are calculated also for the FCSA tables using the same system as for the ETA, see Table 10 and Table 11. Neither FCSA product declarations nor ETA specifications give separate rules for profiles in tension, thus values for

columns are used for all truss members. The paint thickness tables have values up to 5 mm, but in reality over 2 mm paint thicknesses often pose difficulties to transportation and installation. However, these practical limitations are not considered here.

If Table 10 and Table 11 are compared with the corresponding tables for FIRETEX FX2002 [14], it can be seen that the FCSA-approved values are valid for a wider range of section factors and temperatures. With lower critical temperatures or higher section factors the ETA produces significantly greater paint thicknesses. Alternatively, when the critical temperature is high and the section factor relatively low, the difference is quite small. For example, consider a tube with 8 mm wall thickness ($A/V \approx 125$) with 650 °C critical temperature in R60 fire. The required intumescent paint thickness is 0.986 mm with FCSA and 1.208 mm with ETA. For 5 mm wall thickness ($A/V \approx 200$), the corresponding values are 1.578 mm and 3.290 mm, respectively. These significant differences in required paint thicknesses probably originate from different paint testing methods used by FCSA and ETA, but the exact reasons have not yet been fully explored.

The method of the critical temperature is also applied to joint design in fire. The geometrical requirements for the joints are the same for ambient and fire conditions. The resistance checks of welded tubular K-joints includes checks for 7 failure modes with axial loads of the braces (Figure 7.3 of EN 1993-1-8): chord face failure, chord side wall failure, chord shear failure, punching shear failure, brace failure, local buckling of the brace, and local buckling of the chord. The resistance of the joint with respect to each failure mode is expressed as the allowable member axial force.

Denote by $N_{i,Ed}$ and $N_{i,Rd}$ the axial force and the resistance of brace i in ambient conditions, respectively. As linear structural analysis is performed, the axial force in fire conditions is $N_{i,Ed,t_0} = 0.40 N_{i,Ed}$. The resistance N_{i,Rd,t_0} is calculated at $t = 0$ for each member of the joint using the limiting failure mode acting on that member. The utilization ratios $\mu_0 = N_{i,Ed,t_0}/N_{i,Rd,t_0}$ can be then calculated for each member. The process is very much similar as in normal member fire design.

In this study, the gas temperature follows the ISO-834 standard curve. It is recognized by the authors that this choice places rather strict requirement for the structures. Switching to natural fire design could often produce much more economical structures regardless of the design approach used. However, as the scope of this paper is to compare the two design approaches rather than to find the most realistic fire scenario, the widely used ISO-834 curve is adopted.

Optimization

Sizing of the truss members is carried out by an optimization procedure, which requires a careful definition the corresponding optimization problem. In this study, the member profiles are taken as the discrete design variables. The profile catalogue is shown in Table 1. It consists of cold-formed square tubes fabricated by SSAB [18]. The objective is the fabrication cost of the truss, and the constraints are derived from EN 1993.

The fabrication costs include material, blasting, sawing, welding, painting and costs of the intumescent paint. The material cost for S420 steel is 1 €/kg, and the cost of the intumescent paint is 40 €/m^2 per 1 mm coating thickness. If the thickness of the coating is smaller or larger than 1 mm then the linear extrapolation is used. The amount of steel and the surface area to be painted are calculated using the exact geometrical form of the truss. Blasting, sawing and welding costs are calculated by a featured-based costing method [8].

Table 1. Catalogue of square hollow sections. The tube dimensions are given in form $h \times t$, where h is the outer dimension (width or height) in millimeters and t is the wall thickness in millimeters.

25x3	70x4	100x5	140x6	180x8
30x3	70x5	100x6	140x8	180x10
40x3	80x3	100x8	150x5	200x8
40x4	80x4	110x4	150x6	200x10
50x3	80x5	110x5	150x8	200x12.5
50x4	80x6	120x4	150x10	250x6
50x5	90x3	120x5	150x12.5	250x8
60x3	90x4	120x6	160x6	250x10
60x4	90x5	120x8	160x8	250x12.5
60x5	90x6	120x10	160x10	300x10
70x3	100x4	140x5	180x6	300x12.5

The numerical values of the different cost factors are very much dependent on the country, contractor and other issues. However, in order to compare different solutions these values must be estimated. In this study the costs mentioned above have been obtained from discussions with contractors in Finland. Transport and erection costs on site are not taken into account in this analysis, because they do not play an important role in this comparison. In the engineering approach the cost of the intumescent paint is not included in the objective function. The cost of fire protection is added to the other fabrication costs of the truss after optimization.

The constraints are derived from the Eurocodes. For members this implies axial force, shear force and bending moment resistances in ambient conditions. Flexural buckling and beam-column behaviour of compression members are taken into account using EN 1993-1-1, Method B. The corresponding resistances are also verified in fire conditions using EN 1993-1-2.

The K-joints (not at support and at the ridge) are checked in ambient conditions according to EN 1993-1-8 and in fire by EN 1993-1-2. The joint constraints include the joint resistance checks and the geometrical conditions which define the range of applicability of the resistance rules. Full strength welds are used at the joints. This implies that for S420 members, the weld size is $1.4t$ where t is the wall thickness of the connected brace. In fire condition the resistance of the welds is not considered. The details of the optimization problem can be found in [19].

Sizing optimization is performed using the metaheuristic Particle Swarm Optimization (PSO) method. PSO cannot guarantee the optimality of the solution, but with sufficiently large swarm size and using proper parameters, satisfactory results can be obtained. The details of PSO can be found in [12] and the applied constraint handling mechanism is described in [16]. The algorithm is run with the following key parameters: population size 250, iterations 120, number of runs 40.

In the engineering approach the truss is optimized in ambient conditions. To exclude impractically thin profiles for fire design, the minimum wall thickness of 5 mm is prescribed. This limitation is not needed in advanced approach due to the more holistic nature of the method.

After optimization, the required intumescent thicknesses are calculated using the critical temperatures for the members and for the joints. If the critical temperature and section factor combination is outside the range of the intumescent paint, the thickness

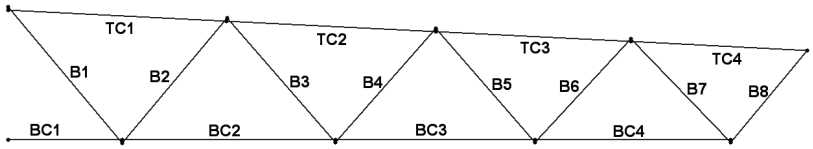

Figure 4. Member labels.

Table 2. Results of optimization. Best found member profiles. The member labels correspond to Fig. 4. TC and BC refer to top and bottom chords, respectively.

Method	Engineering				Advanced			
Paint	ETA		FCSA		ETA		FCSA	
Fire	R30	R60	R30	R60	R30	R60	R30	R60
TC	180x10	180x10	180x10	180x10	180x10	180x10	180x10	180x10
BC	120x8	120x8	120x8	120x8	120x8	150x10	120x8	120x10
B1	50x5	50x5	50x5	50x5	50x3	80x6	80x4	50x4
B2	70x5	70x5	70x5	70x5	70x3	80x6	70x4	80x4
B3	90x5	90x5	90x5	90x5	110x4	120x6	90x5	80x6
B4	70x5	70x5	70x5	70x5	80x3	100x6	70x4	70x5
B5	100x5	100x6	100x5	100x5	100x5	150x6	100x5	100x6
B6	70x5	70x5	70x5	70x5	70x4	100x6	70x4	80x6
B7	120x5	120x6	120x5	120x5	120x5	140x8	120x5	120x6
B8	90x5	90x5	90x5	90x5	90x4	120x6	90x6	80x6

of the member is increased for the next possible. Altogether four different intumescent coating thicknesses are allowed in the truss: one for the top chord, one for the bottom chord and two for the braces. This reflects the fact that at employing individual coating thicknesses at the workshop is time-consuming and prone to errors. In the engineering approach the grouping of the braces is done after the intumescent coating thickness is defined to all members separately. In the advanced approach this sorting is done during the optimization.

Results

The member profiles obtained by PSO are listed in Table 2 for different fire cases and for the two approaches described above. As can be expected, the profiles obtained by the engineering approach are nearly identical in all four cases. Only the braces B5 and B7 needed to be changed in R60 fire using ETA. In the advanced approach the member sizes vary considerably depending on the case. Only the top chord profile remains constant among the different cases.

The fire paint thicknesses for the optimized designs are shown in Table 3. For R30, the paint thicknesses are nearly identical for both approaches and ETA and FCSA tables. On the other hand, for R60, substantial differences can be observed. Using the advanced approach clearly leads to thinner coating, especially when ETA approval is adopted. For example, using the ETA approval, the engineering approach leads to paint thickness of 1.949 mm for the bottom chord, whereas only 0.506 mm layer is required when the advanced approach is utilized. Similar ratio applies for the braces as well, but for the

Table 3. Fire paint thicknesses (mm).

Method	Engineering				Advanced			
Paint	ETA		FCSA		ETA		FCSA	
Fire	R30	R60	R30	R60	R30	R60	R30	R60
Top Chord	0.462	0.980	0.325	0.885	0.462	0.987	0.325	0.885
Bottom Chord	0.462	1.949	0.427	1.166	0.462	0.506	0.427	0.879
B1	0.462	2.846	0.500	1.494	0.462	1.062	0.435	1.091
B2	0.462	2.846	0.500	1.494	0.462	1.062	0.435	1.091
B3	0.462	3.813	0.742	1.968	0.462	0.768	0.742	1.584
B4	0.462	2.846	0.500	1.494	0.462	0.768	0.435	1.091
B5	0.522	3.813	0.742	1.968	0.523	0.768	0.742	1.584
B6	0.522	2.846	0.500	1.494	0.523	0.768	0.742	1.091
B7	0.522	3.813	0.742	1.968	0.523	1.062	0.742	1.584
B8	0.522	3.813	0.742	1.968	0.523	1.062	0.435	1.584

Table 4. Minimum costs, the corresponding weights and costs distributions.

Method	Engineering				Advanced			
Paint	ETA		FCSA		ETA		FCSA	
Fire	R30	R60	R30	R60	R30	R60	R30	R60
Weight (kg)	1651	1670	1651	1651	1607	2105	1650	1764
Cost (€)	2569	4273	2543	3411	2499	3746	2534	3327
Material	1651	1670	1651	1651	1607	2105	1650	1764
Welding	146	165	146	146	108	297	139	176
Sawing	97	98	97	97	97	103	97	97
Blasting	22	22	22	22	22	22	22	22
Painting	128	127	128	128	130	147	130	127
Fire Paint	525	2191	499	1367	535	1071	496	1140

top chord, the paint thickness is virtually identical for both approaches. When the paint thickness is determined according to FCSA, the difference between the two approaches is smaller. The engineering approach leads to 25–36% greater paint thickness, except for the top chord.

The costs and weights of the obtained designs are given in Table 4. The advanced approach leads to slightly more economical designs with ETA in R30 and FCSA in R60. There is practically no difference in cost using FCSA in R30. However, in R60 with ETA, the advanced approach gives 12 % from the solution obtained by the engineering approach. Note that in this case, the weight of the more economical solution is 26% greater than the weight of the less economical design.

The cost distributions of the solutions, shown in Table 4, illustrate the fact that in R60 the cost of the intumescent coating can be as great as (or greater than) the cost of steel when engineering approach is employed. Using the advanced approach the cost of the fire paint is always smaller than the material cost. Note that with the adopted unit costs, the cost of fire paint is greater than the other fabrication costs combined.

Table 5. Utilities of members with respect to the resistances.

Method	Engineering				Advanced			
Paint	ETA		FCSA		ETA		FCSA	
Fire	R30	R60	R30	R60	R30	R60	R30	R60
B1	0.01	0.01	0.01	0.01	0.01	0	0	0.01
B2	0.01	0.01	0.01	0.01	0	0.01	0.01	0.01
B3	0.60	0.60	0.60	0.60	0.43	0.25	0.60	0.73
B4	0.26	0.26	0.26	0.26	0.36	0.15	0.32	0.26
B5	0.89	0.77	0.89	0.89	0.89	0.31	0.89	0.77
B6	0.58	0.58	0.58	0.58	0.70	0.33	0.70	0.42
B7	0.93	0.80	0.93	0.93	0.93	0.46	0.93	0.80
B8	0.71	0.71	0.71	0.71	0.86	0.44	0.60	0.69
TC1	0.85	0.85	0.85	0.85	0.85	0.85	0.85	0.85
TC2	0.82	0.81	0.82	0.82	0.81	0.82	0.82	0.81
TC3	0.64	0.63	0.64	0.64	0.63	0.63	0.63	0.63
TC4	0.41	0.41	0.41	0.41	0.41	0.41	0.41	0.41
BC1	0.80	0.80	0.80	0.80	0.79	0.52	0.80	0.66
BC2	0.87	0.87	0.87	0.87	0.89	0.56	0.87	0.72
BC3	0.72	0.72	0.72	0.72	0.73	0.49	0.72	0.61
BC4	0.99	0.99	0.99	0.99	0.99	0.59	0.99	0.80

In order to evaluate the performance of PSO in this problem the utilization ratios of members and joints with respect to the resistances are given in Table 5 and Table 6. The "utilities" with respect to the geometrical properties of the joints are given in Table 7, and the maximum utilization ratios for all members, including member and joint resistances and the geometrical "utilities" are given in Table 8. It can be seen, that very high utilization ratios (values near 1.00) are obtained in all cases, which implies excellent performance of the designs.

The sensitivity of the solutions with respect to the initial cost data is examined by re-optimizing the structures using the steel material cost 0.8 €/kg instead of 1.0 €/kg. The obtained costs and the corresponding weights are given in Table 9.

Table 6. Utilities of joints with respect to the resistance.

Method	Engineering				Advanced			
Paint	ETA		FCSA		ETA		FCSA	
Fire	R30	R60	R30	R60	R30	R60	R30	R60
B1-BC-B2	0.88	0.88	0.88	0.88	0.88	0.57	0.88	0.73
B2-TC-B3	0.46	0.46	0.46	0.46	0.46	0.46	0.46	0.46
B3-BC-B4	0.89	0.89	0.89	0.89	0.89	0.57	0.89	0.74
B4-TC-B5	0.58	0.59	0.58	0.58	0.53	0.44	0.58	0.6
B5-BC-B6	0.82	0.82	0.82	0.82	0.82	0.52	0.82	0.66
B6-TC-B7	0.81	0.81	0.81	0.81	0.81	0.58	0.82	0.75
B7-BC-B8	0.95	0.95	0.95	0.95	0.95	0.5	0.95	0.79

Table 7. "Utilities" of geometrical constraints at joints.

Method	Engineering				Advanced			
Paint	ETA		FCSA		ETA		FCSA	
Fire	R30	R60	R30	R60	R30	R60	R30	R60
B1-BC-B2	0.84	0.84	0.84	0.84	0.84	0.70	0.74	0.84
B2-TC-B3	1.00	1.00	1.00	1.00	0.90	0.90	1.00	1.00
B3-BC-B4	0.83	0.83	0.83	0.83	0.92	0.83	0.83	0.74
B4-TC-B5	0.95	0.95	0.95	0.95	0.90	0.83	0.95	0.95
B5-BC-B6	0.95	0.95	0.95	0.95	0.95	1.00	0.95	0.90
B6-TC-B7	0.90	0.90	0.90	0.90	0.90	0.78	0.90	0.80
B7-BC-B8	1.00	1.00	1.00	1.00	1.00	0.93	1.00	1.00

Table 8. Combined utilities.

Method	Engineering				Advanced			
Paint	ETA		FCSA		ETA		FCSA	
Fire	R30	R60	R30	R60	R30	R60	R30	R60
B1	0.88	0.88	0.88	0.88	0.88	0.70	0.88	0.84
B2	1.00	1.00	1.00	1.00	0.90	0.90	1.00	1.00
B3	1.00	1.00	1.00	1.00	0.92	0.90	1.00	1.00
B4	0.95	0.95	0.95	0.95	0.92	0.83	0.95	0.95
B5	0.95	0.95	0.95	0.95	0.95	1.00	0.95	0.95
B6	0.95	0.95	0.95	0.95	0.95	1.00	0.95	0.90
B7	1.00	1.00	1.00	1.00	1.00	0.93	1.00	1.00
B8	1.00	1.00	1.00	1.00	1.00	0.93	1.00	1.00
TC1	1.00	1.00	1.00	1.00	0.90	0.90	1.00	1.00
TC2	1.00	1.00	1.00	1.00	0.90	0.90	1.00	1.00
TC3	0.95	0.95	0.95	0.95	0.90	0.83	0.95	0.95
TC4	0.90	0.90	0.90	0.90	0.90	0.78	0.90	0.80
BC1	0.88	0.88	0.88	0.88	0.88	0.70	0.88	0.84
BC2	0.89	0.89	0.89	0.89	0.92	0.83	0.89	0.84
BC3	0.95	0.95	0.95	0.95	0.95	1.00	0.95	0.90
BC4	1.00	1.00	1.00	1.00	1.00	0.93	1.00	1.00

As the material unit cost is decreased, the advanced approach leads to greater savings than in the first scenario, where the unit cost of steel was 1.0 €/kg. Using ETA in R60, the advanced approach gives 23 % more economical design than the engineering approach. For the other cases, from 4 % to 8 % savings can be achieved by the advanced approach.

Conclusions

The findings of the present study indicate that the proposed "advanced approach" should be employed in fire design of tubular trusses in all cases. Especially when the fire resistance requirement is high traditional method of finding the least weight solution does not seem to produce the most economical solution. The single drawback of the advanced approach

Table 9. Costs and weights of optimal cases using the steel material cost 0.8 €/kg.

Method	Engineering				Advanced			
Paint	ETA		FCSA		ETA		FCSA	
Fire	R30	R60	R30	R60	R30	R60	R30	R60
Cost (€)	2317	4303	2292	3286	2197	3315	2210	3020
Weight (kg)	1630	1640	1630	1630	1619	1977	1643	1824

is that it requires unit costs for steel, intumescent paint and other fabrication phases. In order to provide the designer with the best possible tools for finding the most economical structures, the authors recommend that the workshops and steel producers make this data available. This can be done, for example, in a closed design software, that enables cost optimization but does not reveal all sensitive cost data.

In this study the particle swarm optimization method was employed, but the automated member sizing can be performed by other means as well, including sophisticated mathematical programming methods, and ad hoc engineering rules. The most important feature of advanced approach is the combined sizing and intumescent paint thickness determination which are done simultaneously in order to find the most economical designs.

Finally, it should be noted that it is the experience of the authors that the discrete optimization problem resulting from detailed structural modelling and constraints derived from the Eurocode is very difficult to solve, and possibly a combination of heuristic methods and mathematical programming algorithms leads to a suitable solution strategy.

Acknowledgements

Ruukki Construction Oy and FIMECC/MANU/Digimap are acknowledged for the financial support for this study.

References

[1] J.A. Diez Albero, T. Tiainen, K. Mela, and M. Heinisuo. Structural analysis of tubular trusses in fire. In E. Batista, P. Vellasco, and L. Lima, editors, *Tubular Structures XV*, Rio de Janeiro, Brazil, May 2015. Proceedings of the 15th international symposium on tubular structures.

[2] Finnish Constructional Steel Association. *Varmennettu Käyttöseloste TRY-107-2011: FIRETEX FX2000 -palosuojamaali putki- ja I-profiilien palosuojaukseen.* Finnish Constructional Steel Association, 2011. In Finnish.

[3] H. Boel. Buckling length factors of hollow section members in lattice girders. Master's thesis, Eindhoven University of Technology, 2010.

[4] EN 1993–1–1. *Eurocode 3: Design of Steel Structures. Part 1-1: General rules and rules for buildings.* CEN, 2005.

[5] EN 1993–1–2. *Eurocode 3: Design of Steel Structures. Part 1-2: General rules – Structural fire design.* CEN, 2005.

[6] EN 1993–1–8. *Eurocode 3: Design of Steel Structures. Part 1-8: Design of joints*. CEN, 2005.

[7] J. Farkas and K. Jármai, editors. *Optimum Design of Steel Structures*. Springer, 2013.

[8] J. Haapio. *Feature-Based Costing Method for Skeletal Steel Structures Based on the Process Approach*. PhD thesis, Tampere University of Technology, 2012.

[9] M. Heinisuo and Ä. Haakana. Buckling of members of welded tubular truss. In Markku Heinisuo and Jari Mäkinen, editors, *Proceedings of The 13th Nordic Steel Construction Conference (NSCC-2015)*, pages 23–25, Tampere, Finland, sep 2015.

[10] J. Jalkanen. *Tubular Truss Optimization Using Heuristic Algorithms*. PhD thesis, Tampere University of Technology, 2007.

[11] K. Jármai and J. Farkas. Cost calculation and optimisation of welded steel structures. *Journal of Constructional Steel Research*, 50:115–135, 1999. doi:10.1016/S0143-974X(98)00241-7.

[12] J. Kennedy and R. Eberhart. Particle swarm optimization. In *IEEE International Conference on Neural Networks*, pages 1942–1948, 1995.

[13] U. Klanšek and S. Kravanja. Cost estimation, optimization and competitiveness of different composite floor systems–part 1: Self-manufacturing cost estimation of composite and steel structures. *Journal of Constructional Steel Research*, 62:434–448, 2006. doi:10.1016/j.jcsr.2005.08.005.

[14] Warrington Certification LTD. *European technical approval ETA-12/0049: FIRETEX FX2002 and FIRETEX FX1002*. EOTA, Warrington, UK, 2013.

[15] L. Pavlovčič, A. Krajnc, and D. Beg. Cost function analysis in the structural optimization of steel frames. *Structural and Multidisciplinary Optimization*, 28:286–295, 2004. doi:10.1007/s00158-004-0430-z.

[16] G.T. Pulido and C.A.C. Coello. A constraint-handling mechanism for particle swarm optimization. In *Congress on Evolutionary Computation*, volume 2, pages 1396 – 1403, june 2004. doi:10.1109/CEC.2004.1331060.

[17] K. C. Sarma and H. Adeli. Cost optimization of steel structures. *Engineering Optimization*, 32:777–802, 2000. doi:10.1080/03052150008941321.

[18] SSAB. *Structural Hollow Section*, 2016. Dimensions and cross-sectional properties.

[19] T. Tiainen, K. Mela, and M. Heinisuo. High strength steel in tubular trusses. *Structures and Buildings*, 2016. Submitted.

[20] K.B. Watson, S. Dallas, N. Van der Kreek, and T. Main. Costing of steelwork from feasibility through to completion. *Journal of Australian Steel Construction*, 30(2):9, 1996.

Timo Jokinen
Palotekninen Insinööritoimisto Markku Kauriala Oy
Hermiankatu 6-8 D
FI-33720 Tampere
Finland
timo.jokinen@kauriala.fi

Kristo Mela, Teemu Tiainen, Markku Heinisuo
Tampere University of Technology
Department of Civil Engineering
P.O.Box 600
FI-33101 Tampere
Finland
kristo.mela@tut.fi teemu.tiainen@tut.fi
markku.heinisuo@tut.fi

Appendix: FIRETEX FX2000 coating thickness tables

The coating thickness values are calculated using procedure described in [2]. The unit system in the Tables is: Intumescent thickness [mm], Critical temperature T[°C], Section factor A/V [1/m].

Table 10. FIRETEX FX2000, RHS, R30.

A/V \ T	350	400	450	500	550	600	650	700	750	800	850
70	0.759	0.558	0.431	0.346	0.300	0.300	0.300	0.300	0.300	0.300	0.300
75	0.813	0.598	0.462	0.371	0.305	0.300	0.300	0.300	0.300	0.300	0.300
80	0.867	0.638	0.493	0.396	0.326	0.300	0.300	0.300	0.300	0.300	0.300
85	0.921	0.678	0.523	0.421	0.346	0.300	0.300	0.300	0.300	0.300	0.300
90	0.976	0.718	0.554	0.445	0.366	0.304	0.300	0.300	0.300	0.300	0.300
95	1.030	0.757	0.585	0.470	0.387	0.321	0.300	0.300	0.300	0.300	0.300
100	1.084	0.797	0.616	0.495	0.407	0.338	0.300	0.300	0.300	0.300	0.300
105	1.138	0.837	0.647	0.520	0.427	0.354	0.300	0.300	0.300	0.300	0.300
110	1.192	0.877	0.677	0.544	0.448	0.371	0.307	0.300	0.300	0.300	0.300
115	1.247	0.917	0.708	0.569	0.468	0.388	0.321	0.300	0.300	0.300	0.300
120	1.301	0.957	0.739	0.594	0.489	0.405	0.335	0.300	0.300	0.300	0.300
125	1.355	0.997	0.770	0.619	0.509	0.422	0.349	0.300	0.300	0.300	0.300
130	1.409	1.037	0.801	0.643	0.529	0.439	0.363	0.300	0.300	0.300	0.300
135	1.463	1.076	0.831	0.668	0.550	0.456	0.376	0.306	0.300	0.300	0.300
140	1.518	1.116	0.862	0.693	0.570	0.473	0.390	0.318	0.300	0.300	0.300
145	1.572	1.156	0.893	0.717	0.590	0.489	0.404	0.329	0.300	0.300	0.300
150	1.626	1.196	0.924	0.742	0.611	0.506	0.418	0.341	0.300	0.300	0.300
155	1.680	1.236	0.955	0.767	0.631	0.523	0.432	0.352	0.300	0.300	0.300
160	1.734	1.276	0.985	0.792	0.651	0.540	0.446	0.363	0.300	0.300	0.300
165	1.789	1.316	1.016	0.816	0.672	0.557	0.460	0.375	0.300	0.300	0.300
170	1.843	1.355	1.047	0.841	0.692	0.574	0.474	0.386	0.300	0.300	0.300
175	1.897	1.395	1.078	0.866	0.712	0.591	0.488	0.397	0.309	0.300	0.300
180	1.951	1.435	1.109	0.891	0.733	0.608	0.502	0.409	0.318	0.300	0.300
185	2.005	1.475	1.139	0.915	0.753	0.624	0.516	0.420	0.327	0.300	0.300
190	2.060	1.515	1.170	0.940	0.774	0.641	0.530	0.431	0.336	0.300	0.300
195	2.114	1.555	1.201	0.965	0.794	0.658	0.544	0.443	0.345	0.300	0.300
200	2.168	1.595	1.232	0.990	0.814	0.675	0.558	0.454	0.353	0.300	0.300
205	2.222	1.635	1.263	1.014	0.835	0.692	0.572	0.465	0.362	0.300	0.300
210	2.276	1.674	1.293	1.039	0.855	0.709	0.586	0.477	0.371	0.300	0.300
215	2.331	1.714	1.324	1.064	0.875	0.726	0.600	0.488	0.380	0.300	0.300
220	2.385	1.754	1.355	1.089	0.896	0.743	0.614	0.499	0.389	0.300	0.300
225	2.439	1.794	1.386	1.113	0.916	0.759	0.627	0.511	0.398	0.300	0.300
230	2.493	1.834	1.417	1.138	0.936	0.776	0.641	0.522	0.406	0.300	0.300
235	2.547	1.874	1.447	1.163	0.957	0.793	0.655	0.533	0.415	0.300	0.300
240	2.602	1.914	1.478	1.188	0.977	0.810	0.669	0.545	0.424	0.300	0.300
245	2.656	1.953	1.509	1.212	0.997	0.827	0.683	0.556	0.433	0.300	0.300
250	2.710	1.993	1.540	1.237	1.018	0.844	0.697	0.568	0.442	0.300	0.300
255	2.764	2.033	1.570	1.262	1.038	0.861	0.711	0.579	0.451	0.300	0.300
260	2.818	2.073	1.601	1.286	1.059	0.878	0.725	0.590	0.460	0.306	0.300
265	2.873	2.113	1.632	1.311	1.079	0.894	0.739	0.602	0.468	0.312	0.300
270	2.927	2.153	1.663	1.336	1.099	0.911	0.753	0.613	0.477	0.318	0.300
275	2.981	2.193	1.694	1.361	1.120	0.928	0.767	0.624	0.486	0.323	0.300
280		2.233	1.724	1.385	1.140	0.945	0.781	0.636	0.495	0.329	0.300
285		2.272	1.755	1.410	1.160	0.962	0.795	0.647	0.504	0.335	0.300
290		2.312	1.786	1.435	1.181	0.979	0.809	0.658	0.513	0.341	0.300
295		2.352	1.817	1.460	1.201	0.996	0.823	0.670	0.521	0.347	0.300
300		2.392	1.848	1.484	1.221	1.013	0.837	0.681	0.530	0.353	0.300

Table 11. FIRETEX FX2000, RHS, R60.

A/V \ T	350	400	450	500	550	600	650	700	750	800	850
70	1.465	1.187	0.993	0.847	0.730	0.634	0.552	0.479	0.409	0.339	0.300
75	1.569	1.272	1.064	0.908	0.782	0.679	0.592	0.513	0.438	0.363	0.300
80	1.674	1.357	1.135	0.968	0.835	0.725	0.631	0.547	0.467	0.387	0.305
85	1.778	1.442	1.206	1.029	0.887	0.770	0.671	0.581	0.496	0.412	0.324
90	1.883	1.526	1.277	1.089	0.939	0.815	0.710	0.616	0.526	0.436	0.343
95	1.988	1.611	1.348	1.150	0.991	0.861	0.750	0.650	0.555	0.460	0.362
100	2.092	1.696	1.419	1.210	1.043	0.906	0.789	0.684	0.584	0.484	0.381
105	2.197	1.781	1.490	1.271	1.095	0.951	0.829	0.718	0.613	0.509	0.400
110	2.302	1.866	1.561	1.331	1.148	0.997	0.868	0.753	0.642	0.533	0.419
115	2.406	1.950	1.632	1.392	1.200	1.042	0.907	0.787	0.672	0.557	0.439
120	2.511	2.035	1.703	1.452	1.252	1.087	0.947	0.821	0.701	0.581	0.458
125	2.615	2.120	1.774	1.513	1.304	1.132	0.986	0.855	0.730	0.605	0.477
130	2.720	2.205	1.845	1.573	1.356	1.178	1.026	0.889	0.759	0.630	0.496
135	2.825	2.290	1.916	1.634	1.408	1.223	1.065	0.924	0.788	0.654	0.515
140	2.929	2.374	1.987	1.694	1.461	1.268	1.105	0.958	0.818	0.678	0.534
145		2.459	2.058	1.755	1.513	1.314	1.144	0.992	0.847	0.702	0.553
150		2.544	2.129	1.815	1.565	1.359	1.184	1.026	0.876	0.726	0.572
155		2.629	2.200	1.876	1.617	1.404	1.223	1.060	0.905	0.751	0.591
160		2.713	2.271	1.936	1.669	1.450	1.263	1.095	0.934	0.775	0.610
165		2.798	2.342	1.997	1.721	1.495	1.302	1.129	0.964	0.799	0.629
170		2.883	2.413	2.057	1.774	1.540	1.341	1.163	0.993	0.823	0.648
175		2.968	2.484	2.118	1.826	1.585	1.381	1.197	1.022	0.848	0.667
180			2.555	2.178	1.878	1.631	1.420	1.231	1.051	0.872	0.686
185			2.626	2.239	1.930	1.676	1.460	1.266	1.081	0.896	0.705
190			2.697	2.299	1.982	1.721	1.499	1.300	1.110	0.920	0.724
195			2.768	2.360	2.034	1.767	1.539	1.334	1.139	0.944	0.744
200			2.839	2.420	2.087	1.812	1.578	1.368	1.168	0.969	0.763
205			2.910	2.481	2.139	1.857	1.618	1.402	1.197	0.993	0.782
210			2.981	2.541	2.191	1.903	1.657	1.437	1.227	1.017	0.801
215				2.602	2.243	1.948	1.697	1.471	1.256	1.041	0.820
220				2.662	2.295	1.993	1.736	1.505	1.285	1.065	0.839
225				2.723	2.347	2.038	1.775	1.539	1.314	1.090	0.858
230				2.784	2.399	2.084	1.815	1.573	1.343	1.114	0.877
235				2.844	2.452	2.129	1.854	1.608	1.373	1.138	0.896
240				2.905	2.504	2.174	1.894	1.642	1.402	1.162	0.915
245				2.965	2.556	2.220	1.933	1.676	1.431	1.187	0.934
250					2.608	2.265	1.973	1.710	1.460	1.211	0.953
255					2.660	2.310	2.012	1.744	1.489	1.235	0.972
260					2.712	2.356	2.052	1.779	1.519	1.259	0.991
265					2.765	2.401	2.091	1.813	1.548	1.283	1.010
270					2.817	2.446	2.131	1.847	1.577	1.308	1.029
275					2.869	2.491	2.170	1.881	1.606	1.332	1.049
280					2.921	2.537	2.209	1.915	1.635	1.356	1.068
285					2.973	2.582	2.249	1.950	1.665	1.380	1.087
290						2.627	2.288	1.984	1.694	1.404	1.106
295						2.673	2.328	2.018	1.723	1.429	1.125
300						2.718	2.367	2.052	1.752	1.453	1.144

Publication II

Title: The effect of steel grade on weight and cost of Warren-type welded tubular trusses
Authors: Teemu Tiainen, Timo Jokinen, Kristo Mela and Markku Heinisuo
Journal: Proceedings of the Institution of Civil Engineers - Structures and Buildings
Volume: 170
Issue: 11
Pages: 854 – 872

Accepted manuscript printed on kind permission from ICE publishing.

Original article available at https://doi.org/10.1680/jstbu.16.00112

The Effect of Steel Grade on Weight and Cost of Warren-Type Welded Tubular Trusses

Teemu Tiainen, Kristo Mela, Timo Jokinen, Markku Heinisuo

Abstract

In this paper, the effect of steel grade in weight and cost of Warren-type welded tubular roof trusses is considered. For unbiased comparison, best truss designs are obtained with optimization. Steel strength ranges from S355 to S960. Costs are calculated based on features of the trusses. The starting point is the exact geometry of the truss from which the finite element analysis model is derived. This approach allows the resistance and other requirements of design standards for both for the members and the joints to be included as constraints in the optimization problem. Design variables are the height of the truss, the locations of the joints, gap width at the joints and the member sections using a catalogue of cold-formed square tubes. Unlike with the optimization formulations found in the literature, the resulting design using this formulation is fully compliant with relevant standards without post-processing steps. In this case the Eurocode 3 standards were applied. The results of the comparison imply a significant saving in weight when using high strength steel. Cost reduction is smaller but existent. The results motivate the use and further research of high strength steels in building products.

1 Introduction

In contemporary automotive applications, high strength steels (HSS) are widely employed but in buildings the prevailing steel grade is S355. Progress in manufacturing technologies has made HSS readily available also for structural applications. Increased strength of the material implies lighter structures, which makes HSS appealing for the designer. However, the material and fabrication costs of HSS are still somewhat higher compared to milder steels. Moreover, certain rules of the Eurocodes impose tighter restrictions on HSS than on S355. For example, the bounds cross-section classes become tighter for HSS as the $\epsilon = \sqrt{235/f_y}$ becomes smaller for increasing yield strength.

Consequently, assessing the economic performance of HSS in relation to milder steels is not a straightforward task. Presumably the actual benefits of HSS depend on the application and in practice on the skills of the designer, and general statements on the matter are difficult to obtain. In this study, the performance of HSS in tubular roof trusses is evaluated. These structures are widely employed when longer spans are required and when precamber can be used to control deflections, the higher strength of the material can be utilised.

The approach of the study is to find minimum cost and minimum weight designs of typical roof trusses for different steel grades. The cost calculation is performed by a general feature-based costing method (Haapio 2012) that adopted for tubular trusses. This approach provides unbiased and quantified data on potential cost and weight savings of HSS compared to S355. In the literature the economical benefits of high strength steel have been presented for bridges (Günther 2005) and sports arenas (Cederfeldt & Sperle 2012). In these studies, the costs are approximated based on the structural weight and unit costs. The ecological benefits of HSS have also been treated (Stroetmann 2012).

Several researches have analysed the cost distribution of steel structures (Nethercot 1998, Carter, Murray & Thornton 2000, Evers & Maatje 2000, Salokangas 2009, Jalkanen 2007). Although

there is some variation in the figures, a general conclusion is that manufacturing cost plays an important role in the economy of steel structures. Therefore, the cost function used in optimisation should include the manufacturing costs. Various cost functions of varying degree of detail have been proposed in the literature (Watson, Dallas, Van der Kreek & Main 1996, Jármai & Farkas 1999, Sarma & Adeli 2000, Jármai & Farkas 2001, Farkas, Simões & Jármai 2005, Pavlovčič, Krajnc & Beg 2004). The feature-based costing method (Haapio 2012) employed in the present study aims at highly detailed expressions of all relevant factors contributing to the total cost of the structure. For tubular trusses, these factors include material, blasting, sawing, welding and painting. Transport and erecting of the truss could also be included, but as these costs are not essentially affected by the results of optimisation, they are omitted.

An essential part of the present study is formulating the tubular truss design task a mathematical optimisation problem to which suitable numerical methods can be applied. The problem formulation should reflect the actual design situation as accurately as possible, because if certain design aspects are omitted from optimisation, the results can be inapplicable in practice. This would distort the comparison of steel grades. In the present study, shape optimisation of the truss is considered, which means that in addition to optimal member profiles, also the optimal joint locations are determined. Member cross-sections are chosen from a catalogue of predefined alternatives. The constraints are derived from the Eurocode 3 (CEN 2006*a*, CEN 2006*c*, CEN 2006*b*), and they include member and joint resistance checks as well as conditions on joint geometry. The structural model is also in accordance with EN 1993 such that bending of the chords and eccentricities of the joints are taken into account. Actual geometry of the joints is utilised in constructing the structural model for determining the internal forces.

The resulting optimisation problem includes discrete and continuous variables and highly nonlinear constraints. Moreover, the constraints are evaluated by a separate structural analysis module such that the mathematical structure of the optimisation problem cannot be effectively utilised. Such optimisation problems can be treated by a limited number of methods. In this study, Particle Swarm Optimisation (PSO) method (Kennedy & Eberhart 1995), which is a stochastic optimisation algorithm capable of treating problems with discrete design variables and constraints derived from design rules. The choice of algorithm is based on previous investigations (Jalkanen 2007).

The structures considered are two Warren-type trusses (with and without verticals). The layouts are based on a preliminary study (Bzdawka & Heinisuo 2012).

The paper is organized as follows. In the Section 2, the basis of the optimisation problem is presented. This include structural modelling of the truss as well as derivation of the constraints and description of the cost evaluation. Next, in Section 3, the optimization procedure and the results are presented. Finally, the findings of the study are discussed in Section 4.

2 Truss evaluation

In order to study the behaviour of trusses using optimization an automatic parametric truss evaluation is obligatory. In this study, the automatic truss evaluation is implemented in Matlab (Mat 2011) and it checks the constraints of a given tubular steel truss with given uniform load at the top chord. The flow chart of the evaluation module is shown in Fig. 1. The constraints are derived from requirements of EN 1993-1-1 (CEN 2006*a*) for members and of EN 1993-1-8 (CEN 2006*c*) for the joints. These standards cover steel grades up to yield strength 460 MPa. For higher strength, the standard EN 1993-1-12 (CEN 2006*b*) is applied. The scope of EN 1993-1-12 is limited to yield strength 700. In this paper, when S960 steel performance is evaluated, the rules given by EN 1993-1-12 were applied.

The truss evaluation output are the scaled values of constraints when the input parameters of the truss are given. The truss is feasible following EN-standards, if the constraint value is in the

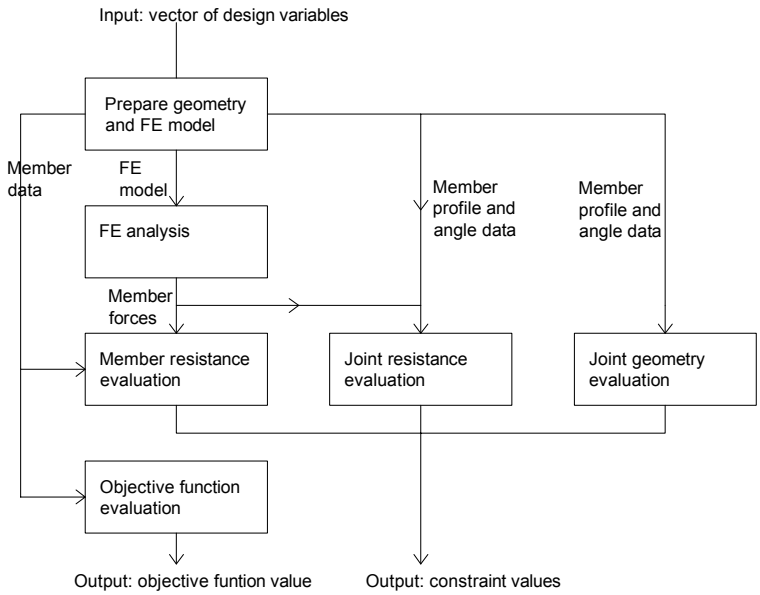

Figure 1: Truss evaluation flow chart.

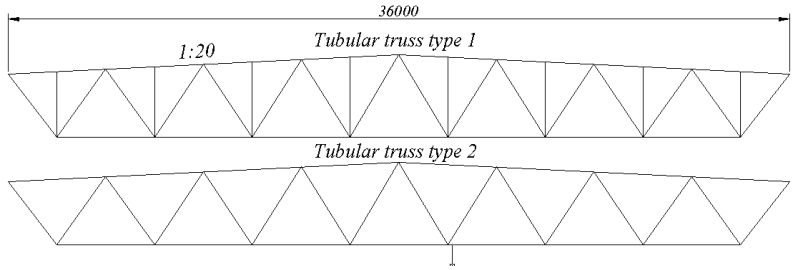

Figure 2: Layouts of the Warren trusses considered.

range $[0, 1]$. The truss module is made for two topologies of Warren type trusses: with vertical members (Type 1) and without verticals (Type 2), see Fig. 2. The trusses are typical one span symmetric roof trusses with fixed roof inclination 1:20 and span of $L = 36$ m. The trusses are tubular trusses with welded gap joints. Eccentricities at the joints are taken into account as described later.

The used library of cold-formed tubular member profiles is shown in Table 1. Only cross-sections with the minimal wall thickness 3 mm are considered due to limitations in the joint design of EN 1993-1-8. The material combinations examined in this paper are shown in Table 2.

The design loads are uniform 23.5 and 47 kN/m at the top chord. These are the loads in the ultimate limit state. Deflections are not considered, because they are compensated typically in these trusses by the pre-camber.

2.1 Truss geometry

The geometry of the truss is defined with 23 (KT-truss) or 19 (K-truss) *design variables*:

Table 1: The list of available cold formed square hollow section profiles. B is the width, H the height and t the wall thickness.

Number	BxHxt [mm]	Number	BxHxt [mm]	Number	BxHxt [mm]
1	25x25x3	19	90x90x4	37	150x150x6
2	30x30x3	20	90x90x5	38	150x150x8
3	40x40x3	21	90x90x6	39	150x150x10
4	40x40x4	22	100x100x4	40	150x150x12.5
5	50x50x3	23	100x100x5	41	160x160x6
6	50x50x4	24	100x100x6	42	160x160x8
7	50x50x5	25	100x100x8	43	160x160x10
8	60x60x3	26	110x110x4	44	180x180x6
9	60x60x4	27	110x110x5	45	180x180x8
10	60x60x5	28	120x120x4	46	180x180x10
11	70x70x3	29	120x120x5	47	200x200x8
12	70x70x4	30	120x120x6	48	200x200x10
13	70x70x5	31	120x120x8	49	200x200x12.5
14	80x80x3	32	120x120x10	50	250x250x6
15	80x80x4	33	140x140x5	51	250x250x8
16	80x80x5	34	140x140x6	52	250x250x10
17	80x80x6	35	140x140x8	53	250x250x12.5
18	90x90x3	36	150x150x5	54	300x300x10
				55	300x300x12.5

Table 2: The material combinations examined.

Chords	Braces
S355	S355
S500	S500
S700	S700
S500	S355
S700	S355
S700	S500
S960	S960
S960	S355
S960	S500
S960	S700

- Distances $a_1, a_2, \ldots, a_7$ between the joints starting from the mid span, range 0.5 - 5 m, see Fig. 3;
- Height H of the truss at the mid span, range 0.5 - 5 m;
- Gap g at the joints, range 10 - 50 mm, step 1 mm.
- Chord member sizes (2 variables, 55 possible sizes seen in Table 1)
- Diagonal brace member sizes (8 variables)
- Vertical brace member sizes (4 variables, present only in type 1 truss)

The shape of the truss is altered by variables a_i and H. The variables a_i control the position of the joints along the span, whereas H is the total height of the truss measured from the top of the top chord to bottom of lower chord as shown in Fig. 4.

The definition of distances a_i is illustrated in Fig. 3. In type 1 truss (with verticals) the a_i are the distances along the horizontal axis between the midpoints of a given vertical and the next gap (or vice versa). In type 2 truss the a_i are measured between the midpoints of two consecutive gaps. The gap with is depicted in Figs. 3–5.

The structural analysis model generation should start from the geometrical model of the structure (Heinisuo, Möttönen, Paloniemi & Nevalainen 1991, Heinisuo, Laasonen, Ronni & Anttila 2010,

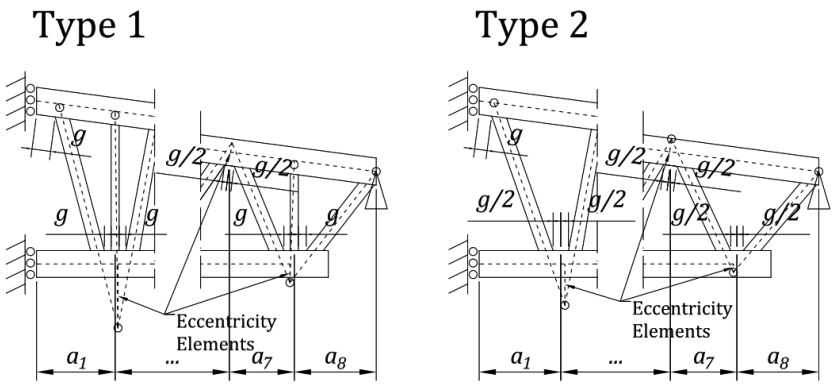

Figure 3: Dimensions a_i and distinction between geometrical and finite element models.

Wardenier, Packer, Zhao & van der Vegte 2010). In this study, the geometrical model is defined by the design variables and it can be seen in Fig. 3 with bold continuous line. The finite element analysis model has the same diagonal member directions but they are extended to the point where two braces next to each other meet. From this point an eccentricity element is needed to connect braces to the chord. The finite element model is seen in Fig. 3 with dashed line. Cross-sectional properties of the eccentricity elements are supposed very rigid (same as HEB 600). If the length of the eccentricity element is smaller than 1 mm then it is not present in the global model. Chords are modeled as continuous beams and braces as hinged members. End support prevents vertical displacement. The eccentricities at the joints between braces and chords are taken into account both at the top chord and at the bottom chord to avoid the constraints given in EN 1993-1-8, clause 5.1.5(5).

At the support the diagonal brace is connected to the support with a hinge without eccentricity (see Fig. 3). In the FE analysis model the elements verticals are not necessary vertical, but the real members are. By these means we avoid the use of inclined eccentricity elements at KT joints, as is done in (Heinisuo et al. 1991). The joint at the support and the joint at the top chord next to the mid-span are not checked in this study, because they are typically designed case by case. Instead, all other K, KT and T joints between braces and chords are considered.

To generate the geometrical model starting from the parameters of the truss module consider Fig. 4. The angle β_i seen in Fig. 4 can be calculated by first calculating the angle β_h from distances y and x by

$$\beta_h = \arctan \frac{y}{x} \tag{1}$$

Distances x and y for the particular diagonal member seen in Fig. 4, they can written as

$$x = a_i - g_i \cos\alpha - \frac{g_{i+1}}{2} \tag{2}$$

and

$$y = H - h_{bc} - \frac{h_{uc}}{\cos\alpha} - g_i \sin\alpha \tag{3}$$

The solution of β_i is based on solution of second order polynomial expression:

$$(h_i^2 - y^2)\frac{1}{\sin\beta_i{}^2} - 2h_i \cos\beta_h \sqrt{x^2+y^2}\frac{1}{\sin\beta_i} + x^2 + y^2 = 0 \tag{4}$$

By shortening

$$b = -2h_i \cos\beta_h \sqrt{x^2+y^2} \tag{5}$$

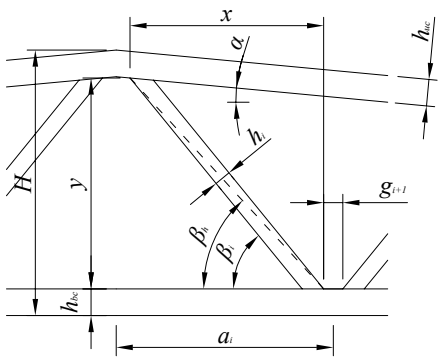

Figure 4: Dimensions for defining the inclination of a brace member.

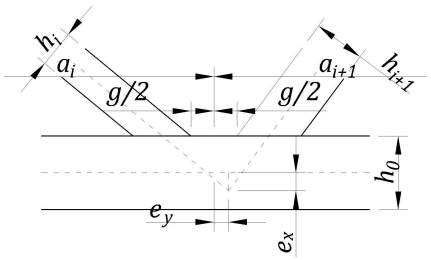

Figure 5: Eccentricities in the joint.

the solution becomes

$$\frac{1}{\sin\beta_i} = \frac{-b \pm \sqrt{b^2 - 4\left(h_i^2 - y^2\right)\left(x^2 + y^2\right)}}{2\left(h_i^2 - y^2\right)} \tag{6}$$

from which $\beta_i > \beta_h$ is chosen.

Consider Fig. 5. Eccentricity in direction perpendicular to chord can be calculated as (Ongelin & Valkonen 2012)

$$e_x = \left(\frac{h_1}{2\sin\beta_1} + \frac{h_2}{2\sin\beta_2} + g\right)\frac{\sin\beta_1\sin\beta_2}{\sin\beta_1 + \beta_2} - \frac{h_0}{2} \tag{7}$$

and in the direction of the chord as

$$e_y = \frac{e_x + h_0}{\tan\beta_2} - \frac{g}{2} - \frac{h_2}{2\sin\beta_2} \tag{8}$$

or with vertical member present

$$e_y = \frac{e_x + h_0}{\tan\beta_2} - g + \frac{h_v}{2} - \frac{h_2}{2\sin\beta_2} \tag{9}$$

where h_0 is the height of the chord, h_v is the height of the vertical, h_1 and h_2 the heights of the diagonals and β_1 and β_2 the angles of respective diagonal braces.

2.2 Constraints

Constraints are derived from requirements described in Eurocode steel design standards (CEN 2006*a*, CEN 2006*c*). For high strength steels, the standard (CEN 2006*b*) is also taken into account. Constraints for the resistances of the members and the joints are called as utilities. The

members are checked for the interaction of the axial force and the bending moment and for shear. For the interaction of the axial force and the moment the EN 1993-1-1, method 2 is used with the recommended material factors γ_{M0} = γ_{M1} = 1.0 and the imperfection factor in buckling is α = 0.49. The factor C_{my} = 1.0 is used for all members, but not for the top chord. The equation used is (EN 1993-1-3 clause 6.3.3(4)):

$$\frac{N_{Ed}}{\frac{\chi_y A f_y}{\gamma_{M1}}} + \frac{k_{yy} M_{y,Ed}}{\frac{W_{pl,y} f_y}{\gamma_{M1}}} \leq 1 \tag{10}$$

where

- χ_y is the reduction factor for the relevant buckling curve c;
- A is the cross-section area of the member;
- f_y is the yield strength of the member;
- γ_{M1} is the partial factor 1.0 in this case;
- k_{yy} is the interaction factor;
- $W_{pl,y}$ is the plastic section modulus.

Eq. 10 can also be written in shortened form by marking

$$\frac{N_{Ed}}{\frac{\chi_y A f_y}{\gamma_{M1}}} = n_y, \ \frac{k_{yy} M_{y,Ed}}{\frac{W_{pl,y} f_y}{\gamma_{M1}}} = m_y \tag{11}$$

$$\Rightarrow n_y + m_y \leq 1 \tag{12}$$

The left hand side of Eq. 10 is the utility of the member for the interaction of the axial force and the moment. The interaction factor k_{yy} is in this case for the top chord (plastic cross-sectional properties)

$$k_{yy} = C_{my} \min[1 + (\bar{\lambda_y} - 0.2) n_y; 1 + 0.8 n_y] \tag{13}$$

where factor C_{my} is

$$C_{my} = 0.1 + 0.8 \frac{M_{span}}{M_{support}} \tag{14}$$

and

$$\bar{\lambda_y} = \sqrt{\frac{A f_y}{N_{cr,y}}} \tag{15}$$

and the buckling load $N_{cr,y}$ is:

$$N_{cr,y} = \frac{\pi^2 E I_y}{L_{cr,y}^2} \tag{16}$$

where buckling lengths $L_{cr,y}$ are 0.9 times the member lengths in the analysis model and E = 210000 MPa. When calculating the cross-sectional property values A, $W_{pl,y}$ and I_y the corner radius of the profile shall be taken into account. The radii are defined following the standard EN 10219-2 (EN 10219-2 2006). They are:

- If the tube wall thickness t is smaller or equal to 6 mm then the outer radius r of the corner is 2 times the wall thickness.
- If the wall thickness is larger than 10 mm then the outer radius is 3 times the wall thickness.
- In between it is 2.5 times the wall thickness.

The effect of shear to resistances of the members is checked using EN 1993-1-1 clauses 6.2.6 and 6.2.8.

The utilities of K-joints are calculated as:

- Utility of brace:

$$\frac{N_{i,Ed}}{N_{i,Rd}} \leq 1,\ i = 1,2 \tag{17}$$

- Utility of chord:

$$\frac{N_{0,Ed}}{N_{0,gap,Rd}} \leq 1,\ i = 1,2 \tag{18}$$

The resistances of braces at K-joints are:

- Chord face failure:

$$N_{i,Rd} = \frac{8.9 k_n f_{y0} t_0^2 \sqrt{\gamma}}{\sin\theta_i}\beta,\ i = 1,2 \tag{19}$$

- Chord shear:

$$N_{i,Rd} = \frac{f_{y0} A_{v0}}{\sqrt{3}\sin\theta_i},\ i = 1,2 \tag{20}$$

- Chord face punching shear if $\beta \leq (1 - 1/\gamma)$:

$$N_{i,Rd} = \frac{f_{y0} t_0}{\sqrt{3}\sin\theta_i}\left(\frac{2h_i}{\sin\theta_i} + b_i + b_{e.p}\right),\ i = 1,2 \tag{21}$$

- Brace failure:

$$N_{i,Rd} = f_{yi} t_i (2h_i - 4t_i + b_i + b_{eff}),\ i = 1,2 \tag{22}$$

The resistance of the chord including the effect of shear in the gap area is:

$$N_{0,gap,Rd} = (A_0 - A_{v0}) f_{y0} + A_{v0} f_{y0} \sqrt{1 - \left(\frac{V_{Ed}}{V_{pl,Rd}}\right)^2} \tag{23}$$

The values for $M_{0,Ed}$ are taken as maximum values at both sides of the joint. The axial force $N_{0,Ed}$ is the axial force from the tension diagonal side. The value for V_{Ed} is calculated as maximum of $[\cos\theta_i N_{i,Ed}, \cos\theta_{i+1} N_{i+1,Ed}]$ where θ_i is the angle between the brace and the chord and $N_{i,Ed}$ is the axial force of the brace. All notations follow EN 1993-1-8. KT-joints are checked using the same equations as K-joints but the resistance of the chord is checked as a series of two K-joints. At T-joints the chord side wall failure is checked as well.

When using S500 and S700 steel the resistances of the joints should be multiplied by 0.8 (CEN 2006*b*). For S960 same values are used. Full strength welds are used at all joints. The weld throat thickness are shown in Table 3.

Other constraints in K-joints deal with:

- Angles between braces and chords

$$\theta_i \geq 30^\circ \Rightarrow \frac{30^\circ}{\theta_i} \leq 1 \tag{24}$$

- Cross-section classes of both chords and compressed braces should be 1 or 2 ;

Table 3: Fillet weld throat thickness a for different material grades for full strength welds connecting tubular members as function of wall thickness t.

Material	a
S355	$1.11t$
S500	$1.61t$
S700	$1.65t$
S960	$1.68t$

- Geometrical constraints

$$\frac{b_i}{b_0} \leq 1,\ i = 1, 2 \tag{25}$$

$$\beta \leq 1 \tag{26}$$

$$g \geq t_1 + t_2 \Rightarrow \frac{t_1 + t_2}{g} \leq 1 \tag{27}$$

$$\frac{g}{b_0} \geq 0.5(1 - \beta) \Rightarrow \frac{0.5(1 - \beta)}{g/b_0} \leq 1 \tag{28}$$

$$\frac{g}{b_0} \leq 1.5(1 - \beta) \Rightarrow \frac{g/b_0}{1.5(1 - \beta)} \leq 1 \tag{29}$$

$$\frac{h_i}{t_i} \leq 35 \Rightarrow \frac{h_i}{35t_i} \leq 1 \tag{30}$$

$$\frac{h_0}{t_0} \leq 35 \Rightarrow \frac{h_0}{35t_0} \leq 1 \tag{31}$$

If $g/b_0 \geq 1.5(1 - \beta)$ and $g \geq t_1 + t_2$ then the K-joint is treated as two separate T-joints.

The length of the last part a_8 is calculated from the span L_{span} and sum of 7 other parts (see also Fig. 3)

$$a_8 = L_{span} - \sum_{i=1}^{7} a_i \tag{32}$$

With large values of $a_1, a_2 \ldots, a_7$ it would be possible to have negative a_8 which would not make sense. Therefore, a_8 is restricted to interval $0.5, \ldots, 5$ m. This is written as constraints

$$\frac{\sum_{i=1}^{7} a_i}{L_{span} - 0.5} \leq 1 \tag{33}$$

$$\frac{L_{span} - 5}{\sum_{i=1}^{7} a_i} \leq 1 \tag{34}$$

For Type 2 truss constraints are:

- Interaction of axial force and bending moment, 4 elements at both chords, 8 member at braces, 16 constraints;
- Shear resistance checks of the elements, 16 constraints;
- Resistance checks of K-joints, 7 joints, $7 \cdot 2 + 7 \cdot 1 = 21$;
- Angles 16 constraints, checked also support and top joints;
- Cross-section class checks, 3x7 = 21;
- Gaps, dimensions and geometrical constraints 13x7 = 91;

Total amount for type 2 truss is thus 183 constraints. For Type 1 truss there are 259 constraints. It should be noted that some of the constraints can be formed in linear form. Depending on optimization method linearity is a highly sought after property. In this case when PSO is used the constraints are normalized to have values at similar range and the linearity is not exploited.

2.3 Fabrication cost of a truss

As described in the introduction fabrication cost of a truss can be approximated in many ways. In this study the feature based approach proposed by Haapio (2012) was adopted. The approach is very general and requires a lot of input parameters and data of the fabrication process. In the following, the method proposed by Haapio is applied to tubular trusses mainly following his notation and parameter values presented in his thesis. The fabrication cost C_T of a truss is calculated as

$$C_T = C_{SM} + \sum C_B + \sum C_S + \sum C_W + C_P \text{ [€]} \tag{35}$$

where C_{SM} is material cost, C_B is member blasting cost, C_S is member sawing cost, C_W is member welding cost and C_P is truss painting cost. Material cost is

$$C_{SM} = \sum_{i=1}^{n} k_{grade,i} 0.8 W_{M,i} \text{ [€]} \tag{36}$$

where $k_{grade,i}$ is the material factor for ith member, $W_{M,i}$ [kg] is the weight of the member i and n is the number of member in the truss.

The costs related to work shop action or a cost centre k can be expressed by

$$C_k = \frac{(T_{Nk} + T_{Pk})(c_{Lk} + c_{Eqk} + c_{Mk} + c_{REk} + c_{Sek})}{u_k} + T_{Pk}(c_{Ck} + c_{Enk}) + C_{Ck} \tag{37}$$

where T_{Nk} is the non-productive time, T_{Pk} is the productive time, c_{Lk} is the labour unit cost, c_{Eqk} is the equipment investment unit cost, c_{Mk} is the equipment maintenance unit cost, c_{REk} is the real estate investment unit cost, c_{Sek} is the real estate maintenance unit cost, c_{Ck} is the unit cost of time related consumables, c_{Enk} is the unit cost of energy needed, C_{Ck} is the total cost of non-time-related consumables used, and u_k is the utilization rate of the cost centre.

The utilization rate is assumed 1 in all workshop actions in this article. Values of other cost factors need to be calculated according to space requirement, equipment, labour etc. needed by the cost centres.

Real estate as well as equipment investment cost can be calculated as

$$c_{inv} = \frac{p_{inv}}{a_w} \frac{i \cdot (1+i)^n}{i \cdot (1+i)^n - 1} \text{ [€/min]}; \tag{38}$$

where p_{inv} is the price for the real estate or equipment, i is the interest rate, a_w is the work year in minutes (120960 min) and n is the investment time in years. In real estate cost, the price is supposed to be proportional to area of the cost centre. With assumed 5 % interest rate, 900 €/m^2 unit price, area of A and 50 year investment time this becomes

$$c_{RE,i} = 4.08 \cdot 10^{-4} A \text{ [€/min]} \tag{39}$$

The cost data used in this article can be seen in Table 4. The values are based on (Haapio 2012).

2.3.1 Blasting

The productive time used in blasting of a member with length L is defined by

$$T_B = \frac{L}{v_c} \tag{40}$$

where v_c is the conveyor speed. In this article $v_c = 3000$ mm/min.

Table 4: Assumed unit cost data. If a symbol instead of a numerical value is present, the value is dependent on the assembly or member properties. If a $-$ sign is present, the cost factor is not relevant in the cost centre.

Action	c_L	c_{Eqk}	c_{Mk}	c_{Rek}	c_{Sek}	c_{Ck}	c_{Enk}	C_{ck}
Blasting	0.46	0.13	0.01	0.16	0.24	0.02	0.07	-
Cutting	0.46	0.21	0.01	0.21	0.31	-	0.02	-
Welding	0.46	0.01	0	c_{ReW}	c_{SeW}	c_{CW}	0.01	-
Painting	0.46	0	0	0.03	0.04	-	0	C_{cP}

2.3.2 Sawing

The productive time in sawing for one cut

$$T_{PSi} = \frac{h}{\left(0.0328 \cdot \left(\frac{t}{\cos\theta_i}\right)^2 - 3.1794 \cdot \frac{t}{\cos\theta_i} + 115.6\right) 0.9} + \frac{A_{hi}}{8800} \text{ [min];}$$

where h [mm] is the profile height, t [mm] is the profile wall thickness, θ_i [°] is the sawing angle, and A_h [mm^2] is the area of horizontal part of the profile.

Total time of sawing one member takes two cuts.

The non-productive time in sawing (saw angle adjustment and conveyor roll) can be calculated as

$$T_{NS} = 6.5 + L_S/20000[min] \tag{41}$$

where L_S is the length of the member to be sawn.

Cost of consumables (wear of saw blade) for one cut can be calculated as

$$C_{CSi} = \frac{100}{T_{PSi}} \cdot \frac{A_{ti}}{\left(-1.188 \cdot \left(\frac{t}{\cos\theta_i}\right)^2 + 188892 \cdot \frac{t}{\cos\theta_i} + 4414608\right)}$$

[€/min];

where A_{ti} total sawing area for the cut.

2.3.3 Welding

The welding time for one connection between brace and chord as a fillet weld can be calculated as

$$T_{PWW} = \frac{L_W}{1000} \cdot \left(0.4988 \cdot a^2 - 0.0005 \cdot a + 0.0021\right)$$

where L_W is the length of the weld and a is the throat thickness. The throat thickness for full strength is dependent on material grade. The values used in this article are shown in Table 3.

Weld assembly preparation time consists of tack welding which is assumed 1,59 min/member.

Area requirement for real estate cost is assumed

$$A_W = (L_{truss} + 2)(H_{truss} + 2) \text{ [m}^2\text{]} \tag{42}$$

This means that the real estate cost is dependent of the truss height which is also a design variable in optimization.

Table 5: Cost factors for different material grades.

Steel	Material	Sawing	Welding
S355	1	1	1
S500	1.15	1.15	1.25
S700	1.30	1.30	1.50
S960	1.6	1.5	2

2.3.4 Painting

Both painting time and paint cost are proportional to painted area A_p. Painting time with alkyd paint system AK 160/3 - FeSa2$\frac{1}{2}$ can be calculated as

$$T_{PP} = (0.513/900000)A_p \text{ [min]} \tag{43}$$

and paint cost as

$$C_{CP} = 3.87 \cdot 10^{-6} A_p \tag{44}$$

2.3.5 Material grade effect

Certain actions are more costly if the material yield strength is higher than S355. Those actions in this paper are sawing and welding. In sawing, according to saw blade manufacturers lower feeding speeds must be used and blade wear is greater. In welding, the welding wire is more expensive and heat input limits defined by steel suppliers lower the maximum possible welding speed. Also the high strength steel tubes are typically more expensive than S355. In the calculations presented in this paper, coefficients shown in Table 5 were used to approximate these higher costs.

3 Optimization

3.1 Optimization problem statement

The truss optimization problem can be written as

$$\begin{aligned}
\min_{\mathbf{x}\in\Omega} \quad & f(\mathbf{x}) \\
\text{such that} \quad & g_{Joint,jn}(\mathbf{x}) \leq 0,\ j = 1,\dots,n_j,\ n = 1,\dots,n_{jn} \\
& g_{Interaction,i}(\mathbf{x}) \leq 0,\ i = 1,\dots,n_e \\
& g_{Shear,i}(\mathbf{x}) \leq 0,\ i = 1,\dots,n_e \\
& g_{Geometry,jl}(\mathbf{x}) \leq 0,\ i = 1,\dots,n_j,\ l = 1,\dots,n_c \\
& g_{Angles,m}(\mathbf{x}) \leq 0,\ m = 1,\dots 16 \\
& g_{a_8,ub}(\mathbf{x}) \leq 0 \\
& g_{a_8,lb}(\mathbf{x}) \leq 0
\end{aligned} \tag{45}$$

where f is the objective function (weight or cost) and $\mathbf{x}$ is the vector of design variables (see Table 6). $g_{Joint,jn}$ is the joint utility constraint for nth brace in joint number j, n_j is the number of joints, n_{jn} is the number of braces in joint j, $g_{Interaction,i}$ is the axial force - moment interaction utility constraint of element i, $g_{Shear,i}$ shear utility of element i, n_e is the number of member elements in the FE model, $g_{Geometry,jl}$ is the utility constraint of geometry check l in joint number j, $g_{Angles,m}$ angle constraint value of angle m and $g_{a_8,ub}$ and $g_{a_8,lb}$ are the utilities of upper and lower bound constraints of length a_8 stated by Eqs. (33) and (34).

Table 6: Design Variables in optimization. Variables 20–23 only present in type 1 truss.

Variable	Description	Values
x_i	a_i $i = 1, 2, \ldots, 7$	$[0.5, 5]$ [m]
x_8	Height H	$[0.5, 5]$ [m]
x_9	Top Chord profile	$1, 2, \ldots, 55$
x_{10}	Bottom Chord profile	$1, 2, \ldots, 55$
x_{11}	Brace 1 profile	$1, 2, \ldots, 55$
x_{12}	Brace 2 profile	$1, 2, \ldots, 55$
x_{13}	Brace 3 profile	$1, 2, \ldots, 55$
x_{14}	Brace 4 profile	$1, 2, \ldots, 55$
x_{15}	Brace 5 profile	$1, 2, \ldots, 55$
x_{16}	Brace 6 profile	$1, 2, \ldots, 55$
x_{17}	Brace 7 profile	$1, 2, \ldots, 55$
x_{18}	Brace 8 profile	$1, 2, \ldots, 55$
x_{19}	Gap	$10, 11, \ldots, 50$ [mm]
x_{20}	Vertical 1 profile	$1, 2, \ldots, 55$
x_{21}	Vertical 2 profile	$1, 2, \ldots, 55$
x_{22}	Vertical 3 profile	$1, 2, \ldots, 55$
x_{23}	Vertical 4 profile	$1, 2, \ldots, 55$

The objective function is either the structural weight or the total cost of the truss. The structural weight is written as

$$W(\mathbf{x}) = \rho_s \sum_{i=1}^{n_m} A_i(\mathbf{x}) L_{i,g}(\mathbf{x}) \tag{46}$$

where ρ_s is the density of steel, and A_i and $L_{i,g}$ are the cross-sectional area and the length of member i, respectively.

The expression of the total cost of the truss is

$$C(\mathbf{x}) = C_{SM}(\mathbf{x}) + \sum_{i=1}^{n_m} (C_B(\mathbf{x}) + C_S(\mathbf{x}) + C_W(\mathbf{x})) + C_P(\mathbf{x}) \tag{47}$$

As the problem includes both continuous and discrete variables and the constraints are non-linear, it can be concluded that the problem is a mixed-integer nonlinear program (MINLP).

3.2 Optimization method and parameters

In optimization, the PSO method (Kennedy & Eberhart 1995) was used. It is a stochastic heuristic method relying on a swarm of individuals moving in the design space. The solution the method produces is usually good but convergence to local nor global optimum can not be proved.

Optimization runs were done using following PSO parameters:

- Inertia: 1.4;
- Factor to reduce the inertia: 0.8;
- Number of iterations without best found value enhancement to change the inertia: 3;
- Penalty factor: 2

There are many approaches in handling constraints in PSO. In the implementation used, a penalty function approach was used. The standard problem

$$\begin{aligned} &\min f(\mathbf{x}) \\ &\text{s.t. } \mathbf{g}(\mathbf{x}) \leq 0 \end{aligned} \tag{48}$$

Table 7: PSO run parameters.

Truss type	Population	Iterations	Runs
KT	400	225	75
K	400	200	100

is replaced with unconstrained problem in which the criterion function is

$$f^*(\mathbf{x}) = f(\mathbf{x}) \left(1 + \sum_{g_i(\mathbf{x}>0)} P g_i(\mathbf{x}) \right) \tag{49}$$

where P is the penalty factor. This approach can lead to a situation in which the best found solution is no longer feasible. Therefore, best found feasible solution is also kept in memory.

First, in order to study convergence characteristics and to find out suitable values, the number of populations and iterations were varied. Consider Type 2 truss which is made of S355 steel grade with the load 23.5 kN/m. Using the truss evaluation module, or using special software developed for the design of tubular trusses, the designer can solve sizing problem rather quickly if the geometry of the truss is fixed. Engineers natural choise would be an evenly distributed design, meaning variables a_i having values a_i = 2.25 m. For truss height commonly used value is $H = L/10$ which is $36/10$ m $= 3.6$ m in this case. Gap was fixed at g = 50 mm.

When evaluating different designs manually it was found that all the constraints, especially dealing with the geometrical entities, were extremely difficult to fulfil. E.g. by allowing different (smaller) gap at the first joint from the support, better solutions were found. At the first joint two rather large braces are joined to the bottom chord and then using large gap the eccentricity at the joint is large increasing the bending moment at the bottom chord. Also, the maximum allowed gap 50 mm was clearly too small in some cases. It could be seen that in the best found solution the gap was at this limit, meaning that allowing larger gaps perhaps better solutions can be found in some cases. The reason to use constant gap are the truss manufacturers. They do not like variable gaps at manual fabrication lines. Perhaps through more automation in the future the the use of many gap values in one truss will be allowed. In many cases the number of sections in different brace members is also an issue. In this study was allowed that all braces may have different sizes. These difficulties reflect to the PSO runs, as well.

3.3 Results

The results for cases were calculated with rather extensive computer runs (Table 7). One function evaluation takes about 0.05 seconds and thus one run takes from one to one-and-half hour with a contemporary pc. The results for Type 1 are given in Table 8 and the results for Type 2 are given in Table Table 9.

The design variable values corresponding to best found structures are shown in Tables 10–13. If the minimum weight and minimum cost designs are different, minimum cost design is shown. The geometry optimization seems to drive towards solutions where compression members become shorter which reduces buckling lengths. The span–height ratio is in average 10.4 for K trusses and 10.8 for KT trusses.

It can be seen that the gap is at the upper bound (50 mm) in many cases. This may imply that allowing larger gaps better solutions can be found. The mean of height of the truss is L/10.7 for type 1 and L/10.4 for type 2.

In the Figs. 6–7 graphical illustration of the performance of different steel grades can be seen.

The Table 14 shows relative cost and weight values of best found designs.

Table 8: Best found results for type 1 truss. If a value is marked with * minimum weight and minimum cost designs were different.

Material		Load [kN/m]	Weight optimization		Cost optimization		Best overall	
Chords	Braces		Cost [€]	Weight [kg]	Cost [€]	Weight [kg]	Cost [€]	Weight [kg]
355	355	23.5	3406	3270	3422	3288	3406	3270
500	500	23.5	3417	2642	3549	2726	3417	2642
500	355	23.5	3200	2678	3288	2764	3200	2678
700	700	23.5	3269	2150	3237	2163	3237*	2150*
700	355	23.5	3125	2343	3184	2397	3125	2343
700	500	23.5	3147	2199	3311	2285	3147	2199
960	960	23.5	3416	1803	3724	2015	3416	1803
960	355	23.5	3390	2196	3391	2213	3390	2196
960	500	23.5	3642	2109	3535	2057	3535	2057
960	700	23.5	3494	1924	3392	1873	3392	1873
355	355	47	6711	6551	6682	6702	6682*	6551*
500	500	47	5866	4738	6080	5121	5866	4738
500	355	47	5631	5000	5597	5030	5597*	5000*
700	700	47	5401	3700	5165	3563	5165	3563
700	355	47	5502	4424	5533	4458	5502	4424
700	500	47	5575	3996	5700	4222	5575	3996
960	960	47	5384	2971	5344	3015	5344*	2971*
960	355	47	5631	3857	5672	3867	5631	3857
960	500	47	6026	3678	5883	3593	5883	3593
960	700	47	5491	3152	5301	3107	5301	3107

Table 9: Best found results for type 2 truss. If a value is marked with * minimum weight and minimum cost designs were different.

Material		Load [kN/m]	Weight optimization		Cost optimization		Best overall	
Chords	Braces		Cost [€]	Weight [kg]	Cost [€]	Weight [kg]	Cost [€]	Weight [kg]
355	355	23.5	3212	3146	3221	3244	3212	3146
500	500	23.5	3357	2753	3352	2736	3352	2736
500	355	23.5	3028	2633	3031	2632	3028*	2632*
700	700	23.5	3024	2165	3215	2318	3024	2165
700	355	23.5	2910	2272	2881	2253	2881	2253
700	500	23.5	3051	2233	3102	2277	3051	2233
960	960	23.5	3478	1987	3565	2088	3478	1987
960	355	23.5	3225	2125	3348	2195	3225	2125
960	500	23.5	3446	2132	3510	2162	3446	2132
960	700	23.5	3369	2026	3434	2046	3369	2026
355	355	47	5795	5981	5885	6086	5795	5981
500	500	47	5426	4407	5301	4600	5301*	4407*
500	355	47	5165	4633	5024	4557	5024	4557
700	700	47	4992	3697	5150	3782	4992	3697
700	355	47	4799	3881	4590	3718	4590	3718
700	500	47	5008	3800	5156	3918	5008	3800
960	960	47	5321	3173	5356	3192	5321	3173
960	355	47	5002	3463	5453	3769	5002	3463
960	500	47	5528	3439	5805	3695	5528	3439
960	700	47	5169	3218	5223	3231	5169	3218

Table 10: Design variable values for best found trusses of type 1, load 23.5 kNm

Chords	355	500	500	700	700	700	960	960	960	960
Braces	355	500	355	700	355	500	960	355	500	700
UC	160x8	160x6	150x6	140x6	150x6	140x6	120x6	120x8	120x6	120x6
BC	150x10	150x8	150x8	120x8	140x6	120x8	120x6	120x6	120x6	120x6
Br1	110x4	60x3	110x4	100x4	50x3	50x3	50x3	50x3	50x3	50x3
Br2	110x4	60x3	60x3	50x3	70x3	50x3	50x3	90x3	110x4	100x4
Br3	110x4	70x3	70x3	60x3	90x3	90x3	60x3	80x3	90x3	70x3
Br4	70x3	60x3	70x3	60x3	80x3	50x3	50x3	50x3	50x3	50x3
Br5	100x4	90x3	90x4	100x4	100x4	90x4	90x4	100x4	110x4	90x4
Br6	90x3	110x4	120x4	70x3	90x3	60x3	50x3	90x3	80x3	60x3
Br7	100x6	120x4	140x5	100x4	120x4	120x4	100x5	120x5	120x4	100x4
Br8	100x5	110x4	120x4	100x4	110x5	100x4	70x4	90x5	80x5	90x4
V1	90x3	60x3	90x3	70x3	90x3	60x3	60x3	90x3	70x3	60x3
V2	70x3	60x3	70x3	50x3	70x3	60x3	50x3	50x3	70x3	60x3
V3	70x3	110x4	60x3	50x3	110x4	50x3	50x3	50x4	90x3	90x4
V4	70x3	110x4	90x3	70x3	100x4	60x3	70x4	60x3	70x3	60x3
Gap [mm]	50	50	47	47	46	50	50	32	50	50
H [m]	3.23	3.44	3.46	2.96	3.43	3.52	3.02	3.41	3.84	2.99
L/H	11.14	10.46	10.40	12.18	10.51	10.22	11.94	10.56	9.38	12.04
a_1	2.38	2.72	1.25	2.20	2.76	1.60	2.18	2.29	2.49	1.82
a_2	2.04	2.00	2.30	2.25	2.27	2.72	2.13	2.79	2.44	2.13
a_3	1.77	1.57	2.13	1.70	2.15	1.95	1.73	1.97	2.27	2.17
a_4	2.39	2.09	2.43	2.40	1.45	2.79	2.20	2.01	2.10	2.17
a_5	2.39	0.75	1.91	2.74	1.06	1.53	2.52	2.10	1.59	2.17
a_6	1.76	2.54	2.31	1.47	2.44	1.46	2.37	1.73	2.60	2.40
a_7	1.96	2.35	1.98	1.84	1.66	2.48	1.86	2.17	0.76	1.88

Table 11: Design variable values for best found trusses of type 1, load 47.0 kNm.

Chords	355	500	500	700	700	700	960	960	960	960
Braces	355	500	355	700	355	500	960	355	500	700
UC	200x12.5	180x10	180x10	160x8	160x10	180x8	150x8	180x10	160x8	160x8
BC	250x12.5	200x10	200x12.5	160x10	200x8	180x8	160x8	160x8	160x8	160x8
Br1	180x6	120x4	70x3	150x6	90x3	120x4	70x4	60x3	70x3	70x3
Br2	180x6	90x3	150x5	70x3	110x4	90x3	60x3	90x3	60x3	70x3
Br3	180x6	110x4	150x5	90x4	150x5	120x4	90x4	90x3	150x5	70x4
Br4	180x6	180x6	70x3	70x3	80x4	90x3	60x3	90x3	70x3	60x3
Br5	180x6	140x5	150x5	110x5	150x5	120x4	110x5	150x5	140x5	120x5
Br6	180x6	100x4	80x5	80x4	120x4	150x5	70x4	90x6	120x4	80x4
Br7	180x6	160x6	160x6	140x6	160x8	180x6	120x6	150x5	160x6	140x6
Br8	180x6	150x5	180x6	100x6	150x5	140x5	100x5	150x6	150x5	120x5
V1	90x3	90x3	100x4	70x3	100x4	90x3	60x3	90x3	90x3	60x3
V2	100x4	70x3	110x4	70x3	110x4	80x3	60x3	80x3	70x3	70x3
V3	90x3	140x5	100x4	60x3	90x3	150x5	60x3	60x3	110x4	60x3
V4	110x4	70x3	90x3	100x4	120x4	80x3	90x4	90x3	90x4	90x4
Gap [mm]	50	50	50	48	50	42	50	50	50	50
H [m]	3.21	3.30	3.59	3.62	4.05	3.86	3.18	3.76	4.32	3.14
L/H	11.2	10.9	10.0	9.9	8.9	9.3	11.3	9.6	8.3	11.5
a_1	1.92	1.01	2.65	1.92	2.72	2.97	2.09	2.17	3.25	1.35
a_2	1.65	2.10	2.05	2.20	1.68	1.04	2.16	1.57	1.23	1.67
a_3	2.02	2.26	1.80	2.19	2.70	1.58	2.31	1.58	1.75	2.48
a_4	2.04	1.52	1.53	2.30	2.56	2.17	2.28	3.35	1.79	2.55
a_5	2.35	2.34	1.90	1.46	1.31	1.89	2.13	1.79	2.00	2.80
a_6	1.66	2.80	1.40	2.00	1.71	2.34	2.66	2.33	2.35	2.00
a_7	2.68	3.31	2.55	2.29	2.60	3.03	1.94	1.59	1.38	2.03

Table 12: Design variable values for best found trusses of type 2, load 23.5 kNm

Chords	355	500	500	700	700	700	960	960	960	960
Braces	355	500	355	700	355	500	960	355	500	700
UC	180x8	180x8	160x8	160x8	150x8	160x8	150x8	150x8	150x8	150x8
BC	140x8	140x6	140x6	110x5	120x5	120x5	90x5	100x5	110x5	100x5
Br1	90x3	50x3	50x3	40x3	50x3	50x3	40x3	40x3	40x3	40x3
Br2	70x3	110x4	90x3	60x3	60x3	60x3	60x3	90x3	60x3	70x3
Br3	90x3	70x3	110x4	70x3	90x3	70x3	70x4	80x3	80x3	70x3
Br4	110x4	70x3	70x3	60x3	70x3	60x3	60x3	60x3	60x3	60x3
Br5	110x4	110x4	90x4	90x4	100x4	90x3	90x4	100x4	90x5	100x4
Br6	140x5	100x4	80x3	60x3	70x3	70x3	70x4	90x3	60x3	70x3
Br7	140x5	120x4	140x5	100x4	120x5	110x4	90x5	100x6	110x4	100x4
Br8	110x4	120x4	120x4	90x4	110x4	100x5	70x4	100x5	100x4	90x4
Gap [mm]	50	47	50	50	50	50	50	50	50	50
H [m]	3.53	3.29	3.82	3.56	3.74	3.36	3.31	3.25	3.57	3.18
H/L	10.2	10.9	9.4	10.1	9.6	10.7	10.9	11.1	10.1	11.3
a_1 [m]	2.17	2.07	2.28	2.34	2.44	1.42	2.61	1.94	1.78	2.34
a_2 [m]	1.58	1.16	1.77	1.56	1.66	2.80	1.52	2.15	2.51	1.70
a_3 [m]	2.37	1.98	1.41	1.37	1.86	1.39	2.12	1.81	0.50	1.82
a_4 [m]	1.53	1.92	2.65	2.25	2.27	2.50	1.83	2.34	3.83	2.16
a_5 [m]	2.55	2.81	0.97	1.66	2.12	1.43	1.90	2.19	2.20	2.09
a_6 [m]	2.13	2.29	3.51	3.20	2.17	2.95	2.55	2.50	1.88	2.49
a_7 [m]	2.78	1.93	1.75	1.41	1.86	1.52	1.55	1.53	1.58	1.65

Table 13: Design variable values for best found trusses of type 2, load 47.0 kNm

Chords	355	500	500	700	700	700	960	960	960	960
Braces	355	500	355	700	355	500	960	355	500	700
UC	250x12.5	200x12.5	200x10	200x10	200x8	200x10	180x10	180x8	180x8	180x10
BC	200x10	160x10	180x8	140x8	160x8	160x8	120x8	160x8	160x8	120x8
Br1	70x3	90x3	140x5	50x3	60x3	60x3	50x3	80x3	110x4	50x3
Br2	180x6	100x4	120x4	100x4	70x3	90x3	70x4	90x3	70x3	70x3
Br3	120x4	100x4	120x4	100x4	140x5	110x4	90x5	100x4	110x4	100x4
Br4	180x6	90x3	120x4	80x4	70x3	90x3	70x4	90x3	100x4	70x3
Br5	140x5	120x5	140x5	120x5	140x5	110x4	100x5	140x5	120x5	110x5
Br6	160x6	100x4	150x5	90x4	150x5	110x4	70x4	100x4	100x4	80x4
Br7	150x6	160x6	160x6	140x6	160x6	140x5	120x6	150x6	150x5	120x6
Br8	180x6	140x5	160x6	110x5	160x6	160x6	90x5	160x6	100x8	110x5
Gap [mm]	50	50	42	50	50	50	50	50	50	50
H [m]	3.57	3.63	4.39	3.66	3.98	3.21	3.59	4.04	4.13	3.57
L/H	10.1	9.9	8.2	9.8	9.0	11.2	10.0	8.9	8.7	10.1
a_1	3.44	2.70	2.52	2.27	3.42	2.30	2.34	2.39	2.73	1.59
a_2	1.53	1.61	1.84	2.23	0.67	1.75	1.83	1.57	1.31	2.55
a_3	1.48	2.11	2.12	2.22	1.76	2.76	1.97	1.75	2.13	2.02
a_4	1.95	2.21	2.18	2.20	2.38	1.30	2.23	2.30	1.95	2.08
a_5	2.24	1.96	1.29	2.05	0.96	1.11	1.40	2.72	1.29	2.00
a_6	1.56	2.35	2.49	1.68	3.52	3.36	2.90	1.97	3.27	2.79
a_7	1.54	2.11	1.61	1.94	0.78	1.68	1.24	1.27	1.29	1.59

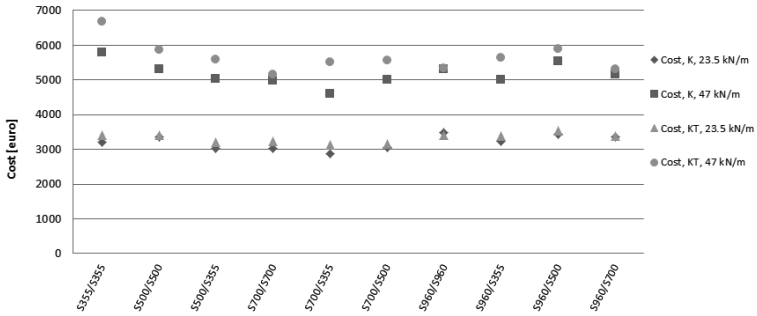

Figure 6: Truss cost. Best found among all the result data.

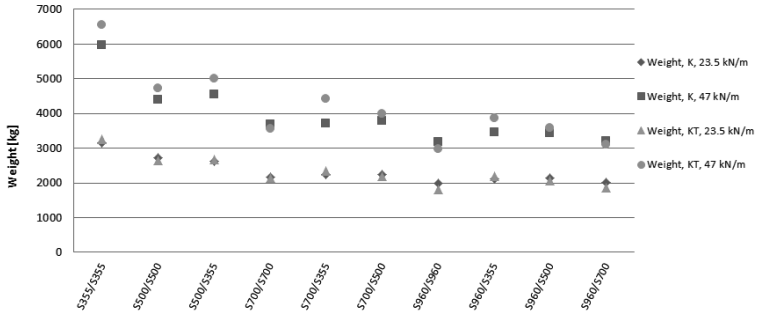

Figure 7: Truss weight. Best found among all the result data.

Table 14: Truss relative cost and weight. Compared to best found S355.

	Cost				Weight			
	K	KT	K	KT	K	KT	K	KT
Material	23.5 kN/m		47 kN/m		23.5 kN/m		47 kN/m	
S355/S355	100 %	106 %	100 %	115 %	100 %	104 %	100 %	110 %
S500/S500	104 %	106 %	91 %	101 %	87 %	84 %	74 %	79 %
S500/S355	94 %	100 %	87 %	97 %	84 %	85 %	76 %	84 %
S700/S700	94 %	101 %	86 %	89 %	69 %	68 %	62 %	60 %
S700/S355	90 %	97 %	79 %	95 %	72 %	74 %	62 %	74 %
S700/S500	95 %	98 %	86 %	96 %	71 %	70 %	64 %	67 %
S960/S960	108 %	106 %	92 %	92 %	63 %	57 %	53 %	50 %
S960/S355	100 %	106 %	86 %	97 %	68 %	70 %	58 %	64 %
S960/S500	107 %	110 %	95 %	102 %	68 %	65 %	58 %	60 %
S960/S700	105 %	106 %	89 %	91 %	64 %	60 %	54 %	52 %

3.4 Sizing optimization vs. shape optimization

To consider effect of including shape variables in the optimization problem the truss was also optimized with fixed geometry and by allowing only the height of the truss to change. The results of this comparison (Table 15) implies that it is beneficial to let the geometry vary. For fixed geometry, the number of iterations was 150.

The results imply a 10–15 % higher cost and weight for fixed geometry solution against the solution where geometry is allowed to vary.

Table 15: Truss relative cost and weight with fixed or partly fixed geometry. OG = optimized geometry, FG = fixed geometry ($H = L/10$), FN = fixed nodes, varying height.

Material	OG	FG	FN	OG	FG	FN
	Relative cost			Relative weight		
S355/S355	1.00	0.99	0.98	1.00	1.01	0.97
S500/S500	1.00	1.19	1.02	1.00	1.19	1.06
S500/S355	1.00	1.14	1.01	1.00	1.15	1.03
S700/S700	1.00	1.12	1.02	1.00	1.15	1.02
S700/S355	1.00	1.14	1.06	1.00	1.17	1.06
S700/S500	1.00	1.10	1.02	1.00	1.13	1.01
S960/S960	1.00	1.15	1.12	1.00	1.14	1.09
S960/S355	1.00	1.14	1.09	1.00	1.14	1.10
S960/S500	1.00	1.09	1.07	1.00	1.11	1.05
S960/S700	1.00	1.15	1.11	1.00	1.13	1.10

3.5 PSO reliability

When applying stochastic methods multiple runs are needed for reliable results. Even multiple runs may fail capturing the global optimum for the problem. The results shown above were obtained with large number of optimization runs resulting in long computational time that is probably not practical for designer. To see the stochastic nature of the PSO method, some statistical evaluation is presented in the following.

For each material combination some statistical figures from the sets of runs are shown in Table 16 and Table 17. It seems, that when dealing with convergence characteristics, there is little or no difference in the performance of optimization regardless of material, objective function or truss type. Only exception is the 355/355 runs when the higher load is applied. In type 1 the deviation is very small and in type 2 on the other hand relatively high. Reason for this behaviour is not known.

Consider histograms in Fig. 8. In the figure, the case of S355 KT truss with the higher load, 47 kN/m, represents a low deviation case, same strength and load but K truss represents the high deviation and the S500 K truss represents the typical deviation.

To consider a practical number of runs expectation value for best found design is calculated based on the sample of 100 runs. The expectation value was created by randomly taking subsets from the set of 100 results. This was done for sets from 1 to 99 elements. The resulting curve can be seen in Fig. 9. The curve implies that if an error of 2% can be accepted, around 25 runs should be enough which means significant reduction to computational time. This should only be understood as a schematic figure, since the sample of 100 runs might be to small to draw solid conclusions.

Table 16: Stastical figures of optimization in type 1 trusses. Figures compared to best found values. 5 % and 10 % is refer to percentages of solutions within 5 or 10 % away from the best found.

Chords	Braces	Objective	Load	Median	Average	Std deviation	5 %	10 %
355	355	c	23.5	1.19	1.18	0.16	0.11	0.27
500	355	c	23.5	1.16	1.14	0.09	0.08	0.28
500	500	c	23.5	1.17	1.14	0.11	0.11	0.32
700	355	c	23.5	1.15	1.14	0.09	0.11	0.27
700	500	c	23.5	1.21	1.19	0.12	0.08	0.13
700	700	c	23.5	1.17	1.15	0.10	0.09	0.25
960	355	c	23.5	1.22	1.21	0.14	0.11	0.27
960	500	c	23.5	1.21	1.14	0.18	0.11	0.36
960	700	c	23.5	1.17	1.14	0.12	0.08	0.24
960	960	c	23.5	1.16	1.13	0.09	0.05	0.24
355	355	c	47	1.03	1.02	0.03	0.76	0.97
500	355	c	47	1.14	1.10	0.10	0.17	0.49
500	500	c	47	1.21	1.13	0.17	0.15	0.31
700	355	c	47	1.12	1.11	0.09	0.13	0.43
700	500	c	47	1.20	1.19	0.10	0.03	0.15
700	700	c	47	1.20	1.18	0.12	0.07	0.25
960	355	c	47	1.21	1.21	0.11	0.04	0.07
960	500	c	47	1.21	1.21	0.11	0.04	0.15
960	700	c	47	1.18	1.17	0.10	0.04	0.31
960	960	c	47	1.14	1.12	0.09	0.13	0.37
355	355	w	23.5	1.16	1.15	0.07	0.07	0.24
500	355	w	23.5	1.22	1.21	0.08	0.01	0.05
500	500	w	23.5	1.18	1.17	0.08	0.08	0.17
700	355	w	23.5	1.18	1.17	0.09	0.04	0.16
700	500	w	23.5	1.19	1.17	0.11	0.04	0.21
700	700	w	23.5	1.15	1.14	0.11	0.19	0.40
960	355	w	23.5	1.17	1.12	0.13	0.12	0.41
960	500	w	23.5	1.12	1.10	0.09	0.12	0.47
960	700	w	23.5	1.17	1.15	0.11	0.04	0.15
960	960	w	23.5	1.22	1.21	0.09	0.01	0.04
355	355	w	47	1.05	1.04	0.02	0.64	0.96
500	355	w	47	1.10	1.09	0.05	0.11	0.56
500	500	w	47	1.12	1.10	0.07	0.11	0.49
700	355	w	47	1.10	1.11	0.05	0.16	0.43
700	500	w	47	1.15	1.15	0.05	0.03	0.20
700	700	w	47	1.14	1.14	0.06	0.05	0.16
960	355	w	47	1.17	1.17	0.06	0.01	0.12
960	500	w	47	1.12	1.12	0.06	0.13	0.37
960	700	w	47	1.10	1.10	0.07	0.27	0.48
960	960	w	47	1.13	1.11	0.07	0.08	0.39

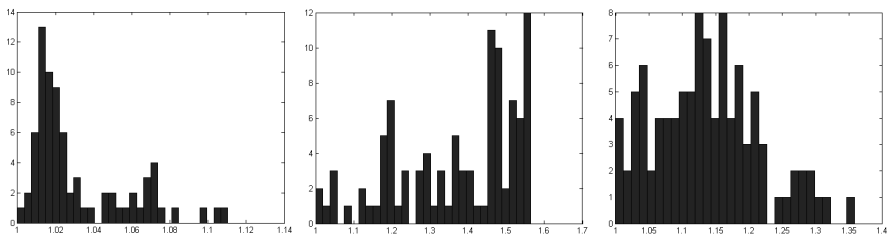

Figure 8: Histograms of the results of all runs in three cases. From left: S355 47 kN/m KT truss, objective: cost; S355 47 kN/m K truss objective: weight; S500 23.5 kN/m K truss, objective: weight.

Table 17: Stastical figures of optimization in type 2 trusses. Figures compared to best found values. 5 % and 10 % is refer to percentages of solutions within 5 or 10 % away from the best found.

Chords	Braces	Objective	Load	Median	Average	Std deviation	5 %	10 %
355	355	c	23.5	1.12	1.11	0.07	0.15	0.43
500	355	c	23.5	1.18	1.15	0.11	0.09	0.26
500	500	c	23.5	1.19	1.15	0.11	0.06	0.23
700	355	c	23.5	1.20	1.17	0.12	0.07	0.19
700	500	c	23.5	1.19	1.16	0.13	0.10	0.24
700	700	c	23.5	1.21	1.18	0.12	0.01	0.14
960	355	c	23.5	1.18	1.12	0.14	0.10	0.31
960	500	c	23.5	1.17	1.12	0.16	0.23	0.43
960	700	c	23.5	1.15	1.11	0.12	0.13	0.44
960	960	c	23.5	1.17	1.13	0.14	0.13	0.35
355	355	c	47	1.39	1.45	0.16	0.03	0.05
500	355	c	47	1.20	1.18	0.09	0.05	0.09
500	500	c	47	1.23	1.21	0.10	0.04	0.08
700	355	c	47	1.21	1.24	0.13	0.10	0.25
700	500	c	47	1.22	1.18	0.13	0.03	0.17
700	700	c	47	1.22	1.15	0.17	0.12	0.30
960	355	c	47	1.12	1.12	0.07	0.14	0.39
960	500	c	47	1.14	1.12	0.12	0.21	0.45
960	700	c	47	1.15	1.12	0.10	0.04	0.35
960	960	c	47	1.26	1.23	0.18	0.07	0.19
355	355	w	23.5	1.15	1.13	0.10	0.11	0.31
500	355	w	23.5	1.20	1.19	0.11	0.05	0.19
500	500	w	23.5	1.14	1.14	0.08	0.17	0.32
700	355	w	23.5	1.19	1.17	0.12	0.10	0.19
700	500	w	23.5	1.19	1.15	0.14	0.11	0.21
700	700	w	23.5	1.16	1.16	0.10	0.09	0.27
960	355	w	23.5	1.20	1.15	0.16	0.09	0.24
960	500	w	23.5	1.13	1.10	0.12	0.20	0.50
960	700	w	23.5	1.15	1.10	0.13	0.10	0.50
960	960	w	23.5	1.16	1.10	0.14	0.08	0.47
355	355	w	47	1.37	1.42	0.16	0.05	0.07
500	355	w	47	1.17	1.16	0.08	0.08	0.13
500	500	w	47	1.20	1.21	0.07	0.04	0.08
700	355	w	47	1.22	1.25	0.13	0.09	0.21
700	500	w	47	1.19	1.19	0.11	0.14	0.33
700	700	w	47	1.19	1.14	0.14	0.17	0.37
960	355	w	47	1.18	1.16	0.09	0.02	0.08
960	500	w	47	1.16	1.14	0.12	0.07	0.31
960	700	w	47	1.18	1.17	0.11	0.02	0.15
960	960	w	47	1.17	1.15	0.10	0.04	0.31

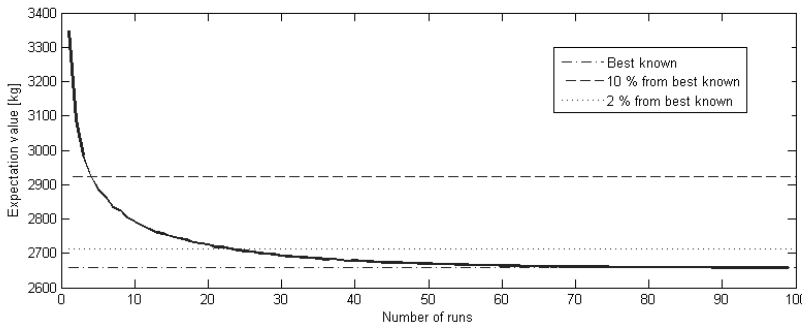

Figure 9: Expectation value based on the results of 100 runs.

4 Discussion

The main idea of used optimization formulation is that the starting point is the exact geometry of truss including gaps and eccentricities in joints. The FE analysis model is derived from the geometrical model using nearly rigid eccentricity elements. In this type of approach all the requirements presented in relevant design standards can be checked and the resulting design is fully compliant with the chosen design standard. The approach, however, results in a fairly large amount of constraints even in a relatively simple structure such as Warren type truss. This causes difficulties in finding feasible solutions and reflects to the convergence of PSO. Especially dealing with geometrical entities originating from requirements of joints from EN 1993-1-8 causes difficulties.

The main scope of this study was to find out if it is economically efficient to use high strength steel in a Warren type truss. The found weight reductions compared to S355 trusses were for around 15–20 % for S500, 30–40 % for S700 and 40–50 % for S960 the higher loading implying higher savings. The cost reductions were smaller and in some cases there was no benefit using higher steel strength. The hybrid solutions seem attractive in cost comparison. The S700/355 K truss with the higher load is around 20 % less costly than the reference truss (S355).

The use of S960 steel does not seem to make extra cost savings in comparison to S700 steel.

Generally, the first span from the support tends to be longer than other spans. This is a natural result when thinking about stress resultants at the top chord. In elements closer to midspan the axial force is weaker than in elements closer to midspan meaning that a longer buckling length can be allowed. The mean height in Type 1 was L/10.8 and in Type 2 L/10.4 which are in line with previous studies (Bzdawka & Heinisuo 2012, Tiainen, Heinisuo, Jokinen & Salminen 2012) and with Wardenier et al. who proposed $L/16 \ldots L/10$ (Wardenier et al. 2010). The large eccentricity at the first joint at the bottom chord (near the support) caused large moments to the first element of the bottom chord, but this element was not critical typically. The joint locations seemed to seek to values that shorten compressed member thus reducing buckling length meaning increased strength.

Using same gap width at each joint does not seem a good choice. The first joint at the bottom chord near the support should be smaller than others. At this joint two typically rather large members are joined and the axial forces are large. If gap is large the joint will be classified as two T-joints meaning lower strength. Still, for other joints large gap seems favourable. The upper bound 50 mm seemed to be too small since optimization lead to the upper bound in most cases. Allowing every gap to be design variable, the problem size also grows meaning that swarm size and number of iterations should be larger. Also the use of rectangular members together with square members may lead to better solutions but it also makes a substantial growth in problem size as the variety of available sections grows.

The environmental impact of S700 is only 5 - 10 % higher than that of S355 depending on indicator (Stroetmann 2012, Sperle 2012). This means that achieved weight reductions lead to more ecological structures.

The reliability of the results using stochastic optimization method with no convergence check possibility is always an issue. In this paper, the results were generated with a rather large number of extensive optimization runs. For every material combination, same parameter values were used. Thus, it seems fair to state that the results can be considered reliable. Even if the best found solutions are not actual optima of the problems fair comparison between the performance of different steel materials in a tubular truss can be made.

Convergence of a single run might be poor and thus multiple runs are needed. As computational time of even a single run is quite long, it seems that optimization approach used in this research paper is not applicable in practical design work without improvement.

Many research questions remain still open. The approach presented could be used in other types of trusses as well. Also, in order to get full economical benefit of HSS, the design rules should be checked thoroughly and updated where needed. Present rules either do not include any guidance or the formulas are very conservative. For example the full strength welds are very large and thus expensive using HSS. Also, the strength factor of 0.8 for HSS joints should be checked. In addition, in some research work it has been found that HSS products could use more favourable buckling curves than proposed by current Eurocode (Rasmussen & Hancock 1994, Ban, Shi, Shi & Bradford 2013).

5 Conclusions

Starting point of the optimization should be the geometrical presentation of the truss in order to check all requirements, such as geometrical rules of codes and correct structural analysis model with eccentricities. In sizing and shape optimization this will result in non-linear mixed-integer optimization for which heuristic methods can used as shown in the paper. As the problems are very demanding and the method does not include checks for optimality, the result might be in some cases sub-optimal. However, by using the proposed optimization technique, the weight of the manually designed solution including evenly distributed joints could be reduced over 10 % allowing joint locations change during optimization.

Weight reductions compared to S355 trusses were for around 15–20 % for S500, 30–40 % for S700 and 40–50 % S960. The cost reduction seems to be effected on the truss type Warren type truss without verticals performing better, at around 10–20 % in comparison to S355 solution. Reductions for hybrid trusses were between these numbers, but for S700/S500 (chords S700, braces S500) the reductions were about the same as for S700/S700 trusses. Hybrid solutions, especially S700/355, seem attractive when considering both weight and cost savings.

The results imply that the use of HSS is economical in tubular trusses applying the design rules of the present Eurocodes even though some of the rules ”penalize” high strength steels. These issues should be solved in the future and the fabrication costs of HSS tubular trusses can be reduced and more savings achieved.

Acknowledgements

This research has been completed in RFCS project RUOSTE. Funding of RFCS is gratefully acknowledged.

References

Ban, H., Shi, G., Shi, Y. & Bradford, M. A. (2013), ‘Experimental investigation of the overall buckling behaviour of 960 MPa high strength steel columns’, *Journal of constructional steel research* **88**, 256–266.

Bzdawka, K. & Heinisuo, M. (2012), *Optimization of Planar Tubular Truss with Eccentric Joint*, Tampere University of Technology. Research Report 157.

Carter, C. J., Murray, T. M. & Thornton, W. A. (2000), ‘Cost-effective steel building design’, *Progress in structural engineering and materials* **2**, 16–25.

Cederfeldt, L. & Sperle, J.-O. (2012), High strength steel in the roof of Swedbank arena savings in weight, cost and environmental impact, *in* ‘Proceedings of Nordic Steel Construction Conference’, Oslo.

CEN (2006*a*), *EN-1993-1-1. Eurocode 3: Design of steel structures. Part 1-1: General rules and rules for buildings.*

CEN (2006*b*), *EN-1993-1-12. Eurocode 3: Design of steel structures. Part 1-12: General - High strength steels.*

CEN (2006*c*), *EN-1993-1-8. Eurocode 3: Design of steel structures. Part 1-8: Design of joints.*

EN 10219-2 (2006), *Cold formed welded structural hollow sections of non-alloy and fine grain steels. Part 2: Tolerances, dimensions and sectional properties*, CEN.

Evers, H. G. A. & Maatje, I. F. (2000), Cost based engineering and production of steel constructions, *in* 'Connections in steel structures IV', Roanoke, Virginia, USA, pp. 14–22.

Farkas, J., Simões, L. M. C. & Jármai, K. (2005), 'Minimum cost design of a welded stiffened square plate loaded by biaxial compression', *Structural and Multidisciplinary Optimization* **29**, 298–303.

Günther, H.-P. (2005), *Use and Application of High-Performance Steels for Steel Structures*, IABSE.

Haapio, J. (2012), Feature-Based Costing Method for Skeletal Steel Structures based on the Process Approach, Phd thesis, Tampere University of Technology.

Heinisuo, M., Laasonen, M., Ronni, H. & Anttila, T. (2010), Integration of joint design of steel structures using product model, *in* W. T., ed., 'Proceedings of The International Conference: Computing in Civil and Building Engineering', Nottingham, pp. 323–324.

Heinisuo, M., Möttönen, A., Paloniemi, T. & Nevalainen, P. (1991), Automatic design of steel frames in a cad-system, *in* 'Proceedings of the 4th Finnish Mechanics days', Lappeenranta.

Jalkanen, J. (2007), Tubular Truss Optimization Using Heuristic Algorithms, Phd thesis, Tampere University of Technology.

Jármai, K. & Farkas, J. (1999), 'Cost calculation and optimisation of welded steel structures', *Journal of Constructional Steel Research* **50**, 115–135.

Jármai, K. & Farkas, J. (2001), 'Optimum cost design of welded box beams with longitudinal stiffeners using advanced backtrack method', *Structural and Multidisciplinary Optimization* **21**, 52–59.

Kennedy, J. & Eberhart, R. (1995), Particle swarm optimization, *in* 'IEEE International Conference on Neural Networks, Vol. 4', pp. 1942–1948.

Mat (2011), *Matlab R2011a*.

Nethercot, D. A. (1998), 'Towards a standardization of the design and detailing of connections', *Journal of constructional Steel Research* **46**, 3–4.

Ongelin, P. & Valkonen, I. (2012), *Rakenneputket*, Rautaruukki Oyj. in Finnish.

Pavlovčič, L., Krajnc, A. & Beg, D. (2004), 'Cost function analysis in the structural optimization of steel frames', *Structural and Multidisciplinary Optimization* **28**, 286–295.

Rasmussen, K. J. R. & Hancock, G. J. (1994), 'Tests of high strength steel columns', *Journal of constructional steel research* **34**, 27–52.

Salokangas, J. (2009), *Costs in steel construction (Teräsrakentamisen kustannukset)*, Teräsrakenneyhdistys. in Finnish.

Sarma, K. C. & Adeli, H. (2000), 'Cost optimization of steel structures', *Engineering Optimization* **32**, 777–802.

Sperle, J.-O. (2012), Environmental advantages of using advanced high strength steel in steel structures, *in* 'Proceedings of Nordic Steel Construction Conference', Oslo.

Stroetmann, R. (2012), Sustainable design of steel structures with high strength steels, *in* 'Proceedings of Nordic Steel Construction Conference', Oslo.

Tiainen, T., Heinisuo, M., Jokinen, T. & Salminen, M. (2012), 'Steel building optimization using metamodel technique', *Rakenteiden Mekaniikka* **45**, 152—-161.

Wardenier, J., Packer, J. A., Zhao, X.-L. & van der Vegte, G. (2010), *Hollow sections in structural applications 2nd edition*, Cidect.

Watson, K. B., Dallas, S., Van der Kreek, N. & Main, T. (1996), 'Costing of steelwork from feasibility through to completion', *Journal of Australian Steel Construction* **30**, 2–9.

Publication III

Title: Mixed-integer linear programming approach for global discrete sizing optimization of frame structures
Authors: Roxane Van Mellaert, Kristo Mela, Teemu Tiainen, Markku Heinisuo, Geert Lombaert, Mattias Schevenels
Journal: Structural and multi–disciplinary optimization
Volume: 57
Issue: 2
Pages: 579 –593

Accepted manuscript printed on kind permission from Springer–Verlag.

Original available at https://doi.org/10.1007/s00158-017-1770-9

Structural and Multidisciplinary Optimization manuscript No.
(will be inserted by the editor)

Mixed-integer linear programming approach for global discrete sizing optimization of frame structures

R. Van Mellaert[1] · **K. Mela**[2] · **T. Tiainen**[2] · **M. Heinisuo**[2] · **G. Lombaert**[3] · **M. Schevenels**[1]

Received: date / Accepted: date

Abstract This paper focuses on discrete sizing optimization of frame structures using commercial profile catalogs. The optimization problem is formulated as a mixed-integer linear programming (MILP) problem by including the equations of structural analysis as constraints. The internal forces of the members are taken as continuous state variables. Binary variables are used for choosing the member profiles from a catalog. Both the displacement and stress constraints are formulated such that for each member limit values can be imposed at predefined locations along the member. A valuable feature of the formulation, lacking in most contemporary approaches, is that global optimality of the solution is guaranteed by solving the MILP using branch-and-bound techniques. The method is applied to three design problems: a portal frame, a two-story frame with three load cases and a multiple-bay multiple-story frame. Performance profiles are determined to compare the MILP reformulation method with a genetic algorithm.

Keywords Global optimization · discrete optimization · sizing optimization · frame structures · mixed-integer linear programming

R. Van Mellaert
Tel.: +32 16 32 13 68
E-mail: roxane.vanmellaert@kuleuven.be

[1]Department of Architecture, Faculty of Engineering Science, KU Leuven, Kasteelpark Arenberg 1 box 2431, 3001 Leuven, Belgium

[2]Department of Civil Engineering, Tampere University of Technology, Finland

[3]Department of Civil Engineering, Faculty of Engineering Science, KU Leuven, Belgium

List of Symbols

$\mathcal{M}$	set of all member indices
$\mathcal{C}_i$	profile catalog for member i
y_{ij}	binary decision variable selecting profile j for member i
c_{ij}	cost for member i [a]
$\mathbf{f}$	nodal load vector [b]
$\mathbf{u}$	nodal displacement vector
$\mathbf{K}_{ij}$	element stiffness matrix for member i [a]
$\mathbf{B}_i$	binary location matrix mapping system dofs to element dofs for member i
$\mathbf{T}_i$	transformation matrix accounting for the orientation of member i
$\mathbf{R}_i$	matrix relating six dependent member end forces to three independent member end forces for member i [b]
$\mathbf{q}_{ij}$	member end forces for member i [a,b]
$\bar{\mathbf{q}}'_{ij}$, $\underline{\mathbf{q}}'_{ij}$	artificial upper/lower bounds for $\mathbf{q}_{ij}$
$\mathbf{d}_{ij}$	displacements of member i [a,c]
$\mathbf{D}_i$	displacement shape functions for member i [b,c]
$\tilde{\mathbf{d}}_{ij}$	displacements of member i in clamped-clamped conditions [a,c]
$\bar{\mathbf{d}}_{ij}$, $\underline{\mathbf{d}}_{ij}$	maximum/minimum allowed values for $\mathbf{d}_{ij}$ [c]
$\bar{\mathbf{d}}'_{ij}$, $\underline{\mathbf{d}}'_{ij}$	artificial upper/lower bounds for $\mathbf{d}_{ij}$ [c]
$\mathbf{s}_{ij}$	stresses in member i [a,c]
$\mathbf{S}_{ij}$	stress shape functions for member i [a,b,c]
$\tilde{\mathbf{s}}_{ij}$	stresses in member i in clamped-clamped conditions [a,c]
$\bar{\mathbf{s}}_{ij}$, $\underline{\mathbf{s}}_{ij}$	maximum/minimum allowed values for $\mathbf{s}_{ij}$ [c]
$\bar{\mathbf{s}}'_{ij}$, $\underline{\mathbf{s}}'_{ij}$	artificial upper/lower bounds for $\mathbf{s}_{ij}$ [c]

[a] assuming that profile j is selected.
[b] assuming that non-nodal loads are replaced with equivalent nodal loads.

[c] these matrices and vectors refer to displacements or stresses at a limited number of prescribed output locations along member i.

1 Introduction

In structural optimization, the problem formulation plays a fundamental role. The mathematical structure of the optimization problem determines which solution methods can be applied, and how difficult it is to find the optimal solution. From the designer's perspective, the problem should include the necessary requirements of design, manufacture and economy [1] such that the results of optimization are applicable in practice. In general, the problem formulation is a compromise between meeting the needs of the designer and the capabilities of contemporary solution procedures.

In practical optimization of frame structures, the member profiles must be chosen from a catalog of commercially available sections. When this feature is coupled with conventional formulations based on elastic structural analysis, the problem is not only nonlinear [2], but it also contains discrete design variables. The resulting mixed-integer nonlinear programming (MINLP) problem can be treated by several optimization methods that have been proposed in the literature on discrete structural design of frames (for reviews, see [3–6]). However, these methods have in common that they cannot guarantee that the global optimum is found.

In a detailed review, Arora [6] discusses various methods for structural optimization with discrete variables. These include branch-and-bound for nonlinear problems, sequential linearization, dynamic rounding-off, penalty approach and various stochastic methods, among others. Some of the more recent approaches include the discrete Lagrangian-based algorithm [7], and a scheme based on the optimality criteria method [8].

Currently, stochastic algorithms are widely used for solving discrete frame optimization problems. These methods include genetic algorithms [9–12], ant colony optimization [13,14], firefly algorithm [15,16], harmony search algorithm [17], particle swarm optimization [18], guided stochastic search heuristic [19], eagle strategy with differential evolution [20], and teaching-learning based optimization [21]. The general idea is to explore the design space in a random fashion, thereby using information collected from previous analyses to gradually improve the design. These algorithms owe their popularity to the fact that they are easy to understand and to implement. They can cope with discrete parameters and are able to take into account complex constraints. However, stochastic algorithms converge slowly, involve algorithmic parameters that require careful tuning, and global optimality cannot be guaranteed since no conclusive convergence checks can be made.

In this paper, global discrete sizing optimization of frame structures is considered. The weight of the structure is minimized, taking into account stress and displacement constraints. The optimization problem is reformulated into a mixed-integer linear programming (MILP) problem. In the classical approach for structural optimization the nested analysis and design (NAND) approach is employed [22]: in every iteration a finite element analysis is performed in order to obtain the state variables (the structural nodal displacements and the member end forces). In order to facilitate the reformulation of the optimization problem as an MILP, the simultaneous analysis and design (SAND) approach [22] is adopted in this study: the state variables are considered as additional design variables and the state equations (the equilibrium equations and member stiffness relations) are enforced by means of additional constraints. In addition, a set of binary decision variables is introduced for each member of the structure to select a profile from the catalog given by the designer. The obtained MILP can be solved for global optimality with well-established algorithms such as branch-and-bound methods [23,24].

The MILP formulation approach has originally been proposed by Ghattas et al. [25] and Grossmann et al. [26] for discrete topology optimization of trusses, later studied by Rasmussen et al. [27], Faustino et al. [28], and Kanno et al. [29]. Mela [30] included member strength and buckling constraints specified by the Eurocode in the truss topology design problem. Van Mellaert et al. [31] included both the member and the joint constraints for sizing optimization of statically determinate trusses. Stolpe [32] proposed a mixed-integer linear programming reformulation approach to solve continuum topology optimization problems. Kureta et al. [33] developed a mixed integer programming approach for topology optimization of periodic frame structures with negative Poisson's ratio, and Hirota et al. [34] developed a mixed integer programming approach for the optimal design of periodic frame structures with negative thermal expansion.

The main differences in the mixed-integer linear programming problem between frames and trusses are related to structural analysis and member resistance constraints. In truss analysis, the only stress resultant is the normal force, which is constant in the member. Thus, for each member, a single state variable is required. For frames modeled with beam elements, shear forces and bending moments in addition to normal forces must be included in the analysis. Moreover, nodal rotations need to be considered in addition to displacements. Conse-

quently, the number of state variables and constraints related to structural analysis increases when the mixed-integer formulation is extended from trusses to frames.

The member resistance and deflection constraints for trusses are imposed by simply limiting the normal force and nodal displacement variables, respectively. For members of frames, the stress resultants typically vary along the member, which implies that resistance constraints must be considered at several locations and not only at member ends. This applies also for deflection constraints. Furthermore, the interaction of stress resultants should be taken into account, which means that the resistance constraints become more complicated than simple bounds on the state variables.

This study focuses on the computational efficiency of the mixed-integer linear programming approach for the discrete sizing optimization of frames. The MILP formulation for topology optimization presented in [32–34] is adopted for sizing optimization. However, the formulation is extended to take into account non-nodal loads. In addition, catalogs consisting of 9 to 24 available profiles are adopted, instead of the smaller catalogs consisting of 3 profiles adopted for the MILP frame problems presented in the literature.

The paper is organized as follows. In Section 2, the mixed-integer linear programming problem for frame optimization is presented: the design variables as well as the constraints are described in detail. In Section 3, the formulation is applied to three example problems: a simple portal frame with an inclined roof, a two-story frame with three load cases, and a three-bay three-story frame. In addition, the performance of the MILP reformulation method is compared with the performance of a genetic algorithm by solving several multiple-bay multiple-story frame problems. Section 4 summarizes the main findings of this study.

2 Mixed-integer linear programming formulation

This section describes the mixed-integer linear programming formulation for the discrete sizing optimization of frame structures. The formulation is written for plane frames with prismatic members analyzed by the theory of linear elasticity. For simplicity, it is assumed that all members are made of the same material. Moreover, only a single load case is considered, but the formulation can easily be extended to multiple load cases. Non-nodal loads are replaced with equivalent nodal loads in the formulation of the problem. The joints are assumed to be rigid, although hinged connections can be incorporated into the formulation.

Consider a frame structure defined by n_m members and n_n nodes with n_dof degrees of freedom. The number of profile alternatives is n_s. Denote by $\mathcal{M} = \{1, 2, \ldots, n_\mathrm{m}\}$ and $\mathcal{C} = \{1, 2, \ldots, n_\mathrm{s}\}$ the index sets for members and profiles. Each member may have its own set of profile alternatives. The index set of profiles of member i is denoted by $\mathcal{C}_i \subseteq \mathcal{C}$.

2.1 Design variables

The design variables include a vector of binary decision variables $\mathbf{y}$, a vector of continuous nodal displacement variables $\mathbf{u}$ (including translations and rotations), and a vector of continuous member end forces $\mathbf{q}$ (caused by the equivalent nodal loads). The binary variables are employed to select member profiles from the set of available alternatives. For member i, profile j is selected when the corresponding variable $y_{ij} = 1$. Profile j is not selected for member i when the corresponding variable $y_{ij} = 0$. For each member i and for each section j a set of three independent member end forces is defined, including the normal end force $N_{1,ij}$, and the bending moment end forces $M_{1,ij}$ and $M_{2,ij}$ as shown in Fig. 1. The member end forces for each member i and for each section j are collected in the vector $\mathbf{q}_{ij}$:

$$\mathbf{q}_{ij} = \begin{bmatrix} N_{1,ij} & M_{1,ij} & M_{2,ij} \end{bmatrix}^\mathrm{T} \tag{1}$$

Fig. 1: Member end forces.

The vector with the design variables $\mathbf{x}$ is given by:

$$\mathbf{x} = \begin{bmatrix} \mathbf{y}^\mathrm{T} & \mathbf{u}^\mathrm{T} & \mathbf{q}^\mathrm{T} \end{bmatrix}^\mathrm{T}, \quad \mathbf{y} \in \mathbb{B}^{n_\mathrm{b}}, \mathbf{u} \in \mathbb{R}^{n_\mathrm{dof}}, \mathbf{q} \in \mathbb{R}^{3n_\mathrm{b}} \tag{2}$$

The total number of binary decision variables is denoted by $n_\mathrm{b} = \sum_{i=1}^{n_\mathrm{m}} n_{\mathrm{s}i}$, where n_m is the total number of members in the structure, and $n_{\mathrm{s}i}$ is the total number of available sections for member i. The total number of degrees of freedom is denoted by n_dof. The total number of force variables is $3n_\mathrm{b}$. The total number of design variables is calculated as $n_\mathrm{dv} = n_\mathrm{dof} + 4n_\mathrm{b}$.

2.2 Problem statement

The mixed-integer linear programming problem for a frame structure is given by Eqs. (3) through (9):

$$\min_{\mathbf{x}} \sum_{i\in\mathcal{M}} \sum_{j\in\mathcal{C}_i} c_{ij} y_{ij} \tag{3}$$

such that

$$\sum_{j\in\mathcal{C}_i} y_{ij} = 1 \qquad \forall\, i \in \mathcal{M} \tag{4}$$

$$\sum_{i\in\mathcal{M}} \sum_{j\in\mathcal{C}_i} \mathbf{B}_i^{\mathrm{T}} \mathbf{T}_i^{\mathrm{T}} \mathbf{R}_i \mathbf{q}_{ij} = \mathbf{f} \tag{5}$$

$$(1-y_{ij})\underline{\mathbf{q}}'_{ij} \leqslant \mathbf{K}_{ij}\mathbf{T}_i\mathbf{B}_i\mathbf{u} - \mathbf{q}_{ij} \leqslant (1-y_{ij})\bar{\mathbf{q}}'_{ij} \qquad \forall\, i \in \mathcal{M},\, \forall\, j \in \mathcal{C}_i \tag{6}$$

$$y_{ij}\underline{\mathbf{q}}'_{ij} \leqslant \mathbf{q}_{ij} \leqslant y_{ij}\bar{\mathbf{q}}'_{ij} \qquad \forall\, i \in \mathcal{M},\, \forall\, j \in \mathcal{C}_i \tag{7}$$

$$\underline{\mathbf{d}}'_{ij} + y_{ij}(\underline{\mathbf{d}}_{ij} - \underline{\mathbf{d}}'_{ij}) \leqslant \mathbf{D}_i\mathbf{T}_i\mathbf{B}_i\mathbf{u} + \tilde{\mathbf{d}}_{ij} \leqslant \bar{\mathbf{d}}'_{ij} + y_{ij}(\bar{\mathbf{d}}_{ij} - \bar{\mathbf{d}}'_{ij}) \qquad \forall\, i \in \mathcal{M},\, \forall\, j \in \mathcal{C}_i \tag{8}$$

$$\underline{\mathbf{s}}'_{ij} + y_{ij}(\underline{\mathbf{s}}_{ij} - \underline{\mathbf{s}}'_{ij}) \leqslant \mathbf{S}_{ij}\mathbf{T}_i\mathbf{B}_i\mathbf{u} + \tilde{\mathbf{s}}_{ij} \leqslant \bar{\mathbf{s}}'_{ij} + y_{ij}(\bar{\mathbf{s}}_{ij} - \bar{\mathbf{s}}'_{ij}) \qquad \forall\, i \in \mathcal{M},\, \forall\, j \in \mathcal{C}_i \tag{9}$$

The objective function is given by Eq. (3), where c_{ij} is the cost of profile j for member i. When the structural weight is taken as the objective function, c_{ij} is the weight of member i with profile j, and it can be written as $c_{ij} = \rho L_i A_{ij}$, where ρ is the density of the material, L_i is the length of member i, and A_{ij} is the section area of profile j for member i. Alternatively, c_{ij} can be written as $c_{ij} = L_i w_{ij}$, where $w_{ij} = \rho_{ij} A_{ij}$ is the weight per unit length of profile j for member i. This expression can be used, if multiple materials are included in the problem.

The subsequent equations are the constraints of the optimization problem. Eq. (4) ensures that a single profile j is chosen from the catalog $\mathcal{C}_i$ for member i. The equilibrium equations and the member stiffness relations are given by Eqs. (5) and (6), respectively. Eq. (7) ensures that if profile j is not selected for member i, the corresponding force variables become zero, i.e. $\mathbf{q}_{ij} = \mathbf{0}$. The derivation of Eqs. (3-7) is given in Appendix A. The displacements and stresses at predefined locations of member i are limited by the constraints of Eqs. (8) and (9), respectively. The derivation of these constraints is given in the subsequent sections. A list of symbols is provided at the beginning of the paper.

It is possible to take into account multiple load cases by introducing additional nodal displacement and force variables and constraints of Eqs. (5) to (9) for each load case [30].

2.3 Displacements along elements

Constraints on deflections along the members are expressed in terms of nodal values using interpolation with shape functions. The idea is that the designer defines *a priori* the locations where chosen displacement components are restricted.

The displacement along the local x-axis as defined in Fig. 2 at location $x \in [0, L_i]$ of member i for profile j is calculated as:

$$u_{ij}(x) = \mathbf{D}_i^u(x)\mathbf{T}_i\mathbf{B}_i\mathbf{u} + \tilde{u}_{ij}(x) \tag{10}$$

where $\tilde{u}_{ij}(x)$ is the displacement at location x of member i due to the element loads, assuming that profile j is selected and that the member ends are clamped. This term compensates for the fact that non-nodal loads are replaced by equivalent nodal loads in the formulation of the problem. The displacements along the local y-axis $v_{ij}(x)$, and the rotation $\varphi_{ij}(x)$ are calculated in the same way. The shape function vectors $\mathbf{D}_i^u(x)$, $\mathbf{D}_i^v(x)$ and $\mathbf{D}_i^\varphi(x)$ are given by Eqs. (44) to (46) in section A.3.

The constrained displacement components of element i with profile j at the locations x_k of interest are collected in the vector $\mathbf{d}_{ij}$. For example, if the transverse displacement v_i of element i is to be constrained at the locations x_1, x_2, and x_3, the vector $\mathbf{d}_{ij}$ is given by:

$$\mathbf{d}_{ij} = \begin{bmatrix} v_{ij}(x_1) \\ v_{ij}(x_2) \\ v_{ij}(x_3) \end{bmatrix} \tag{11}$$

This vector is obtained as follows:

$$\mathbf{d}_{ij} = \mathbf{D}_i\mathbf{T}_i\mathbf{B}_i\mathbf{u} + \tilde{\mathbf{d}}_{ij} \tag{12}$$

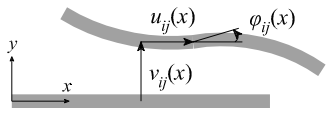

Fig. 2: Local displacements

where the matrix $\mathbf{D}_i$ and the vector $\tilde{\mathbf{d}}_{ij}$ are (in this case):

$$\mathbf{D}_i = \begin{bmatrix} \mathbf{D}_i^v(x_1) \\ \mathbf{D}_i^v(x_2) \\ \mathbf{D}_i^v(x_3) \end{bmatrix} \qquad \tilde{\mathbf{d}}_{ij} = \begin{bmatrix} \tilde{v}_{ij}(x_1) \\ \tilde{v}_{ij}(x_2) \\ \tilde{v}_{ij}(x_3) \end{bmatrix} \tag{13}$$

In order to limit the relevant displacement components at all predefined locations of member i, the constraints given by Eq. (8) are introduced, where $\underline{\mathbf{d}}_{ij}$ and $\bar{\mathbf{d}}_{ij}$ are the prescribed minimum and maximum allowed value of displacements, respectively. The artificial bounds $\underline{\mathbf{d}}'_{ij}$ and $\bar{\mathbf{d}}'_{ij}$ ensure that when profile j is not selected for member i, the constraints Eq. (8) do not impose any limits on the nodal displacements $\mathbf{u}$. When profile j is selected for member i ($y_{ij} = 1$), Eq. (8) becomes $\underline{\mathbf{d}}_{ij} \leqslant \mathbf{D}_i\mathbf{T}_i\mathbf{B}_i\mathbf{u} + \tilde{\mathbf{d}}_{ij} \leqslant \bar{\mathbf{d}}_{ij}$ and the appropriate displacement components are constrained. When profile j is not selected for member i ($y_{ij} = 0$), Eq. (8) reduces to $\underline{\mathbf{d}}'_{ij} \leqslant \mathbf{D}_i\mathbf{T}_i\mathbf{B}_i\mathbf{u} + \tilde{\mathbf{d}}_{ij} \leqslant \bar{\mathbf{d}}'_{ij}$. The bounds $\underline{\mathbf{d}}'_{ij}$ and $\bar{\mathbf{d}}'_{ij}$ are calculated similarly to $\underline{\mathbf{q}}'_{ij}$ and $\bar{\mathbf{q}}'_{ij}$ (Eqs. (42) and (43)) for each row k of matrix $\mathbf{D}_i$ and vector $\tilde{\mathbf{d}}_{ij}$ as:

$$\underline{d}'_{k,ij} = \min_{\mathbf{u}} \quad \mathbf{D}_{k,i}\mathbf{T}_i\mathbf{B}_i\mathbf{u} + \tilde{\mathbf{d}}_{k,ij} \qquad \text{s.t.} \quad \underline{\mathbf{u}} \leqslant \mathbf{u} \leqslant \overline{\mathbf{u}} \tag{14}$$

$$\bar{d}'_{k,ij} = \max_{\mathbf{u}} \quad \mathbf{D}_{k,i}\mathbf{T}_i\mathbf{B}_i\mathbf{u} + \tilde{\mathbf{d}}_{k,ij} \qquad \text{s.t.} \quad \underline{\mathbf{u}} \leqslant \mathbf{u} \leqslant \overline{\mathbf{u}} \tag{15}$$

where $\underline{\mathbf{u}}$ and $\overline{\mathbf{u}}$ are the minimum and maximum allowed nodal displacements, respectively.

When only nodal displacements are limited, the constraints given by Eq. (8) can be substituted by the following constraints:

$$\underline{\mathbf{u}} \leqslant \mathbf{u} \leqslant \overline{\mathbf{u}} \tag{16}$$

2.4 Stresses

The resistance of cross-sections subjected to shear forces, normal forces, and bending moments is checked at predefined locations along the members. For elastic design, the resistance constraints can be written in terms of stresses as:

$$\sigma_{\min} \leqslant \sigma_{\mathrm{t},ij}(x) \leqslant \sigma_{\max} \tag{17}$$

where $\sigma_{\mathrm{t},ij}(x)$ is the normal stress at the top fiber of the cross-section of member i for profile j at location x. The normal stress at the bottom fiber of the cross-section $\sigma_{\mathrm{b},ij}(x)$, and the maximum shear stress $\tau_{ij}(x)$ of member i for profile j at location x are limited in the same way. These stresses are calculated as

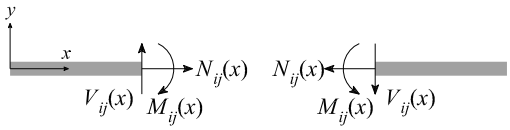

Fig. 3: Internal forces of member i for profile j at location x

$$\sigma_{\mathrm{t},ij}(x) = \frac{N_{ij}(x)}{A_{ij}} + \frac{M_{ij}(x)}{W_{\mathrm{t},ij}} \tag{18}$$

$$\sigma_{\mathrm{b},ij}(x) = \frac{N_{ij}(x)}{A_{ij}} - \frac{M_{ij}(x)}{W_{\mathrm{b},ij}} \tag{19}$$

$$\tau_{ij}(x) = \frac{V_{ij}(x)S_{ij}}{I_{ij}b_{ij}} \tag{20}$$

where $W_{\mathrm{t},ij}$ and $W_{\mathrm{b},ij}$ are the section moduli with respect to the top and bottom fibers of the cross-section, respectively, I_{ij} is the second moment of area, S_{ij} is the first moment of area, and b_{ij} is the width of the profile at the point where the maximum shear stress occurs. $N_{ij}(x)$, $V_{ij}(x)$, and $M_{ij}(x)$ are, respectively, the normal force, shear force, and bending moment at location x as given by Fig. 3. For plastic design, similar constraints related to the stress resultants can be formulated.

The stress $\sigma_{\mathrm{t},ij}(x)$ at location x of member i for profile j is calculated as:

$$\sigma_{\mathrm{t},ij}(x) = \mathbf{S}_{ij}^{\sigma_{\mathrm{t}}}(x)\mathbf{T}_i\mathbf{B}_i\mathbf{u} + \tilde{\sigma}_{\mathrm{t},ij}(x) \tag{21}$$

where $\tilde{\sigma}_{\mathrm{t},ij}(x)$ is the stress of the beam at location x due to the element loads, assuming that profile j is selected and that the member ends are clamped, calculated in a similar way as given by Eq. (18). The stresses $\sigma_{\mathrm{b},ij}(x)$ and $\tau_{ij}(x)$ are calculated in the same was as in Eq. (21).

The stresses can be calculated from the nodal displacements $\mathbf{u}$ using the vectors $\mathbf{S}_i^{\sigma_{\mathrm{t}}}(x)$, $\mathbf{S}_i^{\sigma_{\mathrm{b}}}(x)$ and $\mathbf{S}_i^{\tau}(x)$, which are given by Eqs. (47) to (49) in section A.4. Stress constraints have been treated similarly in the literature [33,34], but only for point loads located at the element nodes. The proposed formulation of Eq. (21) takes into account distributed loads and point loads not located at the nodes.

The constrained stress components $\sigma_{\mathrm{t},ij}$, $\sigma_{\mathrm{b},ij}$ and/or τ_{ij} of element i with profile j at locations x_k are collected in the vector $\mathbf{s}_{ij}$. For example, if the normal stress at the top of element i is to be constrained at locations x_1, x_2, and x_3, the vector $\mathbf{s}_{ij}$ is given by:

$$\mathbf{s}_{ij} = \begin{bmatrix} \sigma_{\mathrm{t},ij}(x_1) \\ \sigma_{\mathrm{t},ij}(x_2) \\ \sigma_{\mathrm{t},ij}(x_3) \end{bmatrix} \tag{22}$$

This vector is obtained as follows:

$$\mathbf{s}_{ij} = \mathbf{S}_{ij}\mathbf{T}_i\mathbf{B}_i\mathbf{u} + \tilde{\mathbf{s}}_{ij} \tag{23}$$

where $\mathbf{S}_{ij}$ and $\tilde{\mathbf{s}}_{ij}$ are in this case

$$\mathbf{S}_{ij} = \begin{bmatrix} \mathbf{S}_{ij}^{\sigma_t}(x_1) \\ \mathbf{S}_{ij}^{\sigma_t}(x_2) \\ \mathbf{S}_{ij}^{\sigma_t}(x_3) \end{bmatrix} \qquad \tilde{\mathbf{s}}_{ij} = \begin{bmatrix} \tilde{\sigma}_{t,ij}(x_1) \\ \tilde{\sigma}_{t,ij}(x_2) \\ \tilde{\sigma}_{t,ij}(x_3) \end{bmatrix} \tag{24}$$

In general, the stress constraints at predefined locations along the members are written in the form of Eq. (9), where $\tilde{\mathbf{s}}_{ij}$ is a vector containing the selected stress components at the predefined locations of the beam with clamped-clamped boundary conditions subjected to the element loads of member i for profile j, and $\underline{\mathbf{s}}_{ij}$ and $\bar{\mathbf{s}}_{ij}$ are the prescribed minimum and maximum allowed stresses. The artificial bounds $\underline{\mathbf{s}}'_{ij}$ and $\bar{\mathbf{s}}'_{ij}$ serve the same purpose as the bounds $\bar{\mathbf{d}}'_{ij}$ and $\underline{\mathbf{d}}'_{ij}$, i.e. they ensure that if profile j is not selected for member i, the nodal displacements are not constrained by Eq. (9). They are computed analogously to Eqs. (14) and (15), using $\tilde{\mathbf{s}}_{ij}$ instead of $\tilde{\mathbf{d}}_{ij}$.

3 Test problems and optimization results

In this Section, the mixed-integer linear programming formulation presented above is applied to three test problems. Firstly, a simple portal frame with an inclined roof subjected to a distributed load is considered. This problem is employed to verify the method because it can also be solved by complete enumeration. Secondly, a two-story frame benchmark problem reported in the literature is treated. Finally, a three-bay three-story frame is considered. This problem represents a case where the optimum design is not easy to find by enumeration.

All test problems are solved by the commercial software Gurobi [37]. The software employs the branch-and-cut method [23], where cutting planes and other enhancements are incorporated in the general branch-and-bound framework in order to reduce the computational time. Several parameters for controlling the details of the algorithm are available. In this study, the default values of these parameters are used, except for feasibility and integer tolerances, respectively, which are set to values given below. Thus, the crucial decisions of the branch-and-cut algorithm, e.g. branching strategy and cutting plane selection, are governed by the software.

According to the principle of branch-and-bound, in each iteration, a lower bound of the objective function, f_{LB}, is computed by solving a linear programming relaxation of the problem, where integer variables are treated as continuous. This lower bound increases over the iterations, whereas the upper bound of the optimum, f_{UB}, decreases as better feasible solutions are found. At any time, the *optimality gap*, defined by

$$\text{Gap} = \frac{f_{UB} - f_{LB}}{f_{UB}} \tag{25}$$

can be calculated to measure the quality of the solution. When the optimality gap becomes 0, the global optimality of the solution is verified. For numerical purposes, a small positive value is employed.

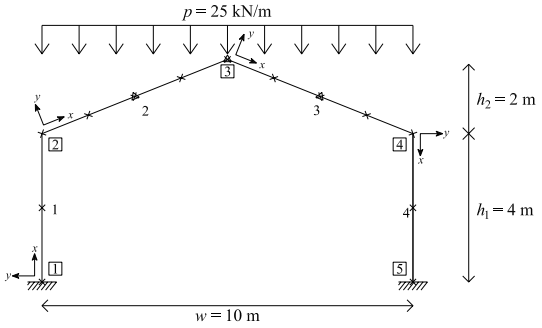

Fig. 4: Schematic of the portal frame. The displacements are constrained at the locations indicated by a triangle (△), the stresses are constrained at the locations indicated by a cross (×).

3.1 Portal frame

Fig. 4 shows a portal frame structure with four members. The height of the frame is $h_1 = 4\,\text{m}$ and $h_2 = 2\,\text{m}$, the span of the frame is $w = 10\,\text{m}$, the value of the distributed load is $p = 25\,\text{kN/m}$.

The objective of the optimization problem is to minimize the weight of the structure. The members are made of steel, and the profiles are chosen from a catalog with 24 HEA alternatives (Table 1). The Young's modulus is 210 GPa, the density is $7850\,\text{kg/m}^3$, and the yield strength is $f_y = 235\text{MPa}$. The allowable normal stress is f_y, while the allowable shear stress is $f_y/\sqrt{3} = 136\text{MPa}$. For members 1 and 4 all stress components are limited at three equidistant locations including the end points of the members. For members 2 and 3 all stress components are limited at five equidistant locations including the end points of the members (see Fig. 4). The stress constraints are given by Eq. (9). For determining the components of the vector $\tilde{\mathbf{s}}_{ij}$ included in this equation, the normal force $\tilde{N}_i(x)$, shear force $\tilde{V}_i(x)$ and bending moment $\tilde{M}_i(x)$ of a beam representing member i with clamped-clamped boundary conditions subjected to the

element loads are required. For member 2 they are calculated as:

$$\tilde{N}_2(x) = \sin(\alpha_2)\cos(\alpha_2)px - \sin(\alpha_2)\frac{pw}{4} \tag{26}$$

$$\tilde{V}_2(x) = \cos^2(\alpha_2)px - \cos(\alpha_2)\frac{pw}{4} \tag{27}$$

$$\tilde{M}_2(x) = \cos^2(\alpha_2)\frac{px^2}{2} - \cos(\alpha_2)\frac{pw}{4}x + \frac{p}{12}\left(\frac{w}{2}\right)^2 \tag{28}$$

where $\alpha_2 = \tan^{-1}(h_2/(w/2))$ is the angle of inclination of member 2. The normal stresses $\tilde{\sigma}_{\mathrm{t},2j}(x)$ and $\tilde{\sigma}_{\mathrm{b},2j}(x)$ at the top and bottom of member 2 for profile j at location x, respectively, and the shear stresses $\tilde{\tau}_{2j}(x)$ at the neutral axis of member 2 for profile j at location x are then obtained by substituting $\tilde{N}_2(x)$, $\tilde{V}_2(x)$, and $\tilde{M}_2(x)$ in Eqs. (18) to (20).

For member 3, the normal force $\tilde{N}_3(x)$, shear force $\tilde{V}_3(x)$ and bending moment $\tilde{M}_3(x)$ are calculated as:

$$\tilde{N}_3(x) = -\sin(\alpha_3)\cos(\alpha_3)px + \sin(\alpha_3)\frac{pw}{4} \tag{29}$$

$$\tilde{V}_3(x) = \cos^2(\alpha_3)px - \cos(\alpha_3)\frac{pw}{4} \tag{30}$$

$$\tilde{M}_3(x) = -\cos^2(\alpha_3)\frac{px^2}{2} + \cos(\alpha_3)\frac{pw}{4}x + \frac{p}{12}\left(\frac{w}{2}\right)^2 \tag{31}$$

The stresses of the beam with clamped-clamped boundary conditions subjected to the element loads at location x of member 3 for profile j are calculated similarly as for member 2.

The maximum allowed displacement is $u_{\max} = 0.05$m. For member 2, the vertical displacement component is limited at $x_1 = L_2/2$ and $x_2 = L_2$, and for member 3 the vertical displacement component is limited at $x_1 = L_3/2$. The displacement constraints are given by Eq. (8). The vector containing the vertical displacements of member 2 at the predefined locations x_1 and x_2 is in this case given by:

$$\mathbf{d}_{2j} = \begin{bmatrix} u_{2j}(x_1)\sin\alpha_2 + v_{2j}(x_1)\cos\alpha_2 \\ u_{2j}(x_2)\sin\alpha_2 + v_{2j}(x_2)\cos\alpha_2 \end{bmatrix} \tag{32}$$

where $u_{2j}(x_k)$ and $v_{2j}(x_k)$ are the displacements along the local x- and y-axes, respectively, of member 2 at location x_k for profile j. The matrix $\mathbf{D}_2$ is:

$$\mathbf{D}_2 = \begin{bmatrix} \mathbf{D}_2^u(x_1)\sin\alpha_2 + \mathbf{D}_2^v(x_1)\cos\alpha_2 \\ \mathbf{D}_2^u(x_2)\sin\alpha_2 + \mathbf{D}_2^v(x_2)\cos\alpha_2 \end{bmatrix} \tag{33}$$

and the vector $\tilde{\mathbf{d}}_{2j}$ is:

$$\tilde{\mathbf{d}}_{2j} = \begin{bmatrix} \tilde{u}_{2j}(x_1)\sin\alpha_2 + \tilde{v}_{2j}(x_1)\cos\alpha_2 \\ \tilde{u}_{2j}(x_2)\sin\alpha_2 + \tilde{v}_{2j}(x_2)\cos\alpha_2 \end{bmatrix} \tag{34}$$

where $\tilde{u}_{2j}(x)$ and $\tilde{v}_{2j}(x)$ are derived from the constitutive relations between stress and strain according to the Euler-Bernoulli beam theory:

$$\tilde{u}_{2j}(x) = \frac{\sin(\alpha_2)\cos(\alpha_2)\,p}{2EA_{2j}}x^2 - \frac{\sin(\alpha_2)\,pw}{4EA_{2j}}x \tag{35}$$

$$\tilde{v}_{2j}(x) = -\frac{\cos^2(\alpha_2)\,p}{24EI_{2j}}x^4 + \frac{\cos(\alpha_2)\,pw}{24EI_{2j}}x^3 - \frac{pw^2}{96EI_{2j}}x^2 \tag{36}$$

The vector containing the vertical displacements of member 3 at the predefined location x_1 is:

$$\mathbf{d}_{3j} = \begin{bmatrix} u_{3j}(x_1)\sin\alpha_3 + v_{3j}(x_1)\cos\alpha_3 \end{bmatrix} \tag{37}$$

where $u_{3j}(x_1)$ and $v_{3j}(x_1)$ are the displacements along the local x- and y-axes, respectively, of member 3 at x_1 for profile j, and $\alpha_3 = -\tan^{-1}(h_2/(w/2))$ is the angle of inclination of member 3. The matrix $\mathbf{D}_3$, the vector $\tilde{\mathbf{d}}_{3j}$, and the displacement components $\tilde{u}_{3j}(x)$ and $\tilde{v}_{3j}(x)$ are composed in the same way as for member 2.

The sizing optimization problem is defined by Eqs. (3) to (9). The total number of members is $n_{\mathrm{m}} = 4$, and for each member the number of available profiles is $n_{\mathrm{s}} = 24$. Thus there are altogether $n_{\mathrm{b}} = 96$ binary decision variables, and $3n_{\mathrm{b}} = 288$ force variables, whereas the number of degrees of freedom is $n_{\mathrm{dof}} = 9$. Consequently, the problem consists of 393 design variables and 4765 constraints, and the constraint coefficient matrix contains 24000 nonzero elements. There are 4 equality constraints to ensure that only one profile is selected for each member (Eq. (4)), 9 nodal equilibrium equality constraints (Eq. (5)), 1152 member stiffness relation inequality constraints (Eq. (6)), 1152 force inequality constraints (Eq. (7)), 144 displacement inequality constraints (Eq. (8)), and 2304 stress inequality constraints (Eq. (9)). The number of profile combinations is $24^4 = 331776$. The problem is solved by Gurobi (version 6.0.2) on a computer with an Intel Core i7-5600U processor (2.6 GHz clock frequency) and 8 GB RAM. The feasibility tolerance is set to 10^{-9}, the integer feasibility tolerance is set to 10^{-9}, and the optimality gap (defined as the relative difference between the

Table 1: HEA profile catalog

Index	Section	Index	Section
1	HEA 100	13	HEA 340
2	HEA 120	14	HEA 360
3	HEA 140	15	HEA 400
4	HEA 160	16	HEA 450
5	HEA 180	17	HEA 500
6	HEA 200	18	HEA 550
7	HEA 220	19	HEA 600
8	HEA 240	20	HEA 650
9	HEA 260	21	HEA 700
10	HEA 280	22	HEA 800
11	HEA 300	23	HEA 900
12	HEA 320	24	HEA 1000

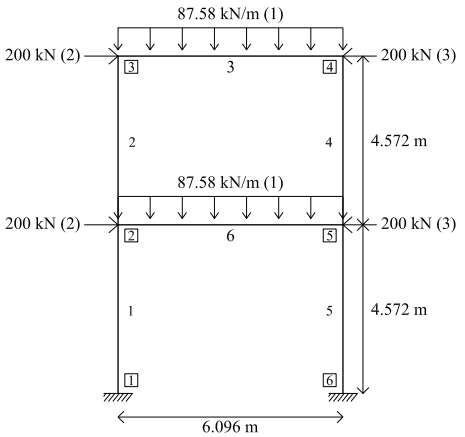

Fig. 5: Schematic of the two-story frame. The three load cases are indicated by (1), (2), and (3).

lower and upper objective bound) is set to 5×10^{-3}. The optimization problem is solved in 26 seconds, and 10510 nodes of the branch-and-bound tree are explored.

The optimum design is obtained by assigning the profile HEA 240 for all members. This can be explained by inspecting the force diagrams (Fig. 11). The critical cross-sections of all members have approximately equal normal forces and bending moments. This suggests that the same profile for all members produces approximately equal normal stresses at all critical cross-sections, which implies that a single profile for the entire frame should yield the minimum weight design as long as the normal stress constraints are decisive. In this case, the shear stress constraints and the displacement constraints are not critical. The total weight of the structure is 1131.63 kg. It is verified by full enumeration of all possible designs that this is indeed the global optimum.

Detailed results for this test problem are given in B, where the deformed shape of the frame, internal force diagrams and constraint margins evaluated at the optimum design are presented.

3.2 Two-story frame

Fig. 5 shows a two-story frame under three load cases. Sizing optimization of this structure has been considered in the literature by Chai et al. [38], Jivotovski [39], and Juang et al. [40]. The horizontal displacements of nodes 2 and 3 are limited to 2.54 cm, whereas the allowable normal stress in all members is 163860 $^{\mathrm{kN}}/_{\mathrm{cm}^2}$. The Young's modulus of the material is 206.88GPa, and the density is 76999.34 $^{\mathrm{N}}/_{\mathrm{cm}^3}$. The members are divided in 4 groups: the columns of the same story must have the same profile, the beams are designed independently. The catalog of available sections is given in Table 2.

Table 2: Profile catalog for the two-story frame

Index	Section area [cm^2]	Section modulus [cm^3]	First moment of area [cm^4]
1	118.39	1690.2	41623
2	144.92	2290.9	62435
3	167.34	2842.5	83246
4	187.10	3360.3	104058
5	204.96	3852.7	124869
6	221.37	4324.9	145681
7	236.66	4780.5	166492
8	251.02	5222.0	187304
9	264.59	5651.4	208115

The mixed-integer linear programming formulation is adopted for multiple load cases by including nodal displacement and member force variables for each load case. Moreover, the constraints of Eqs. (5) through (9) are written for each load case. Altogether, the sizing optimization problem of Eqs. (3) through (9) contains 576 variables (54 binary, 522 continuous) and 5268 constraints.

The MILP problem is solved by Gurobi (version 6.5) on a computer with an Intel Core i5-3470 processor (3.2 GHz clock frequency) and 16 GB RAM. The optimality gap is set to 5×10^{-3}, and default values are used for the other parameters. The runtime of the algorithm is 7 seconds, and 1461 nodes of the branch-and-bound tree are explored. At termination, the global optimality of the solution is verified. The weight of the solution is 42.53 kN. Profile number 5 is assigned to members 1 and 5, profile number 2 is assigned to members 2, 3, and 4, and profile number 7 is assigned to member 6 (see Table 1). This solution is the same as the solution reported by Juang and Chang, who have carried out a complete enumeration to verify that 42.53 kN is indeed the global optimum.

3.3 Three-bay three-story frame

Fig. 6 shows a three-bay three-story frame with 21 members. The height of each story is $h = 3.5\,\mathrm{m}$, the width of each bay is $w = 6\,\mathrm{m}$, the value of the horizontal load is $F = 22.05\,\mathrm{kN}$, and the value of the distributed vertical load is $p = 50.1\,^{\mathrm{kN}}/_{\mathrm{m}}$. The members are divided in seven groups, and in each group, all members must have the same profile. The beams (members 13 to 21) form one group, whereas, the columns are organized in six groups such that for each story, two groups are generated: the outer columns (members 1 and 4, 5 and 8, and 9 and 12) and inner columns (members 2 and 3, 6 and 7, and 10 and 11). Among group members, identical profiles are enforced by introducing additional linear constraints in

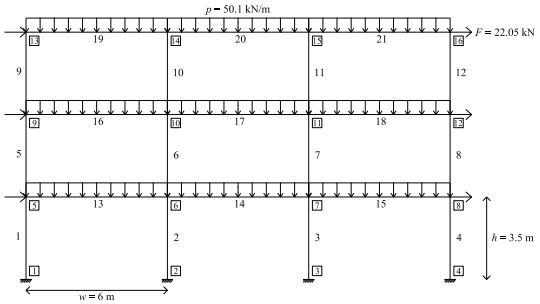

Fig. 6: Schematic of the three-bay three-story frame.

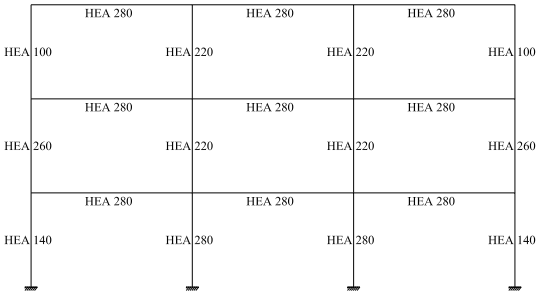

Fig. 7: Optimal design of the three-bay three-story frame

terms of the profile selection variables, y_{ij}. For example, the profiles of columns 1 and 4 are set to be identical by the following constraints:

$$y_{1j} = y_{4j} \quad \forall\, j \in \mathcal{C} \tag{38}$$

The objective of the optimization problem is to minimize the structural weight. In order to reduce the computation time, a limited set of available profiles is used: 15 profile alternatives ranging from HEA 100 to HEA 400 (Table 1) are included in the catalog. The material properties and allowed stresses are as in the previous example. For each member, all stress components are limited at three equidistant locations $x_1 = 0$, $x_2 = L_i/2$, and $x_3 = L_i$. For each column, the interstory drift, $\triangle u$, is limited by $h/300 = 0.0117\,\mathrm{m}$. For example, the interstory drift constraint of column 5 is

$$-\triangle u \leqslant u_9 - u_5 \leqslant \triangle u \tag{39}$$

where u_9, and u_5 are the horizontal displacements of nodes 9 and 5, respectively. The other interstory drift constraints are composed similarly. For each beam, the vertical deflection is limited at location $x_1 = L_i/2$ by $w/200 = 0.03\,\mathrm{m}$.

The minimum weight problem is given by Eqs. (3) through (9). The total number of members is $n_\mathrm{m} = 21$, and for each member the number of available profiles is $n_\mathrm{s} = 15$, resulting in $n_\mathrm{b} = 315$ binary decision variables. The number of force variables is $3n_\mathrm{b} = 945$, and the number of degrees of freedom is $n_\mathrm{dof} = 36$. The MILP consists of 1296 design variables, 13791 constraints, and the constraint coefficient matrix has 64195 nonzero elements. The number of design combinations is $15^7 = 171 \times 10^6$. There are 21 equality constraints to ensure that only one profile is selected for each member (Eq. (4)), 36 nodal equilibrium equality constraints (Eq. (5)), 3780 member stiffness relation inequality constraints (Eq. (6)), 3780 force inequality constraints (Eq. (7)), 270 deflection constraints (Eq. (8)), 5670 stress inequality constraints (Eq. (9)), and 210 grouping constraints. The interstory drift constraints are imposed by limiting the difference of the horizontal nodal displacements at the top and bottom of each column. Consequently, there are 24 interstory drift constraints.

The MILP is solved by Gurobi (version 6.5) on the same computer as the first example problem. The optimality gap is set to 5×10^{-3}, the feasibility tolerance is set to 10^{-6}, and default values are used for the other parameters. The runtime of the algorithm is 19249 seconds (5.3 hours), and 140066 nodes of the branch-and-bound tree are explored. At termination, the global optimality of the solution is verified.

The convergence of the algorithm is illustrated in Fig. 8. The progress of the upper and lower bound, respectively, are shown by the two curves. It can be seen that feasible solutions close to the global optimum are found quickly.

The optimum design is shown in Fig. 7. The weight of the frame is 6131.87 kg. Detailed results for this test problem are given in C, where the deformed shape of the frame, internal force diagrams and constraint margins evaluated at the optimum design are presented.

The deflections of the beams (Table 5) are small and not decisive for the optimal design. As can be seen from Table 6, the utilization ratio of the interstory drift constraints ranges from 0.90 to 1.00 for the bottom two rows of columns. This means that the interstory drift is decisive for the optimal design.

Stresses in the members vary significantly throughout the frame (Table 7). The utilization ratios of the stress constraints range from 0.65 to 0.96 for the beams, and from 0.38 to 0.96 for the columns. Highest utilization ratios appear in the members of the first story. As interstory drift and profile grouping constraints are enforced, a fully stressed design is not obtained.

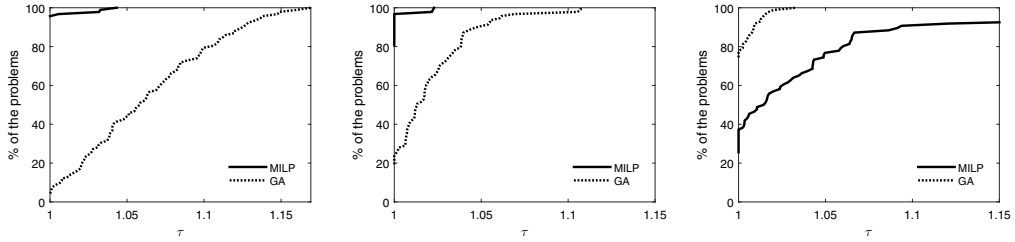

(a) Two-bay two-story frame (b) Three-bay three-story frame (c) Four-bay four-story frame

Fig. 10: Performance measured for the objective function value of the MILP reformulation approach (solid line) and genetic algorithm (dotted line) solving the two-bay two-story, three-bay three-story, and four-bay four-story frame problems.

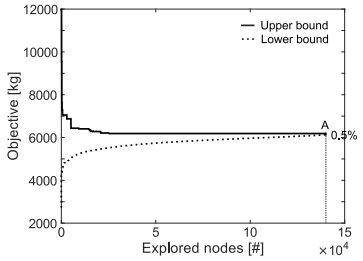

Fig. 8: Convergence curves of the optimization. After exploring 140066 nodes of the branch-and-bound tree, an optimality gap of 0.5 % is reached in point A and the optimization is terminated.

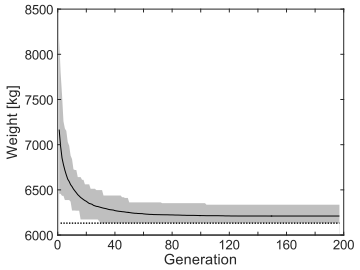

Fig. 9: Performance of the genetic algorithm. The mean objective function value of 100 runs in each generation is represented by the black curve. The gray region delimits the highest and lowest obtained objective function value in each generation. The global optimum is indicated by the dotted line.

3.4 Comparison with a genetic algorithm

It is interesting to compare the performance of the mixed-integer linear programming approach with metaheuristic methods in order to assess the computational cost that comes with the ability of the MILP formulation to find and verify the global optimum.

In this paper, the genetic algorithm (GA) function from the Matlab 2015 Global Optimization Toolbox is chosen as the metaheuristic solution method. Now the problem formulation follows the conventional nested analysis and design approach, where only member cross-sections are taken as design variables, and the values of the internal forces and displacements used in constraint evaluation are computed by the finite element method for given cross-sections. Default stopping criteria and parameter values are used, except for the constraint tolerance, which is set to 10^{-6} instead of the using the default value of 10^{-3} to make a fair comparison.

The three-bay three-story frame problem is solved by performing 100 different runs of the genetic algorithm with a population size of 70 for each generation. The results are shown in Fig. 9. The mean objective function value of all runs in each generation is represented by the solid black curve. The mean value of all solutions is 6210.5 kg, which is 1.3 % greater than the global optimum. The gray region delimits the highest and lowest obtained objective function value in each generation. The global optimum is indicated by the dotted line. For 32 % of the runs, the global optimum is reached. 54 % of all runs reach a solution which is heavier than the mean objective function value. The weight of the heaviest solution is 6335.7 kg (3.3 % greater than the global optimum). The computation time to perform 100 runs is 9.7 hours, giving an average of 350 seconds for 1 run.

This analysis depicts the typical stochastic nature of the genetic algorithm. For the majority of the runs, the global optimum is not obtained, although the solution deviates by only few percents, and the results of the genetic algorithm are satisfactory. On the other hand, during the computations, the quality of the solution cannot be assessed with the genetic algorithm, and eventually, the algorithm is simply stopped when no better solution is found, or when the maximum number of iterations has been reached. On the contrary, the solution process of the MILP ends precisely when the global optimality of the solution is verified. If global optimality of the solution is not required, the branch-and-cut method can be terminated when the optimality gap has become sufficiently small.

Therefore, in addition, a comparison of the performance obtained by setting a limit on the computation time is made. The performance measured for the objective function value is illustrated by optimizing a two-bay two-story, three-bay three-story, and four-bay four-story frame imposing the same dimensions, loads, and constraints of the three-bay three-story frame example problem discussed in the previous section. For each case, multiple optimization problems are solved using a different subset of 5 available profiles. The different subsets are composed by dividing the catalog consisting of 15 profile alternatives ranging from HEA 100 to HEA 400 (Table 1) in five equidistant intervals, and randomly selecting a section from each interval.

For the two-bay two-story, three-bay three-story, and four-bay four-story frame a time limit of respectively 5, 50, and 500 seconds is set for each optimization. For each example case, 100 different optimization problems are solved. The performance profiles [41,42] of the MILP reformulation method and the genetic algorithm are shown in Fig. 10. In this figure, the x-axis represents the parameter τ which is the relative ratio of the objective function value and the best obtained objective function value using the same subset of sections. The y-axis represents the percentage of optimization problems reaching an objective function value that is at most τ-times higher than the best obtained objective function value. The intersection of the plotted curves with the y-axis indicates the percentage of winning solutions. It can be seen that the MILP reformulation method performs better for the two-bay two-story (Fig. 10a) and three-bay three-story frame (Fig. 10b). In these cases, the winning solution is obtained with the MILP approach for respectively 96 % and 80 % of the optimization problems. For 80 % of the problems, the genetic algorithm yields solutions with an objective function value that is at most respectively 10 % and 5 % higher than the solution obtained with the MILP approach. In the case of the four-bay four-story frame (Fig. 10c), the winning solution is obtained with the genetic algorithm for 75 % of the optimization problems, and for 80 % of the problems the MILP method yields solutions with an objective function value that is at most 6 % higher than the solution obtained with the genetic algorithm. In this case, the genetic algorithm performs better. Due to the simplicity of implementing the genetic algorithm, adopting this approach might be preferable for practitioners. However, the quality of the solution can only be assessed by means of the optimality gap provided by the MILP approach. Therefore, the computation time can be reduced when adopting the MILP approach by terminating the optimization when the optimality gap is sufficiently small, say 5 % to 10 %. In addition, the method can be used to benchmark the efficiency of other methods.

4 Conclusion

This paper addresses a mixed-integer linear programming approach for discrete sizing optimization of frame structures using commercial profile catalogs. The performance of the method is compared with the performance of a genetic algorithm. The main benefit of the MILP formulation is that it allows for finding the global optimum of frames using well-established deterministic solution methods such as branch-and-bound. The formulation can be adopted for various materials and applications. In order to make the approach more relevant for practical applications, constraints derived from design codes can be included. In extending the formulation presented in this paper, the linearity of the problem should be preserved, because otherwise a large-scale *nonlinear* mixed-integer problem needs to be solved, which implies a substantial increase of computational burden.

The critical point of the mixed-integer formulation is the problem size. The problem includes hundreds of variables and thousands of constraints even for modest design tasks. The problem size increases rapidly as more members and profiles as well as additional load cases are introduced, which, due to the nature of MILP problems, implies that the computational time will grow significantly. The multiple-bay multiple-story frame gives some indication of this. In some cases the genetic algorithm appears to be more efficient than the MILP approach. However, even if the computational time for finding and verifying the global optimum becomes prohibitively large, the MILP formulation can still be used for finding good designs. Moreover, the branch-and-bound method provides the optimality gap throughout the iterations. This information can be used to reduce

the computational time by terminating the algorithm when the optimality gap becomes sufficiently small.

In order to draw definitive conclusions on the applicability of the MILP approach to practical design problems, the capabilities of the branch-and-cut method should be thoroughly studied in order to reduce the computational times. The convergence behavior depicted in Fig. 8 shows that while contemporary branch-and-cut algorithms are able to find feasible solutions (including the global optimum) relatively quickly, the improvement of the lower bound is rather slow. Consequently, further research efforts should be targeted at producing tighter relaxations of the MILP problem in order to obtain greater lower bounds more quickly. For this task, special-purpose cutting planes that efficiently exploit the specific mathematical structure of the MILP problem should be considered. Additionally, various case studies of actual design tasks should be treated. For a given design problem, engineering judgment and problem-specific additional constraints can often be employed to improve the solution process.

A Mixed-integer linear programming problem

A.1 Equilibrium equations

The nodal equilibrium is imposed by the equality constraints of Eq. (5). In this equation, $\mathbf{B}_i$ is a $6 \times n_{\text{dof}}$ binary location matrix that maps the system degrees of freedom to the element degrees of freedom, $\mathbf{T}_i$ is a 6×6 transformation matrix that accounts for the orientation of the element [35], and $\mathbf{f}$ is the $n_{\text{dof}} \times 1$ nodal load vector. Element loads are taken into account as equivalent nodal loads in the nodal load vector $\mathbf{f}$. $\mathbf{R}_i$ is a 6×3 matrix giving the relation between the six member end forces as shown in Fig. 1, and the three independent force variables $\mathbf{q}_{ij}$ (see Eq. (1)) as follows:

$$\begin{bmatrix} N_{1,ij} \\ V_{1,ij} \\ M_{1,ij} \\ N_{2,ij} \\ V_{2,ij} \\ M_{2,ij} \end{bmatrix} = \begin{bmatrix} 1 & 0 & 0 \\ 0 & \frac{1}{L_i} & \frac{1}{L_i} \\ 0 & 1 & 0 \\ -1 & 0 & 0 \\ 0 & -\frac{1}{L_i} & -\frac{1}{L_i} \\ 0 & 0 & 1 \end{bmatrix} \begin{bmatrix} N_{1,ij} \\ M_{1,ij} \\ M_{2,ij} \end{bmatrix} \tag{40}$$

A.2 Member stiffness relations

In addition to nodal equilibrium, the material law and compatibility conditions are needed in structural analysis. For trusses, Hooke's law and compatibility conditions can be written as a single equation, because the normal force is the only stress resultant appearing in the members [27]. As frame members have three (6 in 3D) stress resultants in each node, altogether six (12 in 3D) force-displacement relations are needed. Thus, the relation between the member end forces and the nodal displacements can be written as:

$$\mathbf{q}_{ij} = y_{ij} \mathbf{K}_{ij} \mathbf{T}_i \mathbf{B}_i \mathbf{u} \quad \forall\, i \in \mathcal{M},\, \forall\, j \in \mathcal{C}_i \tag{41}$$

where the matrix $\mathbf{K}_{ij}$ assembles the first, third and sixth row of the element stiffness matrix:

$$\mathbf{K}_{ij} = \begin{bmatrix} \frac{EA_{ij}}{L_i} & 0 & 0 & -\frac{EA_{ij}}{L_i} & 0 & 0 \\ 0 & \frac{6EI_{ij}}{L_i^2} & \frac{4EI_{ij}}{L_i} & 0 & -\frac{6EI_{ij}}{L_i^2} & \frac{2EI_{ij}}{L_i} \\ 0 & \frac{6EI_{ij}}{L_i^2} & \frac{2EI_{ij}}{L_i} & 0 & -\frac{6EI_{ij}}{L_i^2} & \frac{4EI_{ij}}{L_i} \end{bmatrix}$$

where E is the Young's modulus of the material, L_i is the length of member i, and A_{ij} and I_{ij} are the section area and second moment of area of profile j for member i, respectively.

Eq. (41) ensures that the force variables $\mathbf{q}_{ij}$ become zero when profile j is not selected for member i ($y_{ij} = 0$) and $\mathbf{q}_{ij} = \mathbf{K}_{ij}\mathbf{T}_i\mathbf{B}_i\mathbf{u}$ when profile j is selected for member i ($y_{ij} = 1$).

In a regular finite element analysis, the global stiffness matrix $\mathbf{K}$ is assembled by replacing $\mathbf{q}_{ij}$ in Eq. (5) with the expression given by Eq. (41). The resulting equilibrium equation can not be reformulated as a linear system of equations in terms of the design variables since the global stiffness matrix depends on the binary decision variables. Therefore, the linear nodal equilibrium, Eq. (5), and the member stiffness relation, Eq. (41), are adopted as separate constraints.

The member stiffness relation in Eq. (41) is nonlinear in terms of the design variables but it can be equivalently reformulated as a set of linear inequality constraints by introducing artificial upper and lower bounds [27] of Eq. (6).In this equation, the force variables become equal to $\mathbf{q}_{ij} = \mathbf{K}_{ij}\mathbf{T}_i\mathbf{B}_i\mathbf{u}$ when profile j is selected for member i ($y_{ij} = 1$). When profile j is not selected for member i ($y_{ij} = 0$), the force variables do not become zero but are bounded by $\mathbf{K}_{ij}\mathbf{T}_i\mathbf{B}_i\mathbf{u} - \bar{\mathbf{q}}'_{ij} \leqslant \mathbf{q}_{ij} \leqslant \mathbf{K}_{ij}\mathbf{T}_i\mathbf{B}_i\mathbf{u} - \underline{\mathbf{q}}'_{ij}$. In order to ensure that the force variables become zero when profile j is not selected for member i, additional constraints given by Eq. (7) are introduced.

The artificial upper and lower bounds $\bar{\mathbf{q}}'_{ij}$ and $\underline{\mathbf{q}}'_{ij}$ ensure that, when profile j is not selected for member i, the nodal displacements are not bounded by Eq. (6). Each element k of the artificial bound vectors is calculated as follows [36]:

$$\begin{aligned} \underline{q}'_{k,ij} = \min_{\mathbf{u}} \quad & \mathbf{k}_{r,ij}\mathbf{T}_i\mathbf{B}_i\mathbf{u} \\ \text{s.t.} \quad & \underline{\mathbf{u}} \leqslant \mathbf{u} \leqslant \overline{\mathbf{u}} \end{aligned} \tag{42}$$

$$\begin{aligned} \bar{q}'_{k,ij} = \max_{\mathbf{u}} \quad & \mathbf{k}_{r,ij}\mathbf{T}_i\mathbf{B}_i\mathbf{u} \\ \text{s.t.} \quad & \underline{\mathbf{u}} \leqslant \mathbf{u} \leqslant \overline{\mathbf{u}} \end{aligned} \tag{43}$$

where $\mathbf{k}_{r,ij}$ represents row $r \in [1, 3, 6]$ of the element stiffness matrix $\mathbf{K}_{ij}$, and $\underline{\mathbf{u}}$ and $\overline{\mathbf{u}}$ are the prescribed minimum and maximum allowed nodal displacements, respectively. Eqs. (42) and (43) are linear optimization problems with bound constraints, that can be solved without effort [36].

A.3 Displacement vectors

$$\mathbf{D}_i^u(x) = \begin{bmatrix} 1 - \frac{x}{L_i} & 0 & 0 & \frac{x}{L_i} & 0 & 0 \end{bmatrix} \tag{44}$$

$$\mathbf{D}_i^v(x) = \begin{bmatrix} 0 & 1 - \frac{3x^2}{L_i^2} + \frac{2x^3}{L_i^3} & x\left(1 - \frac{x}{L_i}\right)^2 & \cdots \\ 0 & \frac{3x^2}{L_i^2} - \frac{2x^3}{L_i^3} & x\left(-\frac{x}{L_i} + \frac{x^2}{L_i^2}\right) & \end{bmatrix} \tag{45}$$

$$\mathbf{D}_i^\varphi(x) = \begin{bmatrix} 0 & \frac{-6x}{L_i^2} + \frac{6x^2}{L_i^3} & 1 - \frac{4x}{L_i} + \frac{3x^2}{L_i^2} & \cdots \\ 0 & \frac{6x}{L_i^2} - \frac{6x^2}{L_i^3} & \frac{-2x}{L_i} + \frac{3x^2}{L_i^2} & \end{bmatrix} \tag{46}$$

A.4 Stress vectors

$$\mathbf{S}_{ij}^{\sigma_\mathrm{t}}(x) = \left[\; -\frac{E}{L_i} \quad \frac{6EI_{ij}}{L_i^2 W_{\mathrm{t},ij}} - \frac{12xEI_{ij}}{L_i^3 W_{\mathrm{t},ij}} \quad \frac{4EI_{ij}}{L_i W_{\mathrm{t},ij}} - \frac{6xEI_{ij}}{L_i^2 W_{\mathrm{t},ij}} \quad \cdots \right.$$
$$\left. \frac{E}{L_i} \quad \frac{12xEI_{ij}}{L_i^3 W_{\mathrm{t},ij}} - \frac{6EI_{ij}}{L_i^2 W_{\mathrm{t},ij}} \quad \frac{2EI_{ij}}{L_i W_{\mathrm{t},ij}} - \frac{6xEI_{ij}}{L_i^2 W_{\mathrm{t},ij}} \; \right] \tag{47}$$

$$\mathbf{S}_{ij}^{\sigma_\mathrm{b}}(x) = \left[\; -\frac{E}{L_i} \quad \frac{12xEI_{ij}}{L_i^3 W_{\mathrm{b},ij}} - \frac{6EI_{ij}}{L_i^2 W_{\mathrm{b},ij}} \quad \frac{6xEI_{ij}}{L_i^2 W_{\mathrm{b},ij}} - \frac{4EI_{ij}}{L_i W_{\mathrm{b},ij}} \quad \cdots \right.$$
$$\left. \frac{E}{L_i} \quad \frac{6EI_{ij}}{L_i^2 W_{\mathrm{b},ij}} - \frac{12xEI_{ij}}{L_i^3 W_{\mathrm{b},ij}} \quad \frac{6xEI_{ij}}{L_i^2 W_{\mathrm{b},ij}} - \frac{2EI_{ij}}{L_i W_{\mathrm{b},ij}} \; \right] \tag{48}$$

$$\mathbf{S}_{ij}^{\tau}(x) = \left[\; 0 \quad -\frac{12ES_{ij}}{L_i^3 b_{ij}} \quad -\frac{6ES_{ij}}{L_i^2 b_{ij}} \quad 0 \quad \frac{12ES_{ij}}{L_i^3 b_{ij}} \quad -\frac{6ES_{ij}}{L_i^2 b_{ij}} \; \right] \tag{49}$$

B Detailed results for the portal frame

Table 3: Constrained displacements evaluated at the optimum design

Member	Location	v [m]	$\frac{\lvert v \rvert}{v_{\max}}$
2	$L/2$	-0.0223	0.45
2	L	-0.0348	0.70
3	$L/2$	-0.0223	0.45

(a) Deformed frame.

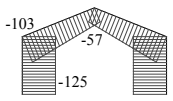

(b) Normal forces [kN].

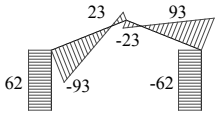

(c) Shear forces [kN].

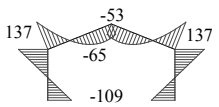

(d) Bending moments [kNm].

Fig. 11: Deformation and internal force diagrams at the optimum design.

Table 4: Constrained stresses evaluated at the optimum design

Member	Location	σ_t [MPa]	$\frac{\lvert\sigma_\mathrm{t}\rvert}{\sigma_{\max}}$	σ_b [MPa]	$\frac{\lvert\sigma_\mathrm{b}\rvert}{\sigma_{\max}}$	τ [MPa]	$\frac{\lvert\tau\rvert}{\tau_{\max}}$
1	0	-178.64	0.76	146.08	0.62	64.79	0.28
1	$L/2$	3.79	0.02	-36.34	0.15	64.79	0.28
1	L	186.21	0.79	-218.76	**0.93**	64.79	0.28
2	0	188.99	0.80	-215.97	**0.92**	-98.06	0.42
2	$L/4$	33.60	0.14	-57.55	0.24	-67.53	0.29
2	$L/2$	-63.94	0.27	43.01	0.18	-37.00	0.16
2	$3L/4$	-103.62	0.44	85.71	0.36	-6.47	0.03
2	L	-85.43	0.36	70.54	0.30	24.06	0.10
3	0	-85.43	0.36	70.54	0.30	-24.06	0.10
3	$L/4$	-103.62	0.44	85.71	0.36	6.47	0.03
3	$L/2$	-63.94	0.27	43.01	0.18	37.00	0.16
3	$3L/4$	33.60	0.14	-57.55	0.24	67.53	0.29
3	L	188.99	0.80	-215.97	**0.92**	98.06	0.42
4	0	-178.64	0.76	146.08	0.62	64.79	0.28
4	$L/2$	3.79	0.02	-36.34	0.15	64.79	0.28
4	L	186.21	0.79	-218.76	**0.93**	64.79	0.28

C Detailed results for the three-bay three-story frame

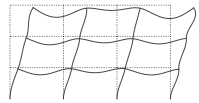

(a) Deformed frame.

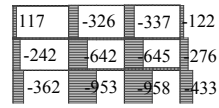

(b) Normal forces [kN].

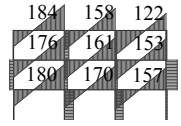

(c) Shear forces [kN].

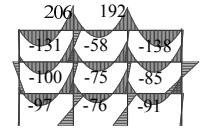

(d) Bending moments [kNm].

Fig. 12: Deformation and internal force diagrams at the optimum design.

Table 5: Constrained deflections evaluated at the optimum design

Member	Location	v [m]	$\frac{\lvert v \rvert}{v_{\max}}$
13	$L/2$	-0.0097	0.19
14	$L/2$	-0.0070	0.14
15	$L/2$	-0.0103	0.21
16	$L/2$	-0.0116	0.23
17	$L/2$	-0.0090	0.18
18	$L/2$	-0.0105	0.21
19	$L/2$	-0.0166	0.33
20	$L/2$	-0.0072	0.14
21	$L/2$	-0.0185	0.37

Table 6: Constrained interstory drifts evaluated at the optimum design

Member	Δu [m]	$\frac{\lvert\Delta u\rvert}{\Delta u_{\max}}$
1	0.0112	0.96
2	0.0112	0.96
3	0.0114	0.98
4	0.0117	1.00
5	0.0115	0.99
6	0.0113	0.97
7	0.0110	0.94
8	0.0105	0.90
9	0.0097	0.83
10	0.0098	0.84
11	0.0099	0.85
12	0.0102	0.87

Table 7: Constrained stresses evaluated at the optimum design

Member	Location	σ_{t} [MPa]	$\frac{\lvert\sigma_{\mathrm{t}}\rvert}{\sigma_{\mathrm{max}}}$	σ_{b} [MPa]	$\frac{\lvert\sigma_{\mathrm{b}}\rvert}{\sigma_{\mathrm{max}}}$	τ [MPa]	$\frac{\lvert\tau\rvert}{\tau_{\mathrm{max}}}$
1	0	-74.18	0.32	-156.20	0.66	-3.03	0.02
1	$L/2$	-97.42	0.41	-132.96	0.57	-3.03	0.02
1	L	-120.66	0.51	-109.72	0.47	-3.03	0.02
2	0	29.49	0.13	-225.30	0.96	-31.60	0.23
2	$L/2$	-83.73	0.36	-112.07	0.48	-31.60	0.23
2	L	-196.96	0.84	1.16	0.00	-31.60	0.23
3	0	19.58	0.08	-216.54	0.92	-27.39	0.20
3	$L/2$	-78.57	0.33	-118.39	0.50	-27.39	0.20
3	L	-176.71	0.75	-20.25	0.09	-27.39	0.20
4	0	-52.12	0.22	-223.61	0.95	-11.56	0.09
4	$L/2$	-140.89	0.60	-134.84	0.57	-11.56	0.09
4	L	-229.67	0.98	-46.07	0.20	-11.56	0.09
5	0	-84.94	0.36	29.29	0.12	15.64	0.12
5	$L/2$	-25.76	0.11	-29.90	0.13	15.64	0.12
5	L	33.43	0.14	-89.08	0.38	15.64	0.12
6	0	-33.59	0.14	-166.09	0.71	-15.08	0.11
6	$L/2$	-104.98	0.45	-94.69	0.40	-15.08	0.11
6	L	-176.37	0.75	-23.30	0.10	-15.08	0.11
7	0	-59.14	0.25	-141.36	0.60	-10.32	0.08
7	$L/2$	-107.99	0.46	-92.50	0.39	-10.32	0.08
7	L	-156.85	0.67	-43.64	0.19	-10.32	0.08
8	0	137.91	0.59	-201.39	0.86	-44.84	0.33
8	$L/2$	-31.75	0.14	-31.74	0.14	-44.84	0.33
8	L	-201.40	0.86	137.92	0.59	-44.84	0.33
9	0	-109.53	0.47	-0.74	0.00	6.04	0.04
9	$L/2$	-44.88	0.19	-65.39	0.28	6.04	0.04
9	L	19.78	0.08	-130.05	0.55	6.04	0.04
10	0	44.20	0.19	-145.61	0.62	-22.66	0.17
10	$L/2$	-63.08	0.27	-38.33	0.16	-22.66	0.17
10	L	-170.36	0.72	68.95	0.29	-22.66	0.17
11	0	-10.02	0.04	-94.70	0.40	-6.97	0.05
11	$L/2$	-43.02	0.18	-61.70	0.26	-6.97	0.05
11	L	-76.03	0.32	-28.70	0.12	-6.97	0.05
12	0	51.49	0.22	-166.76	0.71	-12.33	0.09
12	$L/2$	-80.56	0.34	-34.72	0.15	-12.33	0.09
12	L	-212.60	0.90	97.33	0.41	-12.33	0.09
13	0	47.17	0.20	-45.46	0.19	-57.93	0.43
13	$L/2$	-86.11	0.37	87.81	0.37	14.53	0.11
13	L	225.73	0.96	-224.02	0.95	87.00	0.64
14	0	97.55	0.42	-86.70	0.37	-62.76	0.46
14	$L/2$	-65.41	0.28	76.26	0.32	9.70	0.07
14	L	216.75	0.92	-205.89	0.88	82.17	0.60
15	0	121.97	0.52	-102.39	0.44	-69.05	0.51
15	$L/2$	-79.60	0.34	99.18	0.42	3.42	0.03
15	L	163.95	0.70	-144.37	0.61	75.88	0.56
16	0	49.58	0.21	-59.38	0.25	-60.10	0.44
16	$L/2$	-97.02	0.41	87.22	0.37	12.37	0.09
16	L	201.49	0.86	-211.29	0.90	84.83	0.62
17	0	113.21	0.48	-125.18	0.53	-67.49	0.50
17	$L/2$	-78.77	0.34	66.80	0.28	4.98	0.04
17	L	174.36	0.74	-186.33	0.79	77.44	0.57
18	0	124.52	0.53	-135.53	0.58	-71.01	0.52
18	$L/2$	-89.09	0.38	78.08	0.33	1.46	0.01
18	L	142.42	0.61	-153.42	0.65	73.92	0.54
19	0	2.84	0.01	-7.92	0.03	-56.36	0.41
19	$L/2$	-120.77	0.51	115.68	0.49	16.11	0.12
19	L	200.74	0.85	-205.83	0.88	88.58	0.65
20	0	143.13	0.61	-141.73	0.60	-68.62	0.50
20	$L/2$	-55.81	0.24	57.21	0.24	3.84	0.03
20	L	190.37	0.81	-188.96	0.80	76.31	0.56
21	0	179.33	0.76	-175.93	0.75	-86.02	0.63
21	$L/2$	-126.48	0.54	129.88	0.55	-13.55	0.10
21	L	12.83	0.05	-9.43	0.04	58.91	0.43

References

1. J. Farkas. Structural optimization as a harmony of design, fabrication and economy. *Structural and Multidisciplinary Optimization*, 30:66–75, 2005.
2. Q. Wang and J. S. Arora. Alternative formulations for structural optimization: An evaluation using frames. *Journal of Structural Engineering*, 132(12):1880–1189, 2006.
3. P.B. Thanedar and G.N. Vanderplaats. Survey of discrete variable optimization for structural design. *Journal of Structural Engineering*, 121:301–306, 1995.
4. J.S. Arora and M.-W. Huang. Discrete structural optimization with commercially available sections. *Structural Engineering/Earthquake Engineering*, 13:93–110, 1996.
5. M.-W. Huang and J.S. Arora. Optimal design of steel structures using standard sections. *Structural Optimization*, 14:24–35, 1997.
6. J. Arora. Methods for discrete variable structural optimization. In Scott A. Burns, editor, *Recent Advances in Optimal Structural Design*, pages 1–40. ASCE, 2002.
7. D.S. Juang and W.T. Chang. A revised discrete lagrangian-based search algorithm for the optimal design of skeletal structures using available sections. *Structural and Multidisciplinary Optimization*, 31:201–210, 2006.
8. M. Schevenels, S. McGinn, A. Rolvink, and J. Coenders. An optimality criteria based method for discrete design optimization taking into account buildability constraints. *Structural and Multidisciplinary Optimization*, 50(5):755–774, 2014.
9. C. Camp, S. Pezeshk, and C. Guozhong. Optimized design of two-dimensional structures using a genetic algorithm. *Journal of Structural Engineering*, 124(5):551–559, 1998.
10. S. Rajeev and C.S. Krishnamoorthy. Discrete optimization of structures using genetic algorithms. *Journal of Structural Engineering*, 118(5):1233–1250, 1992.
11. M. B. P. Gero, A. B. Garcia, and J. J. C. Diaz. Design optimization of 3d steel structures: Genetic algorithms vs. classical techniques. *Journal of Constructional Steel Research*, 62(12):1303–1309, 2006.
12. P. Kripakaran, H. Brian, and G. Abhinav. A genetic algorithm for design of moment-resisting steel frames. *Structural and Multidisciplinary Optimization*, 32(3):559–574, 2010.
13. C.V. Camp, B.J. Bichon, and S.P. Stovall. Design of steel frames using ant colony optimization. *Journal of Structural Engineering*, 131(7):369–379, 2005.
14. A. Kaveh and S. Talatahari. An improved ant colony optimization for the design of planar steel frames. *Engineering Structures*, 32(3):864–873, 2010.
15. A.H. Gandomi, X.S. Yang, and A.H. Alavi. Mixed variable structural optimization using firefly algorithm. *Computers & Structures*, 89(23):2325–2336, 2011.
16. S. Carbas. Design optimization of steel frames using an enhanced firefly algorithm. *Engineering Optimization*, pages 1–19, 2016.
17. M. P. Saka. Optimum design of steel sway frames to bs5950 using harmony search algorithm. *Journal of Constructional Steel Research*, 65(1):36–43, 2009.
18. G. Venter and J. Sobieszczanski-Sobieski. Particle swarm optimization. *AIAA Journal*, 41(8):1583–1589, 2003.
19. S. Kazemzadeh Azad and O. Hasancebi. Computationally efficient discrete sizing of steel frames via guided

stochastic search heuristic. *Computers & Structures*, 156:12–28, 2015.
20. S. Talatahari, A. H. Gandomi, X.-S. Yang, and S. Deb. Optimum design of frame structures using the eagle strategy with differential evolution. *Engineering Structures*, 91:16–25, 2015.
21. V. Togan. Design of planar steel frames using teaching-learning based optimization. *Engineering Structures*, 34:225(8), 2012.
22. J.S. Arora and Q. Wang. Review of formulations for structural and mechanical system optimization. *Structural and Multidisciplinary Optimization*, 30(4):251–272, 2005.
23. Laurence A. Wolsey. *Integer Programming*. John Wiley & Sons, 1998.
24. G. Nemhauser and L. Wolsey. *Integer and Combinatorial Optimization*. John Wiley & Sons, 1999.
25. O. Ghattas and I.E. Grossmann. MINLP and MILP strategies for discrete sizing structural optimization problems. In O. Ural and T. L. Wang, editors, *Proceedings of the 10th Conference on Electronic Computation*, pages 197–204. ASCE, 1991.
26. I.E. Grossmann, V.T. Voudouris, and O. Ghattas. Mixed-integer linear programming reformulations for some nonlinear discrete design optimization problems. In C.A. Floudas and P.M. Pardalos, editors, *Recent Advances in Global Optimization*, pages 478–512. Princeton University Press, 1992.
27. M.H. Rasmussen and M. Stolpe. Global optimization of discrete truss topology design problems using a parallel cut-and-branch method. *Computers & Structures*, 86(13):1527–1538, 2008.
28. A.M. Faustino, J.J. Júdice, I.M. Ribeiro, and A.S. Neves. An integer programming model for truss topology optimization. *Investigação Operacional*, 26:111–127, 2006.
29. Yoshihiro Kanno and Xu Guo. A mixed integer programming for robust truss topology optimization with stress constraints. *International Journal for Numerical Methods in Engineering*, 83(13):1675–1699, 2010.
30. K. Mela. Resolving issues with member buckling in truss topology optimization using a mixed variable approach. *Structural and Multidisciplinary Optimization*, 50(6):1037–1049, 2014.
31. R. Van Mellaert, G. Lombaert, and M. Schevenels. Global size optimization of statically determinate trusses considering displacement, member, and joint constraints. *Journal of Structural Engineering*, 142(2):04015120, 2015.
32. M. Stolpe. On the refomulation of topology optimization problems as linear or convex quadratic mixed 0-1 programs. *Optimization in Engineering*, (8):163–192, May 2007.
33. R. Kureta and Y. Kanno. A mixed integer programming approach to designing periodic frame structures with negative poissons ratio. *Optimization and Engineering*, 15(3):773–800, 2014.
34. M. Hirota and Y. Kanno. Optimal design of periodic frame structures with negative thermal expansion via mixed integer programming. *Optimization and Engineering*, 16(4):767–809, 2015.
35. A. Kassimali. *Matrix Analysis of Structures*. Brooks/Cole Publishing Company, London, UK, 1999.
36. M. Stolpe and K. Svanberg. Modelling topology optimization problems as linear mixed 0-1 programs. *International Journal for Numerical Methods in Engineering*, 57:723–739, 2003.
37. Gurobi Optimization Inc. Gurobi optimizer reference manual, 2015.
38. S. Chai and H.C. Sun. A relative difference quotient algorithm for discrete optimization. *Structural Optimization*, 12(1):46–56, 1996.
39. G. Jivotovski. A gradient based heuristic algorithm and its application to discrete optimization of bar structures. *Structural and Multidisciplinary Optimization*, 19(3):237–248, 2000.
40. D.S. Juang and W.T. Chang. A revised discrete lagrangian-based search algorithm for the optimal design of skeletal structures using available sections. *Structural and Multidisciplinary Optimization*, 31(3):201–210, 2006.
41. Susana Rojas-Labanda and Mathias Stolpe. Benchmarking optimization solvers for structural topology optimization. *Structural and Multidisciplinary Optimization*, 52(3):527–547, 2015.
42. Elizabeth D Dolan and Jorge J Moré. Benchmarking optimization software with performance profiles. *Mathematical programming*, 91(2):201–213, 2002.

Publication IV

Title: Buckling Length in Mixed-Integer Linear Frame Optimization
Authors: Teemu Tiainen, Kristo Mela and Markku Heinisuo
Collection: Advances in Structural and Multidisciplinary Optimization
Pages: 1923–1936

Accepted manuscript printed on kind permission from Springer–Verlag.

Original available at https://link.springer.com/chapter/10.1007/978-3-319-67988-4_143

12th World Congress on Structural and Multidisciplinary Optimization
5th - 9th, June 2017, Braunschweig, Germany

Buckling length in mixed-integer linear frame optimization

Teemu Tiainen[1], Kristo Mela[2], Markku Heinisuo[3]

[1] Tampere university of technology, Finland, teemu.tiainen@tut.fi
[2] Tampere university of technology, Finland, kristo.mela@tut.fi
[2] Tampere university of technology, Finland, markku.heinisuo@tut.fi

1. Abstract
In structural optimization of trusses and frames, the member profiles have to be selected from material suppliers selection. This means that the optimization problem becomes discrete. The discrete frame optimization problem can be formulated as mixed-integer linear program (MILP) and thus solved for global optimality using well-known deterministic methods such as branch-and-cut. Within the formulation it is possible to include member buckling constraints. When using design standards as basis for member buckling resistance evaluation, the critical forces or buckling lengths of the members are required. Buckling length can be determined using many methods, both numerical and analytical. Regardless of the method, buckling length of a single member is dependent on surrounding members stiffness which makes it practically impossible to include the correct buckling lengths in MILP formulation directly. In general, the question of buckling length in frame optimization has rarely been discussed in the structural optimization literature. Therefore, in this paper, an iterative approach to determine the correct buckling lengths is presented. In this approach, the MILP optimization is run several times. Linear stability analysis is performed between MILP runs to update buckling length data. The performance of the proposed method is illustrated in example calculations. The example structures are steel frames and Eurocode 3 is used as basis for member resistance constraints. In the examples, the method converges with a relatively low number of iterations.
2.Keywords:global optimization, frames, stability constraints

3. Introduction
In frame or truss design, the respective optimization problem is typically discrete meaning the sections must be chosen from a set of profiles given by steel supplier. On the other hand, the design is not only limited by stress or displacement as found in classical structural optimization literature but more complex constraints of design codes and standards. These documents typically present ways to handle local and global instabilities as well as stress measures. In optimization, the design rules can easily result in non-linear, non-convex and even non-continuous constraint functions depending on formulation.
When adopting the SAND (simultaneous analysis and design) approach and discrete design variables the truss design problem can be formulated as MILP (mixed integer linear program) [1]. Recently, the similar approach has also been used in topology optimization of frames [2, 3]. This type of optimization problem can be solved to verified global optimum with well-known branch-and-cut method. Moreover, since internal forces are state variables in optimization, the SAND approach seems tempting since steel design code formulas typically constrain forces rather than stresses.
When applying the design codes as basis for design, the buckling length or critical force for each member is needed. In EN 1993-1-1 [4] for certain structures, such as tubular trusses, straight-forward coefficients multiplying member length are given as constant values. This has been utilized in MILP approach of trusses [5]. In frames, however, the buckling length or critical force is dependent of support conditions and surrounding members' stiffness which are typically dependent on the design variables in optimization. Therefore, the stability analysis should somehow be included in the optimization to properly take the stability into account. The well-known linear stability eigenvalue analysis or analytical approaches (for example [6]) have been presented in the literature but within MILP the use of both of these approaches would require very large amount of constraints.
The mathematical properties of the constraint functions or discrete design variables do not cause problems if meta-heuristic optimization approach such as genetic algorithm (GA), particle swarm optimization (PSO) and harmony search (HS) – among many others – is adopted. For example, harmony search has been used in frame design examples with AISC based design constraints using approximate effective lengths with a finding that HS performs better than GA [7]. When using these approaches, however, the optimality of the obtained solution cannot typically be verified.
Therefore in this paper, an approach to use the MILP scheme by sequentially updating parameter values needed in design code buckling analysis according to EN 1993-1-1 is presented. The formulas are presented for planar

frame made of European standard hot-rolled I sections. Paper is organized as follows: In next section, the MILP formulation is presented, after that EN 1993-1-1 member design formulas are formulated and – when needed – linearized to fit the MILP scheme. In following section a sequential procedure to handle buckling constraint related parameter values is proposed. The convergence of proposed procedure is verified in numerical examples.

4. MILP in frame structures

The mixed integer linear scheme was introduced to beam elements was written by [2]. However, the work aims for topology optimization of special structures under special consideration and involves only one possible size for each existing member. For a plane frame found in buildings, the weight minimization with displacement and stress constraints can be written as ([8], notation follows the reference):

$$\min_{\mathbf{x}} \sum_{i\in\mathscr{M}} \sum_{j\in\mathscr{C}_i} c_{ij} y_{ij} \tag{1}$$

such that

$$\sum_{j\in\mathscr{C}_i} y_{ij} = 1 \qquad \forall\, i \in \mathscr{M} \tag{2}$$

$$\sum_{i\in\mathscr{M}} \sum_{j\in\mathscr{C}_i} \mathbf{B}_i^{\mathrm{T}} \mathbf{T}_i^{\mathrm{T}} \mathbf{q}_{ij} = \mathbf{f} \tag{3}$$

$$(1-y_{ij})\underline{\mathbf{q}}'_{ij} \leqslant \mathbf{K}_{ij}\mathbf{T}_i\mathbf{B}_i\mathbf{u} - \mathbf{q}_{ij} \leqslant (1-y_{ij})\bar{\mathbf{q}}'_{ij} \qquad \forall\, i \in \mathscr{M}, \forall\, j \in \mathscr{C}_i \tag{4}$$

$$\underline{\mathbf{q}}'_{ij} y_{ij} \leqslant \mathbf{q}_{ij} \leqslant \bar{\mathbf{q}}'_{ij} y_{ij} \qquad \forall\, i \in \mathscr{M}, \forall\, j \in \mathscr{C}_i \tag{5}$$

$$\underline{\mathbf{d}}'_{ij} + (\underline{\mathbf{d}}_{ij} - \underline{\mathbf{d}}'_{ij}) y_{ij} \leqslant \mathbf{D}_i\mathbf{T}_i\mathbf{B}_i\mathbf{u} + \tilde{\mathbf{d}}_{ij} \leqslant \bar{\mathbf{d}}'_{ij} + (\bar{\mathbf{d}}_{ij} - \bar{\mathbf{d}}'_{ij}) y_{ij} \qquad \forall\, i \in \mathscr{M}, \forall\, j \in \mathscr{C}_i \tag{6}$$

$$\underline{\mathbf{s}}'_{ij} + (\underline{\mathbf{s}}_{ij} - \underline{\mathbf{s}}'_{ij}) y_{ij} \leqslant \mathbf{S}_{ij}\mathbf{T}_i\mathbf{B}_i\mathbf{u} + \tilde{\mathbf{s}}_{ij} \leqslant \bar{\mathbf{s}}'_{ij} + (\bar{\mathbf{s}}_{ij} - \bar{\mathbf{s}}'_{ij}) y_{ij} \qquad \forall\, i \in \mathscr{M}, \forall\, j \in \mathscr{C}_i \tag{7}$$

The stress constraints are found in structural optimization literature, but design codes focus on member resistances. Thus, in the following section the EN 1993-1-1 member design rules are written within the MILP scheme.

5. MILP and Eurocode

Consider a planar steel frame with support conditions such that lateral torsion buckling is restricted. Moreover, hot-rolled I or H profiles are used. The respective EN 1993-1-1 member design constraints are as follows. In cross-section check, the bending moment resistance is lowered to take into account the axial force as (EN 1993-1-1, clause 6.2.9.1(5)):

$$M_{y,Ed} \leq M_{N,y,Rd} = M_{pl,y,Rd} \min\left\{\frac{1-n}{1-0.5a}; 1\right\} \tag{8}$$

where

$$n = \frac{|N|}{N_{pl,Rd}} \tag{9}$$

and

$$a = \min\left\{\frac{A-2bt_f}{A}; 0.5\right\} \tag{10}$$

The cross-section dimensions and local axes are shown in Figure 1.
This can be written as six linear constraints for each member, profile choice and location where the check is needed as:

$$\frac{N}{N_{Rd}} + \left(1 - \frac{N_n}{N_{Rd}}\right)\frac{M}{M_{Rd}} \leq 1 \tag{11}$$

$$-\frac{N}{N_{Rd}} + \left(1 - \frac{N_n}{N_{Rd}}\right)\frac{M}{M_{Rd}} \leq 1 \tag{12}$$

$$\frac{N}{N_{Rd}} - \left(1 - \frac{N_n}{N_{Rd}}\right)\frac{M}{M_{Rd}} \leq 1 \tag{13}$$

$$-\frac{N}{N_{Rd}} - \left(1 - \frac{N_n}{N_{Rd}}\right)\frac{M}{M_{Rd}} \leq 1 \tag{14}$$

$$\frac{M}{M_{Rd}} \leq 1 \tag{15}$$

$$-\frac{M}{M_{Rd}} \leq 1 \tag{16}$$

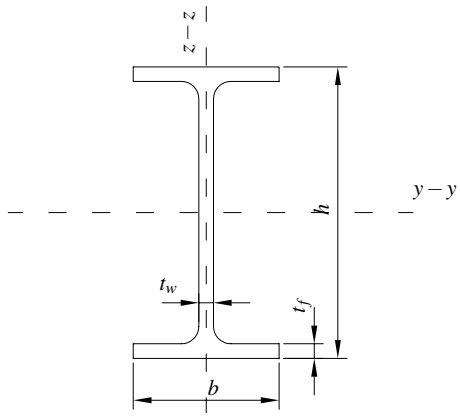

Figure 1: Dimensions and local axes of hot-rolled I section.

where

$$N_n = 0.5 \min \left\{ \frac{A - 2bt_f}{A}; 0.5 \right\} A f_y \tag{17}$$

The EN 1993-1-1 member stability or compression-bending interaction formulas are:

$$\frac{N_{Ed}}{\chi_y N_{Rd}} + k_{yy} \frac{M_{y,Ed}}{\chi_{LT} M_{y,Rd}} + k_{yz} \frac{M_{z,Ed}}{M_{z,Rd}} \leq 1 \tag{18}$$

and

$$\frac{N_{Ed}}{\chi_z N_{Rd}} + k_{zy} \frac{M_{y,Ed}}{\chi_{LT} M_{y,Rd}} + k_{zz} \frac{M_{z,Ed}}{M_{z,Rd}} \leq 1 \tag{19}$$

in which χ_y is the reduction factor in buckling in plane and χ_z is the reduction factor in buckling out of plane and χ_{LT} is the reduction factor in lateral torsion buckling. The factors k_{ij} are interaction factors.
Members are assumed not susceptible to lateral torsion buckling, and thus $\chi_{LT} = 1$. Moreover, $k_{zy} = 0$ (EN 1993-1-1 table B1) and obviously $M_{z,Ed} = 0$. Thus, the interaction formulas are reduced to

$$\frac{N_{Ed}}{\chi_y N_{Rd}} + k_{yy} \frac{M_{y,Ed}}{M_{y,Rd}} \leq 1 \tag{20}$$

and

$$\frac{N_{Ed}}{\chi_z N_{Rd}} \leq 1 \tag{21}$$

Interaction factor k_{yy} is a function of both axial force and bending moment. For hot-rolled I-profile in cross-section class 1 or 2 according to method 2 in EN 1993-1-1 annex B

$$k_{yy} = C_{my} \min \left(1 + (\lambda_y - 0.2) \frac{N_{Ed}}{\chi_y N_{Rd}}; 1 + 0.8 \frac{N_{Ed}}{\chi_y N_{Rd}} \right) \tag{22}$$

where C_{my} is the equivalent moment factor. For columns with no distributed transverse loads only end bending moments need to be considered and the EN 1993-1-1 annex B table gives formula

$$C_{my} = \max \{0.4; 0.6 + 0.4\psi\} \tag{23}$$

where

$$\psi = \frac{M_1}{M_2} \text{ if } |M_2| > |M_1| \text{ else } \psi = \frac{M_2}{M_1} \tag{24}$$

where M_1 and M_2 are the member end bending moments.
Reduction factor χ_y is calculated by

$$\chi_y = \min \left(\frac{1}{\phi_y + \sqrt{\phi_y^2 - \bar{\lambda}_y^2}}, 1 \right) \tag{25}$$

where

$$\phi_y = 0.5\left[1 + \alpha_y\left(\bar{\lambda}_y - 0.2\right) + \bar{\lambda}_y^2\right] \tag{26}$$

and

$$\bar{\lambda}_y = \sqrt{\frac{f_y A}{N_{cr,y}}} \tag{27}$$

where α_y is the imperfection factor and $N_{cr,y}$ the critical load of the column in buckling about y-axis. Critical load is calculated as

$$N_{cr,y} = \frac{\pi^2 E I_y}{L_{cr,y}^2} = \frac{\pi^2 E I_y}{\left(k_y L_{sys}\right)^2} \tag{28}$$

where $L_{cr,y}$ is the buckling length of the member, k_y is the buckling length factor and L_{sys} is the member system length in the model.
χ_z is calculated similarly but by using values $N_{cr,z}$ and α_z.
Thus, it is evident that stability constraints in MILP are non-linear. However, by assuming constant values for C_{my}, k_y and k_z a linear approximation of the non-linear constraint can be made.
Consider that the evaluation formula Eq. (20) is relevant only for compression ($N \leq 0$) and abbreviate $n = -\frac{N}{N_{Rd}}$ and $m = \frac{M_{Ed}}{M_{Rd}}$. By considering Eq. (20) as an equality, and solving for m as a function of n yields

$$m = m(n) = \frac{1 + \dfrac{n}{\chi_y}}{C_{my}\left(1 - \underline{\lambda}\dfrac{n}{\chi_y}\right)} \tag{29}$$

The curve is linearized at point $n = n_l$. The derivative of $m(n)$ is

$$m'(n) = \frac{1 + \underline{\lambda}}{C_{my}\chi_y\left(1 - \underline{\lambda}\dfrac{n}{\chi_y}\right)^2} \tag{30}$$

The linearization or first order Taylor approximation can be written

$$m_{lin}(n) = m(n_l) + m'(n_l)\left(n - n_l\right) \tag{31}$$

The point n_l is chosen as the mid point of decisive buckling strength $n_b = \min\left(\chi_z, \chi_y\right)$ and intersection point plastic interaction and compression-bending interaction curves or zero if the inter-section point n_c is positive.

$$n_l = \frac{\min\left(0, n_c\right)}{2} + \frac{n_b}{2} \tag{32}$$

The relevant plastic interaction (acting in when $n < 0$ and $M > 0$) is defined by

$$m(n) = \frac{1+n}{1-n_0} \tag{33}$$

where n_0 is largest absolute value of n when bending moment resistance is not affected by axial force which can be calculated as

$$n_0 = \frac{N_n}{N_{Rd}} \tag{34}$$

The compression bending interaction is defined by Eq. (29). The intersection of the curves is defined by a second degree polynomial

$$-\frac{C_{my}\underline{\lambda}}{\chi_y}n^2 + \left[-\frac{C_{my}\underline{\lambda}}{\chi_y} + C_{my} - \frac{1}{\chi_y} + \frac{n_0}{\chi_y}\right]n + C_{my} - 1 + n_0 = 0 \tag{35}$$

By marking

$$A = -\frac{C_{my}\underline{\lambda}}{\chi_y} \tag{36}$$

$$B = -\frac{C_{my}\underline{\lambda}}{\chi_y} + C_{my} - \frac{1}{\chi_y} + \frac{n_0}{\chi_y} \tag{37}$$

$$C = C_{my} - 1 + n_0 \tag{38}$$

the solution can be written

$$n_c = \frac{-B \pm \sqrt{B^2 - 4AC}}{2A} \tag{39}$$

From $\pm$ the subtraction is chosen.
The linear constraint thus obtained can be written as

$$m(n_l) + m'(n_l)\,(n - n_l) \leq m \tag{40}$$

for positive bending moment and

$$-m(n_l) - m'(n_l)\,(n - n_l) \geq m \tag{41}$$

for negative bending moment.
In total, linearized EN 1993-1-1 member design requirements considering stability expressed in N, M space ($N < 0$ compression):

$$\frac{N}{N_{Rd}} \geq -\chi_z \tag{42}$$

$$k\frac{N}{N_{Rd}} - \frac{M}{M_{Rd}} \leq c \tag{43}$$

$$-k\frac{N}{N_{Rd}} - \frac{M}{M_{Rd}} \leq c \tag{44}$$

$$\tag{45}$$

where

$$k = m'(n_l) = \frac{1 + \underline{\lambda}}{C_{my}\chi_y\left(1 - \underline{\lambda}\dfrac{n_l}{\chi_y}\right)^2} \tag{46}$$

$$c = \frac{1 + \dfrac{n_l}{\chi_y}}{C_{my}\left(1 - \dfrac{\lambda n_l}{\chi_y}\right)} - \frac{1 + \underline{\lambda}}{C_{my}\chi_y\left(1 - \underline{\lambda}\dfrac{n_l}{\chi_y}\right)^2} n_l \tag{47}$$

The linearization is clearly an approximation and introduces some error. The error made by linearization of Eq. (20) is dependent of both buckling length factors k_y and k_z and equivalent moment factor C_{my}. For three sets of parameter values the error is visualized in Figure 2. It seems that high values of k_y and C_{my} contribute to high curvature of the interaction and thus high error at the ends. In all cases the error is conservative. With buckling length close to system length the error can be considered to be at acceptable level. With high out-of-plane buckling length in comparison to in-plane buckling length, the design might be limited only by plastic resistance of the cross-section and out-of-plane buckling. Obviously, the choice of the linearization point affects the error. The choice presented above seems to produce a balanced and usable result.

6. Problem formulation with Eurocode 3 member design constraints

The problem formulation with linearized Eurocode 3 member design constraints can be written as:

$$\min_{\mathbf{x}} \sum_{i \in \mathscr{M}} \sum_{j \in \mathscr{C}_i} c_{ij} y_{ij} \tag{48}$$

$$\text{such that} \sum_{j \in \mathscr{C}_i} y_{ij} = 1 \;\; \forall\, i \in \mathscr{M} \tag{49}$$

$$\sum_{i \in \mathscr{M}} \sum_{j \in \mathscr{C}_i} \mathbf{B}_i^{\mathrm{T}} \mathbf{T}_i^{\mathrm{T}} \mathbf{q}_{ij} = \mathbf{f} \tag{50}$$

$$(1 - y_{ij})\underline{\mathbf{q}}'_{ij} \leqslant \mathbf{K}_{ij}\mathbf{T}_i\mathbf{B}_i\mathbf{u} - \mathbf{q}_{ij} \leqslant (1 - y_{ij})\bar{\mathbf{q}}'_{ij} \quad \forall\, i \in \mathscr{M}, \forall\, j \in \mathscr{C}_i \tag{51}$$

$$\underline{\mathbf{q}}'_{ij} y_{ij} \leqslant \mathbf{q}_{ij} \leqslant \bar{\mathbf{q}}'_{ij} y_{ij} \quad \forall\, i \in \mathscr{M}, \forall\, j \in \mathscr{C}_i \tag{52}$$

$$\underline{\mathbf{d}}'_{ij} + (\underline{\mathbf{d}}_{ij} - \underline{\mathbf{d}}'_{ij})y_{ij} \leqslant \mathbf{D}_{ik}\mathbf{T}_i\mathbf{B}_i\mathbf{u} + \tilde{\mathbf{d}}_{ij} \leqslant \bar{\mathbf{d}}'_{ij} + (\bar{\mathbf{d}}_{ij} - \bar{\mathbf{d}}'_{ij})y_{ij} \quad \forall\, i \in \mathscr{M}, \forall\, j \in \mathscr{C}_i\, k \in \mathscr{D}_i \tag{53}$$

$$\mathbf{c}_{ijl,cb}\mathbf{q}_{ij} + b_{ijl,cb}y_{ij} \leqslant c_{ij,cb} \quad \forall\, i \in \mathscr{M}, \forall\, j \in \mathscr{C}_i\, l \in \mathscr{E}_i \tag{54}$$

$$\mathbf{c}_{ijl,pl}\mathbf{q}_{ij} + b_{ijl,pl}y_{ij} \leqslant 1 \quad \forall\, i \in \mathscr{M}, \forall\, j \in \mathscr{C}_i\, l \in \mathscr{E}_i \tag{55}$$

$$\mathbf{c}_{ijl,M}\mathbf{q}_{ij} + b_{ijl,M}y_{ij} \leqslant 1 \quad \forall\, i \in \mathscr{M}, \forall\, j \in \mathscr{C}_i\, l \in \mathscr{E}_i \tag{56}$$

$$\mathbf{c}_{ij,o}\mathbf{q}_{ij} \leqslant 1 \quad \forall\, i \in \mathscr{M}, \forall\, j \in \mathscr{C}_i \tag{57}$$

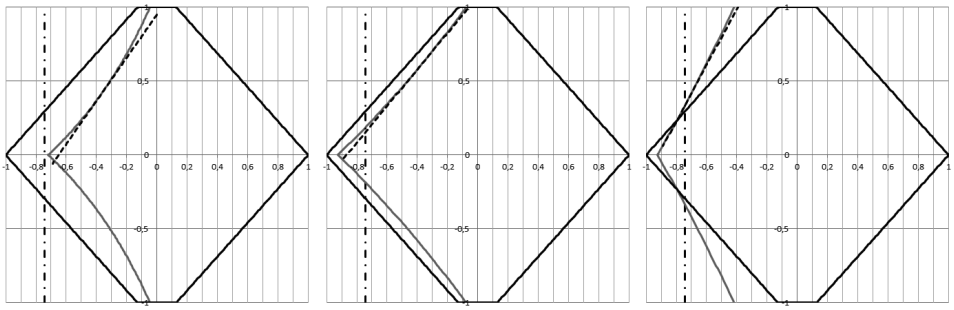

Figure 2: Three different scenarios for linearization with 2500 mm long HEA 200 member. Cross section resistance solid black line, linearization dashed line, compression and bending interaction solid grey line and out-of-plane buckling dash dot line. Left: $k_y = 2$, $k_z = 1$, $C_{my} = 0.9$, middle: $k_y = 1$, $k_z = 1$, $C_{my} = 0.9$, right: $k_y = 1$, $k_z = 1$, $C_{my} = 0.5$.

where constraints 49 - 52 are similar to those shown in Section 2 and the original reference. In the displacement constraint (Eq. (53)), index k is added to emphasize that displacement is constrained in finite number of points along the member. The stress constraint found in the original formulation is replaced with constraints including the compression bending interaction in plane (Eq. (54)), plastic cross-sectional resistance (Eq. (55) and Eq. (56)) and compression including the effect of out-of-plane buckling (Eq. (57)).
The constant vectors and scalars found in Eqs 54-57 are

$$\mathbf{c}_{ij,cb} = \left[\frac{-k_{ij,cb}}{N_{ij,Rd,pl}} \; \frac{x_l L_i}{M_{ij,Rd,pl}} \; \frac{-1}{M_{ij,Rd,pl}} \; 0 \; 0 \; 0 \right]^\mathsf{T} \in \mathbb{R}^6 \tag{58}$$

$$b_{ij,cb} = -\frac{p_i \left(x_l L_i\right)^2}{2M_{ij,Rd,pl}} \tag{59}$$

$$c_{ij,cb} = \frac{1 + \dfrac{n_{l,ij}}{\chi_y}}{C_{my}\left(1 - \dfrac{\lambda n_{l,ij}}{\chi_y}\right)} - \frac{1 + \underline{\lambda}}{C_{my}\chi_y \left(1 - \underline{\lambda}\dfrac{n_{l,ij}}{\chi_y}\right)^2} n_{l,ij} \tag{60}$$

$$\mathbf{c}_{ij,pl} = \left[\frac{-1}{N_{ij,Rd,pl}} \; \frac{k_{m,ij} x_l L_i}{M_{ij,Rd,pl}} \; \frac{-k_{m,ij}}{M_{ij,Rd,pl}} \; 0 \; 0 \; 0 \right]^\mathsf{T} \in \mathbb{R}^6 \tag{61}$$

$$b_{ijk,pl} = -\frac{k_{m,ij} p_i \left(x_l L_i\right)^2}{2M_{ij,Rd,pl}} \tag{62}$$

$$\mathbf{c}_{ij,M} = \left[0 \; \frac{x_l L_i}{M_{ij,Rd,pl}} \; \frac{-k_{m,ij}}{M_{ij,Rd,pl}} \; 0 \; 0 \; 0 \right]^\mathsf{T} \in \mathbb{R}^6 \tag{63}$$

$$b_{ij,M} = -\frac{p_i \left(x_l L_i\right)^2}{2M_{ij,Rd,pl}} \tag{64}$$

$$\mathbf{c}_{ij,o} = \left[\frac{-1}{\chi_{z,ij} N_{ij,Rd,pl}} \; 0 \; 0 \; 0 \; 0 \; 0 \right]^\mathsf{T} \in \mathbb{R}^6 \tag{65}$$

where $k_{m,ij} = 1 - n_{0,ij}$ (see Eq. (33)), x_l is the coordinate along the element in which the resistance is evaluated, p_i is the transverse distributed loading on element i and $k_{ij,cb}$ is calculated using Eq. (46) and $n_{l,ij}$ is the point of linearization (see Eq. (32)).

7. Buckling length factors

When calculating the reduction factors χ_y and χ_z, the respective critical forces, buckling lengths or buckling length factors are needed. Both buckling lengths are dependent on joint type and surrounding member stiffness. They can be calculated by linear eigenvalue analysis or analytical methods but both approaches are practically impossible to be included in the MILP approach as the number of constraints for each member would be very high (for example, with 15 possible profiles and six connecting members the number of combinations is $15^7 \approx 1.5 \cdot 10^9$).

By using the global linear stability (eigenproblem) analysis solution the buckling length can be calculated as

$$L_{cr,y} = \sqrt{\frac{\pi^2 E I_y}{\lambda_i N}} \tag{66}$$

where λ_i is the eigenvalue of the eigenmode connected buckling of member under inspection and N is the absolute value of axial force present in the member. Note, that λ_i is not necessarily the lowest positive eigenvalue (α_{cr} in EN 1993-1-1 notation), especially in a complicated structure, but the lowest value can be used as a safe approximation for all members.

8. Sequential approach for handling stability parameter values

In last section it was assumed for C_{my}, k_y and k_z to be independent of optimization design or state variables. This assumption is known to be incorrect and the values of the named parameters may depend on them. To ensure they have correct values in the optimization a sequential approach is proposed. First, initial values are introduced for compressed members in structure. Then the structure is optimized with these values. For the obtained design full analysis including global linear stability analysis is performed. By the results from this calculation, the parameter values are updated. The procedure flow chart is seen in Figure 3.

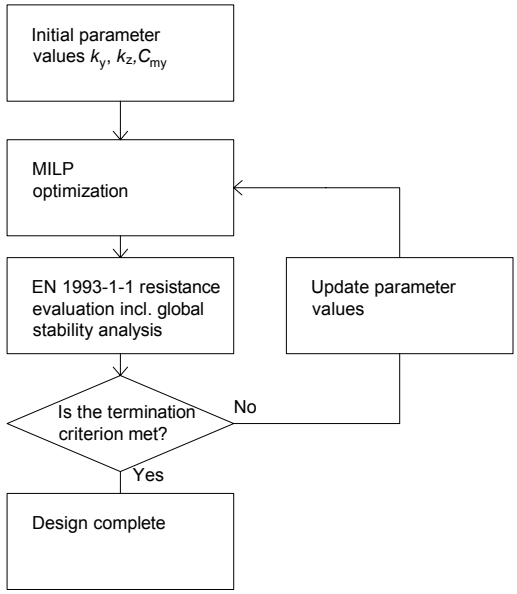

Figure 3: Flow chart of the proposed design procedure.

The iteration is terminated if the design is fully compliant with Eurocode 3. Based on previous Sections, conditions for EN 1993-1-1 resistance evaluation for frame problem could be written as:

$$U_y = \frac{N_{Ed}}{\chi_y N_{Rd}} + k_{yy} \frac{M_{y,Ed}}{M_{y,Rd}} \leq 1 \tag{67}$$

$$U_z = \frac{N_{Ed}}{\chi_z N_{Rd}} \leq 1 \tag{68}$$

$$U_{pl} = \frac{M_{y,Ed}}{M_{y,Rd} \min\left\{\frac{1-n}{1-0.5a}; 1\right\}} \leq 1 \tag{69}$$

$$U_a = \frac{N_{y,Ed}}{N_{y,Rd}} \leq 1 \tag{70}$$

$$U_b = \frac{M_{y,Ed}}{M_{y,Rd}} \leq 1 \tag{71}$$

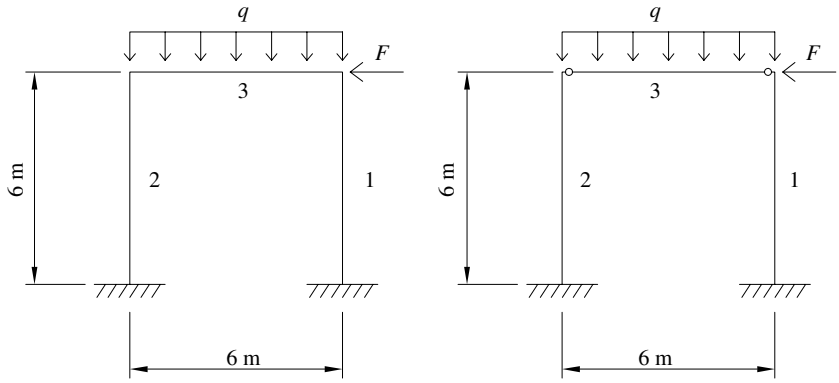

Figure 4: The example frame dimensions, loads, member numbering and in-plane support conditions.

Table 1: Parameter and objective function values at each iteration for hinged frame.

Iteration	C_{my}			k_y			f [kg]
	1	2	3	1	2	3	
0	0.5	0.5	0.5	1	1	1	721
1	0.7	0.7	0.5	1.22	1.22	1	802

The proposed update procedure for the mentioned parameter values is

$$k_y^{n+1} = \alpha k_y^n + (1-\alpha)\, k_y^* \tag{72}$$

$$C_{my}^{n+1} = \alpha C_{my}^n + (1-\alpha)\, C_{my}^* \tag{73}$$

where superscript $n+1$ and n refer to values used in the MILP at iteration $n+1$ and n, respectively, and $*$ to values obtained from non-linearized analysis to design obtained at iteration n. The parameter $\alpha \in [0,1]$ is used to control the step size to alter the parameter values k_y and C_{my}.

9. Numerical examples

Consider a portal frame shown in Figure 4. The columns are chosen from European HEA selection and beams from IPE selection both having 15 possible profiles ranging from HEA100 to HEA400 and IPE100 to IPE400, respectively. The objective function is structural weight. The frame is forced to be symmetric thus leaving only two free sizing variables. The out of plane support is supposed to result buckling length factor $k_z = 1$. Two instances are considered. First, the beam is connected with ideally hinged joints and in second, where beam is connected with ideally rigid joints.

Both cases are optimized with the linearized sequential procedure described in earlier. In the MILP, the resistance constraints are written for 21 evenly distributed points along each member. The initial parameter values are $k_y = 1$ and $C_{my} = 0.5$ for the frame with rigid joints and $k_y = 0.8$ and $C_{my} = 0.5$ for the frame with hinged joints. The stopping criterion for the iteration is that feasible solution according to accurate EN 1993-1-1 member evaluation is found. Therefore, the initial values for the parameters are chosen to be unconservative. The update step size parameter value $\alpha = 0.5$ is used. Displacement constraints are not used. The results and progress of the iteration are seen in Tables 1–2.

Table 2: Parameter and objective function values at each iteration for rigid frame.

Iteration	C_{my}			k_y			f [kg]
	1	2	3	1	2	3	
0	0.5	0.5	0.5	0.8	0.8	0.8	680
1	0.7	0.7	0.7	0.96	0.90	0.8	680
2	0.8	0.8	0.8	1.04	0.94	0.8	721
3	0.85	0.85	0.85	1.07	0.96	0.8	725

Table 3: Parameter values and critical load factor for the exact global optima.

Case	C_{my}			k_y			α_{cr}	f [kg]
	1	2	3	1	2	3		
Rigid	0.84	0.4	0.9	1.18	1.05	2.69	11.6	725
Hinged	0.9	0.9	0.9	1.50	1.50	7.56	6.3	802

For comparison, the global optimum of non-linearized problem is also sought by exhaustive enumeration. The result is 725 kg for the frame with rigid joints and 802 kg for the frame with hinged joints. The buckling length and C_{my} values for the optimal designs are seen in Table 3. In the global linear buckling analysis, 10 elements for each member is used to find the lowest positive eigenmode and eigenvalue.
Thus, it is seen that global optimum is found in both cases with the proposed procedure. However, the convergence of the procedure is dependent of both initial parameter values and step size parameter (α in Eq. (72)) for updating the parameter values especially with the case with rigid joints. With update procedure based only on the obtained design ($\alpha = 1$), suboptimal design ($f = 760$ kg) is obtained. The design thus obtained fulfils the termination criterion but as the design was known to be suboptimal, the iteration was continued resulting in situation where the obtained design jumps between two designs.
In beams, the critical length in Table 3 is relatively high. This happens because the lowest positive eigenvalue that is used on calculating the length is connected to buckling of columns rather than the beam. If the eigenmode and eigenvalue connected to beam buckling was sought, lower values would be expected. However, since the axial force is very low in comparison to bending moment this does not affect the design.

10. Conclusions

In this paper, the effect of buckling length in frame MILP optimization with code-based member resistance constraints is considered. In numerical examples it is shown that buckling length is important parameter since incorrect value will yield that the result obtained in the optimization does not comply with the codes. Therefore, a sequential approach to include member buckling constraints to frame optimization is presented. By this approach, the buckling length dependent on multiple design variables can be used within the MILP scheme. In the numerical examples of small scale the procedure finds the global optima of the non-linearized sizing problem. However, the sequential procedure presented in this paper is not robust in a sense that obtained design might be suboptimal depending on both initial design parameter values and parameter values connected to the solution procedure. Therefore, more research effort is needed to find out proper values for mentioned parameters and limits for the procedure applicability.

11. Acknowledgements

The financial support of Finnish Cultural Foundation, Pirkanmaa Regional fund is gratefully acknowledged.

12. References

[1] O. Ghattas and I. E. Grossmann. MINLP and MILP strategies for discrete sizing structural optimization problems. O. Ural and T. L. Wang (Eds.), *Proceedings of the 10th conference on electronic computation*, pages 197–204, ASCE, 1991.

[2] R. Kureta and Y. Kanno. A mixed integer programming approach to designing periodic frame structures with negative poisson's ratio. *Optimization and Engineering*, 15, 773–800, 2014.

[3] M. Hirota and Y. Kanno. Optimal design of periodic frame structures with negative thermal expansion via mixed integer programming. *Optimization and Engineering*, 16, 767–809, 2015.

[4] EN 1993-1-1. *EN-1993-1-1. Eurocode 3: Design of steel structures. Part 1-1: General rules and rules for buildings.* CEN, 2006.

[5] K. Mela. Resolving issues with member buckling in truss topology optimization using a mixed variable approach. *Structural and Multidisclipinary Optimization*, 50, 1037–1049, 2014.

[6] A. Webber, J. Orr, P. Shepherd and K. Crothers. The effective length of columns in multi-storey frames. *Engineering Structures*, 102, 132–143, 2015.

[7] S. O. Degertekin. Optimum design of steel frames using harmony search algorithm. *Structural and Multidisclipinary Optimization*, 36, 393–401, 2008.

[8] R. Van Mellaert, K. Mela, T. Tiainen, M. Heinisuo, G. Lombaert and M. Schevenels. A mixed-integer linear programming approach for global discrete size optimization of frame structures. M. Papadrakakis, V. Papadopoulos, G. Stefanou and V. Plevris (Eds.), *ECCOMAS Congress*, pages 3395–3408, Greece, 2016.

Publication V

Title: Buckling length of a frame member
Authors: Teemu Tiainen and Markku Heinisuo
Journal: Rakenteiden Mekaniikka (Journal of Structural Mechanics)
Volume: 51
Number: 2
Pages: 49–61

Print permission based on CC BY-SA 4.0 license.

Original available at https://doi.org/10.23998/rm.66836

Rakenteiden Mekaniikka (Journal of Structural Mechanics)
Vol. 51, No 2, 2018, pp. 49 – 61
https://rakenteidenmekaniikka.journal.fi/index
https://doi.org/10.23998/rm.66836
©The author(s) 2018.
Open access under CC BY-SA 4.0 license.

VERTAISARVIOITU
KOLLEGIALT GRANSKAD
PEER-REVIEWED
www.tsv.fi/tunnus

Buckling length of a frame member

Teemu Tiainen[1] and Markku Heinisuo

Summary. In the design of steel frames, the definition of buckling length of its members is a basic task. Computers can be used to calculate the eigenmodes and corresponding eigenvalues for the frame and using these the buckling length of the members can be defined by using the well-known Euler's equation. However, it is not always easy to say, which eigenmode should be used for the definition of the buckling length of a specific member. Conservatively, the lowest positive eigenvalue can be used for all members. In this paper, two methods to define the buckling length of a specific member are presented. The first one uses geometric stiffness matrix locally and the other one uses strain energy measures to identify members taking part in a buckling mode. The applicability of the methods is shown in several numerical examples. Both methods can be implemented into automated frame design, removing one big gap in the integrated design. This is essential when optimization of frames is considered.

Key words: effective length, frame analysis, elastic buckling

Received 6 November 2017. Accepted 19 October 2018. Published online 8 December 2018.

Introduction

In the code-based structural design, the buckling length (also *effective* length) or load of a member is still an important design parameter. For certain structures, the design codes and standards give values for the length factors, as is the case with tubular trusses in EN 1993-1-1 for example, but in general the task is left to the designer.

Multiple methods have been proposed for finding the effective length of a frame member. Widely used simplified approach has been presented by Dumonteil [1]. In this contribution, the transcendental equation is solved approximately with simplified formulas. Multiple extensions for this work have been carried out by several other authors. For example, semi-rigid joints have been considered in [5]. Webber et al. [8] has proposed an extension to cover the effect of axial force in columns adjoining the considered member as well as the effect of axial force in other columns in the same floor. In the examples, it is shown that this approach gives very accurate values in comparison to results given by a finite element software.

Even if the presented simplified methods can be considered to be accurate enough to be applicable with design codes, they do not necessarily fit well in integrated design systems.

[1]Corresponding author. teemu.tiainen@tut.fi

For example, in approach proposed by Webber et al., the user needs to identify other columns in the floor which is not always straightforward task in a complicated structure.

It should also be noted that according to standards, such as the EN 1993-1-1, the concept of buckling length is not needed if geometrically non-linear analysis is employed. However, application of non-linear models will result in greater computational effort needed for the analysis. In case of a single analysis, this is clearly not a problem with contemporary computational tools. However, when optimization is performed the analysis needs to be carried out multiple – even thousands of – times.

Therefore, in this contribution, two approaches for a programmable procedure to assess the effective length are presented. The methods cannot practically be used with hand calculation but need a finite element code that can be altered. However, the routines needed for the proposed methods are relatively easy to implement for an experienced user. The paper is organized as follows. The concept of buckling length and the methods are presented in the following sections and their performance is evaluated in three numerical examples.

Linear stability analysis and buckling length

Typical approach using linear stability theory for elastic buckling yields the well-known linear system of equations

$$\mathbf{f} = \mathbf{K}\mathbf{u} \tag{1}$$

where $\mathbf{f}$ is the vector of nodal forces, $\mathbf{K}$ is the stiffness matrix, to be solved for nodal displacements $\mathbf{u}$. With the nodal displacements, respective internal forces in the elements can be calculated

$$\mathbf{f}^e = \mathbf{k}^e\mathbf{u}^e + \mathbf{r}^e \tag{2}$$

where $\mathbf{f}^e$ is the vector of internal forces in element e, $\mathbf{k}^e$ is the stiffness matrix of element e, $\mathbf{u}^e$ is the vector of displacements for the element e and $\mathbf{r}^e$ is the vector of equivalent external nodal loads.

For the linear stability analysis, the axial forces in each element are picked to form a geometrical stiffness matrix $\mathbf{K}_g$ which is used for writing an eigenvalue problem

$$(\mathbf{K} + \lambda\mathbf{K}_g)\,\mathbf{q} = \mathbf{0} \tag{3}$$

where λ is the eigenvalue and $\mathbf{q}$ is the respective eigenvector representing the buckling mode.

When assessing the buckling length of a single member with the finite element approach it should be recognized which eigenpair should be used. Let us assume it is pair with eigenvalue λ_j for member i.

The critical axial force in flexural buckling by axis y is defined by

$$N_{cr,y} = \frac{\pi^2 E I_y}{L_{cr,y}^2} \tag{4}$$

where E is the Young's modulus for the material, I_y is the second moment of the section in the plane of buckling and $L_{cr,y}$ is the critical length or buckling length for buckling about y axis. Nomenclature and axis definition follow those of EN 1993-1-1 (see Fig. 1). From this expression, the buckling length can be solved

$$L_{cr,y} = \pi\sqrt{\frac{EI_y}{N_{cr,y}}} \tag{5}$$

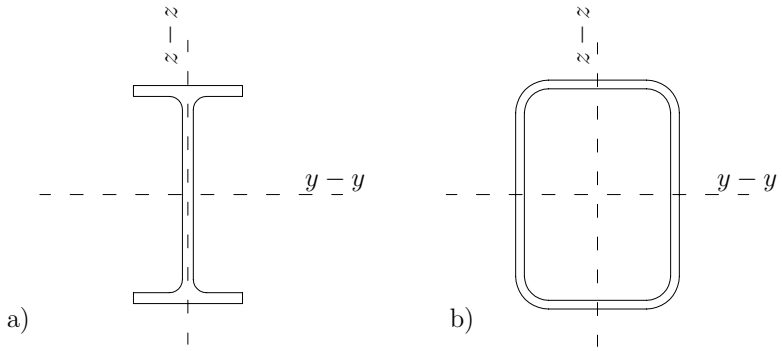

Figure 1: Local axes definition according to EN 1993-1-1 for a) I section b) rectangular hollow section.

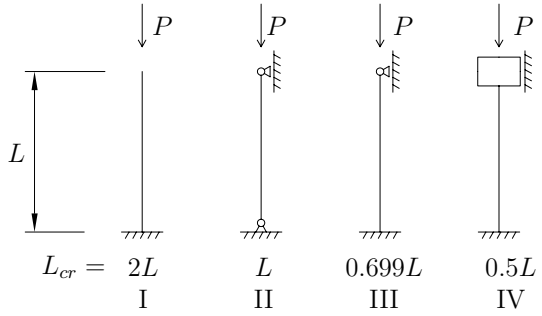

Figure 2: Euler buckling cases.

On the other hand, for member i, the buckling force can be expressed with eigenvalue as $N_{cr,y,i} = \lambda_j |N_i|$, thus

$$L_{cr,y} = \pi \sqrt{\frac{EI_y}{\lambda_j |N_i|}} \tag{6}$$

The buckling length can be best understood when it is compared to the member system length L_{sys}[2]. This can be assessed by formula

$$L_{cr,y} = kL_{sys} \tag{7}$$

where k is a buckling length factor for given direction of buckling (also referred to as K-factor in literature). In the well-known *Euler* cases the factor gets values shown in Tab. 2 but typical members in real frames or other structures rarely fit these support conditions.

Proposed approach with local geometric stiffness

To help the task of choosing the correct eigenpair, the first proposed idea is to include only the finite elements in the evaluated member in the eigenproblem

$$\left(\mathbf{K} + \lambda \mathbf{K}_g^i\right) \mathbf{q} = \mathbf{0} \tag{8}$$

[2]The system length is a concept used by EN 1993-1-1. The length means member length in the mechanical model.

in which

$$\mathbf{K}_g^i = \sum \mathbf{K}_g^e \tag{9}$$

in which the sum is taken over elements belonging to member i.

This implies that instead of one eigenproblem, the design engineer should solve as many eigenproblems as there are compressed members in the structure. However, it is very straightforward that only the lowest positive eigenvalue from each analysis is used.

Proposed approach with strain energy measure

The second proposed approach is based on strain energy. In the well-known linear finite element framework, the element strain energy is calculated as

$$E^e = \frac{1}{2}\mathbf{q}^T\mathbf{k}^e\mathbf{q} \tag{10}$$

where $\mathbf{k}^e$ is the element stiffness matrix and $\mathbf{q}$ is the vector of displacements. Moreover, the member strain energy can be calculated as

$$E^m = \frac{1}{2}\mathbf{q}^T\sum \mathbf{k}^e\mathbf{q} \tag{11}$$

Respectively, for the whole structure, the total strain energy can be calculated when the global stiffness matrix $\mathbf{K}$ is used

$$E = \frac{1}{2}\mathbf{q}^T\mathbf{K}\mathbf{q} \tag{12}$$

The ratio for each member in a deformed shape can be thus calculated as

$$R_m = \frac{E^m}{E} \tag{13}$$

This can be done separately for each member and each eigenmode with positive eigenvalue. The problem related to scaling of eigenvectors disappears when only the relation to total strain energy is considered.

To judge whether a single member is taking part in a buckling mode, it is assumed that the member will have a substantial share of the total strain energy. The share which can be considered substantial is, however, not easily judged. The initial proposal for the criterion is

$$R_m \geq \frac{1}{n} \tag{14}$$

where n is number of members in the structure.

The rationale behind the proposal is purely empirical, based on manual trials on several rectangular 2D frames. However, more rigorous testing might be needed to find out a general criterion to suit other types of structures (frames with diagonal members et cetera).

Numerical examples

Three numerical examples are considered. The first two are extremely simple and academic with only two members but they show some very basic features about the methods rather nicely. The third is an example of a more realistic design situation where a tubular steel truss is connected to columns forming a building frame.

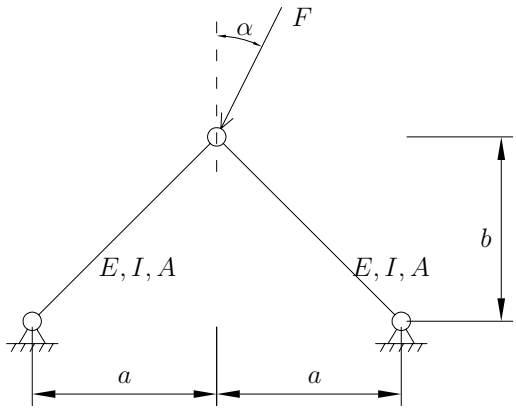

Figure 3: Two member truss.

Two member truss

Consider a two member truss in Fig. 3. Each member is modeled by using five *Euler-Bernoulli* beam elements with element stiffness matrix

$$\mathbf{k} = \frac{E}{l}\begin{bmatrix} A & 0 & 0 & -A & 0 & 0 \\ & \frac{12I}{l^2} & \frac{6I}{l} & 0 & -\frac{12I}{l^2} & \frac{6I}{l} \\ & & 4I & 0 & -\frac{6I}{l} & 2I \\ & & & A & 0 & 0 \\ & & & & \frac{12I}{l^2} & -\frac{6I}{l} \\ \text{sym} & & & & & 4I \end{bmatrix} \tag{15}$$

and element geometric stiffness matrix

$$\mathbf{k}_g = \frac{1}{30l}\begin{bmatrix} 0 & 0 & 0 & 0 & 0 & 0 \\ & 36 & 3l & 0 & -36 & 3l \\ & & 4l^2 & 0 & -3l & -l^2 \\ & & & 0 & 0 & 0 \\ & & & & 36 & -3l \\ \text{sym} & & & & & 4l^2 \end{bmatrix} \tag{16}$$

The ratio of measures a/b is set to 1. The buckling length is calculated with ten values of angle α. The results are seen in Tab. 1. The local approach gives exact value for buckling length factor with each value. The situation is illustrated for $\alpha = 40°$ in Fig. 4 where it can be seen that first three modes represent the buckling of left member and the fourth represents the mode where the member on the right hand side buckles. The respective shares of strain energies are shown in Tab. 2.

Clearly, both proposed methods give exact values for buckling length of both members. The use of lowest eigenmode will result error that grows when α approaches 45°. When $\alpha = 45°$, there is no compressive force in the member 2 and therefore buckling force or buckling length factor cannot be calculated.

Two member frame

Consider a two member frame in Fig. 5. Similarly to previous example, five Euler-Bernoulli elements are used in modeling each member.

Table 1: Buckling length factors with local approach for the two-member truss.

	Local $\mathbf{k}_g$		Lowest eigenmode	
α [°]	k_1 [-]	k_2 [-]	k_1 [-]	k_2 [-]
0	1.00	1.00	1.00	1.00
5	1.00	1.00	1.00	1.09
10	1.00	1.00	1.00	1.19
15	1.00	1.00	1.00	1.32
20	1.00	1.00	1.00	1.46
25	1.00	1.00	1.00	1.66
30	1.00	1.00	1.00	1.93
35	1.00	1.00	1.00	2.38
40	1.00	1.00	1.00	3.38
45	1.00	-	1.00	-

Table 2: Relative strain energy of the five lowest modes in the two-member truss example.

	Mode				
Member	1	2	3	4	5
Left	1.00	1.00	1.00	0.00	1.00
Right	0.00	0.00	0.00	1.00	0.00

The corresponding results as in previous example are shown for this example in Tabs. 3 and 4. In this example, the buckling of members is coupled with small α values. This implies error for the local approach. With the energy based approach the buckling of member with higher load is clearly correct but the buckling of the other member gets very low buckling length values. With $\alpha = 25°$, there is not even a mode within the first ten lowest ones which would give strain energy content of 50 % (see Eq. 14) or more. However, in Tab. 5 it can be seen that in the third mode the strain energy content of the member is 49 %. Thus, it seems that the rule specified in Eq. 14 is not applicable in this example.

Truss frame

Consider a truss frame in Fig. 6. The structure is constructed from cold formed square hollow sections with member profile dimensions shown in Tab. 6. The chosen profiles are a result of optimization [7] with fixed values of buckling length proposed by EN 1993-1-1 for the truss members and simply $0.9L$ for the columns. Cross-sectional properties are calculated following EN 10219-2 [2]. In the mechanical model, the brace-to-chord and chord-to-column joints are hinged, chords and columns are continuous and modeled with beam elements without hinges.

In standard [3], the buckling length factor value for chords is 0.9 and for braces 0.9 (According to Finnish national annex for EN 1993-1-1, value 0.75 can be used). For braces, the model with ideal hinges gives length factor $k = 1.0$ and the value suggested by the standard is lower. This is due to fact that in welded tubular trusses the joints are not necessarily ideally hinged but semi-rigid.

Therefore, some rotational stiffness for the joints is approximated. Joint fixity factor

Table 3: Buckling length factors with local approach for the two-member frame.

	Local $\mathbf{k}_g$		Energy		Lowest eigenmode	
α [°]	k_1 [-]	k_2 [-]	k_1 [-]	k_2 [-]	k_1 [-]	k_2 [-]
0	0.84	0.84	1.00	0.70	1.00	1.00
5	0.84	0.84	0.96	0.73	0.96	1.05
10	0.84	0.84	0.93	0.76	0.93	1.11
15	0.84	0.84	0.91	0.79	0.91	1.20
20	0.84	0.84	0.89	0.41	0.89	1.31
25	0.84	0.84	0.88	-	0.88	1.46
30	0.84	0.84	0.87	0.41	0.87	1.68
35	0.84	0.84	0.86	0.69	0.86	2.05
40	0.84	0.84	0.85	0.72	0.85	2.90
45	0.84	-	0.84	-	0.84	-

Table 4: Relative strain energy of first five modes in the two-member frame, $\alpha = 40°$.

	Mode				
Member	1	2	3	4	5
Left	0.80	0.89	0.92	0.87	0.40
Right	0.20	0.11	0.08	0.13	0.60

Table 5: Relative strain energy of first five modes in the two-member frame, $\alpha = 25°$.

	Mode				
Member	1	2	3	4	5
Left	0.74	0.66	0.51	0.73	0.55
Right	0.26	0.33	0.49	0.27	0.44

Table 6: Truss-frame profile dimensions.

Member	b [mm]	t [mm]
Top Chord	150	8
Bottom Chord	150	5
Columns	180	8
Brace (20 & 33)	100	4
Brace (21 & 32)	90	3
Brace (22 & 31)	90	3
Brace (23 & 30)	60	4
Brace (24 & 29)	60	4
Brace (25 & 28)	50	3
Brace (26 & 27)	50	3

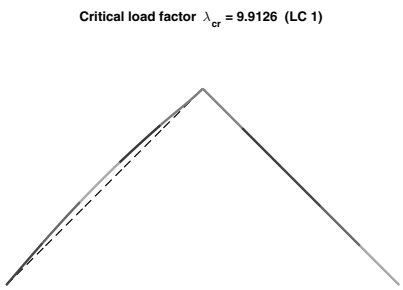

(a) Mode 1.

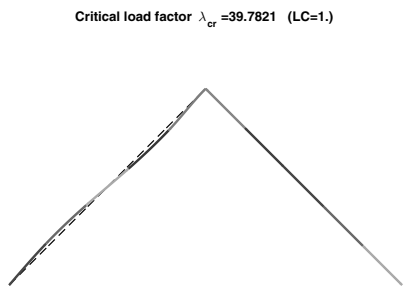

(b) Mode 2.

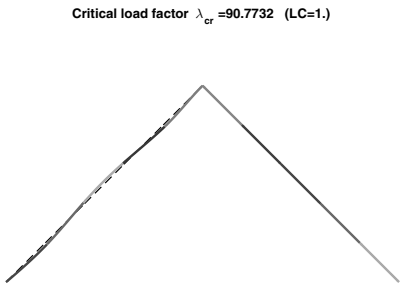

(c) Mode 3.

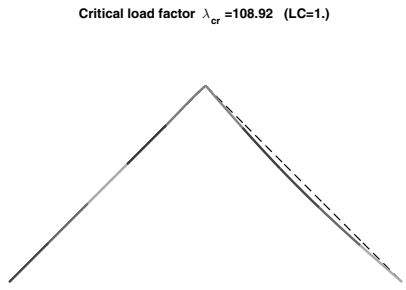

(d) Mode 4.

Figure 4: Four lowest buckling modes for the two member truss. Colouring shows the used finite element division.

α [6] is defined as

$$\alpha = \frac{1}{1 + \dfrac{3EI}{kL}} \tag{17}$$

where k is the rotational stiffness of the joint. Clearly, $\alpha = 0$ means ideal hinge and $\alpha = 1$ ideally rigid connection. The standard EN 1993-1-8 [4] specifies upper limit for ideally hinged joint to be

$$k \leq \frac{EI}{2L} \tag{18}$$

this means

$$\alpha = \frac{1}{7} \approx 0.143 \tag{19}$$

In the calculation, fixity factor value $\alpha = 0.1$ is assumed for brace-to-chord joints. Every member is modeled again with five elements. The results for relative strain energy in ten lowest positive modes can be seen in Table 7. In this structure, the member that is buckling exhibits over 90 % share of the total strain energy. Therefore, it is clear which member buckles in the first ten modes. This can be verified from Fig. 7 for the eight lowest modes.

The lowest four modes are connected to buckling of braces and the fifth one is a sway mode connected to column buckling. Upper chord buckling is seen in mode eight. The respective buckling length factors are seen in Table 8.

It seems that the local approach can predict the buckling length of braces (members from 20 to 33) consistently. In the column buckling mode (Fig. 7 mode 5) both columns

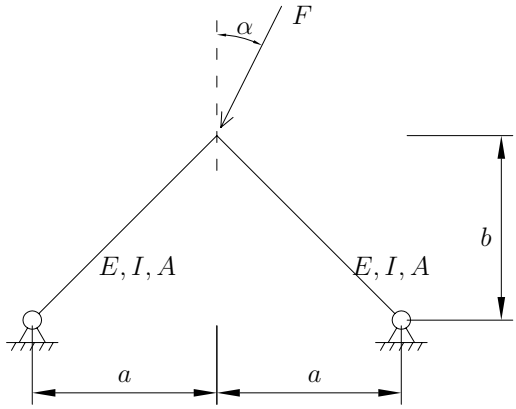

Figure 5: Two member frame.

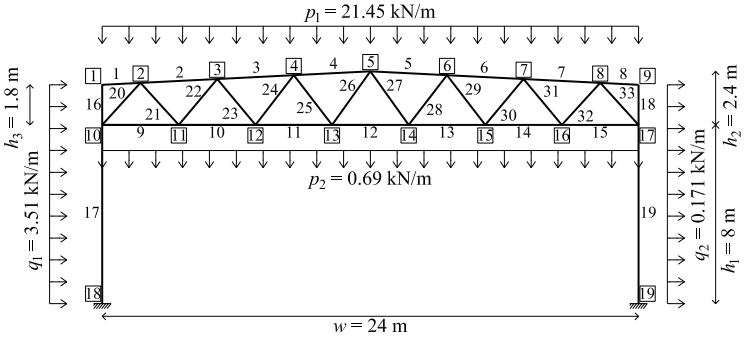

Figure 6: Truss frame example structure, loads and member numbering.

Table 7: Relative strain energy of members of the truss frame in ten lowest positive modes.

	Mode									
Member	1	2	3	4	5	6	7	8	9	10
Columns	0.00	0.00	0.00	0.00	0.98	0.01	0.01	0.00	0.00	0.00
Upper chord	0.00	0.00	0.01	0.01	0.00	0.01	0.01	0.94	0.03	0.01
Brace (20 & 33)	0.00	0.00	0.00	0.00	0.02	0.98	0.98	0.00	0.00	0.00
Brace (21 & 32)	0.00	0.00	0.00	0.00	0.00	0.00	0.00	0.00	0.00	0.00
Brace (22 & 31)	0.00	0.00	0.99	0.99	0.00	0.00	0.00	0.01	0.00	0.00
Brace (23 & 30)	0.00	0.00	0.00	0.00	0.00	0.00	0.00	0.00	0.00	0.00
Brace (24 & 29)	1.00	1.00	0.00	0.00	0.00	0.00	0.00	0.05	0.97	0.99
Brace (25 & 28)	0.00	0.00	0.00	0.00	0.00	0.00	0.00	0.00	0.00	0.00
Brace (26 & 27)	0.00	0.00	0.00	0.00	0.00	0.00	0.00	0.00	0.00	0.00

Table 8: Buckling length factors of compressed members obtained with the proposed methods and with the lowest eigenmode.

Member	Local approach	Energy method	Lowest eigenmode
1	0.80	1.38	30.84
2	0.67	1.18	1.97
3	0.70	0.96	1.59
4	0.70	0.91	1.52
5	0.70	0.92	1.52
6	0.70	0.97	1.61
7	0.67	1.22	2.03
16	0.95	24.65	31.38
17	0.77	1.08	1.38
18	0.95	27.62	35.17
19	0.77	1.07	1.36
20	0.80	0.80	1.13
22	0.80	0.80	1.01
24	0.80	0.80	0.83
26	0.80	0.80	3.27
27	0.80	0.80	1.70
29	0.80	0.80	0.80
31	0.80	0.80	0.99
33	0.80	0.80	1.12

buckle simultaneously and the roof sways horizontally. Thus geometrical stiffness matrix would have to be applied in both columns to capture the mode accurately. By doing this, eigenvalue 2.691 and buckling length factor 1.07 are obtained. These values are very close to the sway mode values.

With the energy method, members 16 and 18 have seemingly very high buckling length factor. However, if the respective buckling forces (Eq. 4) are calculated and the member resistance evaluated according to EN 1993-1-1, approximately 39 % utilization ratio is obtained for members 16 and 18 whereas approximately 50 % ratio is found in members 17 and 19. Thus the high buckling length factor for members 16 and 18 does not seem to have effect on the sizing of the column.

Discussion and conclusions

Both proposed methods are tested in three examples. The first two represent simplified and extreme structures with only two members. In the first one, the buckling modes are totally uncoupled. In the second one the coupling is very strong and there are some parameter values with which the methods fail to give correct buckling length values.

The local approach seems to work well in structures where eigenmodes are not coupled to other members' behaviour or coupling is moderate. If a sway buckling mode is expected, the global geometric stiffness matrix should be used or local matrix should be applied to all columns. However, to authors' knowledge, most of the typical structures found in buildings are braced (no sway modes) and connected with semirigid joints. This means that the applicability range of the method covers many typical structures. Moreover, the

method is very straightforward to be implemented.

The approach based on energy measures can be considered very accurate but at this stage it is not clear how to formulate a criterion for choosing the correct eigenmode in a way that it would work with all frame structures. With the rather simple criterion proposed in the text, good results are obtained in the third design example but the second one reveals that the criterion is not general. Thus more research is needed for a more general criterion.

The computational effort is an important evaluation aspect of structural analysis methods in structural optimization where the objective and constraint functions may need to be evaluated thousands of times in a single optimization run. Of the two proposed methods, the energy based method seems more efficient since only one set of eigenpairs needs to be solved whereas in the local approach the eigenvalue solution needs to be repeated for each compressed member.

In the examples, prismatic members with Euler-Bernoulli beam assumptions are considered. However, both of the methods can theoretically handle also non-prismatic members and also distributed axial loading. Moreover, other types of assumptions of beam behaviour such as the *Timoshenko* beam theory and respective finite elements can be used with these methods.

In this contribution, only planar steel frames were considered. Thus, in further studies, extension to three dimensional structures including flexural buckling out-of-plane as well as torsional buckling behaviour should be considered.

Acknowledgement

The financial support of Finnish Cultural Foundation, Pirkanmaa Regional fund is gratefully acknowledged.

References

[1] Pierre Dumonteil. Simple equations for effective length factors. *Eng J AISC*, 29(3): 111–115, 1992.

[2] EN 10219-2. *Cold formed welded structural hollow sections of non-alloy and fine grain steels. Part 2: Tolerances, dimensions and sectional properties.* CEN, 2006.

[3] EN 1993-1-1. *EN-1993-1-1. Eurocode 3: Design of steel structures. Part 1-1: General rules and rules for buildings.* CEN, 2006.

[4] EN 1993-1-8. *EN-1993-1-8. Eurocode 3: Design of steel structures. Part 1-8: Design of joints.* CEN, 2006.

[5] Georgios E. Mageirou and Charis J. Gantes. Buckling strength of multi-story sway, non-sway and partially-sway frames with semi-rigid connections. *Journal of Constructional Steel Research*, 62(9):893 – 905, 2006. ISSN 0143-974X. doi:https://doi.org/10.1016/j.jcsr.2005.11.019.

[6] G. R. Monforton and Tien Hsing Wu. Matrix analysis of semi-rigid connected frames. *Journal of the Structural Division*, 89:13–24, 1963.

[7] R. Van Mellaert, K. Mela, T. Tiainen, M. Heinisuo, G. Lombaert, and M. Schevenels. Mixed-integer linear programming reformulation approach for global discrete sizing optimization of trussed steel portal frames. In Kai-Uwe Bletzinger, Sierk Fiebig, Kurt Maute, Axel Schumacher, and Thomas Vietor, editors, *WCSMO-12*, Germany, 2017. doi:https://doi.org/10.1007/978-3-319-67988-4_56.

[8] A. Webber, J.J. Orr, P. Shepherd, and K. Crothers. The effective length of columns in multi-storey frames. *Engineering Structures*, 102:132–143, 2015. doi:https://doi.org/10.1016/j.engstruct.2015.07.039.

Teemu Tiainen, Markku Heinisuo
Tampere university of technology
PO box 601 33101 Tampere, Finland
`teemu.tiainen@tut.fi, markku.heinisuo@tut.fi`

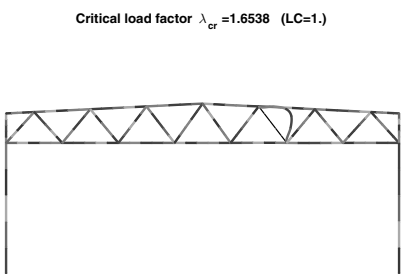

(a) Mode 1.

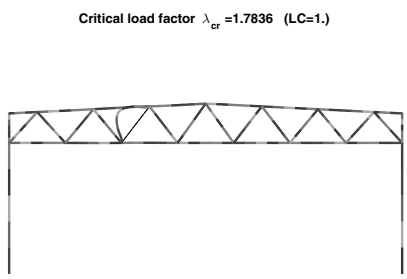

(b) Mode 2.

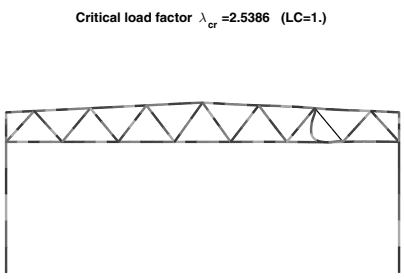

(c) Mode 3.

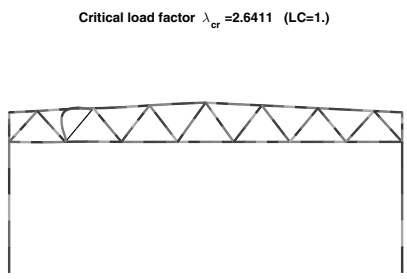

(d) Mode 4.

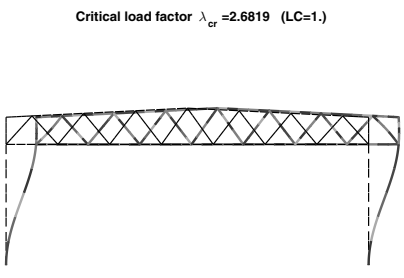

(e) Mode 5.

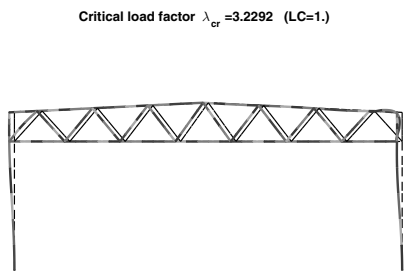

(f) Mode 6.

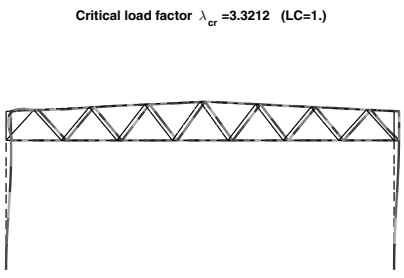

(g) Mode 7.

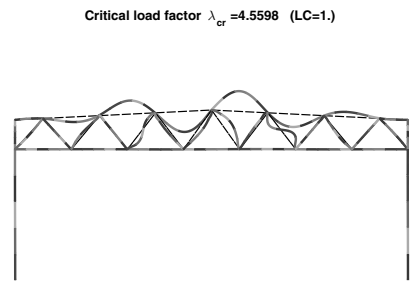

(h) Mode 8.

Figure 7: First eight buckling modes for truss frame.

Publication VI

Title: Two-phase approach in discrete structural sizing optimization
Authors: Teemu Tiainen and Kristo Mela
Journal: manuscript submitted for review

Manuscript

Two-phase approach in discrete structural sizing optimization

Teemu Tiainen · Kristo Mela

–

Teemu Tiainen, Doctoral Researcher, corresponding author
Tampere University
PO box 601 33101 Tampere Finland
email: teemu.tiainen@tuni.fi

Kristo Mela, Assistant Professor
Tampere university
PO box 601 33101 Tampere Finland
email: kristo.mela@tuni.fi

Abstract

In this study, steel frame optimization is treated. The member profiles are taken from a catalogue of commercially available sections, which implies a discrete optimization problem. Member resistance constraints are derived from prevailing design codes in order to ensure applicability of the solution. A two-phase approach is studied as a solution method, where the problem is solved in two stages. Firstly, a continuous relaxation of the discrete problem is formulated and solved. In the second phase, a subset of the discrete set of profile alternatives is constructed around the solution of the relaxation. The discrete problem is then solved using this neighborhood as the set of available profiles. The details of the two-phase procedure are described in this study, and the method is applied on several benchmark problems with comparison to previous studies. Moreover, weight minimization of tubular roof truss is considered with member and joint constraints derived from the European steel design code. The results indicate that the two-phase approach is a viable method for discrete optimization of skeletal structures.

1 Introduction

Optimization of steel frames and trusses leads to a discrete problem in most practical cases, because the member profiles must be chosen from a commercially available list of alternatives. Moreover, the problem is typically nonlinear, as the constraints are derived from the governing design standards, e.g. (EN 1993-1-1 2006) and (Ame 2016), as well as from manufacturing requirements. Although the nonlinearity of the problem increases its complexity, arguably the real difficulty of solving frame and truss optimization problems is mainly because of the discrete variables. For example, it has been shown that discrete truss optimization problems with stress and displacement constraints are NP-hard (Yates, Templeman & Boffey 1982), which implies that the computational effort to solve them increases exponentially as the problem size increases. Similar behaviour is to be expected for frame optimization problems, although the authors are not aware of a mathematical proof of the NP-hardness of frame problems.

These inherent difficulties highlight the importance of problem formulation, as it dictates the range of applicable methods. If the problem formulation is based on the nested analysis and design (NAND) approach, the constraint functions that depend on the structural responses (internal forces, displacements) are known only implicitly. This renders those solution methods inapplicable that rely on the explicit mathematical

Tampere University

structure of the optimization problem. Such methods are, for example, outer approximation and cutting plane methods. If simultaneous analysis and design (SAND) formulation is employed, the problem becomes explicitly defined, which allows to use a wider range of solution methods. However, the problem is then typically a mixed-integer nonlinear programming (MINLP) problem (Kravanja & Zula 2010, Kravanja, Turkalj, Silih & Zula 2013) with a large number of variables and constraints, and such problems are often computationally prohibitive. For truss sizing and topology optimization and frame sizing optimization a mixed-integer linear (MILP) formulation can be derived (Ghattas & Grossmann 1991, Rasmussen & Stolpe 2008, Mela 2014, Kureta & Kanno 2014, Hirota & Kanno 2015, Van Mellaert, Mela, Tiainen, Heinisuo, Lombaert & Schevenels 2018), which is computationally more appealing than the MINLP formulation, but still limited to relatively small problems by the capacity of present solvers and computers.

Conventional deterministic methods used in discrete structural optimization are, among others, branch-and-bound, sequential linear programming, and Lagrangian relaxation (Arora, Huang & Hsieh 1994, Arora & Huang 1996, Arora 2000). Stolpe (2016) provides a comprehensive review on truss optimization with discrete variables, with the valuable remark, that some of the older solution techniques should be re-examined using contemporary computational capabilities. Saka & Geem (2013) have reviewed methods for frame optimization problems, presenting the claim that for discrete problems, *"the solution techniques available among the mathematical programming methods for obtaining the solution of such problems are somewhat cumbersome and not very efficient for practical use."* While this statement was possibly the reason for seeking alternative solution methods, the authors of this study believe that it should be constantly challenged by developing and testing methods based on mathematical programming in conjunction with the increased computational power of contemporary computers.

Since the 1990s, active research on using meta-heuristic methods to solve discrete design optimization problems has been carried out. These methods include genetic algorithms (GA), particle swarm optimization (PSO), harmony search (HS), simulated annealing (SA) and many others. The methods can be applied to discrete problems with black-box function evaluations, as they do not rely on gradient information or on the mathematical structure of the problem. Many of the methods can even be applied when the functions of the optimization problem are discontinuous, which may happen when constraints are derived from the design standards. Different meta-heuristics used in structural sizing problems have been used by Camp, Bichon & Stovall (2005), Kaveh & Talahatari (2009), and Kaveh & Talahatari (2013) among many others.

One drawback of meta-heuristic methods is that they usually require a very large number of function evaluations without any information about the optimality of the obtained solution. The large amount of function evaluations becomes evident particularly when meta-heuristic methods are applied to problems that can also be solved by mathematical programming methods such that the two approaches can be compared (Stolpe 2016). Moreover, meta-heuristic methods do not utilize the mathematical structure of the optimization problem, which means that a great deal of information is lost during the calculations. Nevertheless, meta-heuristic methods are valuable for problems where other methods are not applicable.

Among with different meta-heuristics, different types of heuristics for discrete and combinatorial problems have been proposed for decades (according to Wolsey (1998) oldest references date back to 1950s). Most heuristics can be used both alone and in conjunction with mathematically rigorous solution procedures. For example finding a feasible initial solution for mathematical programming algorithm can be done by heuristic approach. In MILP solution procedures used by commercially available contemporary solvers the branch-and-cut method is assisted with the relaxation induced neighbourhood search (RINS) (Danna, Rothberg & Pape 2005) and feasibility pump (Fischetti, Glover & Lodi 2005).

For practical purposes, finding the global optimum is often not as important as it is to obtain a good design with moderate computational effort. To this end, a method that combines the effectiveness of gradient-based methods for continuous problems with the ability of (meta-)heuristic methods to treat discrete variables would be tempting. Such a *two-phase approach* has been proposed by Hager & Balling (1988), with discussion in (Arora et al. 1994, Arora & Huang 1996). The idea is to solve the discrete design optimization problem in two phases. In the first phase, the discrete variables are relaxed and treated as continuous variables. The *relaxation* of the discrete problem is solved by a chosen gradient-based algorithm for continuous variables. In the second phase, a neighborhood of the solution of the relaxation is generated. This neighborhood consists of discrete variable values corresponding to a subset of the available profiles. The optimum of the original discrete problem is sought from this neighborhood by an appropriate method.

The central idea of the two-phase approach is that only a small subset of the complete set of profile alternatives is explored in the second phase. The premise is that the point generated in the first phase is close to the actual optimum of the original discrete problem. It is appreciated that this assumption does not hold in general. It is also foreseeable that if the neighborhood around the solution of the relaxation is too small, it may not contain any feasible designs. Also, in general there is no guarantee that the global optimum has been

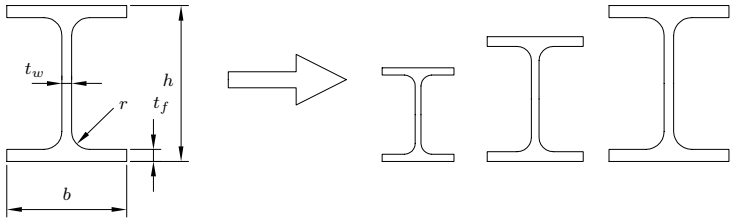

Fig. 1 I profile dimensions in continuous relaxation and discrete sizes.

found at termination of the procedure, as only a subset of the discrete variable values is explored. Therefore, to have any practical value, the two-phase approach should reduce the computational effort compared to other methods while simultaneously producing "good enough" designs.

To the authors' knowledge the first use of a two-phase approach was reported by Hager & Balling (1988). They used cross sectional properties (area, section modulus and moment of inertia) as independent variables. However, they found out that continuous optimum obtained in the first phase was typically far away from discrete profiles. Thus, convex hull constraints were used to direct continuous solution closer to discrete alternatives. Later, Huang & Arora (1997) employed the approach with sequential quadratic programming (SQP) for the continuous solution in the first phase and either branch-and-bound, genetic algorithm or simulated annealing for the discrete problem in the second phase. The numerical examples were steel frames using American standard selection of I profiles. In phase I, four dimensions of the profile (Figure 1) were used as design variables instead of cross-sectional properties used by Hager & Balling (1988). For the branch-and-bound to be applicable, the problem had an approximate convex relaxation.

In this study, the two-phase approach is re-visited and applied to various sizing optimization problems of frames and trusses. A generally applicable metric is presented for the selection of profiles in the second phase. In the first phase, contemporary solvers are used for finding the continuous solution. The discrete subset of profiles is explored both by a genetic algorithm and by a branch-and-cut algorithm, and for the latter, a mixed-integer linear formulation is employed (Van Mellaert et al. 2018). Various design variable choices are explored for the relaxation in different problems. The results obtained by the two-phase approach are compared with solutions found in the literature on selected benchmark problems. Moreover, the method is applied on a tubular truss design problem that includes both member and joint design constraints derived from Eurocode 3. The results indicate that the two-phase approach is indeed a viable solution strategy for optimization of skeletal structures under constraints derived from design standards.

2 Two-phase approach

Consider the sizing optimization problem of a truss or a frame, written in general form as

$$\min_{\mathbf{x}\in\Omega} f(\mathbf{x}) \tag{1}$$

where f is the objective function and Ω is the feasible set including constraints for member and joint resistance, displacements etc. It is assumed that members are divided to n groups, representing, for example, the columns or beams of a particular floor in a multi-storey frame. The design variable vector $\mathbf{x}$ is then partitioned as

$$\mathbf{x} = \{\mathbf{x}_1, \mathbf{x}_2, \ldots, \mathbf{x}_n\} \tag{2}$$

where $\mathbf{x}_k \in \mathrm{R}^{m_k}$ defines the profile of the member group k. All $\mathbf{x}_k$ are discrete variables and can take values appearing in the steel manufacturer's catalogue. Moreover, if the elements of $\mathbf{x}_k$ are the dimensions of a profile they are linked according to the catalogue.

The idea of the two-phase approach is to find a solution in two distinct phases as follows:

Phase I A continuous relaxation of the original problem is formulated and solved. In the relaxation, only continuous variables are used and efficient gradient-based methods can be employed.

Phase II The discrete problem is solved in a neighbourhood of the continuous design obtained in phase I. This neighbourhood is a subset of the original discrete set of alternatives.

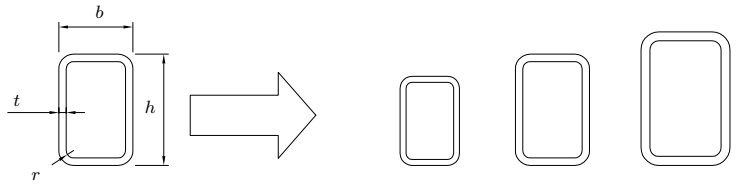

Fig. 2 Rectangular hollow section profile dimensions.

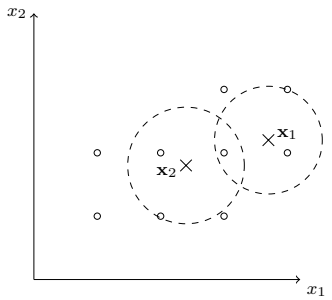

Fig. 3 Two continuous designs ($\mathbf{x}_1$ and $\mathbf{x}_2$) in a two dimensional space (x_1, x_2) with discrete alternatives available in profile catalogue (white dots). Discrete options can be sorted according to their distance from continuous designs $\mathbf{x}_1$ and $\mathbf{x}_2$. Dashed circles show the distance within which three closest alternatives can be found.

In the relaxation each discrete variable is replaced with one or more continuous variables. It is important to notice that the variables in the relaxation can be different from the variables in the second phase. For example, cross-sectional properties (area, moment of inertia, etc.) of the members with approximated dependencies can be used as variables in the first phase, leading to a simpler problem formulation. Then, in the second phase, for each member an integer variable stating the index of a profile in the catalogue of available alternatives can be used.

When profile dimensions are used as design variables the number of variables is dependent on the profile type. For example, for I profiles, the profile is defined by the four (or five if rounding r is included) dimensions shown in Figure 1. Similarly, for rectangular hollow sections the dimensions shown in Figure 2 can be used as design variables.

In the second phase, the first task is to determine the limited search space for the discrete problem. Here, a discrete neighbourhood of the continuous design obtained in phase I is identified using a chosen metric. Various metrics can be used but a general one proposed here is the normalized Euclidean distance between the continuous solution $\mathbf{x}_k^*$ (for group k) and discrete alternative j defined by

$$d_{j,k} = \sqrt{\sum_{i=1}^{m_k} \left(\frac{x_{j,i} - x_{k,i}^*}{x_{i,max} - x_{i,min}} \right)^2} \quad \forall k = 1, 2, \ldots, n \tag{3}$$

where $d_{j,k}$ is the distance for the discrete profile j, $x_{j,i}$ is the value of design variable i for the profile j, $x_{k,i}^*$ is the respective design variable value obtained in phase I and $x_{i,max}$ and $x_{i,min}$ are the maximum and minimum values, respectively, found in the set of discrete alternatives. This idea is depicted in Figure 3.

For each member group the profile alternatives are sorted in ascending order with respect to the distance calculated with Eq. (3). A predefined number of closest alternatives are chosen for the second phase. To limit the design space in the second phase effectively, the predefined number should be considerably lower than the number of alternatives in the catalogue.

In structural optimization, many relaxed problem formulations result in non-convex problems (Svanberg 1984, Stolpe 2016). This holds especially when the constraints are based on structural design standards or codes. This means that it is likely that the relaxed problem will have several local optima. In the procedure proposed here, multiple initial points can be employed in the first phase for solving the continuous relaxation to avoid local minima. If the initial designs are random, the algorithm chosen to this phase must be able to handle infeasible starting points, since it is likely that a random design point is infeasible.

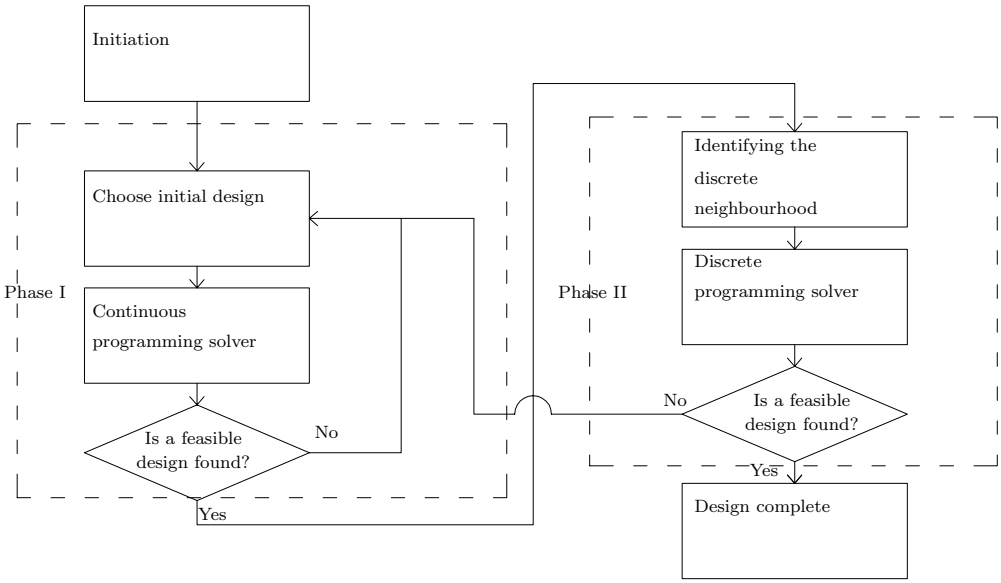

Fig. 4 Flow chart of the two-phase procedure.

Constraints based on structural design standards or codes might include conditional function definitions which can lead to discontinuities in the constraint functions. In such cases, gradient-based optimization methods may fail to find a feasible design in the first phase. Then, a new random starting point will be chosen. Also, it is possible that no feasible point is found in the second phase, for example, if the limited search space is too small. Also in this case, a new random starting point for the first phase is chosen. Another approach to tackle the problem caused by discontinuities in constraint functions would be to create continuous approximations that can be used in the first phase.

The two-phase procedure is illustrated in Figure 4. Depending on the choice of initial point phase I and the optimization method used in phase II the procedure may include stochastics. Thus it is likely – as is the case for other stochastic approaches such as most of the meta-heuristic methods – that multiple runs are needed to ensure good results. Moreover, in general no conclusive checks for global optimality can be made in the second phase. The performance of the two-phase approach is then evaluated through comparison to other methods in various design optimization problems.

If the problem objective and constraint functions allow, the resulting discrete problem in the second phase can also be solved by deterministic approaches such as the MILP reformulation. Then, obviously, the stochastics are limited to the random starting point in phase I.

3 Numerical examples

Four numerical examples are used to demonstrate the applicability of the two-phase procedure. In the first two examples, the behaviour of the approach is compared to a procedure resulting in global optimum of the problem obtained with the MILP reformulation.In the third problem, a tubular roof truss is considered under constraints derived from European steel standards. Finally, a plane frame with American design codes is optimized. For the latter two problems, the performance of the two-phase approach is compared with various metaheuristics.

The two-phase approach was implemented in *Matlab* (version R2016a). The continuous problems of the first phase were solved by the *active-set method* included in the *Matlab optimization toolbox*, whereas the *genetic algorithm* in *Global optimization toolbox* was employed in the second phase. The discrete problems in the second phase were formulated using the indices of profiles in the catalogue as design variables. The algorithms were run with default parameter values unless otherwise noted in the problem description.

The MILPs were solved with *Gurobi* software (Gurobi Optimization 2018) using optimality gap of 0.5 %. With the MILP approach the profile choice is made with binary variables.

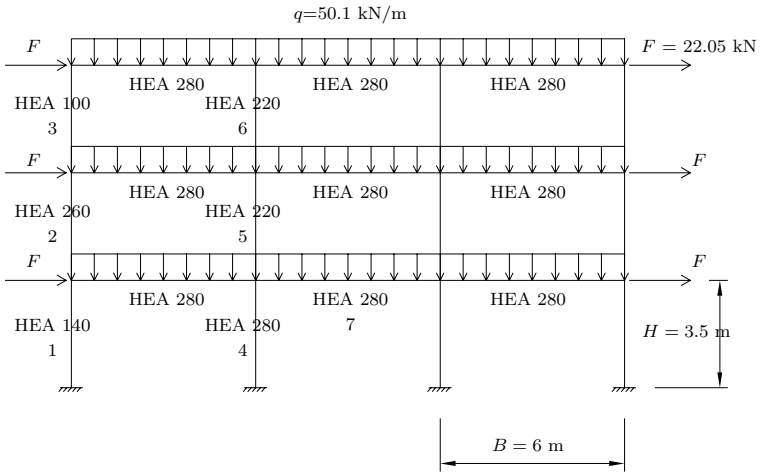

Fig. 5 3x3 frame dimensions, loads, member group numbering and optimal design obtained with MILP by Van Mellaert et al. (2018).

It should be noted that in some test problems the chosen relaxation results in discontinuities in derivatives of the objective and constraint functions. The active-set method belongs to the SQP family where the continuity of the derivatives of the functions is needed to ensure convergence. Therefore, mathematical properties of the relaxed problems are discussed in each design example.

3.1 Three-bay three-story plane frame

Consider the 3x3 plane frame shown in Figure 5. The global optimum for this problem can be obtained by the reformulating it as a mixed-integer linear problem (Van Mellaert et al. 2018). In the design problem, the European hot-rolled HEA selection (Table 1) was used. The constraints were written for axial stress in both ends and mid-span for each member. Stress on both edges of the section were considered as

$$-f_y \leq \frac{N}{A} + \frac{M}{W} \leq f_y \tag{4}$$

$$-f_y \leq \frac{N}{A} - \frac{M}{W} \leq f_y \tag{5}$$

where N is the axial force in the member and M is the bending moment, A is the cross-sectional area and W is the elastic section modulus and f_y is the yield strength. Moreover, inter-story drift was limited to the value $d < H/300 = 11.7$ mm. Also, the vertical deflection of the beams was limited to the value $B/200 = 30$ mm. Material properties were as follows: yield strength $f_y = 355$ MPa, Young's modulus $E = 210$ GPa and density $\rho = 7850$ kg/m^3. The members were grouped such that beams formed one group and inner and outer columns formed their own groups for each story. Thus, there is one independent beam and six column sizing variables making seven in total.

The relaxation scheme in this case could include four dimensions of the I profile as suggested by Huang & Arora (1997) and Figure 1. However, when only HEA catalogue (Table 1) is employed, a single variable, namely the height of the profile is sufficient to define the cross-section. The cross-sectional properties are approximated with the scheme proposed first by Moses & Onoda (1969) according to Haftka & Gürdal (1992). For the given selection, curve fitting results in following approximations

$$I(h) = 0.282h^{3.5677} \quad [\text{mm}^4] \tag{6}$$

$$W(h) = 0.566h^{2.5671} \quad [\text{mm}^3] \tag{7}$$

$$A(h) = 1.81h^{1.5324} \quad [\text{mm}^2] \tag{8}$$

Table 1 Cross-sectional properties of the HEA selection used in the 3x3 frame problem.

HEA	A [mm^2]	W [cm^3]	I [cm^4]	h [mm]
100	2124	72.8	349	96
120	2534	106.3	606	114
140	3142	155.4	1033	133
160	3877	220.1	1673	152
180	4525	294	2510	171
200	5383	389	3692	190
220	6434	515	5410	210
240	7684	675	7763	230
260	8682	836	10455	250
280	9726	1013	13673	270
300	11253	1260	18263	290
320	12437	1479	22929	310
340	13347	1678	27693	330
360	14276	1891	33090	350
400	15898	2311	45069	390

The continuous problem statement for phase I can then be written as

$$\min_{\mathbf{h}} f(\mathbf{h}) = \rho \mathbf{L}^T \mathbf{A}(\mathbf{h}) \tag{9}$$

$$-1 \leq \frac{N_{ik}(\mathbf{h})}{A(h_j) f_y} - \frac{M_{ik}(\mathbf{h})}{W(h_j) f_y} \leq 1 \qquad j : i \in G_j \ \forall i = 1, 2, \ldots, n_M, k = 1, 2, 3 \tag{10}$$

$$-1 \leq \frac{N_{ik}(\mathbf{h})}{A(h_j) f_y} + \frac{M_{ik}(\mathbf{h})}{W(h_j) f_y} \leq 1 \qquad j : i \in G_j \ \forall i = 1, 2, \ldots, n_M, k = 1, 2, 3 \tag{11}$$

$$\frac{300 d_{c,m}(\mathbf{h})}{H} - 1 \leq 0 \qquad \forall m = 1, 2, 3 \tag{12}$$

$$\frac{200 d_{b,n}(\mathbf{h})}{B} - 1 \leq 0 \qquad \forall n = 1, 2, \ldots, 9 \tag{13}$$

$$h_{lb} = 96 \leq h_i \leq h_{ub} = 400 \qquad \forall i = 1, 2, \ldots, 7 \tag{14}$$

where index k refers to predefined location along the member, $d_{c,m}$ is the drift of floor m, and $d_{b,n}$ the vertical displacement on mid-span of beam n.

The constraints of Eqs. (10) and (11) include rational functions of the design variables. The internal forces are evaluated numerically and thus known only implicitly as functions of the design variables. Nevertheless, there are no discontinuities for these functions. Similarly, the displacement constraints of Eqs. (12) and (13) are continuous and differentiable implict functions of the design variables.

For the second phase, three closest HEA profiles are chosen to form the discrete neighbourhood around the solution of the relaxation. As the dimension of the relaxed problem is reduced to contain only the height h of the profile the distance of (Eq. (3)) reduces to

$$d_j = \sqrt{\left(\frac{h_j - h^*}{h_{max} - h_{min}}\right)^2} = \left|\frac{h_j - h^*}{h_{max} - h_{min}}\right| \tag{15}$$

The original discrete problem has $15^7 = 170859375$ possible combinations. When only 3 alternatives per each variable are considered, the number reduces to $3^7 = 2187$ combinations which is only a fraction of the number of combinations in the original discrete problem.

The weight of the optimum design is 6132 kg (Van Mellaert et al. 2018) and the design is seen in Figure 5. With the MILP approach, finding the optimum and proving the optimality took reportedly 5.3 hours (with Intel Core i5-3470 processor 3.2 GHz and 16 GB RAM, Gurobi 6.5). As the optimization approach is deterministic only one run is needed.

The results obtained with the two-phase approach and genetic algorithm are shown in Table 2. Due to their stochastic nature, both GA and the two-phase approach are run 50 times. Note that the two-phase approach is stochastic in this case only because the GA was used in the second phase. Both approaches seem computationally more efficient than the MILP approach and are able to find the global optimum on multiple runs out of 50. The two-phase approach finds the optimum 14 times and GA 16 times. In the continuous phase, the optimization converged to three different designs seen in Table 3 with 50 random initial designs as a starting point. This implies that the relaxed problem has several local optima. Additionally, the profile heights of the global discrete optimum are listed in Table 3. It can be seen that best of the obtained continuous

Table 2 Main results of the 3x3 plane frame example. MILP result reported by Van Mellaert et al. (2018)

Method	Runs	Objective function value [kg] Best found	Mean	Std.	Time per run [h]
MILP	1	6132	-	-	5.3
GA	50	6132	6210	53	0.05
2-phase	50	6132	6287	125	0.02

Table 3 Phase I results and the known global optimum in the 3x3 plane frame example.

n [-]	f^* [kg]	Profile height h [mm] 1	2	3	4	5	6	Beam
17	5933	125.5	253.6	96.0	267.6	199.0	192.5	267.6
25	5939	313.8	96.0	226.2	190.1	268.5	96.0	259.2
8	6081	139.4	250.7	197.2	265.1	205.5	145.1	268.1
Discrete optimum		133	250	96	270	210	210	270

Table 4 Available profiles for the 52-bar planar truss.

No.	A [mm^2]	No.	A [mm^2]	No.	A [mm^2]	No.	A [mm^2]
1	71.613	17	1008.385	33	2477.414	49	7419.340
2	90.968	18	1045.159	34	2496.769	50	8709.660
3	126.451	19	1161.288	35	2503.221	51	8967.724
4	161.290	20	1283.868	36	2696.769	52	9161.272
5	198.064	21	1374.191	37	2722.575	53	9999.980
6	252.258	22	1535.481	38	2896.768	54	10322.560
7	285.161	23	1690.319	39	2961.284	55	10903.204
8	363.225	24	1696.771	40	3096.768	56	12129.008
9	388.386	25	1858.061	41	3206.445	57	12838.684
10	494.193	26	1890.319	42	3303.219	58	14193.520
11	506.451	27	1993.544	43	3703.218	59	14774.164
12	641.289	28	2019.351	44	4658.055	60	15806.420
13	645.160	29	2180.641	45	5141.925	61	17096.740
14	792.256	30	2283.705	46	5503.215	62	18064.480
15	816.773	31	2290.318	47	5999.988	63	19354.800
16	939.998	32	2341.931	48	6999.986	64	21612.860

designs is close to the discrete optimum but the other locally optimal designs differ from it substantially to a degree that the actual discrete optimum is not included in the discrete neighbourhood with three closest profiles.

3.2 52-member planar truss

Consider the plane truss in Figure 6. This example has been treated by several previous optimization researchers (Wu & Chow 1995, Lee, Geem, Lee & Bae 2005, Kaveh & Talahatari 2009, Li, Huang & Liu 2009, Sadollah, Bahreininejad, Eskandar & Hamdi 2012) using different meta-heuristic approaches.

The problem is discrete with 64 possible shapes ranging from cross-sectional area $A = 71.613$ mm^2 to 21612.860 mm^2 (Table 4) and 52 members arranged in 12 groups (Table 5). The material properties are: Young's modulus $E = 207$ GPa and yield stress $f_y = 180$ MPa. The structure is modeled with truss elements and the constraints are mathematically rather straightforward stress constraints which means the problem can be reformulated as MILP and thus the verified global optimum for the problem can be found. However, finding the solution of the resulting MILP turned out to be computationally very demanding. After 10 days of calculation (with Intel Core i5-6200U 2.3 GHz and 8 GB RAM), the optimality gap (gap between the best found discrete design and the relaxed solution) was still 8.4 %, the best found design having the weight of 1898 kg which is lower value than reported by the previous contributors (1902 kg by Sadollah et al. (2012)).

The continuous relaxation for the two-phase approach is straightforward since only cross-sectional areas are used in the structural analysis and member resistance evaluation. Thus cross-sectional areas can be used directly as design variables. The members are divided into 12 groups, denoted by G_j, and one design variable A_j sets the cross-sectional area of the members belonging to the group j. The grouping is shown in Table 5.

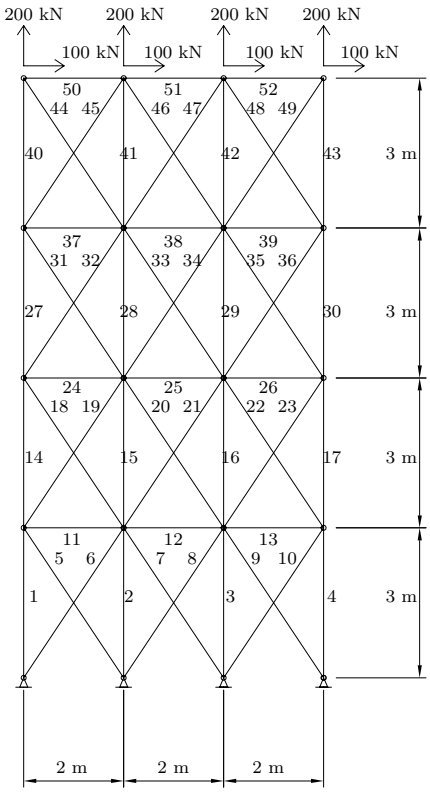

Fig. 6 52-bar planar truss dimensions, topology, loads and member numbering.

The continuous relaxation can be formulated as

$$\begin{aligned} &\min_{\mathbf{A}} \ \rho \mathbf{L}^T \mathbf{A} \\ &\text{such that} \quad N_i(\mathbf{A}) - A_j f_y \leq 0, \quad \forall\, j,\ i \in G_j \\ &\qquad\qquad -N_i(\mathbf{A}) - A_j f_y \leq 0, \quad \forall\, j,\ i \in G_j \\ &\qquad\qquad A_{lb} \leq A_j \leq A_{ub}, \quad j = 1, 2, \ldots, 12 \end{aligned} \tag{16}$$

where axial forces N_j are implicit functions of the variable vector $\mathbf{A}$, and $A_{lb} = 71.612\,\mathrm{mm}^2$ and $A_{ub} = 21612.860\,\mathrm{mm}^2$ are the lower and upper bounds of the cross-sectional areas, respectively. It has been shown by Svanberg (1984) that this kind of formulation can be non-convex which seems to be the case in this problem too since the active-set method converges to several different designs depending on the initial design.

In this problem, the search was tested with discrete search space of 5, 10 and 15 closest discrete profiles around the continuous solution. For each case, 50 complete runs were executed. The original discrete problem has $64^{12} = 4.72 \cdot 10^{21}$ possible combinations whereas the limited spaces have $5^{12} = 2.33 \cdot 10^{8}$, 10^{12} and $15^{12} = 1.30 \cdot 10^{14}$ combinations. Clearly, with these values, total enumeration is not possible in feasible time span.

The main results including those reported in the literature can be seen in Table 6. As in the previous problem, several locally optimal designs are obtained in the continuous phase. Moreover, it can be noted that in the two-phase approach, the MILP reformulation can be used with limited search space in the second phase. The MILP approach was tested with 5 and 10 profiles closest to the best found local optimum of the relaxation. Even with reduced space of ten profiles for each sizing variable, the run was manually stopped after five days without reaching the optimality gap stopping criterion. However, with five profiles the solution was obtained rather quickly. It is shown that 1913 kg is the optimum of the limited search space of five profiles.

Table 5 Member grouping and design variable values of the best found continuous and discrete designs for the 52-bar planar truss.

		A [mm^2]	
j	G_j	Continuous	Discrete
1	1-4	4417.9	4658.1
2	5-10	1113.7	1161.3
3	11-13	241.81	506.45
4	14-17	3394.5	3303.2
5	18-23	863.89	940
6	24-26	221.46	506.45
7	27-30	2311.2	2238.7
8	31-36	956.37	1008.4
9	37-39	259.01	363.23
10	40-43	1318.3	1283.9
11	44-49	1052.8	1161.3
12	50-52	417.44	506.45

Table 6 Main results from 52-member planar truss example. The results of GA, HS, PSO and MBA reported in the literature. n_{fe} is the number of function evalutions.

		Objective function value [kg]			
Method	Runs	Best found	Mean	Std	Mean n_{fe} [-]
GA (Wu & Chow 1995)	-	1970	-	-	-
HS (Lee et al. 2005)	-	1906	-	-	-
PSO (Li et al. 2009)	-	2230	-	-	150000[a]
PSOPC (Li et al. 2009)	-	2147	-	-	150000[a]
HPSO (Li et al. 2009)	-	1905	-	-	150000[a]
DHPSACO (Kaveh & Talahatari 2009)	-	1905	-	-	-
MBA (Sadollah et al. 2012)	-	1902	1906	4.09	-
2-phase GA, 5	50	1913	2063	359	11603
2-phase GA, 10	50	1903	2198	652	17072
2-phase GA, 15	50	1898	1977	107	20128
2-phase MILP, 5	1	1913	n/a	n/a	n/a
2-phase MILP, 10	1	1902[b]	n/a	n/a	n/a
MILP	1	1898[b]	n/a	n/a	n/a
GA	25	1907	1986	86	27089

[a] calculated from set number of iterations
[b] with optimality gap above stopping criterion

Table 7 Number of function evaluations using the two-phase approach with different number of local search options n_d.

	Phase I		Phase II	
n_d	Min	Mean	Min	Mean
5	728	1136	7801	10467
10	741	1110	6701	15961
15	718	1105	7701	19023

In this example, the two-phase approach yields the same design as the MILP reformulation, with slightly lower objective function value than reported in the literature. The best found design variable values are listed in Table 5. HS, particle swarm optimization (HPSO), discrete hybrid particle swarm ant colony optimization (DHPSACO) and mine-blast algorithm (MBA) seem to perform equally well in terms of objective function value but MBA and DHPSACO are computationally more efficient when the number of function evaluations is considered. In the two-phase approach, most of the function evaluations are connected to phase II (Table 7). This implies that using MBA or DHPSACO with the two-phase approach in the second phase instead of GA might be beneficial.

This problem was also tested with direct application of GA. It was observed that the implementation of GA in Matlab seems to be more efficient than the implementation used by Wu & Chow (1995) and different PSO versions considered by Li et al. (2009).

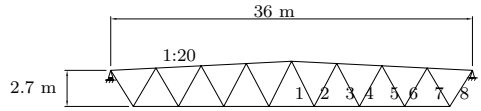

Fig. 7 Truss dimensions, topology and brace numbering. The truss is symmetric with respect to midspan.

Table 8 The list of available cold-formed square hollow section profiles for the truss design problem. b is the width, h the height and t the wall thickness.

Number	*bxhxt* [mm]	Number	*bxhxt* [mm]	Number	*bxhxt* [mm]
1	25x25x3	20	90x90x5	39	150x150x10
2	30x30x3	21	90x90x6	40	150x150x12.5
3	40x40x3	22	100x100x4	41	160x160x6
4	40x40x4	23	100x100x5	42	160x160x8
5	50x50x3	24	100x100x6	43	160x160x10
6	50x50x4	25	100x100x8	44	180x180x6
7	50x50x5	26	110x110x4	45	180x180x8
8	60x60x3	27	110x110x5	46	180x180x10
9	60x60x4	28	120x120x4	47	200x200x8
10	60x60x5	29	120x120x5	48	200x200x10
11	70x70x3	30	120x120x6	49	200x200x12.5
12	70x70x4	31	120x120x8	50	250x250x6
13	70x70x5	32	120x120x10	51	250x250x8
14	80x80x3	33	140x140x5	52	250x250x10
15	80x80x4	34	140x140x6	53	250x250x12.5
16	80x80x5	35	140x140x8	54	300x300x10
17	80x80x6	36	150x150x5	55	300x300x12.5
18	90x90x3	37	150x150x6		
19	90x90x4	38	150x150x8		

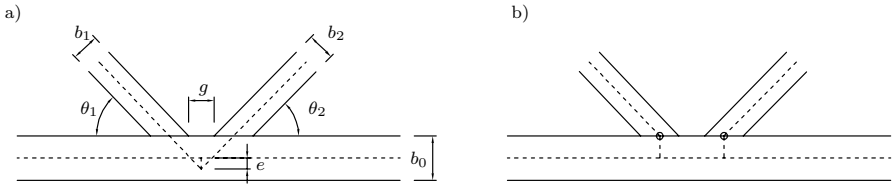

Fig. 8 Tubular truss joint area. a) dimensions and b) schematic representation of the finite element model.

3.3 Tubular roof truss

Consider the sizing optimization of the tubular roof truss shown in Figure 7. The member profiles are chosen from a set of cold-formed square hollow-sections shown in Table 8. There are in total ten sizing variables: eight for braces and one for each chord. The material properties are as follows: Young's modulus $E = 210$ GPa, density $\rho = 7850$ kg/m^3 and yield strength $f_y = 355$ MPa. The truss is subjected to a uniform distributed load of 25 kN/m applied at the top chord.

The truss is modeled with beam elements such that the bending moment of the chords can be taken into account. Moreover, in the joint area, the extensions of brace members do not necessarily meet at the center line of the chord which means that there is eccentricity in the joint. The bending moment caused by the eccentricity is taken into account by modeling the joint area as illustrated in Figure 8. The eccentricity is taken into account with very rigid short beam element and braces are connected to it with ideally hinged joint. The gap is in the example fixed to the value $g = 50$ mm. When brace width b is altered, the intersection point of center line extensions of the braces moves as well. This creates a rather complicated dependency between member profile dimensions, joint eccentricities and brace-to-chord angles. The details of joint geometry and finite element modeling can be found in (Tiainen, Mela, Heinisuo & Jokinen 2017).

In the two-phase approach, each discrete sizing variable is replaced with two continuous sizing variables, namely the outer dimension of the member b_i and the wall thickness of the member t_i (see Figure 2). The cross-sectional properties are calculated according to standard EN 10219-2 (EN 10219-2 2006). The corner

294 outer radius is a piecewise linear function of t:

$$r(t) = \begin{cases} 2t & \text{if } t \leq 6 \text{ mm} \\ 2.5t & \text{if } 6 \text{ mm } < t \leq 10 \text{ mm} \\ 3t & \text{if } t \geq 10 \text{ mm} \end{cases} \tag{17}$$

295 This results in discontinuity in the functions of cross-sectional properties (A, W and I) which are found in the
296 member resistance evaluation formulas and thus the related constraints. Thus, in phase I the relaxed problem
297 is considered with the approximated rounding of

$$r(t) = 2.5t \quad \text{mm} \tag{18}$$

The EN 1993-1-1 (2006) member design requirements in the planar case with square hollow sections reduce to

$$\frac{N_{Ed}}{Af_y} \leq 1 \qquad \text{(axial force)} \tag{19}$$

$$\frac{M_{Ed}}{M_{Rd}} \leq 1 \qquad \text{(bending moment)} \tag{20}$$

$$\frac{N_{Ed}}{Af_y} + \left(1 - \frac{N_n}{Af_y}\right)\frac{M_{Ed}}{M_{Rd}} \leq 1 \qquad \text{(combined axial force and bending)} \tag{21}$$

$$\frac{N_{Ed}}{\chi_y Af_y} + k_{yy}\frac{M_{Ed}}{W_{ply}f_y} \leq 1 \qquad \text{beam-column stability, for compressed members} \tag{22}$$

298 where N_{Ed} is the axial force in the member, M_{Ed} is the in-plane bending moment, W_{ply} is the plastic section
299 modulus of the profile and N_n is defined by

$$N_n = 0.5 \min\left\{\frac{A - 2bt}{A}; 0.5\right\} Af_y \tag{23}$$

The design requirements are clearly non-linear with respect to the design variables b and t. They can be written as optimization constraints as

$$-1 \leq \frac{N(\mathbf{x})}{A(\mathbf{x})f_y} \leq 1 \tag{24}$$

$$-1 \leq \frac{M(\mathbf{x})}{W_{ply}(\mathbf{x})f_y} \leq 1 \tag{25}$$

$$-1 \leq \frac{N(\mathbf{x})}{A(\mathbf{x})f_y} + \left(1 - \frac{N_n(\mathbf{x})}{A(\mathbf{x})f_y}\right)\frac{M(\mathbf{x})}{W_{ply}(\mathbf{x})f_y} \leq 1 \tag{26}$$

$$-1 \leq \frac{N(\mathbf{x})}{A(\mathbf{x})f_y} - \left(1 - \frac{N_n(\mathbf{x})}{A(\mathbf{x})f_y}\right)\frac{M(\mathbf{x})}{W_{ply}(\mathbf{x})f_y} \leq 1 \tag{27}$$

$$-\frac{N(\mathbf{x})}{\chi_y(\mathbf{x})A(\mathbf{x})f_y} + k_{yy}(\mathbf{x})\frac{M(\mathbf{x})}{W_{ply}(\mathbf{x})f_y} \leq 1 \qquad \text{only for compressed members} \tag{28}$$

$$-\frac{N(\mathbf{x})}{\chi_y(\mathbf{x})A(\mathbf{x})f_y} - k_{yy}(\mathbf{x})\frac{M(\mathbf{x})}{W_{ply}(\mathbf{x})f_y} \leq 1 \qquad \text{only for compressed members} \tag{29}$$

300 These constraints are collected to member resistance constraint vector $\mathbf{g}_{M,i}$ for each member i.
301 The design of welded tubular joints according to EN 1993-1-8 (2006) is carried out by comparing the axial
302 force of the braces with the resistance of the joints for the relevant failure modes. Additionally, to ensure that
303 the joint is within the range of applicability of the design equations, a set of constraints regarding the geometry
304 of the joint are provided. In general the joint resistance evaluation formulas are non-linear with respect to the
305 continuous relaxation. For example, the resistance in probably the most important failure mode of a K joint
306 (Figure 8), chord face yielding failure, is calculated as (EN 1993-1-8 2006, Table 7.12)

$$N_{Rd,cfy} = \frac{8.9k_n f_{y0} t_0^2}{\sin\theta_i}\frac{2b_1 + 2b_2}{4b_0}\sqrt{\frac{b_0}{2t_0}} \tag{30}$$

307 where k_n is a factor taking into account the compressive stress in the chord face, f_{y0} is the yield strength of
308 the chord material, t_0 is the chord wall thickness, θ_i is the angle between chord and brace member, b_i and h_i
309 are the dimensions of the members with subscript 0 referring to chord and 1 and 2 referring to braces (see

Table 9 Results of 50 runs for tubular truss example.

	Objective function value [kg]				Function evaluations [-]	
Approach	Best found	Mean	Median	Std	Mean	Std
GA	1669	2323	1950	948	22549	9573
2-phase	1584	1739	1715	88	11608	3639

also Figure 8). In continuous problem, the dimensions b_i and t_i are the design variables. Moreover, k_n depends on the internal forces and the cross-sectional properties of the chord. With fixed gap g, changing the member profile outer dimensions results in change of angles θ_i as well.

The corresponding joint resistance constraint can be formulated as

$$-1 \leq \frac{N}{N_{Rd,cfy}} \leq 1 \tag{31}$$

where N is the axial force in brace member. These constraints are collected to a constraint vector $\mathbf{g}_{R,j}$. Each joint j then has 16 resistance constraints, 8 for each brace.

The range of validity of the design rules for welded joints induce constraints for the joint geometry and for the dimensions of the profiles of the connecting members (EN 1993-1-8 2006, Table 7.8). Additional constraints can be employed to ensure manufacturability of the joints. For example, the brace width b_i should not exceed the chord width b_0. This can be written as

$$\frac{b_i}{b_0} - 1 \leq 0 \tag{32}$$

The joint geometry constraints are collected to the vector $\mathbf{g}_{G,j}$ for each joint j.

The weight minimization problem for the tubular roof truss can be written as

$$\begin{aligned} \min_{\mathbf{x}} \ & \rho \mathbf{L}^T \mathbf{A}\left(\mathbf{x}\right) \\ \text{such that } & \mathbf{g}_{M,i}\left(\mathbf{x}\right) \leq 0, \quad i = 1, 2, \ldots, n_M \\ & \mathbf{g}_{R,j}\left(\mathbf{x}\right) \leq 0, \quad j = 1, 2, \ldots, n_J \\ & \mathbf{g}_{G,j}\left(\mathbf{x}\right) \leq 0, \quad j = 1, 2, \ldots, n_J \end{aligned} \tag{33}$$

where n_J is the number of joints and n_M is the number of members. For more details on joint constraints, see (Jokinen, Mela, Tiainen & Heinisuo 2016, Tiainen et al. 2017, EN 1993-1-8 2006).

In the second phase, discrete neighbourhood consists of five closest profiles for each member, sorted by the distance (see Eq. (3))

$$d_j = \sqrt{\left(\frac{b_j - b^*}{b_{max} - b_{min}}\right)^2 + \left(\frac{t_j - t^*}{t_{max} - t_{min}}\right)^2} \tag{34}$$

where b_j and t_j are the dimensions of profile alternative j, and b^* and t^* the dimensions of the best found continuous solution.

The tubular truss sizing optimization is performed with the two-phase approach and GA. The performance of both approaches is evaluated by taking the results of 50 complete runs. The main results are seen in Table 9 and design variable values for the best found designs in Table 10. The two-phase approach found approximately 6 % better design in terms of objective function value and the performance is better with every criterion in Table 9. However, the main benefit of the two-phase approach is the reduced computational effort (on average 50 % lower number of function evaluations).

With random initial point in the relaxed phase, the optimization fails to converge in about 9 % of the cases. This is probably due to the fact that some constraint functions include non-differentiable points even though the discontinuities related to Eq. (17) have been replaced by the approximation in Eq. (18). If the approximation is not used, the continuous optimization failed to converge in 60 % of cases.

Based on the results of successful continuous runs, the design space contains multiple local optima. In addition, in 1 out of 50 runs the GA did not find a feasible solution in the second phase. Despite these findings the two-phase procedure seems to be efficient on average in comparison with GA. However, due to high possibility of not finding a feasible solution, the deviation in needed computational effort for one complete run seems high. However, the deviation in the function evaluation is considerable also when GA is applied directly.

Table 10 Design variable values for the best found designs for the tubular truss problem.

Member	Continuous	GA	Two-phase
Top chord	214.5x6.6	200x8	200x8
Bottom chord	178.0x5.2	180x6	160x6
Brace 1	78.4x3.0	80x4	70x3
Brace 2	169.4x5.0	150x6	150x6
Brace 3	126.8x7.3	150x6	120x8
Brace 4	104.6x3.0	90x4	90x3
Brace 5	133.4x3.8	110x4	110x4
Brace 6	139.4x4.0	100x4	110x4
Brace 7	178.0x5.3	180x6	160x6
Brace 8	114.4x8.1	120x8	120x8

3.4 Three-bay twenty-four-story frame

Consider the planar frame (Figure 9) which has been treated extensively in the literature, for example, by Saka & Kameshki (1998), Camp et al. (2005), Degertekin (2008), Kaveh & Talahatari (2010*a*), Kaveh & Talahatari (2010*b*), Kaveh & Talahatari (2012), and Kaveh & Talahatari (2013).

The members are organized in 20 groups (the numbering is shown in Figure 9). The member profiles are chosen from the 3rd edition AISC LRFD selection of W profiles with the beams (groups 1-4) having 267 possible shapes. The column profiles (groups 5-20) are chosen from the set of 37 W14 profiles. Constraints are derived from AISC LRFD specification. The material properties are $E = 205$ GPa (29732 ksi) and $f_y = 230$ MPa (33.4 ksi). The constraints are based on the following member design rule:

$$\frac{P_u}{2\phi_c P_n} + \frac{M_u}{\phi_b M_n} \leq 1 \text{ for } \frac{P_u}{\phi_c P_n} < 0.2 \tag{35}$$

$$\frac{P_u}{\phi_c P_n} + \frac{8}{9}\frac{M_u}{\phi_b M_n} \leq 1 \text{ for } \frac{P_u}{\phi_c P_n} \geq 0.2 \tag{36}$$

where P_u is the required strength (tension or compression), P_n is the nominal axial strength (tension or compression, including flexural buckling), ϕ_c is the resistance reduction factor (for tension 0.9, for compression 0.85), M_u is the required bending moment strength, M_n the nominal bending moment strength, and ϕ_b is the bending moment resistance reduction factor (0.9). Additionally, the inter-story drift limit

$$\frac{d_j}{h_j} \leq \frac{1}{300},\ j = 1, 2, \ldots, 24 \tag{37}$$

is imposed, where d_j is the lateral drift in story j and h_j is the height of story j.

These design conditions are written as constraints as follows:

$$g_m(\mathbf{x}) = \begin{cases} \dfrac{P_u}{2\phi_c P_n} + \dfrac{M_u}{\phi_b M_n} - 1 \leq 0 \text{ for } \dfrac{P_u}{\phi_c P_n} < 0.2 \\ \dfrac{P_u}{\phi_C P_n} + \dfrac{8}{9}\dfrac{M_u}{\phi_b M_n} - 1 \leq 0 \text{ for } \dfrac{P_u}{\phi_c P_n} \geq 0.2 \end{cases} \tag{38}$$

and

$$g_d(\mathbf{x}) = \frac{300 d_j}{h_j} - 1 \leq 0,\ j = 1, 2, \ldots, 24 \tag{39}$$

The continuous relaxation for the two-phase approach is now implemented using four design variables for each profile choice as suggested in Figure 1.

In the first phase, the cross-sectional properties are calculated without the rounding r, for example the second moment of the area becomes

$$I_y = \frac{bh^3}{12} - \frac{(b - t_w)\left(h - 2t_f\right)^3}{12} \tag{40}$$

represented with the chosen four design variables.

To ensure compliance with the AISC code, relations of dimensions h, b, t_w and t_f need to be constrained due to local buckling. It is recognized that the selection includes only compact cross-sections which are not

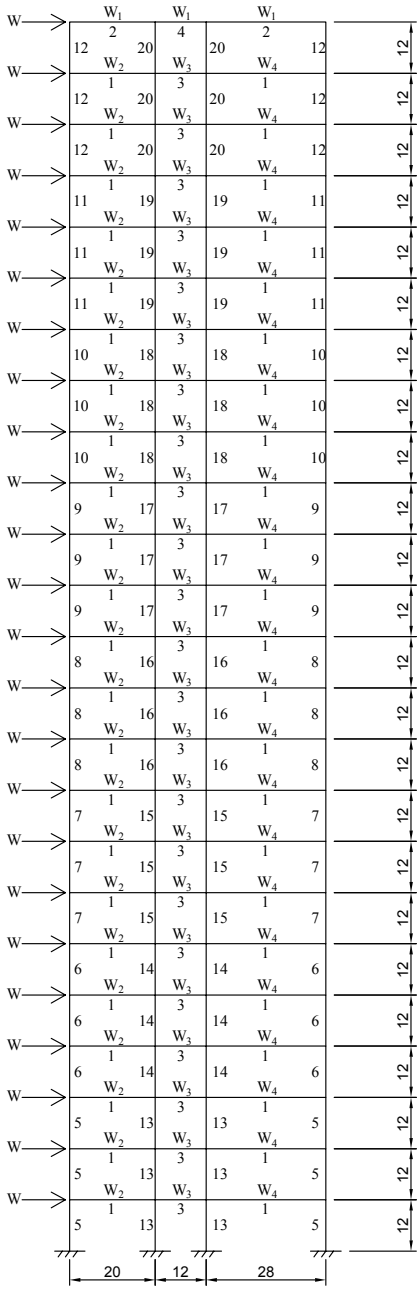

Fig. 9 Layout, member grouping and loading for three-bay twenty-four-story frame. Frame bay width and floor height dimensions in ft (304.8 mm). Load values $W = 5,761.85$ lb, $W_1 = 300$ lb/ft, $W_2 = 436$ lb/ft, $W_3 = 474$ lb/ft, and $W_4 = 408$lb/ft.

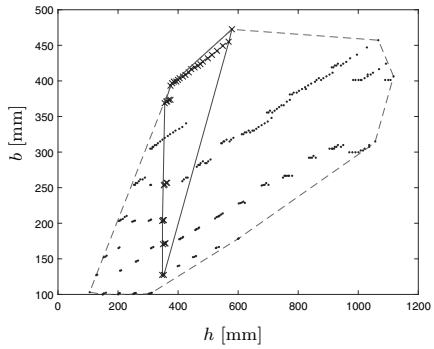

Fig. 10 Convex hull around W14 selection (37 alternatives marked with cross) and total W selection (267 alternatives marked with dot) in (h,b) space. Convex hulls drawn in dashed line for total W selection and solid line for W14 selection.

susceptible to local buckling. The continuous search is guided towards such cross-sections by adding a set of linear constraints that form a convex hull of the profile alternatives. These constraints are written as

$$\mathbf{A}_j \mathbf{x}_j \leq \mathbf{b}_j \tag{41}$$

where $\mathbf{A}_j$ is a constant matrix, $\mathbf{b}_j$ is a constant vector and the variable vector is

$$\mathbf{x}_j = \left[b_j,\ h_j,\ t_{w,j},\ t_{f,j}\right] \tag{42}$$

The dimensions of $\mathbf{A}_j$ and $\mathbf{b}_j$ are different for beams and columns, since the profile alternatives are different. The convex hull constraints are demonstrated in Figure 10. In total, there are 1060 linear convex hull constraints.

Alternatively for the W14 shapes, the height of the profile, h, can be taken as the independent variable, and the remaining dimensions can be expressed by the approximations

$$b\left(h\right) = \begin{cases} 9.3819h - 3099, h < 372 \\ 0.3357h + 266.7, h \geq 372 \end{cases} \quad \text{[mm]} \tag{43}$$

$$t_w\left(h\right) = 0.3347h - 109.4 \quad \text{[mm]} \tag{44}$$

$$t_f\left(h\right) = 0.5104h - 164.9 \quad \text{[mm]} \tag{45}$$

The bilinear approximation of Eq. (43) for b as a function of h is shown in Figure 11. By using the approximate functions, the column profiles can be defined with single variable h instead of four variables thus reducing the dimension of the continuous relaxation.

The objective function is the weight of the frame and it is written as

$$f\left(\mathbf{x}\right) = \rho \sum_{i=1}^{168} A_i L_i = \rho \sum_{i=1}^{168} \left[2b_i t_{f,i} + \left(h_i - 2t_{f,i}\right) t_{w,i}\right] L_i \tag{46}$$

The objective function is clearly nonlinear and non-convex due to the bilinear terms $b_i t_{f,i}$, $h_i t_{w,i}$ and $t_{f,i} t_{w,i}$.

The problem statement for the continuous relaxation can be written as

$$\begin{aligned} &\min_{\mathbf{x}} \ f(\mathbf{x}) \\ &\text{such that } g_m\left(\mathbf{x}\right) \leq 0 \quad \text{(for all members)} \\ &\qquad\quad g_d\left(\mathbf{x}\right) \leq 0 \quad \text{(for all floors)} \\ &\qquad\quad \mathbf{A}_j \mathbf{x}_j \leq \mathbf{b}_j \quad \text{(for all members with convex hull constraints)} \end{aligned} \tag{47}$$

When the profile selection for each of the 20 groups is defined with four variables there are in total 80 design variables in the continuous problem of the first phase. If the approximate functions (Eq. (43)-Eq. (45)) are adopted for the columns, the dimension of the relaxed problem is reduced to 32 design variables.

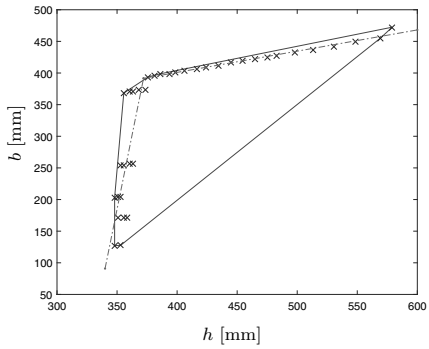

Fig. 11 Convex hull around W14 selection in (h,b) space (solid line) and the bilinear approximation defined by Eq. (43) (dashed line).

Table 11 Four different combinations of continuous and discrete spaces. n_c is the number of continuous design variables and n_d is the number of discrete profile alternatives used in the second phase.

Case	n_c [-]	n_d [-]
1	80	5
2	80	10
3	80	15
4	32	5

Table 12 Main results from Three-bay twenty-four-story frame example.

Method	Runs	Best found [kg]	Mean [kg]	Std [kg]	Mean n_{fe} [-]
ACO (Camp et al. 2005)	100	100001	104124	2069	15500
HS (Degertekin 2008)	100	97459	100979	2631	14651
IACO(Kaveh & Talahatari 2010a)	100	98969	-	-	-
ICA (Kaveh & Talahatari 2010b)	-	96584	-	-	-
CSS (Kaveh & Talahatari 2012)	50	96692	97731	1111	-
DE (Kaveh & Talahatari 2013)	-	93339	-	-	-
2-phase case 1	50	91834	92950	1288	26709
2-phase case 2	50	92958	94960	1042	24024
2-phase case 3	50	93480	95990	1839	29120
2-phase case 4	50	91648	92360	2395	19928

In the second phase, three neighbourhoods were tested, with 5, 10 or 15 profiles closest to the solution from phase I for each member group. The normalized Euclidean distance (see Eq. (3)) is now

$$d_j = \sqrt{\left(\frac{t_{f,j} - t_f^*}{t_{f,max} - t_{f,min}}\right)^2 + \left(\frac{t_{w,j} - t_w^*}{t_{w,max} - t_{w,min}}\right)^2 + \left(\frac{h_j - h^*}{h_{max} - h_{min}}\right)^2 + \left(\frac{b_j - b_f^*}{b_{max} - b_{min}}\right)^2} \tag{48}$$

where b_j, h_j, $t_{w,j}$ and $t_{f,j}$ are the dimensions of profile alternative j and b^*, h^*, t_w^* and t_f^* are the dimensions of the best found continuous solution.

The two-phase approach was applied to the minimum weight problem with 80 variables (i.e. 4 variables for each of the 20 member groups) in the first phase and 5, 10 or 15 profile alternatives in the second phase. In addition, the continuous formulation with 32 design variables was employed with five profile alternatives in the second phase. Thus, the four cases listed in Table 11 were considered.

The results of optimization runs as well as some results from literature are shown in Table 12. The two-phase approach yields better designs than reported in the literature except in case 3. Case 4 provides the best design having 1.8 % smaller weight than obtained by Kaveh & Talahatari (2013). However, the number of function evaluations is in general greater than reported in the literature. As in the 52-bar-truss problem, the phase II requires more function evaluations (Table 13). For the first phase, notable improvement in computational efficiency is observed in case 4 (with 32 variables instead of 80): the number of function

Table 13 Number of function evaluations using the two-phase approach.

	Phase I		Phase II	
Case	Min	Mean	Min	Mean
1	6492	8146	6801	18563
2	6492	7999	6801	16025
3	6917	7997	8801	17169
4	719	2711	7001	17217

Table 14 The best found designs of the three-bay twenty-four-story frame.

	Profiles			
Member	Case			
group	1	2	3	4
1	W30x90	W30x90	W30x90	W30x90
2	W6x15	W8x18	W10x22	W8x18
3	W24x55	W24x55	W24x55	W24x55
4	W12x16	W10x12	W8x15	W6x8.5
5	W14x159	W14x193	W14x159	W14x145
6	W14x109	W14x99	W14x132	W14x132
7	W14x99	W14x109	W14x109	W14x99
8	W14x74	W14x74	W14x90	W14x68
9	W14x68	W14x68	W14x61	W14x74
10	W14x43	W14x68	W14x61	W14x43
11	W14x43	W14x38	W14x30	W14x30
12	W14x22	W14x22	W14x22	W14x22
13	W14x90	W14x90	W14x90	W14x99
14	W14x109	W14x109	W14x99	W14x99
15	W14x99	W14x90	W14x109	W14x99
16	W14x99	W14x99	W14x82	W14x99
17	W14x74	W14x74	W14x90	W14x68
18	W14x61	W14x48	W14x61	W14x61
19	W14x34	W14x30	W14x34	W14x38
20	W14x22	W14x26	W14x22	W14x22

evaluations is approximately at best 89 % and on average 66 % smaller than in cases 1-3. Case 4 also provides the best found design.

Contrary to the previous examples, the best results are obtained with the smallest number of profile alternatives in the second phase. The best found designs are shown in Table 14.

4 Conclusions

In this study, the two-phase approach for discrete variable structural optimization was revisited with applications to skeletal steel structures. The numerical results indicate that the two-phase approach is a viable procedure that performs well when compared to the popular metaheuristics in terms of the quality of the obtained design. Either as good or better solutions than reported in the literature were obtained in all the examples.

Comparing the computational effort of the procedures is difficult as in many references only results of a single run are reported even though the stochastic nature of meta-heuristic methods require multiple runs for reliable performance assessment. By considering the average number of function evaluations the two-phase approach seems better option than GA. On the other hand, for ICA, IACO, DE, CSS, MBA and DHPSACO a lower number of function evaluations is reported for the best run. However, it cannot be said how well the number describes the performance on average.

For further development of the two-phase approach, the following key points should be addressed:

Phase I:
- *Initial point for the continuous solver.* In this study, the initial point was chosen randomly. For conventional frame structures, engineering judgment or other heuristic can be employed to find a design that is based on approximation of internal forces. For example, the beams of the 24-storey frame can be considered separately as beams with fixed supports under uniform load, and the entire profile catalogue can be explored to find the minimum profile.
- *Problem formulation.* The central idea of solving the relaxation is that only a (hopefully) good approximation of the optimum design for the original discrete problem is obtained with a moder-

ate computational effort. Therefore, finding the global optimum or including all the requirements from the design codes that cause discontinuities to the problem are not of primary interest. In order to facilitate the overall solution process, the problem formulation of the relaxation can be manipulated, such that it can be solved quickly by efficient gradient-based algorithms.

Phase II:
- *Problem formulation.* For the second phase, all the requirements of the design codes and fabrication need to be included as constraints and as allowable discrete variable values. The main question is, how to treat the discrete variables for selecting the member profiles. In the examples considered in this study, the indices of the profiles in the catalogue were taken as design variables. In the MILP formulation, binary variables are used for selecting the profile. Other possibilities for defining the discrete variables should be explored.
- *Neighbourhood of the solution of the relaxation.* The Euclidean distance for choosing the subset of discrete profiles for the second phase is a straightforward and generally applicable metric. An important question is then, how many profiles per member (or member group) should be included in the neighbourhood. The neighbourhood should be substantially smaller than the original profile catalogue in order to reduce the computational effort, but large enough to include feasible designs.
- *Solution method.* Instead of the population-based meta-heuristics that intrinsically require a substantial amount of function evaluations, other methods applicable for discrete optimization should be studied. If the MILP formulation or other deterministic approaches are not available (due to problem size or the form of the constraints derived from the design codes), basically any heuristic method can be employed. If the assumption holds that the solution of the relaxation is close to the discrete optimum, most feasible discrete designs should be satisfying for the designer.

Acknowledgements

The financial support of Finnish Cultural Foundation, Pirkanmaa Regional fund is gratefully acknowledged.

5 Data availability statement

Literal replication of results presented in this paper may be impossible due to stochasticity involved in the used solution process. However, as dozens of runs were performed in each example problem, it is believed by the authors that similar results with similar deviation will be obtained.

Three out of four design problems are picked from literature and are well documented and therefore considered straightforward to replicate. For the tubular truss design problem, the authors can upon request send the relevant code files.

Conflict of interest

On behalf of all authors, the corresponding author states that there is no conflict of interest.

References

Ame (2016), *ANSI/AISC 360-16 Specification for Structural Steel Buildings.*

Arora, J. S. (2000), *Methods for Discrete Variable Structural Optimization*, pp. 1–8.

Arora, J. S. & Huang, M.-W. (1996), 'Discrete structural optimization with commercially available sections', *J. Struct. Mech. Earthquake Eng., JSCE* **1996**(549), 1–18.

Arora, J. S., Huang, M. W. & Hsieh, C. C. (1994), 'Methods for optimization of nonlinear problems with discrete variables: A review', *Structural Optimization* **8**, 69–85.

Camp, C. V., Bichon, B. J. & Stovall, S. P. (2005), 'Design of steel frames using ant colony optimization.', *Journal of Structural Engineering* **131**, 369–379.

Danna, E., Rothberg, E. & Pape, C. L. (2005), 'Exploring relaxation induced neighborhoods to improve mip solutions', *Mathematical Programming* **102**, 71–90.

Degertekin, S. O. (2008), 'Optimum design of steel frames using harmony search algorithm', *Structural and Multidisclipinary Optimization* **36**, 393–401.

EN 10219-2 (2006), *Cold formed welded structural hollow sections of non-alloy and fine grain steels. Part 2: Tolerances, dimensions and sectional properties*, CEN.

EN 1993-1-1 (2006), *EN-1993-1-1. Eurocode 3: Design of steel structures. Part 1-1: General rules and rules for buildings.*, CEN.

EN 1993-1-8 (2006), *EN-1993-1-8. Eurocode 3: Design of steel structures. Part 1-8: Design of joints.*, CEN.

Fischetti, M., Glover, F. & Lodi, A. (2005), 'The feasibility pump', *Mathematical Programming* **104**, 91–104.

Ghattas, O. & Grossmann, I. E. (1991), MINLP and MILP strategies for discrete sizing structural optimization problems, *in* O. Ural & T. L. Wang, eds, 'Proceedings of the 10th conference on electronic computation', ASCE, pp. 197–204.

Gurobi Optimization, L. (2018), 'Gurobi optimizer reference manual'.
URL: *http://www.gurobi.com*

Haftka, R. T. & Gürdal, Z. (1992), *Elements of structural optimization*, Kluwer academic publishers.

Hager, K. & Balling, R. (1988), 'New approach for discrete structural optimization', *Journal of Structural Engineering* **114**(5), 1120–1134.

Hirota, M. & Kanno, Y. (2015), 'Optimal design of periodic frame structures with negative thermal expansion via mixed integer programming', *Optimization and Engineering* **16**, 767–809.

Huang, M. W. & Arora, J. S. (1997), 'Optimal design of steel structures using standard sections', *Structural optimization* **14**, 24–35.

Jokinen, T., Mela, K., Tiainen, T. & Heinisuo, M. (2016), 'Optimization of tubular trusses using intumescent coating in fire', *Journal of Structural Mechanics* **49**(4), 854–872.

Kaveh, A. & Talahatari, S. (2009), 'A particle swarm ant colony optimization for truss structures with discrete variables', *Journal of Constructional Steel Research* **65**, 1558–1568.

Kaveh, A. & Talahatari, S. (2010*a*), 'An improved ant colony optimization for design of planar steel frames', *Engineering Structures* **32**, 864–876.

Kaveh, A. & Talahatari, S. (2010*b*), 'Optimum design of skeletal structures using imperialist competitive algorithm', *Computers and Structures* **88**, 1220–1229.

Kaveh, A. & Talahatari, S. (2012), 'Charged system search for optimal design of planar frame structures', *Applied Soft Computing* **12**, 382–393.

Kaveh, A. & Talahatari, S. (2013), 'A new optimization method: Dolphin echolocation', *Advances in engineering software* **59**, 53–70.

Kravanja, S., Turkalj, G., Silih, S. & Zula, T. (2013), 'Optimal design of single-story steel buildigng based on parametric minlp optimization', *Journal of Constructional Steel Research* **81**, 86–103.

Kravanja, S. & Zula, T. (2010), 'Cost optimization of industrial steel building structures', *Advances in Engineering software* **41**, 442–450.

Kureta, R. & Kanno, Y. (2014), 'A mixed integer programming approach to designing periodic frame structures with negative poisson's ratio', *Optimization and Engineering* **15**, 773–800.

Lee, K. S., Geem, Z. W., Lee, S. H. & Bae, K. W. (2005), 'The harmony search heuristic algorithm for discrete structural optimization', *Engineering Optimization* **37**, 663–687.

Li, L., Huang, Z. & Liu, F. (2009), 'A heuristic particle swarm optimization method for truss structures with discrete variables', *Computers and Structures* **87**, 435–443.

Mela, K. (2014), 'Resolving issues with member buckling in truss topology optimization using a mixed variable approach', *Structural and Multidisclipinary Optimization* **50**, 1037–1049.

Moses, F. & Onoda, S. (1969), 'Minimum weight design of structures with application to elastic grillages', *International Journal of numerical methods in engineering* **1**, 311–331.

Rasmussen, M. & Stolpe, M. (2008), 'Global optimization of discrete truss topology design problems using parallel cut-and-branch method', *Computers and structures* **86**, 1527–1538.

Sadollah, A., Bahreininejad, A., Eskandar, H. & Hamdi, M. (2012), 'Mine blast algorithm for optimization of truss structures with discrete variables', *Computers and Structures* **102–103**, 49–63.

Saka, M. & Kameshki, E. (1998), 'Optimum design of unbraced rigid frames', *Computers and Structures* **69**, 433–442.

Saka, M. P. & Geem, Z. W. (2013), 'Mathematical and metaheuristic applications in design optimization of steel frame structures: an extensive review', *Mathematical programming in engineering* **2013**, 33.

Stolpe, M. (2016), 'Truss optimization with discrete design variables: a critical review', *Structural and multi-disclipinary optimization* **53**, 349–374.

Svanberg, K. (1984), On local and global minima in structural optimization, *in* E. Atrek, R. H. Gallagher, K. M. Ragsdell & O. C. Zienkiewicz, eds, 'New Directions in Optimum Structural Design', John Wiley & Sons Ltd, pp. 327–341.

Tiainen, T., Mela, K., Heinisuo, M. & Jokinen, T. (2017), 'The effect of steel grade in weight and cost of warren-type welded tubular trusses', *Proceedings of the institution of civil engineers: Structures and buildings* **170**(11), 854–872.

Van Mellaert, R., Mela, K., Tiainen, T., Heinisuo, M., Lombaert, G. & Schevenels, M. (2018), 'Mixed-integer linear programming approach for global discrete sizing optimization of frame structures', *Structural and Multidisciplinary Optimization* **57**(2), 579–593.
URL: *https://doi.org/10.1007/s00158-017-1770-9*

Wolsey, L. A. (1998), *Integer Programming*, John Wiley & Sons.

Wu, S. J. & Chow, P. T. (1995), 'Steady-state genetic algorithms for discrete optimization of trusses', *Computers and Structures* **56**, 979–991.

Yates, D., Templeman, A. & Boffey, T. (1982), 'The complexity of procedures for determining minimum weight trusses with discrete member sizes', *International Journal of Solids and Structures* **18**, 487–495.

6.1 Errata in original publications

While collecting and revising the thesis some typing mistakes were found in the original publications. Those are listed in the following.

Publication I:

page 161: the sentence ”The paint producers provide tables that give the required intumescent coating thickness for given critical temperature at and cross-section section factor at specific time.” should read ”The paint producers provide tables that give the required intumescent coating thickness for given critical temperature and cross-section section factor at specific time.”

page 168: the sentence ”However, in R60 with ETA, the advanced approach gives 12 % from the solution obtained by the engineering approach.” should read ” However, in R60 with ETA, the advanced approach gives 12 % reduction from the solution obtained by the engineering approach.”

Publication III:

Table 2: The right-most column is incorrectly named ”First moment of area”. It should read ”Second moment of area”.

Incorrect material properties are stated in the 3x3 frame example. The correct ones are: ”Material properties are $f_y = 355$ MPa, $E = 210$ GPa and $\rho = 7850$ kg/m^3”

Publication IV:

The force values F and q are missing from the design example. The force values used are $F = 37.8$ kN and $q = 50.1$ kN/m.

Publication V:

Following Eq. 7, instead of Table 2, reference should be made to Figure 2.

Table 3: Value 0.7 in the first row should be 1.0.